

**DEFORMATION WITHIN A BASEMENT-CORED ANTICLINE:  
TEAPOT DOME, WYOMING**

Scott Patrick Cooper

Department of Earth and Environmental Science

New Mexico Tech

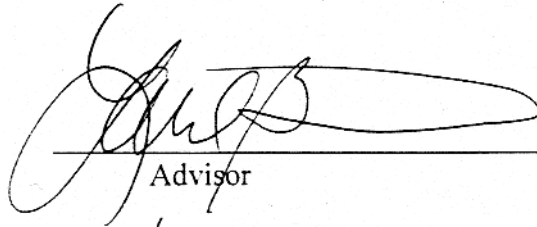
Socorro, New Mexico

Submitted in partial fulfillment of the requirements for the degree of  
Master of Science in Geology

May 2000

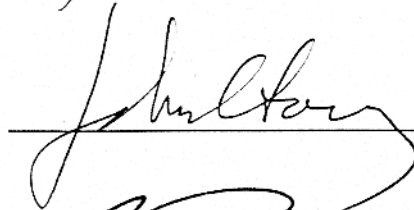
This thesis is accepted on behalf of the faculty

of the institute by the following committee:

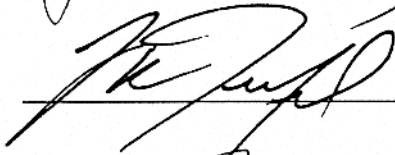


---


Advisor



---



---



---

March 28, 2000

---

Date

## ABSTRACT

Teapot Dome is an asymmetric, doubly plunging, basement-cored, Laramide-age anticline. A systematic study of natural fractures within the Cretaceous Mesaverde Formation at Teapot Dome, Wyoming indicates that lithology and structural position control outcrop fracture patterns. Lithology controls fracture, deformation band and fault patterns in the following ways: 1) fracture intensity increases with increased cementation, 2) fracture spacing increases proportionally with bed thickness within two sandstone facies, but not in carbonaceous shales where fracture spacing is inversely proportional to bed thickness, 3) coal cleats are generally oblique, by up to 20 degrees, to fractures in sandstones, 4) most fractures in sandstone units terminate at contacts with shale layers, 5) deformation bands occur almost exclusively in a poorly cemented, high porosity, beach-sand facies, 6) normal faults within well cemented sandstones are generally expressed as fracture zones, whereas the same faults within poorly cemented sandstones are diffuse zones of subparallel deformation bands.

Three primary throughgoing fracture sets were documented at Teapot Dome. The oldest fracture set is oblique to the fold hinge. The vast majority of these fractures strike NW to WNW. A small number of these oblique fractures strike roughly NNE. Fractures that strike oblique to the fold hinge appear to predate folding. The most common fractures, which are found throughout the fold, are bed-normal extension fractures striking subparallel to the fold hinge. A third set consists of bed-normal extension fractures striking perpendicular to the fold hinge. In many areas this fracture set is spatially related and subparallel to NE-striking, normal oblique-slip faults. The normal oblique-slip faults are common along the eastern limb, but more than 90% of these faults

terminate before intersecting the western limb. Conjugate fractures, deformation bands and faults, oriented such that they have a vertical bisector to the acute angle and striking subparallel to the axis of the anticline, are common in the southwestern limb and southern arc of the anticline. Hinge-parallel and hinge-perpendicular fractures and faults are probably broadly contemporaneous with basement-involved thrusting and folding at Teapot Dome, as suggested by their spatial relationship to the fold. Further observations suggest that fault-related, hinge-perpendicular fractures are generally the same age as hinge-parallel fractures, and NE-striking, normal oblique-slip faults are oriented roughly perpendicular to the fold hinge, even where it bends, and terminate toward the SW limb of the anticline. The oblique movement recorded on some of these NE-striking faults may be related to differential movement across individual segments of the basement-involved thrust.

Based on the Teapot Dome natural fracture data set, a 3-D conceptual model of fractures associated with basement-cored anticlines suggests significant horizontal permeability anisotropy. Depending on structural position and the interaction between fracture sets, the direction of maximum permeability can be either parallel or perpendicular to the fold hinge.

This work is dedicated to my family and, in particular,  
to the memory of my father  
Patrick H. Cooper



## ACKNOWLEDGEMENTS

I would like to thank Laurel B. Goodwin, John C. Lorenz, Lawrence W. Teufel, and Peter S. Mozley for serving on my thesis committee. Each provided valuable help throughout the entire thesis and graduate study process. Dr. Laurel Goodwin deserves special thanks for serving as my advisor, for her input into this project and the critical reviews of each paper and presentation that was developed from this research. Special thanks also to Dr. John Lorenz for his advice, help, time invested in the field, and for arranging my internship with Sandia National Laboratories. I would also like to acknowledge John for suggesting Teapot Dome as a thesis topic and research area – I am grateful. I have been fortunate to have both Laurel Goodwin and John Lorenz providing advice and support - Thank you.

I wish thank to Dr. Lawrence Teufel for providing the funding and the opportunity to work with him, the Naturally Fractured and Stress Sensitive Reservoir Consortium, and New Mexico Tech. Thanks Larry. I would also like to thank Dr. Bruce Hart at the New Mexico Bureau of Mines and Mineral Resources for all his help and support – especially in things seismic. Thanks to Dr. Steve Ralser for all the great comments and advice.

I gratefully acknowledge and thank the landowners and operators (Tom Allemand and family, Bill and Mary Owens, John Beaton, and Leland Bertagnole) surrounding NPR #3 for permission to describe and measure the outcrops on their property. This project would not have been possible without their understanding and support.

Thanks also to the Rocky Mountain Oilfield Testing Center, The Department of Energy and the previous contractor Fluor Daniel for providing safety training, logistical

support, funding and data. I would also like to thank all the great people at NPR #3 who have helped with this project over the last two years, including Mark Milliken, Steve Hardy, Jay LaBeau and everyone else who has come and gone over the life of this project.

Thanks to Matt Herrin and Tony Lupo for taking the time to review the roughest forms of this manuscript. I would also like to acknowledge every member of Dr. Goodwin's structural research group – each of you has listened intently (even when you were not interested hearing another petroleum junkie talk). Your comments and interactions have helped mold my thoughts and research.

Last, but definitely not least, thanks to my family. What can I say – Karen, your understanding, love, support and willingness to help a middle-aged student keep the dream of a higher education alive is what made this whole thing possible and worthwhile (I owe you big time!). To my in-laws (Rick and Hilde Doyle), for supporting us monetarily and for supporting our decision to leave the work place and enter college. To my Mom (Jean Cooper), I know it has not been easy since Dad died and Karen and I left for New Mexico – but every time I talked with you I gained support from the love and pride in your voice for a son who chose a college education. Thanks also for coming down these last two semesters and being a Granny-nanny for the boys. Dad, any success I have is from simply trying to live like the man you were/are and this thesis is dedicated to you. To my boys, Sean and Ryan, I know you do not understand why you had to leave Daddy alone to work so much or why you had to stay behind when I was working in the field, however you have always kept me conscious of those things that really do matter most in this life – I promise to never forget.

## TABLE OF CONTENTS

Abstract .....	i
Dedication .....	iii
Acknowledgments .....	iii
Table of Contents .....	v
List of Appendices .....	vii
List of Figures .....	viii
INTRODUCTION .....	1
Part I: LITHOLOGIC CONTROLS .....	6
Introduction .....	6
Previous Work .....	8
Geologic setting .....	8
Lithologic controls on fracturing .....	11
Influence of porosity on deformation processes .....	14
Teapot Dome .....	16
Methods .....	16
Mesaverde Formation Stratigraphy .....	17
Fractures at Teapot Dome .....	21
Lithologic controls .....	23
Bed thickness .....	27
Porosity .....	35



Lithologic controls on faulting .....	42
Mineralization .....	42
Discussion .....	44
Fracture spacing vs. bed thickness .....	44
Impact of structures on fluid flow .....	46
Conclusions .....	48
Part II: STRUCTURAL CONTROLS .....	50
Introduction .....	50
Fracture-Fold Relationships .....	53
Folds associated with thin-skinned thrusts .....	53
Folds associated with deep-seated thrusts .....	55
Geologic Setting .....	57
Structural Analysis of Teapot Dome .....	61
Distribution of faults and fractures with respect to the fold .....	61
Faults .....	61
Fractures .....	65
Spatial relationship between faults and fractures .....	74
Discussion .....	74
3-D conceptual model of basement-cored anticlines .....	78
Fluid flow implications .....	82
Conclusions .....	84

APPENDICES .....	87
APPENDIX A: Brittle deformation of clastic sediments .....	87
APPENDIX B: Measured stratigraphic sections .....	92
APPENDIX C: Field data charts .....	101
APPENDIX D: Fracture spacing and bed thickness data .....	261
APPENDIX E: Representative fracture orientation data .....	263
APPENDIX F: Representative fracture orientation data for locations away from Teapot Dome .....	266
REFERENCES .....	268

## LIST OF FIGURES

### Deformation within a Basement-Cored Anticline, Part I: Lithologic Controls

Figure 1-1: Location map of Teapot Dome and surrounding Laramide uplifts .....	10
Figure 1-2: Generalized stratigraphic column of the Mesaverde Formation .....	18
Figure 1-3: Fracture map .....	22
Figure 1-4: Lithology related differences in fracture spacing and orientation .....	24
Figure 1-5: Fracture spacing and bed thickness relationships .....	25
Figure 1-6: Rose diagrams illustrating fracture and cleat orientations .....	26
Figure 1-7: Bed thickness and cementation relationship .....	28
Figure 1-8: Fracture spacing and bed thickness relationships .....	30
Figure 1-9: Fracture spacing vs. bed thickness in fluvial sandstones .....	33
Figure 1-10: Fracture spacing vs. bed thickness in Unit 1 sandstones .....	34
Figure 1-11: Fracture spacing and relative age relationships .....	36
Figure 1-12 Photomicrograph of a deformation band .....	39

Figure 1-13: Conjugate deformation bands .....	41
Figure 1-14: Fracture/fault relationship .....	43
Deformation within a Basement-Cored Anticline, Part II: Structural Controls	
Figure 2-1: Stearns and Friedman (1972) model of preferred fracture orientations .....	54
Figure 2-2: Location map of Teapot Dome and surrounding Laramide uplifts .....	59
Figure 2-3: Diagrammatic cross-section of Teapot Dome .....	60
Figure 2-4: Teapot Dome fault map .....	63
Figure 2-5: Western limb segmentation .....	64
Figure 2-6: Equal area net plot of representative fracture orientations .....	66
Figure 2-7: Map of WNW striking fracture set at Teapot Dome .....	68
Figure 2-8: Map of fracture sets at and away from Teapot Dome .....	69
Figure 2-9: Map of the hinge-perpendicular fracture set at Teapot Dome .....	71
Figure 2-10: Map of the hinge-parallel fracture set at Teapot Dome .....	72
Figure 2-11: Photograph and fracture map illustrating fracture patterns .....	73
Figure 2-12: Outcrop transect across a fault .....	75
Figure 2-13: Comparison of 3-D conceptual fracture models .....	80
Figure 2-14: Conceptual 3-D model of fracture patterns from Teapot Dome data .....	83

## Tables

Deformation within a Basement-Cored Anticline, Part I: Lithologic Controls	
Table 1-1: Fracture spacing and lithology relationships .....	29
Table 1-2: Deformation band petrographic data .....	37

## INTRODUCTION

Basement-cored anticlines within the Rocky Mountain region have been hydrocarbon exploration targets since the turn of the century. Structures of this type can also be found in many other areas of the world (e.g. DeSitter, 1964; Harding and Lowell, 1979). One of the primary reasons basement-cored anticlines are exploration targets is that they can provide excellent four-way closure. Four-way closure can allow the entrapment of migrating hydrocarbons in economically significant amounts. To maximize recovery of these trapped hydrocarbons it is essential to accurately model any permeability anisotropy associated with these structures.

An important first step in understanding the nature of permeability anisotropy is developing a conceptual model of the orientations and distribution of structures that influence flow, such as fractures and faults. Various models have been proposed to explain the variation in orientation, location and spacing of fractures in basement-cored anticlines (DeSitter, 1956; Stearns and Friedman, 1972; Pollard and Aydin, 1988; Lorenz, 1997). Many of these conceptual models were developed from field observations at petroleum reservoirs and outcrops. These models are then applied to similar reservoirs for predictive purposes. This use of analogous reservoirs for prediction of permeability anisotropy and localized areas of hydrocarbon accumulation is quite common within the petroleum industry (Stearns and Friedman, 1972; Nelson, 1985; Pollard and Aydin, 1988).

The main purpose of this research was to evaluate the utility of existing conceptual models by comparing the orientation and distribution of predicted structures with those observed at Teapot Dome, Wyoming. Similarities exist between the patterns

observed at Teapot Dome and those described or postulated by DeSitter (1956), Murray (1967), Garrett and Lorenz (1990), Engelder et al. (1997), Hennings et al. (1998) and Unruh and Twiss (1998). However, the orientations of two primary fracture sets predicted by one of the most widely used models (i.e. Stearns and Friedman, 1972) are significantly different from those observed at Teapot Dome. The importance of using a model most analogous to a specific petroleum reservoir for analysis and prediction of permeability anisotropy cannot be overemphasized. In general, the most analogous reservoirs and models would be those with mechanically similar stratigraphic units, which formed under a similar tectonic regime.

### ***Geologic setting***

Teapot Dome is located in central Wyoming, near the southwestern edge of the Powder River Basin. It is an asymmetrical, doubly plunging, Laramide age anticline with a curvilinear fold hinge in map view. NE-striking normal oblique faults, striking predominately perpendicular to the curvilinear fold hinge, are common along the eastern limb (Thom and Speiker, 1931). Mesaverde Formation sandstones are exposed within a resistant rim along the eastern, southern and western limbs of the anticline. Maximum dips along the western limb are near  $30^{\circ}$ , along the eastern limb dips range from  $7^{\circ}$  to  $14^{\circ}$ . Exposures of the Mesaverde Formation along the northern portion are absent due to erosion. The Steele Shale is exposed at the surface within the central portion of this breached anticline. Teapot Dome is one of several productive hydrocarbon traps in Wyoming associated with Laramide structures.

Oil seeps were known to exist in the Teapot Dome and Salt Creek areas prior to 1880. The first oil well in the area was drilled in 1889 near one of the seeps north of the

Salt Creek anticline. The well was drilled to a depth of approximately 213 m (700 ft) and had a production of 10-15 barrels per day (b/d) from sand lenses in the Steele Shale (Curry, 1977). Teapot Dome was established as a Naval Petroleum reserve by President Wilson in 1915 (Doll et al., 1995). The first production at Teapot Dome was 830 barrels in October 1922, representing two days of flow from a shale well (ID # 301-2; Trexel, 1930). Peak production in 1923 was 138,081 barrels in October from 51 wells or 4460 barrels per day (Trexel, 1930).

The infamous Teapot Dome scandal of the Harding Administration involved leasing of this Government-owned reserve to Harry F. Sinclair's Mammoth Oil Company in 1922. Daily production when placed in the hands of the receivers in 1924 was approximately 3790 barrels per day (b/d). Trexel (1930) provides monthly sales and royalty figures for this period. These data show total oil and gas sold by that date by Mammoth Oil Company was 1,442,496 barrels. Trexel (1930) also indicates that Mammoth Oil produced between 2 and 2.5 billion cubic feet of gas by March 13, 1924. Reports indicate that during this period some shale-crevice wells had production rates as high as 25,000 b/d (Curry, 1977). Production dropped to 22,626 barrels per month by December 1927. Therefore, during the scandal, wells were producing at a maximum rate and much of the reservoir pressure was depleted (Curry, 1977; Doll et al., 1995).

The current manager of Teapot Dome, also known as Naval Petroleum Reserve #3 (NPR #3), is The Department of Energy. Cumulative production for the year 1998 was 250,000 barrels of sweet crude oil, and 26,000 barrels of sour crude oil from an average of 500 production wells (Milliken, pers. com., 1999). NPR#3 is slated for closure and reclamation by 2003. At present one of the major uses of the Teapot Dome

Field is as a testing center for new technologies. This research is managed through the Rocky Mountain Oilfield Testing Center located in Casper, Wyoming and on site at Teapot Dome.

### ***Organization***

This thesis provides a new look at how fractures and faults can be formed above a basement-involved thrust. The 3-D model developed herein conceptually illustrates the possible orientations of fractures, deformation bands and faults in this type of deformational regime, which in turn allows one to assess the permeability anisotropy associated with these features. In the interest of disseminating this information to the public and thereby providing industry with another reservoir analog, portions of this thesis are designed as separate papers to be submitted for publication in professional journals. With this in mind, the thesis comprises two papers to be published as Parts I & II. Part I is focused on lithologic controls, whereas Part II addresses structural controls on the distribution and character of faults, fractures and deformation bands. The possible influence of fault, fracture, and deformation band characteristics, such as spacing and orientation, on permeability is also discussed. Field data are included in the appendices.

### ***Additional questions***

The 3-D conceptual model developed in this thesis should not be applied equally to all anticlines. Although the model does provide another useful tool to help determine fluid flow directionality in one type of fractured reservoir, several questions remain unresolved: 1) How deep into the subsurface can the model adequately predict fracture and fault orientations and distributions? Further study of fractures at basement-cored anticlines with exposures of strata lower in the section, such as work done by Hennings et

al. (1998), may help. 2) Are the qualitative permeability anisotropy observations accurate? These could be tested by comparing in-situ well tests with a fluid flow simulation based on Teapot Dome stratigraphy and structure, as provided from well data, seismic sections, and the 3-D conceptual model. 3) How tight can the anticline be before the model becomes invalid? This may require an outcrop study of anticlines with limbs that dip at angles higher than the maximum 30 degree dip angle observed at Teapot Dome. Other important considerations in comparing various sites are differences or similarities in lithology, mechanical stratigraphy and tectonic setting.



## **Deformation within a Basement-Cored Anticline, Part I:**

### **Lithologic Controls**

#### **Introduction**

Structures such as fractures, fracture networks and faults can influence permeability and therefore fluid flow within an aquifer or petroleum reservoir (Lorenz and Finley, 1989; Lorenz et al., 1991; Teufel and Farrell, 1992). A distinct permeability anisotropy has been observed in reservoirs with low matrix permeability and a well developed, open fracture system (Elkins and Skov, 1960; Lorenz and Finley, 1989; Teufel and Farrell, 1992), with the highest permeability parallel to the fractures. Within a given rock volume fractures generally result in an overall permeability increase. There may also be significant interaction between the fracture surface and the matrix, allowing for better drainage of the rock matrix. This matrix/fracture interaction could allow for a substantial increase in recoverable hydrocarbon reserves.

In contrast, mineralized fractures and deformation bands (small-displacement faults, characterized by cataclasis and/or pore reduction through compaction) are typically characterized by significant permeability reduction (Nelson, 1985; Antonellini and Aydin, 1994; Antonellini et al., 1994). Where fractures are mineralized or the rock is cut by deformation bands, the rock matrix is more permeable than the structures, so the rock is most permeable parallel to, and between, fractures and deformation bands. Therefore, within a given rock volume containing mineralized fractures and/or deformation bands there will be an overall permeability decrease and possible reservoir

compartmentalization. Partially mineralized fractures may still have some permeability. However, there could be a significant reduction in the interaction between the remaining open fracture fluid pathway and the rock matrix (Nelson, 1985). Either mineralized or partially mineralized fractures could have the effect of decreasing the total amount of producible reserves.

Because structures such as fractures and faults can increase or decrease permeability in certain directions and thus introduce permeability anisotropy and heterogeneity it is important, from a production standpoint, that they be modeled accurately. It can be very difficult, however, to predict the location, spacing, and orientation of fractures and small-displacement faults in the subsurface (e.g., Lorenz, 1997). Most regional fractures are subvertical, and are thus unlikely to be sampled in vertical boreholes (Lorenz and Hill, 1992). Reasonable predictions of permeability anisotropy require an understanding of controls on the distribution and orientation of such features.

Previous work indicates that lithology and bed thickness are primary controls on fracture spacing and orientation, reflecting the fact that different rock units are mechanically distinct (Nelson, 1985; Fjaer et al., 1992; Long et al., 1997; Lorenz, 1997). Fracture spacing (also referred to as fracture density) has been correlated with the mineralogical composition of the matrix grains, porosity, and bed thickness. In general, more brittle rocks will have more closely spaced fractures than less brittle rocks (Nelson, 1985). Therefore, rock units that contain high percentages of well-cemented brittle constituents will generally have more closely spaced fractures. The primary brittle constituents within a rock are quartz, feldspar, dolomite and calcite. However, it should

be noted that the elastic properties of a given rock unit, which have a direct influence upon fracture spacing, need not always be associated with the amount of brittle constituents. For example cleat or fracture spacing within carbonaceous shales and coals with few quartz grains is in many cases much closer than the fracture spacing within quartz-rich sandstone beds of similar thickness. Even though coal has fewer brittle constituent grains relative to sandstone, Price (1966) notes that Young's modulus for coal is significantly higher than sandstone. Therefore the difference in fracture spacing is more directly attributed to Young's modulus than to brittle constituents.

When loading conditions and all other rock parameters are equal, thin beds will have a higher fracture density than thicker beds (Price, 1966; Ladeira and Price, 1981; Nelson, 1985). With a few exceptions fracture spacing is locally proportional to bed thickness (Price, 1966; Hobbs, 1967; Nelson, 1985; Huang and Angelier, 1989; Lorenz et al., 1996; Bai and Pollard, 2000).

Examination of natural fracture and fault patterns within Mesaverde Formation outcrops at Teapot Dome, Wyoming was undertaken, in part, to develop a better understanding of the influence of lithology and bed thickness on the development of these structures. Additional work (presented in Part II) addresses variations in fault and fracture density and orientation with respect to structural position within the dome. Together, these two studies provide insight into controls on deformation of a heterogeneous sequence of clastic sedimentary rocks in a basement-cored anticline.

## **Previous Work**

### ***Geologic Setting***

Teapot Dome is located in central Wyoming, near the southwestern edge of the

Powder River Basin (Figure 1-1). The deepest portions of the Powder River Basin contain nearly 5,500 m of sedimentary rocks, approximately 2,440 m of which are nonmarine Upper Cretaceous and lower Tertiary clastic sedimentary rocks related to Laramide orogenesis (Fox et al., 1991). Fox et al. (1991) note that the tectonic style of Laramide uplifts varies around the basin, with the greatest deformation along the western and southern margins. Teapot Dome is one of several productive structural-style hydrocarbon traps associated with Laramide structures in this area.

A resistant rim of Mesaverde Formation sandstones is exposed along the eastern, southern and western limbs of Teapot Dome. At this location, the Mesaverde Formation can be subdivided into two members: the Teapot Sandstone Member and the Parkman Sandstone Member (Wegemann, 1918; Thom and Spieker, 1931). The Teapot Sandstone Member overlies the Parkman Sandstone Member with an intervening layer of marine shale between the two members. This relationship suggests sea regression during deposition of the Parkman Sandstone Member, followed by a brief transgression, then regression during the deposition of the Teapot Sandstone Member (Weimer, 1960; Zapp and Cobban, 1962; Gill and Cobban, 1966). An unconformity at the base of the Teapot Sandstone Member represents probable subaerial exposure and erosion associated with eustatic sea level change driven by regional tectonism (Gill and Cobban, 1966; Weimer, 1984; Merewether, 1990; Martinsen et al., 1993). Fractures within the Parkman Sandstone Member are the principle focus of this study.

The Steele Shale is exposed at the surface within the central portion of this breached anticline. An exploratory well (No. 1-G-10) near the apex of the anticline encountered granitic basement at a depth of 2084 m (6849 ft; Gribbin, 1952).

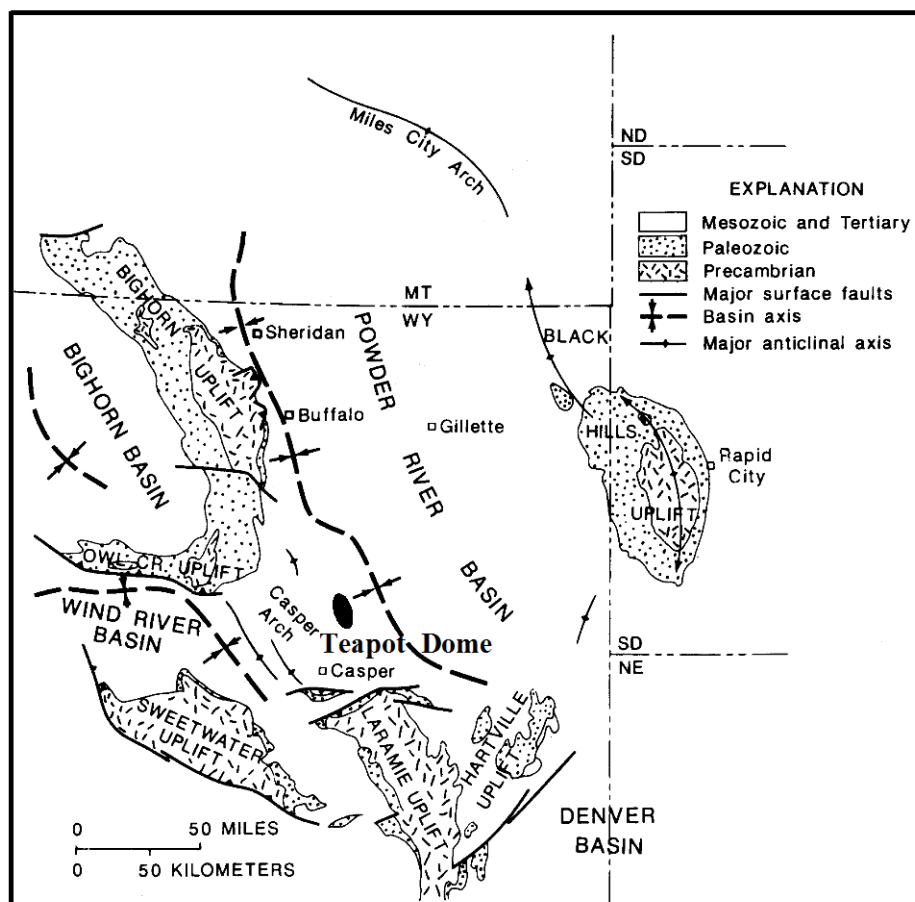


**Figure 1-1:** Index map illustrating the general location of Teapot Dome relative to the Powder River Basin and surrounding Laramide uplifts (after Fox et al., 1991).

The shallowest reservoirs at Teapot Dome are within the Shannon Formation. This formation is also one of the major producing intervals and is located at depths between 75-200m. The sandstones within this formation were deposited as offshore bars along the margin of the Cretaceous Western Interior Seaway (Tillman and Martinsen, 1984).

A major set of faults and fractures striking perpendicular to the hinge of the anticline and a secondary set parallel to the fold hinge were recognized and described at Teapot Dome by Thom and Spieker (1931). Thom and Spieker (1931) suggested that these faults and fractures may inhibit fluid flow if they are cemented, and discussed the possibility of increased hydrocarbon flow if a production well should intersect open fracture zones. They assumed that fractures would penetrate both sandstones and shales. These fractures would therefore allow communication between reservoir units and pressures would equalize. Because different pressures were observed within different reservoirs the authors assumed that fractures did not significantly influence hydrocarbon flow.

Part II (Structural Controls) describes three dominant fracture patterns observed at Teapot Dome. Two of the fracture sets appear to be related to the folding process and are oriented roughly parallel and perpendicular to the fold hinge. The third set predates folding and predominately strikes WNW.

### ***Lithologic Controls on Fracturing***

Fracture spacing is generally proportional to bed thickness (McQuillan, 1973; Narr and Suppe, 1991; Gross, 1993; Ji and Saruwatari, 1998; Bai and Pollard, 2000). Bai and Pollard (2000) evaluated previous studies and showed that spacing to layer thickness ratios range from greater than 10 to less than 0.1. Bogdanov (1947) mathematically

described a relationship where spacing (S) varied as a function of bed thickness (B) and some constant (K). The constant (K) has been related to lithology (Ladeira and Price, 1981).

$$\text{Equation 1:} \quad S = K B$$

Price (1966) attributed differences in spacing between fractures in a sandstone and coal cleats in an adjacent carbonaceous unit to differences in Young's modulus. In beds of similar thickness and within the same area, coal cleat spacing can be less than 3 cm whereas fracture spacing within sandstone can be over 35 cm. In evaluating this relationship, Price (1966) equated strain energy (w) to the applied stress ( $\sigma$ ) and Young's modulus (E):

$$\text{Equation 2:} \quad w = \sigma^2 / 2E$$

Given generalized Young's moduli of  $E = 2 \times 10^5$  and  $E = 1 \times 10^7$  for coal and sandstone, respectively, the strain energy stored in the carbonaceous unit can be several times that of the sandstone. The difference in stored strain energy is the same order of magnitude as the difference in fracture spacing.

With respect to fracture spacing within a single bed Price (1966) suggests that at some distance L from a preexisting fracture forces become large enough to form a second fracture. Therefore L is the limit of influence of the preexisting fracture and is the minimum distance at which a second fracture can be formed. Further, if bed thickness is doubled, a distance of 2L is required for the forces to become large enough to form a second fracture. Essentially Price (1966) implies a linear relationship between bed thickness and fracture spacing. Harris et al. (1960) suggests that fracture density is nearly the inverse of bed thickness. However, bed orientation, thickness of cover, and

the degree of cohesion between adjacent units all influence normal stress on the rock units. Also small lithologic changes, such as grain size, sorting and cementation, will influence both tensile strength and the coefficient of friction (Price, 1966). Price (1966) suggested these mitigating factors produce only second-order fluctuations in the bed thickness to fracture spacing relationship. Other workers (Stearns and Friedman, 1972; Lorenz et al., 1991; Agarwal et al., 1997; Lorenz, 1997) have observed that lithologic changes and sedimentary heterogeneities, such as grain composition, cementation and orientation of lenticular fluvial sandbodies relative to the stress field, can influence mechanical behavior and have a visible effect on fracture distribution and spacing. Fracture spacing has also been related to the rock properties and thickness of the adjacent rock units as well as the rock properties of the fractured bed (Ladeira and Price, 1981; Ji and Saruwatari, 1998; Bai and Pollard, 2000). Hobbs (1967) suggested that fracture spacing is proportional to the square root of Young's modulus for the fractured bed and the inverse of the square root of the neighboring units' shear moduli. Ji and Saruwatari (1998) devised a mathematical model to describe a fractured bed interlayered between two unfractured beds. In the model fracture spacing (s) depends on the fractured layer thickness (t) and the surrounding non-fractured layer thickness (d).

$$\text{Equation 3:} \quad s = n (td)^{1/2}$$

The constant n is dependent on material properties of the rock units and the decay modes of the shear stress in the bounding layers. The model is supported by field data from Ladeira and Price (1981).

Methods of evaluating layer thickness to fracture spacing include the Fracture Spacing Index (Narr and Suppe, 1991), Fracture Spacing Ratio (Gross, 1993) and



Fracture Spacing to Layer Thickness Ratio (Bai and Pollard, 2000). The Fracture Spacing Index (FSI) is the slope of a best-fit line through the origin on plots of mechanical layer thickness vs. median fracture spacing from a number of layers of varying thickness. In these plots thickness is on the y-axis however fracture spacing is held as the dependent variable. The plots are arranged in this manner so that FSI values correlate to higher fracture density. The Fracture Spacing Ratio (FSR) is the ratio of median fracture spacing vs. layer thickness for a single layer. Bia and Pollard (2000) use the Spacing to Layer Thickness Ratio ( $S/T_f$ ) as the inverse of either of the two previous measures assuming equal spacing (i.e. mean and median spacing values are the same). Mean rather than median fracture spacing has also been described as directly proportional to bed thickness (Huang and Angelier, 1988). The Spacing to Layer Thickness Ratio was used by Bia and Pollard (2000) because they wished to focus on “fracture spacing rather than on fracture density”.

### ***Influence of Porosity on Deformation Processes***

Rock strength has generally been shown to decrease in a nonlinear fashion with increasing porosity (Price, 1966; Dunn et al., 1973; Hoshino, 1974). Therefore, the breaking or fracturing strength of clastic sedimentary rocks is closely related to porosity. Hoshino (1974) derived an empirical relationship between rock strength and porosity:

$$\text{Equation 4:} \quad n = A e^{-b\sigma_s}$$

Where rock strength ( $\sigma_s$ ) is proportional to porosity ( $n$ ).  $A$  is the porosity at strength zero and  $b$  is related to the amount of strength change for a specific change in porosity. Dunn et al. (1973) expressed this relationship as:

$$\text{Equation 5:} \quad y = a n^b ,$$

where  $y$  is the stress difference at failure,  $n$  equals porosity, constants  $a > 0 > b$  and “through-going fractures develop by coalescence of grain-boundary cracks, porosity and extension fractures”. In the case of low porosity rocks, where there is limited open pore space, a through-going fracture will consist primarily or exclusively of linked extension fractures and grain boundary cracks. Therefore, low-porosity rocks are relatively strong because extension fractures must propagate through a relatively large number of grains within a given volume. In contrast, rocks of higher porosity have numerous open pore spaces, which requires fewer grains to be fractured. As through-going fractures develop, they will use open pore spaces whenever possible because crack propagation in this way requires the least energy (Dunn et al., 1973).

High porosity sandstones commonly deform by a mechanism different than less porous, more brittle sandstones. Deformation within relatively high porosity sandstones can occur by a combination of sand grain fragmentation and pore collapse localized within very narrow bands accommodating displacements of a few millimeters to centimeters (Engelder, 1974; Aydin, 1978; Jamison and Stearns, 1982; Antonellini et al., 1994). These generally planar small-displacement faults are defined as deformation bands (cf. Aydin, 1978). They are typically thin (1mm wide average) with along strike lengths from a few centimeters to some tens of meters in length. Three major groups of these small-displacement faults have been described (Antonellini et al., 1994): 1) deformation bands with no cataclasis, 2) deformation bands with cataclasis and 3) deformation bands with clay smearing. Formation of deformation bands of the first group is believed to be the result of early, transient dilatancy during grain boundary sliding. This can be followed by the formation of deformation bands of the second

group through grain breakage and pore collapse (Antonellini et al., 1994). The rotation and crushing of grains results in reduced permeability relative to the surrounding matrix (Antonellini et al., 1994). Experimental analyses indicate that the effective pressure required for failure at the transition between brittle faulting and cataclastic flow in porous sandstones decreases with increasing porosity and grain size (Wong et al., 1997). This observation is in accordance with field and experimental observations that porous sandstones tend to be less brittle and fail through a combination of early dilatancy, then pore collapse and grain fragmentation (Wong et al., 1992; Antonellini et al., 1994; Wong et al., 1997; Wong, 1998).

There is a direct relationship between grain size and deformation band width. This relationship is generally described as linear, with the thickness of deformation bands as some multiple (5-15) of average grain diameter (Roscoe, 1970; Muhlhaus and Vardoulakis, 1988; Antonellini et al., 1994). Further discussion of deformation bands is provided in Appendix A.

## **Teapot Dome**

### ***Methods***

Data collection sites were chosen to provide 1) a generally uniform distribution with regard to the large-scale anticlinal structure, and 2) representative samples from the five different stratigraphic units within the Mesaverde Formation. Data were collected by systematically recording the grain size, degree of cementation, bed thickness, and orientation of a given lithologic unit and the type, orientation, spacing, trace length, degree of mineralization, aperture width, surface characteristics, and abutting

relationships of fractures cutting that unit (Appendix C). At certain charted locations the fracture patterns were mapped to scale. These maps help to illustrate the abutting relationships in areas where two or more sets exist. Preference was given to localities that provided a 3-D view (e.g., combined pavement and cross-sectional views).

### ***Mesaverde Formation Stratigraphy***

As previously described, early workers (Wegemann, 1918; Thom and Spieker, 1931) subdivided the Mesaverde Formation at Teapot Dome into two members: the Parkman Sandstone Member and the Teapot Sandstone Member. For this study, a different approach was utilized. The Parkman Sandstone Member was divided into five units according to lithology and depositional environment. These divisions best create units with inherently different mechanical properties. Separating units according to mechanical properties is important due to mechanical influences on fracture characteristics. The majority of the fracture measurements were obtained from these five newly defined lithologic units within the Parkman Sandstone Member. From oldest to youngest, these units are a shallow-marine, interbedded sandstone/shale, foreshore/beach sandstone, a white beach sandstone, a non-marine carbonaceous shale, and lenticular fluvial sandstones within the carbonaceous shale unit. Appendix B details five measured sections at Teapot Dome; a generalized stratigraphic column is provided in Figure 1-2.

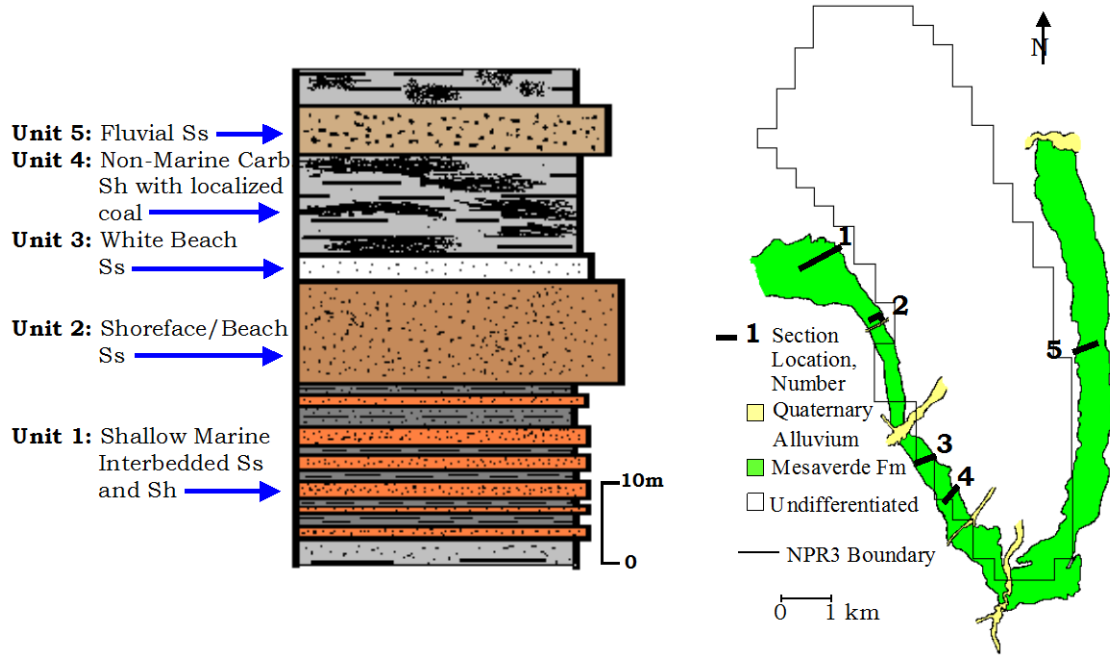


**Figure 1-2:** Generalized stratigraphic column based on measured sections illustrating the relative positions and thicknesses of the five Parkman Sandstone Member stratigraphic units from which fracture orientation data were recorded at Teapot Dome. Location of measured sections shown in map view and keyed to sections provided in Appendix B.

The stratigraphic sections allow consideration of spatial variations in thickness as well as facies variations within the units studied. Key observations and justifications for the environments of deposition within this progradational sequence are summarized in the following paragraphs.

Unit 1 consists of interbedded shallow-marine sandstones and shales and ranges in thickness from 10 to 20 m, with individual bed thicknesses from 5 cm to 150 cm. This unit is similar to a basal unit described by Thom and Spieker (1931). This unit is thicker in the northern half of the anticline. Grain sizes coarsen upward from 62-125  $\mu$  in the lower sandstones to 88-177  $\mu$  in the upper beds. The alternating beds of shale and sandstone, numerous trace fossils, current ripples and occasional hummocky cross-stratified beds found within this unit are evidence that these sandstones were deposited in a shallow-marine environment near wave base. When below wave base, the clay was deposited and not reworked/redistributed farther offshore into the deeper marine environments. When above wave base, sands were reworked into hummocky cross-stratified beds. Reworking was intermittent because trace fossils and current ripples were not always destroyed before burial.

The foreshore/beach sandstone unit (Unit 2) has an average thickness of 15-20 m. Grain sizes average between 88 and 177  $\mu$ . The thickest portion of this unit is found along the southeastern extent of the anticline (up to 20m thick). The basal (transitional) portion of this unit locally displays rip-up clasts, ball, pillow and flame primary structures, and *Ophiomorpha* trace fossils. The lack of trace fossils (except for the armored *Ophiomorpha* burrows) indicates that these deposits were shallow enough for constant reworking by wave and storm processes. Half-meter scale unidirectional crossbedding is suggestive of long-shore currents and offshore bars. Thicker sandstone beds with fewer and thinner shale beds relative to the shallow-marine facies suggest stronger shoreface currents during transport. The ball and pillow structures may represent rapidly deposited sandstones. The sands could be derived from surging

currents directed offshore, after storms flooded low-lying coastal areas. Alternatively, these structures could be related to synsedimentary earthquake activity (Kuenen, 1958; Potter and Pettijohn, 1977).

The white beach sandstone unit (Unit 3) is distinctive due to its snowy white color, higher porosity and lesser amount of cementation relative to any of the other Mesaverde Formation sandstones. Thom and Spieker (1931) also described this unit. This unit is absent along the northwestern portion of the dome, is present as a thin (up to 2 m) unit along the western and southern portions, and thickens to a maximum of 4.5 m along the eastern limb of the anticline. Grain sizes are between 125 and 250  $\mu$ . While sedimentary structures in this unit are typically obscure, carbonaceous shales deposited in paludal/swamp environments directly overlie it, suggesting this unit represents the bedding deposits expected between shallow marine and paludal environments.

The non-marine carbonaceous shale (Unit 4) averages 40 m in thickness and is locally interbedded with coal. A distinctive black color, generally poor induration, and a very fine grain size (less than 62  $\mu$ ) characterize this unit. These organic-rich carbonaceous shales are indicative of swampy environments. There are no distinct paleosols or rooted zones to indicate subaerial exposure. However, there are pieces of fossilized wood as well as twig/leaf imprints in the rock.

Laterally discontinuous, over a scale of 10s of meters, fluvial sandstones (Unit 5) are located within the carbonaceous shale unit. For the purposes of this study, fluvial sandstones are treated separately from the carbonaceous shales because of significant differences in grain size and cementation (and therefore inferred differences in mechanical properties). Unlike the other stratigraphic units, which have a tabular or

sheeted geometry, the fluvial sandstones are lenticular. Individual fluvial sandstone units range between 1 and 6 m in thickness. Sandstone lenses are generally poorly sorted with grain sizes varying between 88 and 250  $\mu$ . Crossbeds are generally uniformly oriented at any single outcrop, but are variable from channel to channel or from location to location along a channel, reflecting channel sinuosity. Associated ripple-bedded, finer-grained, thin-bedded overbank and levee deposits occur lateral to the channels or overlie the channel deposits. In the later case these deposits may have formed during channel abandonment.

### ***Fractures at Teapot Dome***

The dominant type of fractures observed at Teapot Dome is extension fractures that are primarily oriented parallel or perpendicular to the fold hinge (see Part II). At most sample locations there are multiple fracture sets, including throughgoing fractures and cross fractures (Figure 1-3). The majority of apertures measured at these locations are the result of recent erosion and thus are not discussed here. Surface features such as plume and rib structures were noticeably absent on almost all exposed throughgoing fracture surfaces. Due to the limited size of outcrop exposures, fracture trace length data were generally unobtainable at Teapot Dome. The throughgoing fractures generally extended from outcrop edge to outcrop edge. In one large pavement surface, within Unit 2 beach sandstones, fracture zones extend along strike over 100m (Appendix C, Chart 34).



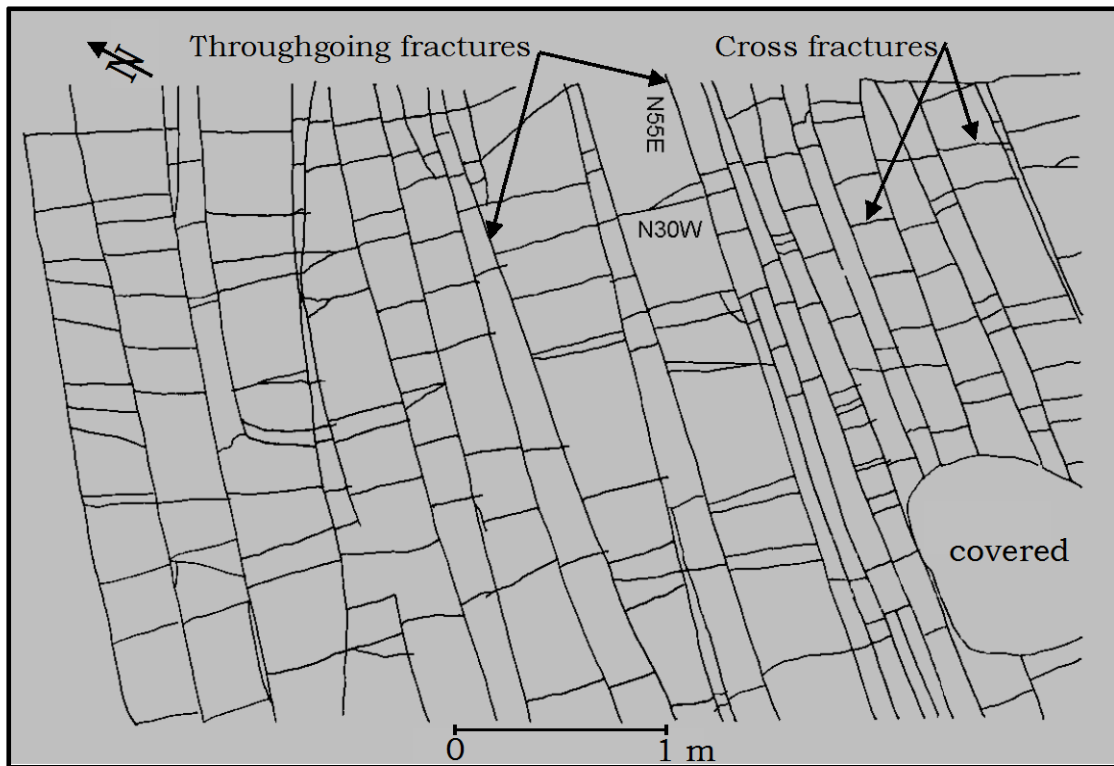


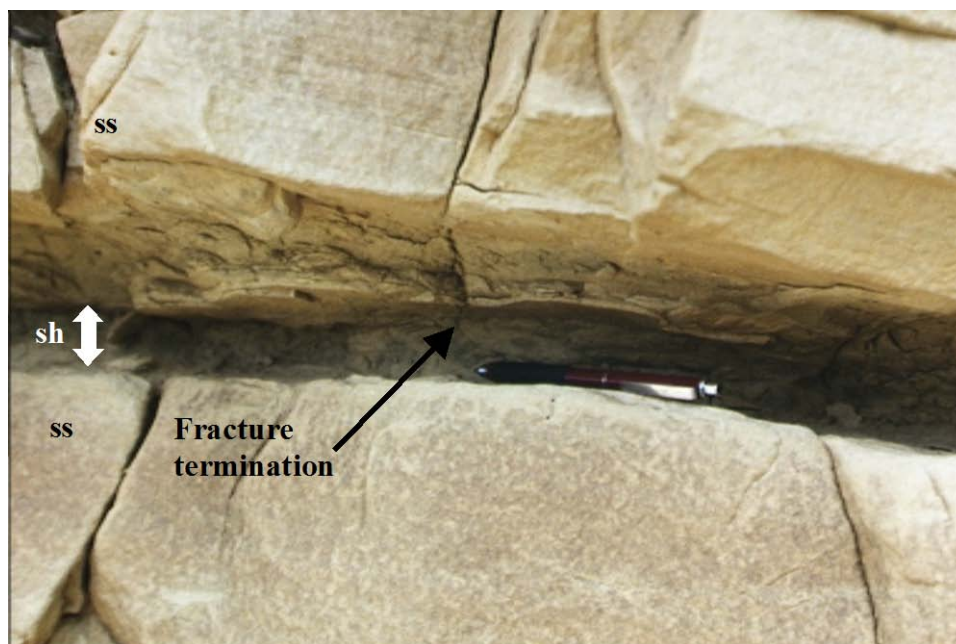
**Figure 1-3:** Fracture map of a pavement surface illustrating the nature of throughgoing fractures and cross fractures at the top of a single sandstone bed at Teapot Dome Wyoming (Appendix D, Chart 15).

### Lithologic Controls

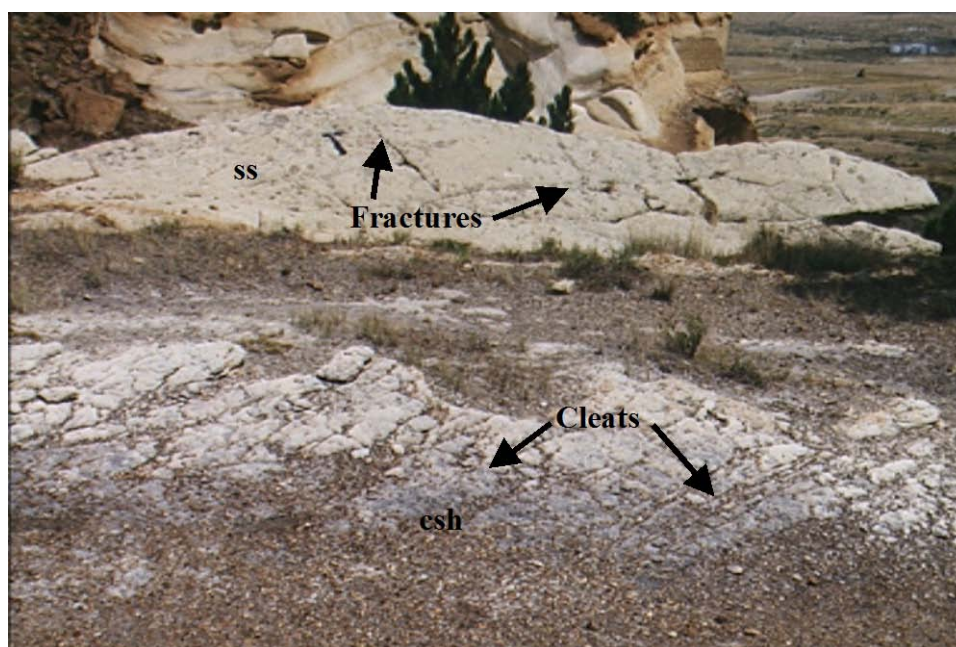
Both fracture spacing and orientation vary with lithology at Teapot Dome. In general, fractures are most closely spaced in carbonaceous shales (Unit 4), more widely

spaced in fluvial (Unit 5) and beach (Unit 2) sands, and most widely spaced in marine shales (Unit 1). Fractures are generally absent, replaced by deformation bands, within the white beach sandstones of Unit 3. Details of these relationships follow.

Unit 1 marine shales exhibit fewer fractures than associated well cemented Unit 1 marine sandstones. Most fractures in the sandstones terminate at sandstone/shale contacts (Figure 1-4a). This fracture termination relationship was observed everywhere Unit 1 was investigated. Unit 4 carbonaceous shales with localized coal seams have a relatively high cleat (extension fracture) density that in many areas is comparable to or greater than the fracture density within well cemented sandstone beds of similar thickness (Figures 1-4b, 1-5a and 1-5b). For example, two distinct fracture sets are observed within the Unit 2 sandstone of Figure 1-6, each with a unique orientation and mean spacing of fractures. The NW-striking fracture set has a mean fracture spacing of 29.5 cm, while the NE-striking fracture set has a mean fracture spacing of 185.5 cm. The mean spacing between NW-striking cleats in the Unit 4 carbonaceous shale is 17.2 cm. Comparing the NW-striking fracture set with NW-striking cleat set gives a ratio of cleats to fractures of 1.7:1. This is consistent with Price's (1966) observations of fracture density in coal vs. sandstone.

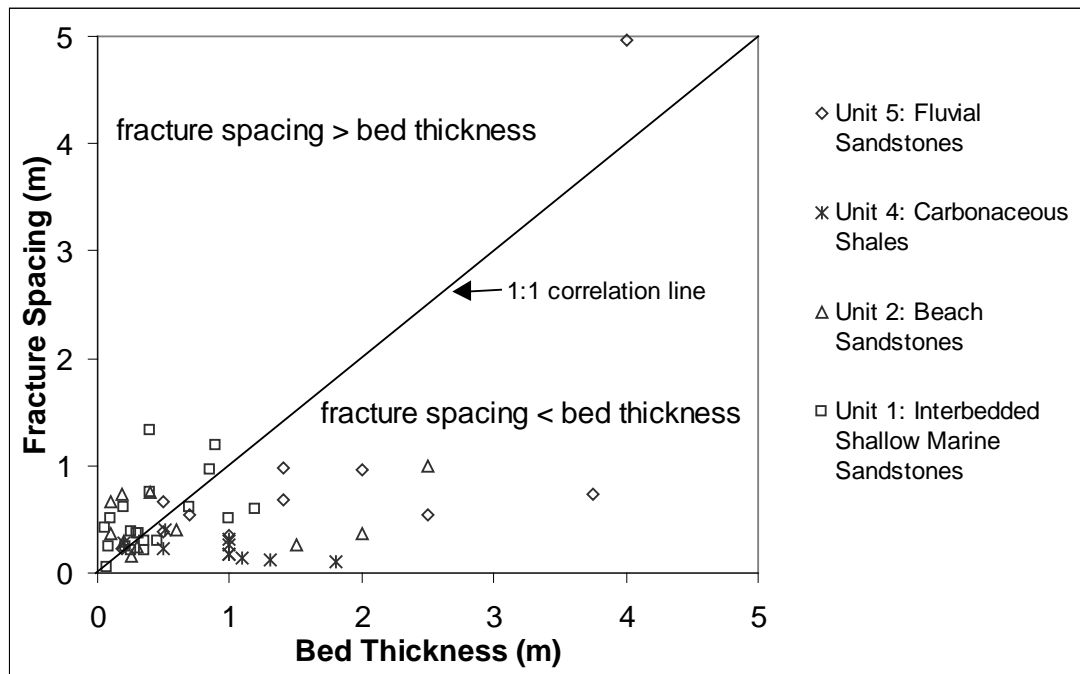


A

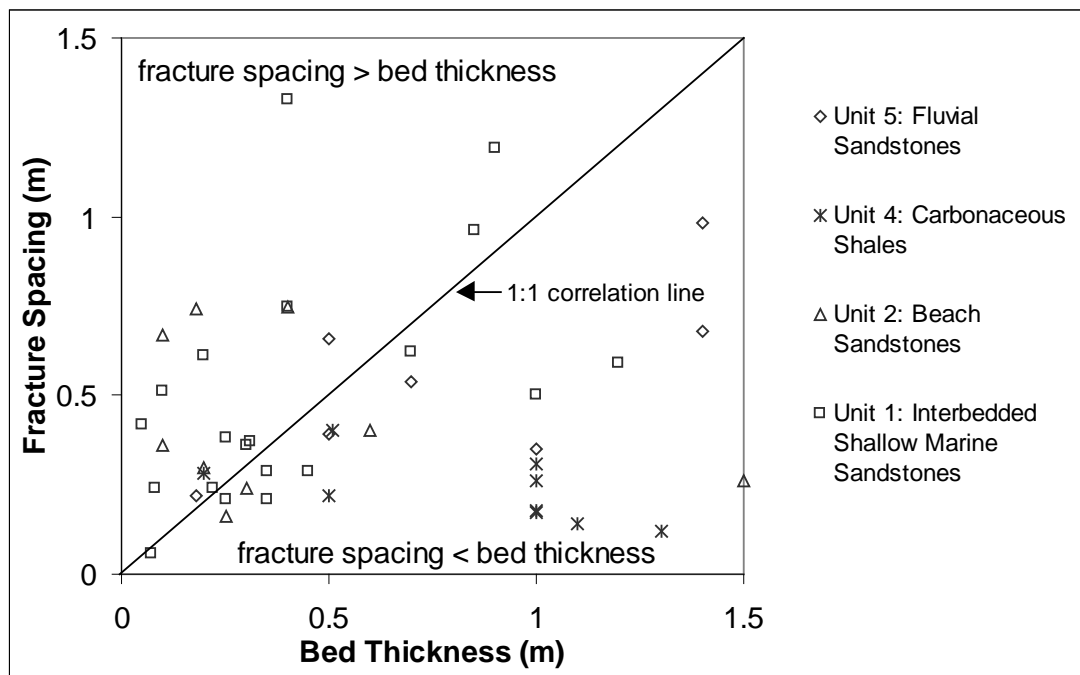


B

**Figure 1-4:** Examples of differences in fracture spacing and orientation related to lithology. (A) Fractures terminate at sandstone (ss) - shale (sh) contacts. Note the absence of fractures in shale. (B) Example of close cleat spacing within carbonaceous shale (csh). Note the two sets of fractures in the sandstone (ss). There is an approximate  $20^\circ$  difference in orientation between one fracture set in the sandstone (ss) and cleats in the carbonaceous shale. The second fracture set is oriented nearly  $70^\circ$  from the cleat set. Hammer on ss for scale.



A



B

**Figure 1-5:** Fracture spacing vs. bed thickness data from 53 locations and 4 lithologic units around Teapot Dome. Locations were selected on the criterion of at least one distinctly older throughgoing fracture set. Fracture spacing was measured perpendicular to the throughgoing fracture set and averaged for each location. 594 total fracture spacing measurements were used. Fracture and bed thickness values are provided in Appendix D.

(A) All data points are shown. (B) Shows data for bed thickness and fracture spacing values below 1.5m.

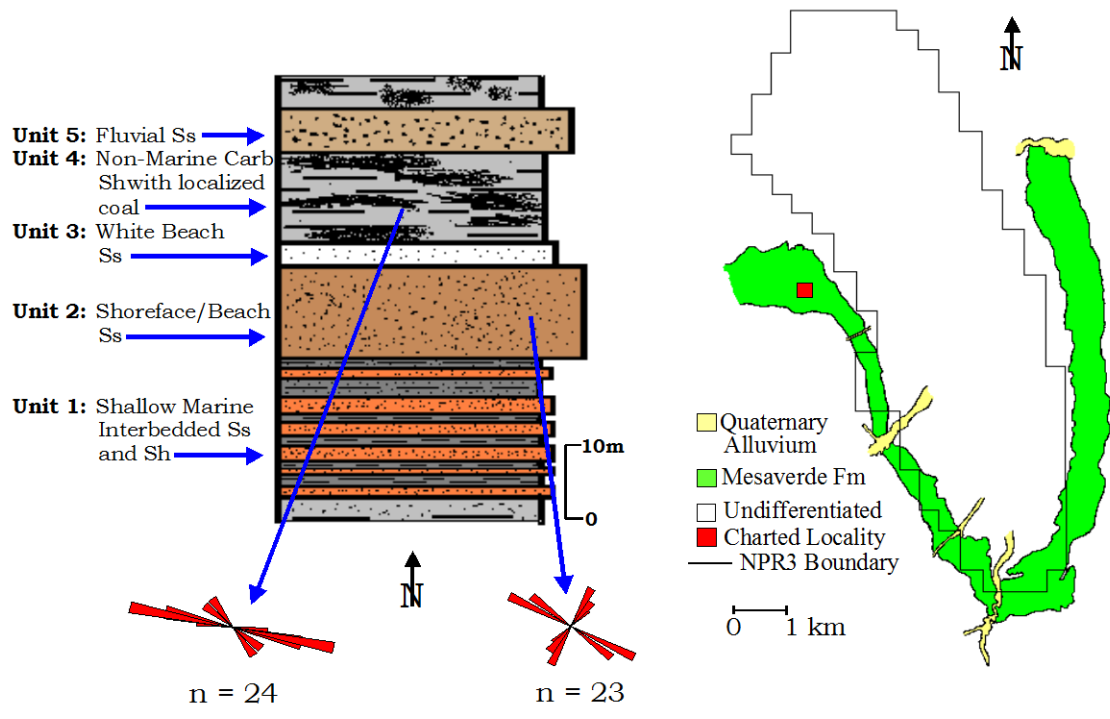


**Figure 1-6:** Example of the approximate 20-degree difference in orientation between fractures in sandstone and in carbonaceous shale. As illustrated by the rose diagrams, the sandstone unit and carbonaceous shale have two distinct fracture sets.

A further comparison suggests a significant difference in orientation between fractures and cleats. Fractures are oblique to cleats by up to  $20^{\circ}$  within beds of similar thickness and relatively close proximity (Figure 1-6).

Given sandstone beds of similar thickness, fractures are more closely spaced within better-cemented sandstones. Measurements obtained from seven adjacent sandstone beds within Unit 2 illustrate the relationship between the amount of cementation and fracture spacing in sandstones observed throughout Teapot Dome (Figure 1-7). Fracture spacing of the oldest throughgoing set was measured perpendicular to fracture strike. The oldest throughgoing set at this location is oblique to the fold hinge and has a representative orientation of  $N55^{\circ}W\ 75^{\circ}NE$ . Note that porosity is inversely related to the amount of cementation within a specific rock unit (Table 1-1).

### Bed Thickness

Data from Figure 1-5 were subdivided by lithology in order to evaluate the common belief that fracture spacing is proportional to bed thickness. Locations with bed normal extension fractures that have unambiguous abutting relationships and are not related to faulting are used in Figures 1-5 and 1-8. Data compiled from Appendix C data charts for this analysis are provided in Appendix D. Only the spacing between fractures in the oldest through-going fracture sets was plotted. This eliminated the necessity of determining the influence of pre-existing fractures on secondary fracture spacing. These data suggest that there is a broad linear relationship as described by Bai and Pollard (2000).

Diagrammatic stratigraphic section  
 Unit 2: shoreface/beach sandstones  
 Beds A-G shown with cementation percentages

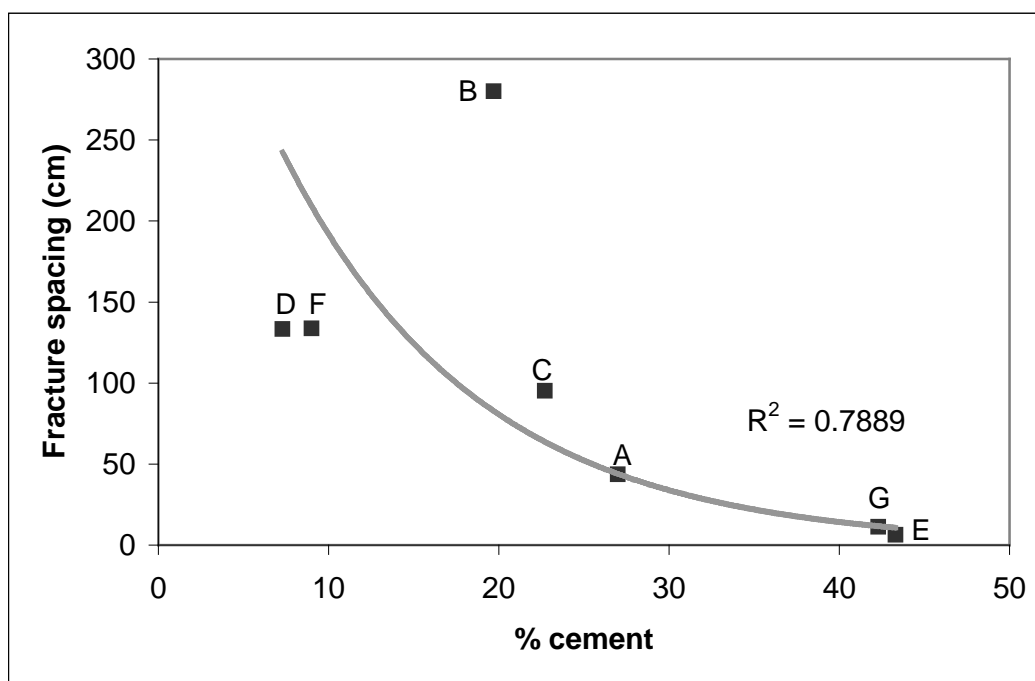
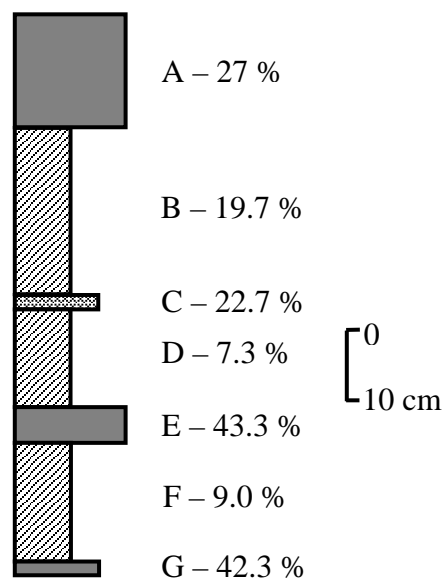
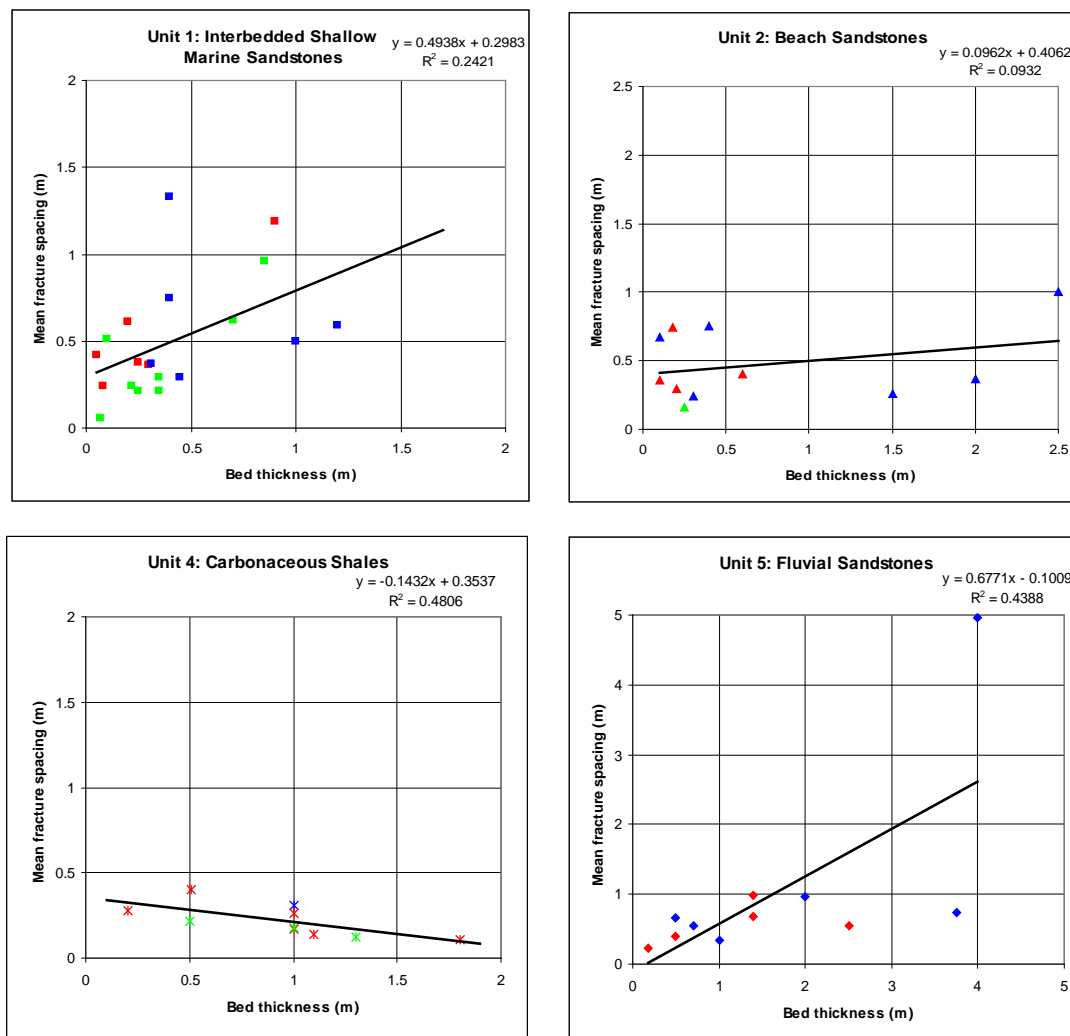


**Figure 1-7:** Fracture spacing generally decreases nonlinearly with increased cementation in a comparison of seven adjacent beds within the shoreface/beach sandstones of Unit 2. Cement percentages were determined from thin section point count data. Fracture spacing is average of measurements from each bed (Table 1). Data table provided in Appendix D – Chart 50.

<b>Bed</b>	<b>A</b>	<b>B</b>	<b>C</b>	<b>D</b>	<b>E</b>	<b>F</b>	<b>G</b>
<b>Number of measurements</b>	11	1	4	3	61	3	40
<b>Mean Fracture Spacing (cm)</b>	43.6	280.0	95.3	133.3	6.2	133.7	11.3
<b>Cement (%)</b>	27	20	23	7	43	9	42
<b>Porosity (%)</b>	18	39	27	36	5	31	11
<b>Bed Thickness (cm)</b>	16	24	4	14	5	17	2

**Table 1-1:** Data illustrating the relationship between fracture spacing and cementation compiled from seven beds within Unit 2 sandstones (stratigraphic section shown in Figure 1-7). Note that porosity is inversely related to cementation. Cementation and porosity measurements are from point counts; 300 points per thin section. Cement is typically calcite with minor amounts of siderite.





Color Key:

Blue Hinge-parallel fracture set

Green Hinge-perpendicular fracture set

Red Hinge-oblique fracture set

**Figure 1-8:** Bed thickness vs. fracture spacing from 53 locations and 4 lithologic units around Teapot Dome. Locations were selected on the criterion that there is at least one throughgoing fracture set. Fracture spacing was measured perpendicular to the throughgoing fracture set and averaged for each location. 594 total fracture spacing measurements were used. Fracture and bed thickness values are provided in Appendix D. This is the same data set used in Figure 1-5. Mean fracture spacing is the dependent variable in all three linear regression analyses.

It is important to consider that bed thickness may or may not be the effective

mechanical thickness. Gross (1993) defines a lithology-controlled mechanical layer as having boundaries where lithologic variation produces distinctly different mechanical properties, so that the layer will respond homogeneously to an applied force. Effective bed thickness is a term used within this paper to describe the total thickness of adjoining stratigraphic units that respond to a deformation process as a single mechanical unit. Therefore, at Teapot Dome, poor correlation coefficients could be attributed to differences between measured bed thickness and effective bed thickness (Figure 1-8).

When evaluating Figures 1-5 and 1-8 it is important to consider the possible mechanical stratigraphic controls on the various units. For example, marine sandsheets separated by shale (shale/sandstone/shale) may be mechanically different than a contiguous sequence of sandstone beds. Unit 1 sandstones are interbedded in shale. They are laterally continuous shallow-marine sandsheets that have a tabular or sheeted geometry. Unit 2 includes beach sandstones generally interbedded within other beach sandstones. These sandstones have a tabular geometry and are laterally continuous. Unit 4 is laterally continuous and is composed of poorly indurated carbonaceous shales and coal. Unit 5 fluvial sandstones have a lenticular geometry and are laterally discontinuous over a scale of 10's of meters. These fluvial sandstones are interbedded with carbonaceous shales.

Unit 5 fluvial sandstones have a fracture to bed thickness relationship closest to a 1:1 correlation line (Figure 1-5). Though the correlation coefficient is poor ( $r^2 = 0.4388$ ), Figure 1-8 does illustrate a broad positive linear relationship between fracture spacing and bed thickness within Unit 5 sandstones. Ladeira and Price (1981) and Huang and Angelier (1988) indicate that the linear correlation between fracture spacing and bed

thickness is no longer observed after beds become a few meters thick. If the three thickest beds are removed from the Unit 5 analysis, a correlation coefficient of 0.6546 is recorded and the equation of the line indicates predicted fracture spacing is approximately 1/3 bed thickness (Figure 1-9). The spacing between cleats within Unit 4 carbonaceous shales is inversely proportional to bed thickness (Figures 1-5 and 1-8). The correlation coefficient for the Unit 4 linear regression is still poor at 0.4806. Fracture spacing within Unit 2 is the most variable with respect to bed thickness of all the units ( $r^2 = 0.2421$ ; Figure 1-8). Unit 1 shallow marine sandstones at first glance show almost no correlation between fracture spacing and bed thickness (Figures 1-5 and 1-8). However, the data in Figure 1-8 are subdivided by orientation of the measured fracture set, and a review of these data shows that hinge-perpendicular fractures within Unit 1 sandstones are better correlated to bed thickness than other fractures ( $r^2 = 0.6719$ ; Figure 1-10). This may be due to Unit 1 sandstones being interbedded with an incompetent (shale) layer and thereby creating the condition wherein bed thickness is equivalent to effective bed thickness. Evaluation of fracture orientations within the remaining lithologic units suggests that better correlation coefficients could be obtained once broken into specific fracture sets. However, breaking the data down into smaller segments (i.e. into fracture sets) can increase the correlation coefficient simply because there are fewer data points relative to the initial data set. There are enough (8) Unit 1 hinge-perpendicular fractures in the sample to suggest that analysis is statistically significant.

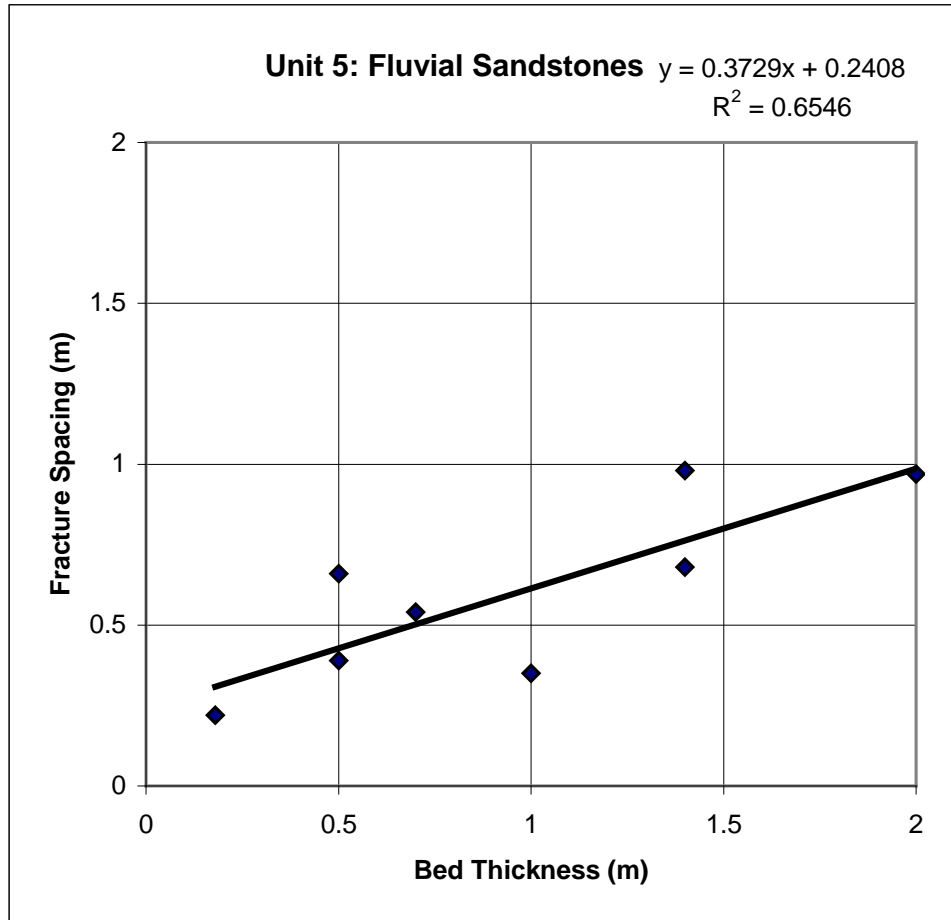


**Figure 1-9:** Fracture spacing vs. bed thickness correlation for Unit 5 fluvial sandstones. This is the same data set as provided in Figures 1-5 and 1-8 minus the three thickest beds.

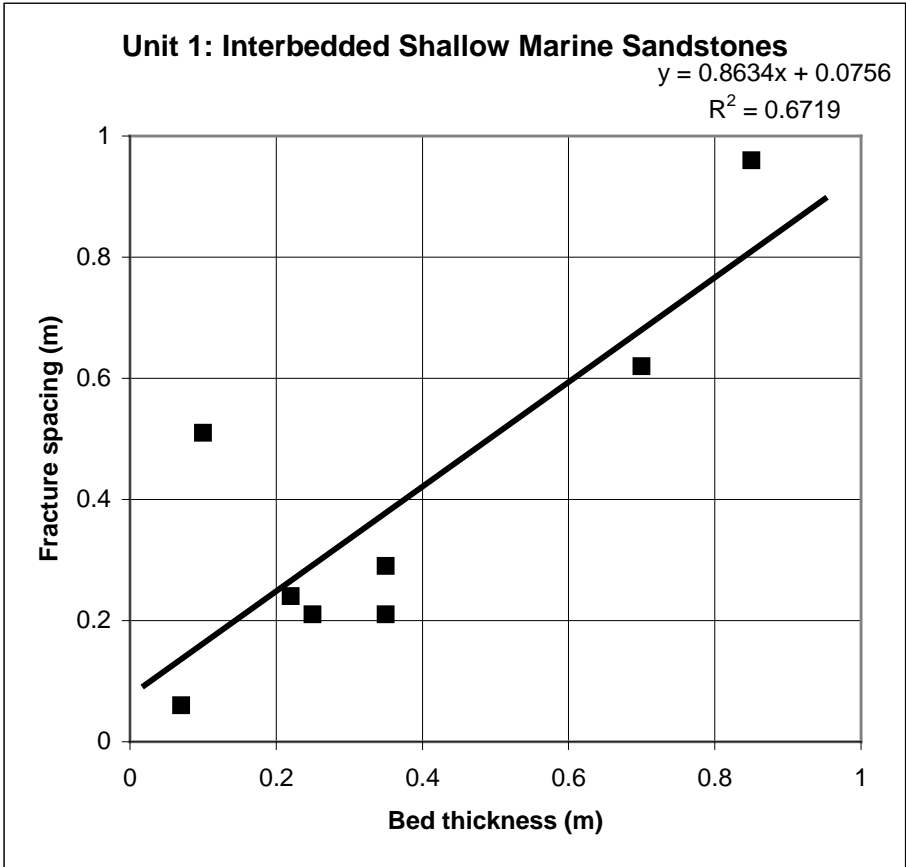


**Figure 1-10:** Spacing vs. bed thickness chart for the fracture set oriented perpendicular to the fold hinge within Unit 1 sandstones. This is the same data set as provided in Figures 1-5 and 1-8 for Unit 1 sandstones minus the other two primary fracture orientations (i.e. parallel and oblique to the fold hinge).

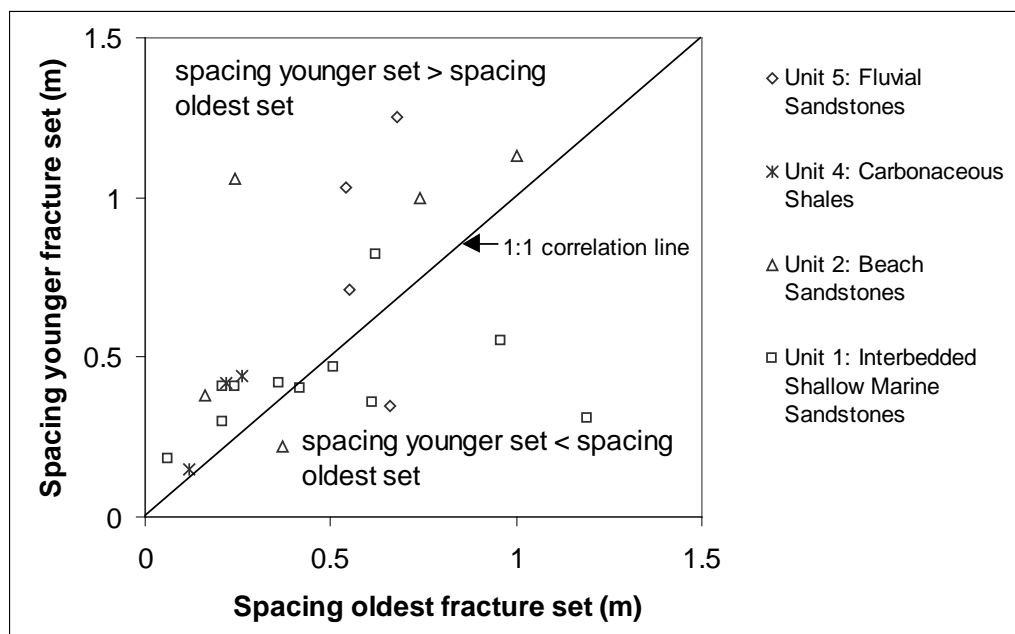
Preexisting fracture sets may affect the spacing of younger fracture sets. For this analysis, data from Appendix D were subdivided in to the oldest throughgoing set,

younger throughgoing sets and cross fractures. Cross fractures strike nearly perpendicular to throughgoing fractures and terminate at intersection with throughgoing fractures. Younger throughgoing fractures can strike oblique or perpendicular to older throughgoing fracture sets. Younger throughgoing fracture sets can extend through points of intersection with an older set. However, after some distance, the younger set will terminate at intersection with an older throughgoing fracture set. In general fracture spacing is greater in younger throughgoing fractures than in the oldest throughgoing fracture set (Figure 1-11a). Specifically, a sampling of 23 locations which have two throughgoing fracture sets indicates that at 16 locations the younger set is more widely spaced than the older set (Figure 1-11a). A comparison of cross fracture spacing to spacing of the oldest throughgoing set indicates cross fracture spacing is greater at 12 out of 16 locations (Figure 1-11b). A linear correlation between the spacing of these two fracture sets is evident for spacing less than 3m. If the outlying data point (4.96,4) is not used in the regression analysis, a correlation coefficient of 0.6225 is obtained.

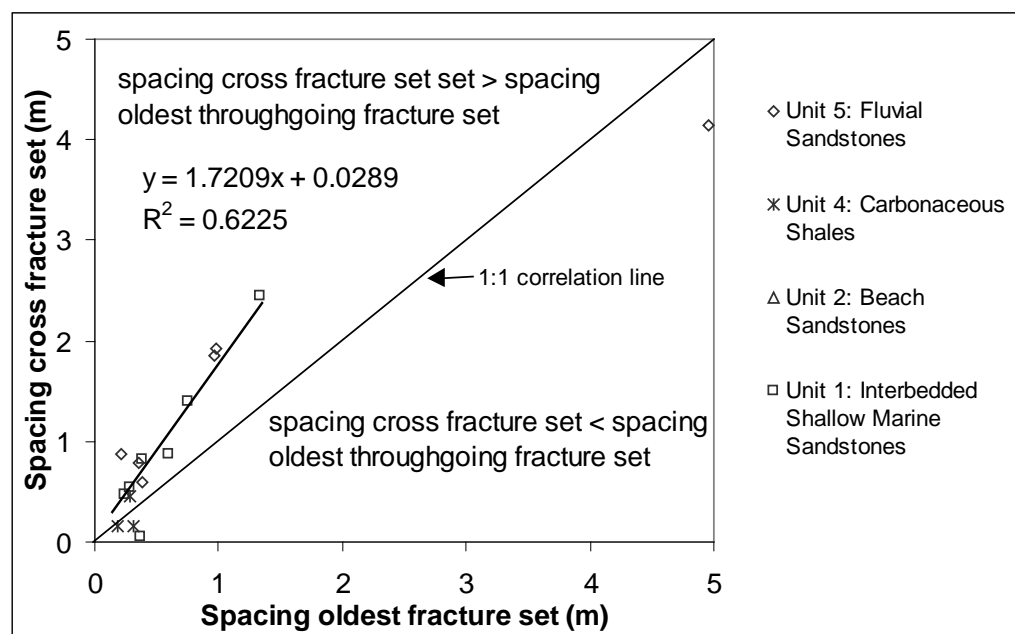
## Porosity

One-millimeter wide deformation bands are common in the high porosity, poorly cemented sandstones of the Unit 3 white beach facies (Unit 3: Figure 1-11). Point count data from four thin sections at two locations within Unit 3 indicate that the rock matrix has a average porosity of 38% at one site and 41% at the second site (Table 1-2).

Average cementation within the matrix is less than 1% at both sites.



A



B

**Figure 1-11:** (A) Fracture spacing of a younger throughgoing fracture set vs. fracture spacing of the oldest throughgoing fracture set. The younger set has generally more widely spaced fractures than the older set. (B) Spacing of cross fractures vs. spacing of the oldest throughgoing fracture set. Cross fractures are generally more widely spaced. Cross fractures were modeled as the dependent variable in the linear regression. One outlying data point at (4.96,4) was withheld from the regression analysis

**A: Unit 3 - matrix**

Sample number	1a	1b	2a	2b
Quartz (monocrystalline)	49	58	36	40
Quartz (polycrystalline)	1	trace	6	4
Chert and lithic fragments	7	5	15	12
Feldspar	1	0	2	1
Muscovite	0	1	trace	0
Undifferentiated clay size material	0	0	0	0
Cement (Fe)	0	0	1	2
Cement (calcite)	0	0	0	0
Cement (chert)	0	2	0	0
Macroporosity (intergranular)	35	28	34	36
Macroporosity (intragranular)	1	1	3	2
Microporosity (intragranular)	5	4	3	3
Microporosity (cement)	1	1	1	1
Number of point counts	300	300	300	300

**B: Unit 3 - deformation bands**

Sample number	1a	1b	2a	2b
Quartz (monocrystalline)	48	68	77	67
Quartz (polycrystalline)	4	1	2	2
Chert and lithic fragments	9	2	4	3
Feldspar	1	0	0	0
Muscovite	0	0	0	1
Undifferentiated clay size material	33	27	20	25
Cement (Fe)	0	0	0	0
Cement (calcite)	0	0	0	0
Cement (chert)	0	0	0	0
Macroporosity (intergranular)	3	2	5	1
Macroporosity (intragranular)	0	0	0	1
Microporosity (intragranular)	1	0	0	0
Microporosity (undifferentiated clay size material)	3	2	2	2
Number of point counts	200	155	108	200

**Table 1-2:** Normalized thin section point count data illustrating the differences in porosity, cementation and composition between matrix (A) and deformation bands (B) within Unit 3 sandstones.



A comparison of this information with the cementation and porosity data supplied in Table 1-1 for seven sandstone beds within Unit 2 indicates that cementation may be more important than porosity in determining whether a unit deforms through fracturing or formation of deformation bands. Porosities within the Unit 2 sandstones ranged from 5-39% while cementation ranged between 9 and 43%. Therefore, some of the porosity values are similar but the cementation values are at least an order of magnitude higher in the Unit 2 sandstones.

The point count data for Unit 3 sandstones described above can also be used for comparing the physical characteristics of the rock matrix to those of the deformation bands. These data suggest that the deformation bands are composed of crushed sand grains within roughly planar margins (Table 1-2; Figure 1-12). The rock matrix has an average porosity of 38% at site 1 and 41% at site 2. Point counts within deformation bands and within the same thin sections indicates average porosity is 5% within deformation bands at sites 1 and 2 (Table 1-2). This is almost a ten-fold reduction in porosity from the matrix. Average cementation within the matrix is 1% at site 1 and site 2. The deformation bands at both sites have no measurable cementation.

Undifferentiated clay-sized material is abundant within the deformation bands, but is absent from the matrix. Deformation bands at site 1 are composed of 30% clay-sized material on average while deformation bands at site 2 include an average of 23% of this material.

At five locations, deformation bands were recorded within other lithologic units (Charts 22, 32, 33, 46, and 57 in Appendix C). Two locations are within Unit 5 fluvial sandstones and three are within Unit 2 sandstones.

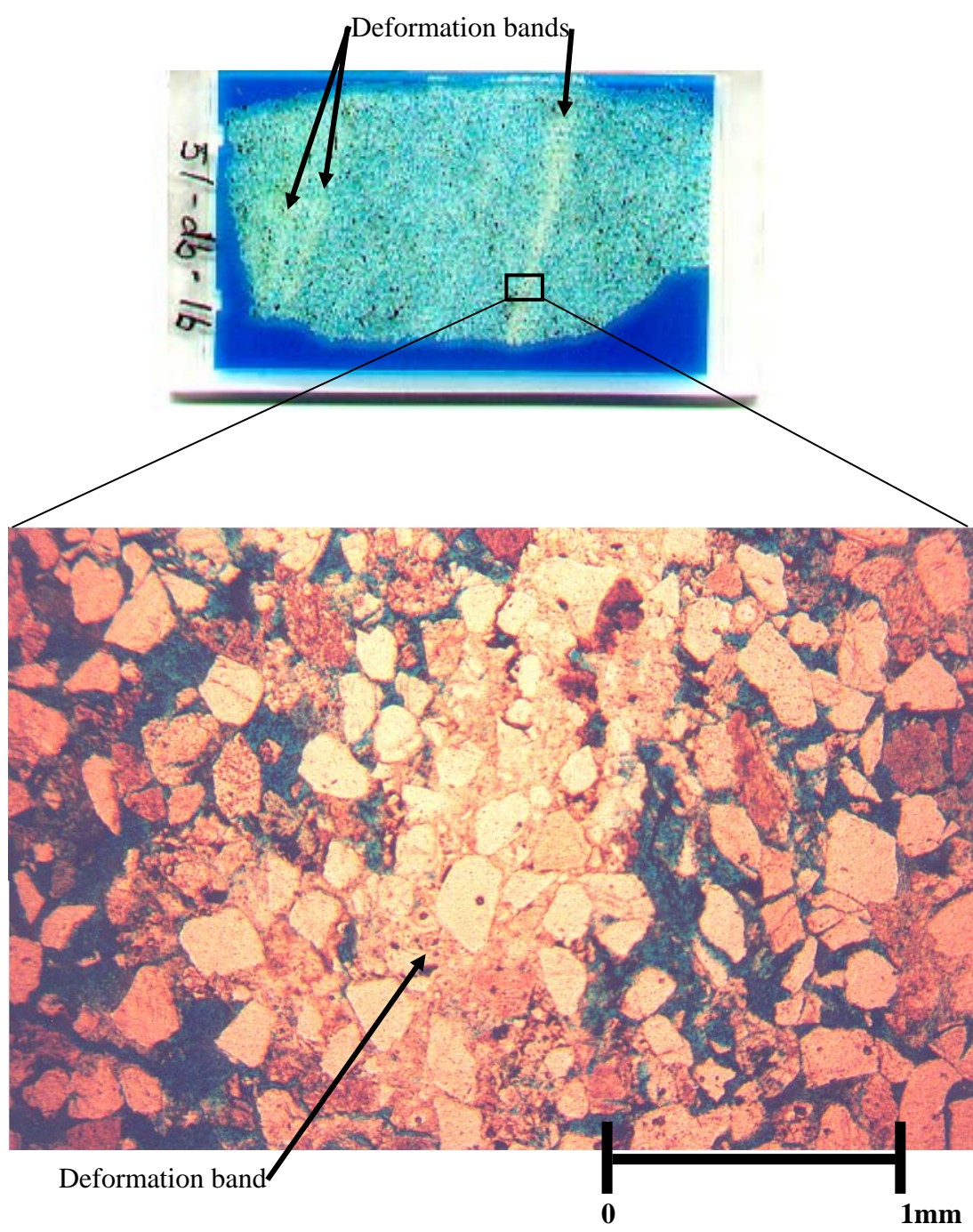


**Figure 1-12:** (A) Scanned image of a petrographic slide showing deformation bands within Unit 3 white beach sandstone. (B) Plain light photomicrograph of a deformation band within the petrographic slide shown in A. Sample was impregnated with blue epoxy to highlight porosity. Note the decreased porosity within the deformation band relative to the surrounding matrix.

Four of these units were observed in the field to be poorly cemented. The field criterion for a poorly cemented sandstone is that it be easily friable with a knife, which will also leave a deep scratch mark. Deformation bands and fractures were found together at four of these locations. At one of these locations, two beds of differing cementation within Unit 2 sandstones were recorded (Chart 57, Appendix C). The upper unit was better cemented and contained a majority of the fractures. These fractures typically terminated at the boundary with the underlying poorly cemented sandstone. At two of the sites, deformation bands were parallel to fractures. At a single Unit 2 site, the deformation bands were nearly perpendicular to the throughgoing fracture set and terminated at intersection with the fracture set (Chart 33, Appendix C). Therefore, at this site the deformation bands post-date fracture formation. Age of the deformation bands relative to fractures at the other sites is undetermined.

Field observations of differential iron staining, related to fluid/groundwater flow, indicate that iron may be reduced on one side of a deformation band, but oxidized on the other (Figure 1-13). It is evident from petrographic study that deformation bands have a lower porosity relative than the surrounding matrix (Figure 1-12; Table 1-2) due to grain breakage and pore collapse. These observations suggest that deformation bands are partial barriers to ground water flow.



**Figure 1-13:** Conjugate deformation bands with a vertical bisector to the acute angle. Note reduced iron above the deformation bands and oxidized iron below.

## Lithologic controls on faulting

Faults at Teapot Dome show variable characteristics associated with differences in porosity and cementation of the rock units cut by the fault. Fault character changes radically where a given fault cuts both poorly cemented sandstone and well cemented sandstone. These changes reflect the differences in deformation behavior documented in previous sections. Faults within well cemented sandstones typically have damage zones characterized by high fracture density (Figure 1-14). The fractures associated with these faults typically strike parallel to the faults and dip normal to bedding. Faults that transect the high porosity, poorly cemented sandstones of the white beach facies (Unit 3) are expressed as zones of subparallel deformation bands.

## Mineralization

Faults and associated fractures are variably cemented. Well cemented faults tend to stand out as erosion-resistant ridges or spurs; poorly cemented or uncemented faults, in contrast, weather into gullies. Cements observed at Teapot Dome are typically calcite, but pyrite is also locally present. Iron staining along fractures and up to 4 cm into the matrix parallel to fracture planes is observed locally. This indicates some fluid flow communication between the fracture and matrix. The degree of cementation of structures varies abruptly in space. In one area, a well cemented fault is located just 50 m from a highly weathered fault that is inferred to have little or no cement.

Thirty-eight sites around Teapot Dome were mineralized with either calcite or iron oxides. Iron oxide mineralization was evidenced by iron staining, both on the fracture surface and at some distance (1 - 4cm) into the matrix from the fracture.

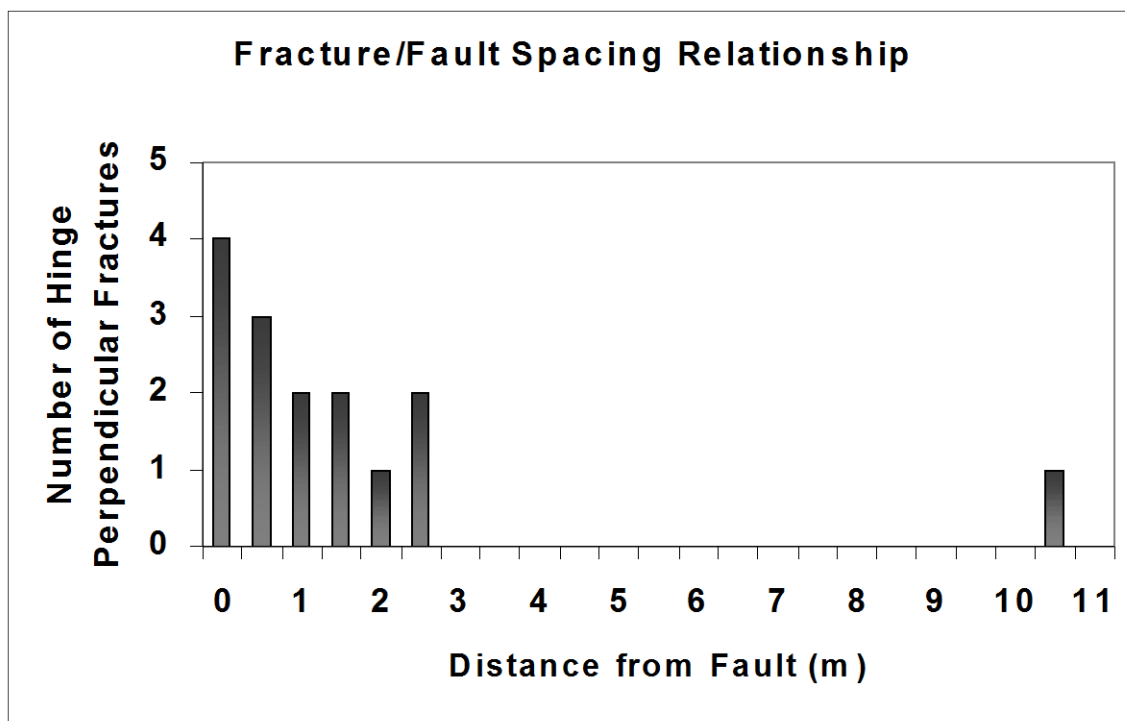


**Figure 1-14:** Histogram of an outcrop transect starting at, and perpendicular to, a fault on the northeastern limb of Teapot Dome. The histogram shows fractures in the damage zone of the fault increasing in number with proximity to the fault. The fault and fractures strike perpendicular to the fold hinge.

Sixteen of the sites were within Unit 1 sandstones, of which eleven were mineralized

with calcite, two were mineralized with calcite and small amounts of pyrite, two were iron stained, and one contained both iron staining and calcite mineralization. The calcite mineralized locations were generally associated with NE-SW oriented faults along the northeastern segment of the anticline. Eleven of the remaining mineralized sites were iron-oxide mineralized cleats within Unit 4 carbonaceous shales. Four sites within Unit 5 fluvial sandstones were mineralized, two with calcite, one with iron oxides and the other with gypsum. Two sites within Unit 3 sandstones were iron stained. Three sites within Unit 2 sandstones were mineralized, two with calcite and one with iron oxides. The two remaining sites were within the Steele Shale and were mineralized with calcite. The majority of mineralized fractures were partially occluded. Four of the five sites containing fractures generally sealed with calcite were within Unit 1 sandstones. The remaining site was within Unit 2 sandstones.

## **Discussion**

### ***Fracture spacing vs. bed thickness***

Exposures of the Mesaverde Formation at Teapot Dome provide an excellent opportunity to study fracture and fault variability related to lithology. One of the first assumptions relating lithology to fractures is that fracture spacing is directly proportional to bed thickness (Bogdanov, 1947; Price, 1966; McQuillan, 1973; Narr and Suppe, 1991; Gross, 1993; Ji and Saruwatari, 1998; Bai and Pollard, 2000). Data at Teapot Dome indicates that this relationship although broadly proportional under certain conditions is not 1:1. In fact, cleat spacing in Unit 4 carbonaceous shales and coals consistently remains below 0.5m no matter what the bed thickness. The data also show that there is

an inverse relationship between cleat spacing and bed thickness within this unit (Figure 8). Price (1966), as noted earlier, uses Young's modulus to explain the differences between fracture spacing in sandstones and cleat spacing in coals; it appears that mechanical controls dominate over bed thickness in these lithologies. The difference between cleat and fracture strike in carbonaceous shales and sandstones respectively, may also be due to differences in mechanical properties. A possible explanation regarding the inverse spacing relationship from a mechanical standpoint is that thinner coals may be less brittle than thicker coals, therefore cleats are more widely spaced in thin units relative to thicker units. However, it is equally possible that there is some difference between measured bed thickness and effective bed thickness, perhaps due to horizontal layering within the carbonaceous shale beds.

As previously discussed Bogdanov (1947) mathematically described a relationship where spacing (S) varied as a function of bed thickness (B) and some constant (K). The amount of variation from an idealized 1:1 fracture spacing to bed thickness ratio can provide some visualization as to how the constant (K) varies with lithology and mechanical controls. Fracture spacing in Unit 2 sandstones is poorly correlated with bed thickness (Figures 1-5 and 1-8). These sandstone beds are generally interbedded with other sandstone beds. In contrast Unit 1 and 5 sandstones, interbedded with marine shale and carbonaceous shale respectively, exhibit the strongest correlation between fracture spacing and bed thickness. Therefore, sandstones within these units have distinctly different boundary layers than Unit 2 sandstones and these bounding layers may contribute significantly to the fracture spacing to bed thickness ratio. Unit 5 is the nearest to 1:1 fracture spacing to bed thickness ratio (when combining all fracture



sets). The Unit 5 sandstones are laterally discontinuous while the other sandstone units are laterally continuous suggesting that there is some lateral mechanical influence on fracturing. The spacing relationships between oldest throughgoing fractures, younger throughgoing fractures and cross fractures also indicates some lateral mechanical influence on fracture spacing. Specifically the younger throughgoing and cross fracture sets have spacings larger than the oldest throughgoing fracture set, suggesting the older fractures are planes of discontinuity that influence fracture spacing in younger fracture sets.

No data was collected concerning the paleoflow direction within any of the units. Therefore, a word of caution is added that some of the variability observed in fracture spacing and fracture orientation may be due to mechanical anisotropy inherent to a bed with a grain fabric related to deposition. Depositional trends such as thickening and thinning of units may also influence local fracture spacing.

### ***Impact of structures on fluid flow***

Depending upon the lithology of the faulted rock unit, a single fault can be expressed as either a zone of deformation bands (partial barriers to flow) or a fault with a primary slip plane and an associated fracture zone (a possible fluid pathway). Unit 3 sandstones, which deform through formation of deformation bands, vary in thickness across the anticline, and are locally absent along the western limb. How this change in thickness influences regional fluid flow is undetermined. However, in both units with deformation-band faults and those with fracture-based faults, maximum permeability would be parallel to fault strike. In the former, fluid flow would be largely confined to the matrix. In the latter, fluid flow would occur preferentially along fractures as long as

they remained unmineralized. Therefore, in low permeability rocks, fractures will be the primary pathways for fluid flow. In contrast, in the high porosity sandstones that host deformation bands, the matrix will provide the main pathway for fluid flow.

Relatively well cemented, low porosity sandstones should not make a better reservoir than poorly cemented, high porosity sandstones. However, it is apparent from this study that fracturing will help increase production in more brittle sandstones while deformation bands may hinder production within high porosity sandstones.

As discussed previously, Thom and Spieker (1931) also recognized that mineralized faults and fractures may inhibit fluid flow and that open fractures could allow for increased fluid flow. However, they assumed that fractures would penetrate both sandstones and shales and that reservoir pressures would equalize. Because pressures within different reservoirs were not equal, the authors concluded that fractures did not significantly influence fluid flow. However, the current study shows that sandstones and shales do not fracture in similar ways. In fact, fractures within sandstone beds often terminate at sandstone/shale contacts. This relationship suggests that shales can create an effective seal between production zones and that pressures need not be similar in this fractured reservoir.

From a production standpoint, fracture permeability is also highly dependent upon the following variables: 1) trace length, 2) aperture width, 3) interconnectivity of the fracture system, and 4) the number of fractures intersecting the well bore. Core data can provide information on aperture width and number of fractures intersecting the well bore. Due to the small size of the core, information with regard to trace length and fracture interconnectivity can be limited. Outcrop fracture studies can help fill in

information for the last two items.

Fractures, in a sense, work like a plumbing system for the reservoir. The longer and more interconnected the drainage system the better the recovery. Fractures with extensive trace lengths have the potential of more effectively draining a reservoir than shorter fractures. The increased fracture surface area associated with increased trace length allows for increased fluid flow communication between the rock matrix and the fracture. Therefore, a well that intersects a fracture set with extensive trace lengths has the potential of draining a significantly larger area than a well that intersects no fractures or fractures with a limited trace length.

## **Conclusions**

Fractures, deformation bands and faults within the Cretaceous Mesaverde Formation at Teapot Dome display patterns that vary with lithology in the following ways: 1) Most fractures in sandstone units terminate at contacts with shale layers. 2) Carbonaceous shales (Unit 4) have cleat spacing densities comparable to or greater than those within sandstones, however, unlike fractures in sandstone, cleat spacing has a unique inverse correlation to bed thickness. 3) In beds of similar thickness and close proximity cleat strike is oblique to fracture strike by up to 20°. 4) Fracture density increases with increased cementation. 5) Sandstones interbedded with marine shales or carbonaceous shales have a fracture spacing to bed thickness ratio that is closer to 1:1 than sandstones interbedded with other sandstones. 6) Fluvial sandstones with lenticular geometries interbedded with carbonaceous shales have a fracture spacing to bed thickness relationship that is closer to 1:1 than that of other units. 7) The poorly cemented, high porosity sandstones of Unit 3 contain deformation bands rather than

fractures. 8) Deformation bands have significantly lower porosities relative to the matrix due to crushing of grains within the deformation band. 9) Normal faults within well cemented sandstones are generally expressed as fracture zones, whereas faults within poorly cemented sandstones are diffuse zones of subparallel deformation bands. 10) Thinner sandstones (< 1m) interbedded within shale may be more likely to be mineralized than thicker sandstone packages.

In the absence of significant subsurface data and because factors such as porosity, cementation and lithology can change with depth, a data set built from observations of outcropping strata that are lithologically analogous to subsurface reservoir rocks may allow a first-order approximation of what features (i.e. fractures, faults, and deformation bands) are present within the subsurface, their spacing and how they may influence permeability and fluid flow.

## **Deformation within a Basement-Cored Anticline, Part II:**

### **Structural Controls**

#### **Introduction**

Fractures can increase effective porosity and permeability and introduce permeability anisotropy, particularly in rocks with low matrix permeability (Rice, 1983; Nelson, 1985; Fassett, 1991; Teufel and Farrell, 1992). Faults can also function as fluid migration pathways, barriers, or a combination of both (e.g. Caine et al., 1996). For modeling and production purposes it is important to document directions of preferred fracture and fault orientations within primary hydrocarbon traps, such as anticlines. By understanding controls on fracture and fault orientation and distribution in a given reservoir the accuracy of flow modeling can be improved, thereby increasing primary and secondary hydrocarbon recovery. Lithologic controls on fracturing as well as some of the consequences of fracture permeability are reviewed in a companion paper (Part I: Lithologic Controls). This paper addresses variations in fracture and fault characteristics, such as spacing and orientation, with structural position on Teapot Dome, Wyoming.

Murray (1968) noted that the relationships between bed thickness, structural curvature and fracture porosity and permeability can be effective in evaluating geologic structures as hydrocarbon reservoirs. Rocks, in general, exhibit increased fracture density with increased deformation (Nelson, 1985). One method of predicting fracture density relative to structural position is the radius-of-curvature or rate-of-change approach (Murray, 1968). The major assumption of this approach is that the greatest density of flexure-related fracturing will occur where the rate of change of dip or

curvature of beds is at a maximum (Nelson, 1985), such as in a fold hinge. Further discussion of fracture initiation and propagation is provided in Appendix A.

Faults also exert structural controls on fracturing. Fault zones in rock generally consist of a fault core and a damage zone, which have permeabilities distinctly different from the protolith (e.g. Caine et al., 1996). The damage zone may include small subsidiary faults, fractures and veins. These structures can vary in character and density along the length of a fault due to variations in lithology and mineralization (see Part I). Displacement also varies along a single fault from a maximum at the center to a minimum at the fault tips (e.g., Nicol et al., 1996). Therefore, the density of secondary fault structures may be greatest near the center of the fault and decrease toward the fault tips, along both strike and dip. Secondary fault structures such as fractures within a damage zone can create areas of increased transmissivity. This can result in preferential fault-parallel fluid flow (e.g. Haneberg, 1995). Huntoon and Lundy (1979) describe a field example near Laramie, Wyoming which suggests increased transmissivity within rock units of the Casper aquifer system adjacent to fault zones and monoclines. The transmissivities of the fracture zones were found to be approximately 100 times greater than transmissivities of unfractured areas. In other situations, decreased porosity within a fault zone could produce a capillary seal given two liquids such as water and oil (e.g. Antonellini and Aydin, 1995; Sigda et al., 1999). Compartmentalization of a petroleum reservoir could occur should the capillary seal prevent cross-fault flow of the nonwetting phase (e.g. oil in a water-wet reservoir; Antonellini and Aydin, 1994).

The permeability of fractures can also be influenced by changes in pore fluid pressure. The effective normal stress can be increased by a decrease in pore fluid

pressure causing fractures at a high angle to the maximum principal stress to close (e.g., Raghaven, 1972; Lorenz et al., 1996; Long et al., 1997). Therefore, as fluids are removed during production of a fractured reservoir, in situ pore pressure may drop, decreasing the aperture widths of critically oriented fractures, which in turn decreases effective permeability and production. Substantial reduction in reservoir pressures at Teapot Dome, for example, is suspected from early production reports (Trexel, 1930; Curry, 1977; Doll et al., 1995).

A systematic study of natural fracture patterns within the outcropping Mesaverde Formation at Teapot Dome was undertaken, in part, to understand variations in fracture characteristics, such as spacing and orientation, with structural position on a doubly plunging anticline. Field observations indicate that extension fractures and normal oblique faults roughly perpendicular to the fold hinge are contemporaneous with hinge-parallel faults and fractures. A third set of fractures with a strike oblique to the fold are interpreted to predate folding.

These fracture and fault data and interpretations from Teapot Dome are used with previous studies to develop a 3-D conceptual model of fractures associated with basement-cored anticlines. A qualitative assessment of the 3-D model suggests that the direction of maximum permeability can be either parallel or perpendicular to the fold hinge depending on the primary fracture pattern within a specific area of the fold.

## **Fracture-Fold Relationships**

Several authors have described preferred fracture orientations associated with folding (DeSitter, 1956; Stearns and Friedman, 1972; Garrett and Lorenz, 1990; Cooper, 1992; Engelder et al., 1997; Hennings et al., 1998). Observations from these studies can

be subdivided into two main categories, those related to thin-skinned thrusts and those related to basement-cored thrusts.

### ***Folds associated with thin-skinned thrusts***

Stearns and Friedman (1972) described five fracture sets associated with folds, only two of which are stated as being sufficiently common to be incorporated into their generalized fracture model. These fracture patterns were documented at the Teton anticlines in northwestern Montana (Stearns, 1964; Stearns, 1967, Friedman and Stearns, 1971; Sinclair, 1980). The Teton anticlines are a pair of Laramide-age structures, and are part of a thrust sheet within the sedimentary section rather than a basement-cored anticline. The larger, western most anticline is hereafter referred to as Teton anticline. The two main fracture sets each consist of extension fractures and conjugate shear fractures (Figure 2-1). The sets locally occur together within the same beds. Both sets are interpreted to record an intermediate principal stress ( $\sigma_2$ ) normal to bedding and maximum ( $\sigma_1$ ) and minimum principal ( $\sigma_3$ ) stresses within the bedding plane. The orientations of maximum and minimum principal stresses were inferred to be different for each fracture set (Figure 2-1). The geometry of these patterns suggests that they accommodated shortening both parallel and perpendicular to the fold hinge. Stearns and Friedman (1972) suggested that these fracture sets resulted from folding because of their consistent orientations relative to bedding and the anticlinal structure.



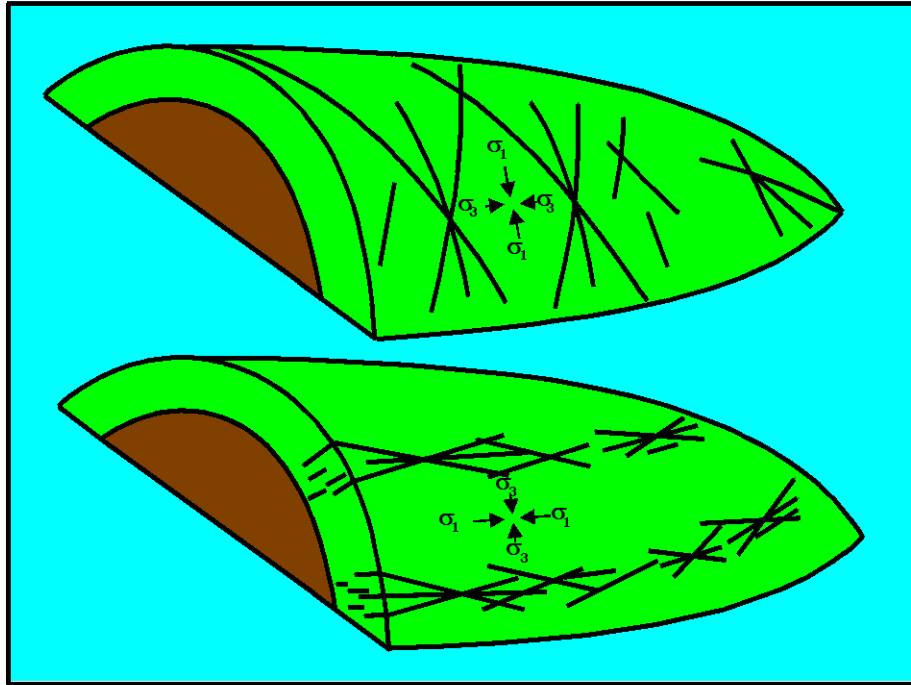


**Figure 2-1:** Stearns and Friedman (1972) model of fractures associated with folding. In both fracture sets the intermediate principal stress ( $\sigma_2$ ) is inferred to be normal to bedding and the maximum ( $\sigma_1$ ) and minimum ( $\sigma_3$ ) principal stresses therefore lie within the bedding plane. The inferred directions of maximum and minimum principle stresses are different for each fracture set.

A third set of fractures, described by Stearns (1964), accommodated extension due to bending of the formations across the anticline.

Cooper (1992) used core analysis along with Formation Microscanner and Array Sonic logs to analyze subsurface fractures associated with a fault-bend fold and a fault-

propagation fold in the foothills of the Canadian Rocky Mountains. Extension fractures parallel and perpendicular to the fold hinge were recorded as were conjugate shear fractures, all of which correspond to the two dominant fracture sets described by Stearns and Friedman (1972).

### ***Folds associated with deep-seated thrusts***

Dominant features associated with basement-cored thrusts include hinge-parallel and hinge-perpendicular faults and fractures. The following examples primarily describe these features and/or describe how they may be related to the folding process. DeSitter (1956) described normal faults parallel to a given hinge that were attributed to tension within the upper arc of an anticline and were observed at Kettleman Hills, California; Quitman Oilfield, Texas; Sand Draw Oilfield, Wyoming; and La Paz Oilfield, Venezuela. Normal faults roughly perpendicular to the axes of folds were attributed to tension resulting from the three-dimensional nature of an uplift (DeSitter, 1956). These faults exhibit maximum displacements near the apex of a given anticline. Further, the displacements on hinge-perpendicular faults decrease toward the limbs of the fold. Both DeSitter (1956) and Engelder et al. (1997) discussed these types of faults using examples from Elk Basin oilfield in Wyoming. Elk Basin anticline is a basement-cored, doubly plunging, breached anticline in the Big Horn Basin with dips on the forelimb in excess of 30° and up to 23° on the backlimb. The anticline strikes roughly NNW and is cut by a number of normal oblique, NE-striking, hinge-perpendicular faults. Fractures striking roughly parallel to the fold hinge are found throughout the fold, but vary more in orientation along the forelimb, perhaps due to local faulting (Engelder et al., 1997). Fractures striking roughly perpendicular to the fold hinge were found in 12% of

measured outcrops and are composed of two basic types: fractures with trace lengths extending several meters and fractures that are confined to the area between hinge-parallel fractures. Thus these later hinge-perpendicular fractures terminate at intersections with hinge-parallel fractures.

Similar joint sets oriented parallel and perpendicular to the hinge of the Grand Hogback Monocline in Colorado were observed Murray (1967). The development of these fractures was inferred to be related to local uplift and rotation of bedding rather than regional shortening. Penecontemporaneous development of the two joint sets was suggested by the lack of consistent abutting relationships to indicate which set is older. However, Garrett and Lorenz (1990) did recognize an older fracture set along the same Grand Hogback Monocline. They interpreted this set, composed of throughgoing regional fractures, to be associated with shortening prior to folding. Two other fracture sets - those recognized by Murray (1967) - were associated with folding along the Hogback.

Hennings et al. (1998) described three joint sets within Frontier Formation sandstones at Oil Mountain, approximately 30 miles west of Casper, Wyoming. Oil Mountain is a NW-striking, doubly plunging, breached anticline. A NW-striking fracture set parallels the fold hinge but is interpreted as a pre-existing regional set due to its presence in Frontier Formation pavements away from the fold. A NE-striking set is roughly perpendicular to the NW-striking set and is attributed to the folding process. The third set is NNW-NNE striking and is oblique to the fold hinge and the other two joint sets. A substantial increase in fracture density was observed within the southern plunging region of the anticline.

Because these anticlines and monoclines are cored by reverse faults it is worth considering strain around a blind thrust. Unruh and Twiss (1998) used coseismic displacements measured after the Northridge earthquake of 1994 (which resulted from movement along a blind thrust fault) to determine the orientations of the principal strain-rate axes for a blind thrust. Horizontal shortening ( $d_3$ ) is perpendicular to the fold hinge, maximum lengthening ( $d_1$ ) is horizontal and parallel to the fold hinge and  $d_2$  is vertical.

Using pseudo-three-dimensional modeling and curvature analysis, Fischer and Wilkerson (2000) described fracture patterns in sedimentary units, modeled as elastically deformed plates, during the evolution of a basement-involved thrust fault. They described joints oblique to the fold hinge as being related to the formation of a fold. These oblique fractures can form early in the folding process. Their work indicates the fracture initiation relative to fold development is a control on fracture orientation. They also noted that fracture orientations may vary with stratigraphic and structural position.

## **Geologic Setting**

Early debates concerning the deformational style of the Laramide orogeny generally centered around two main models: 1) forced folding related to near vertical uplifts (Prucha et al., 1965; Stearns, 1971; Stearns, 1975; Stearns, 1978) and 2) high-angle reverse faulting related to crustal shortening (Blackstone, 1940; Berg, 1962; Blackstone, 1980). Over time, evidence has accumulated for crustal shortening accommodated in the area of interest - Wyoming, Montana, and South Dakota - by thrusts, many of which are basement-cored (Willis and Brown, 1993). This evidence includes seismic reflection data (Gries, 1983; Gries and Dyer, 1985) and a deep crustal line across the Wind River Range by COCORP (Oldow et al., 1989). Teapot Dome is

typical of the structures formed by this deformation process.

Teapot Dome is located in central Wyoming, near the southwestern edge of the Powder River Basin. It is part of a larger structural complex, comprised of Salt Creek anticline to the north and the Sage Spring Creek and Cole Creek oil fields to the south (Figure 2-2; Doelger et al., 1993; Gay, 1999). Teapot Dome is similar to other Laramide structures such as Elk Basin anticline and Oil Mountain (Engelder et al., 1997; Hennings et al., 1998; described in the previous section). At Teapot Dome, a basement-involved thrust that terminates within the sedimentary section (Figure 2-3) is evident in 2-D seismic data (LeBeau, 1996). The dome itself is a doubly plunging anticline. Normal oblique faults that strike predominately perpendicular to the curvilinear fold hinge are common along the eastern limb (Olsen et al., 1993; Doll et al., 1995). Mesaverde Formation sandstones and shales are exposed along the western, eastern and southern limbs of Teapot Dome. Maximum dips along the western limb are near 30°; along the eastern limb dips range from 7° to 14°.

A major set of hinge-perpendicular faults and fractures has been recognized at Teapot Dome and described as the product of the forces that caused the folding (Thom and Speiker, 1931). These faults and fractures were described as characteristic features of Rocky Mountain anticlines.

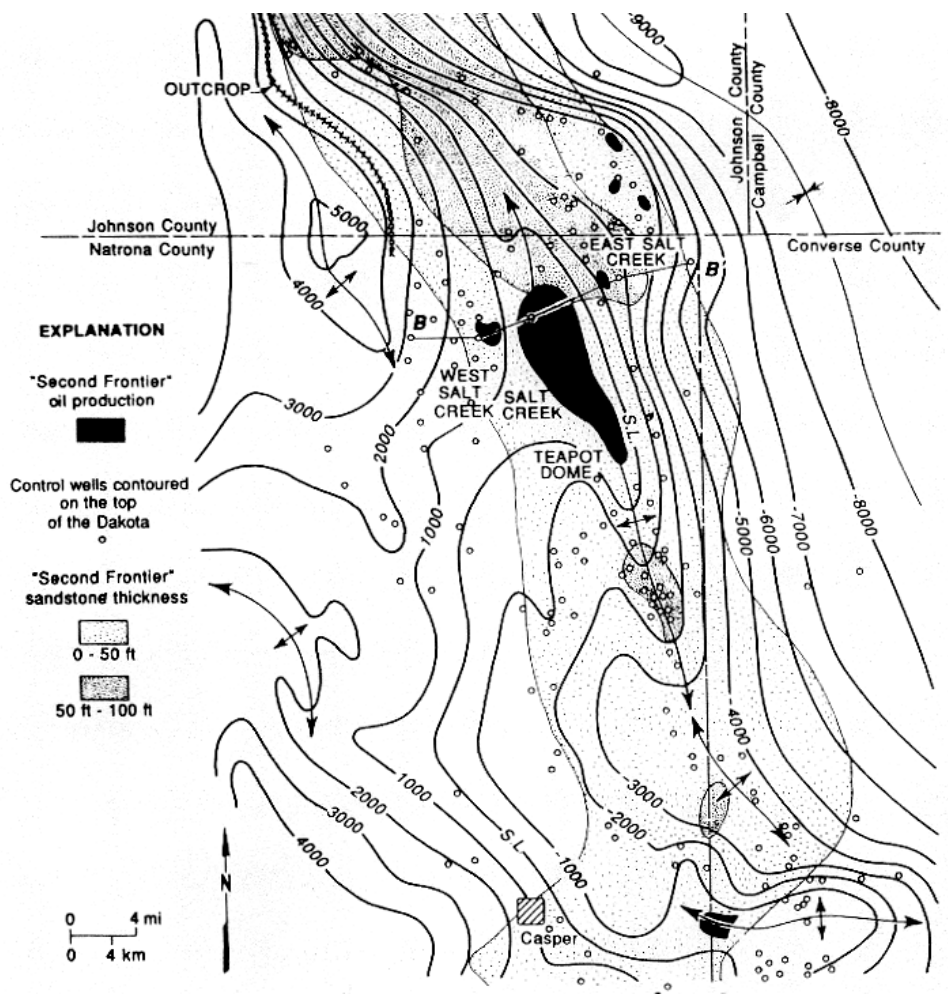


**Figure 2-2:** Structure contour map of the top of the Dakota Sandstone. The map illustrates the location of Teapot Dome relative to nearby Laramide structures (Doelger et al., 1993).

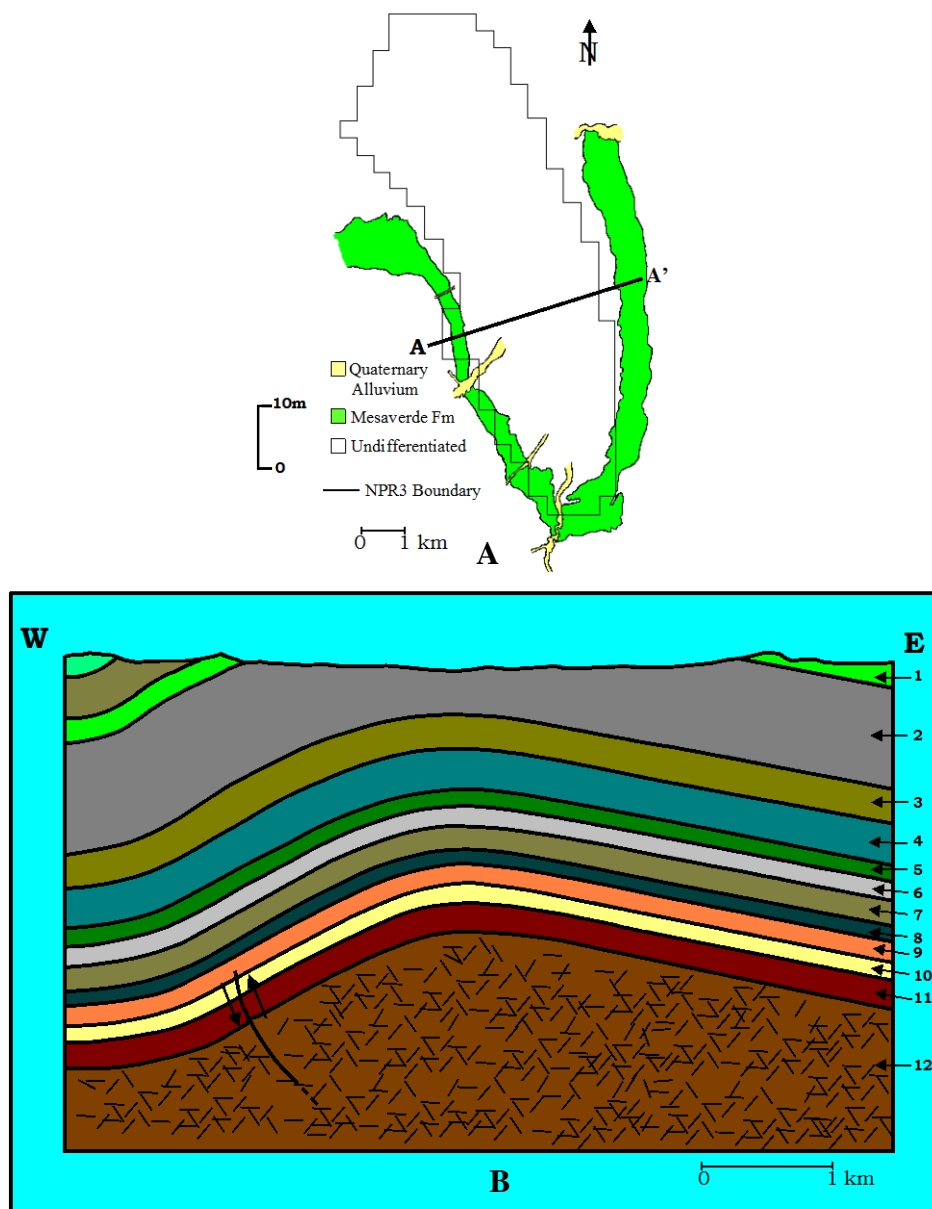


**Figure 2-3.** A. Map view of cross section transect. B. Diagrammatic cross section illustrating general structure and the basement-involved thrust that tips out within the sedimentary section. Cross section was constructed from surface data, well logs and 2-D seismic reflection data. No vertical exaggeration. Numbers correlate to the following stratigraphic units and systems as provided from Doll et al. (1995) and from well logs of exploratory well no. 1-G-10: 1. Cretaceous Mesaverde Formation (Fm). 2. Cretaceous Sussex Sandstone (Ss), Shannon Ss, Steele Shale (Sh), Niobrara Sh, Frontier Fm. 3. Cretaceous Mowry Sh, Muddy Ss, Thermopolis Sh, Dakota Ss, Lakota Ss. 4. Jurassic Morrison Fm, Sundance Fm. 5. Triassic Chugwater Group. 6. Permian; Goose Egg Fm. 7. Pennsylvanian Tensleep Ss. 8. Pennsylvanian Amsden Fm. 9. Mississippian Madison Limestone (Ls). 10. Devonian through Ordovician; Undifferentiated. 11. Cambrian; Deadwood Fm. 12. Precambrian; Granite.

Thom and Speiker (1931) also documented a secondary set of faults and joints

that strike roughly normal to the major set of faults and fractures and are, therefore, oriented approximately parallel to the axis of the anticline. This subsidiary fracture and fault set was attributed to extension across the fold. Doll et al. (1995) inferred three primary fracture directions in the subsurface from steam flood response data. These orientations were perpendicular to the fold hinge, N65°W, and parallel to the hinge. Using indirect surface geochemical techniques such as surface hydrocarbons, Eh, pH, soil electrical conductivity, iodine, and bacteria, Fausnaugh and LeBeau (1997) observed trends in the data suggesting NE-striking faults. Geochemical signatures perpendicular to the NE-striking faults were also observed and attributed to either faulting or to overlapping stratigraphic relationships of subsurface reservoirs.

## **Structural Analysis of Teapot Dome**

Fractures, faults, and deformation bands were studied in five lithologically distinct stratigraphic units within the Mesaverde Formation at Teapot Dome. These units are (from oldest to youngest): a shallow marine interbedded sandstone/shale, a foreshore/beach sandstone, a white beach sandstone, a non-marine carbonaceous shale, and a unit composed of fluvial sandstones within the carbonaceous shale unit. Detailed discussion of these units and of lithologic controls on fracturing is provided in Part I.

### ***Distribution of faults and fractures with respect to the fold***

#### **Faults**

Two dominant sets of faults are observed in outcrops of the Mesaverde Formation at Teapot Dome. The first set consists of NE-striking normal oblique faults shown on Figure 2-4. These faults are common along the eastern limb and most terminate before



intersecting the western limb; displacements therefore decrease to the SW. A normal component of displacement is recorded by stratigraphic separation whereas the strike-slip component is inferred from slickenlines on three fault surfaces with rakes of  $20^{\circ}$ – $35^{\circ}$ . Sense slip for these three faults is oblique right lateral. These faults are generally perpendicular to the fold hinge, even where it bends, and are characterized by vertical separations that vary across the fold. The largest separations, up to 40 m, are observed on the eastern limb. The few hinge-perpendicular faults observed on the western limb exhibit vertical separations that range between 0.5 and 1 m. Although continuous exposure is not available around the dome, these hinge-perpendicular faults appear to be densest near the culmination of the fold (Figure 2-4).

The second set consists of normal faults that strike subparallel to the fold hinge and are observed primarily along the southern arc of the anticline where curvature is at a maximum (Figure 2-4). Normal motion on these faults is recorded by stratigraphic separation.

Two faults observed near the apex of the anticline in 2-D seismic reflection profiles (from the Rocky Mountain Oilfield Testing Center) can be projected into valleys with no surface exposure along the western limb. Individual segments of the western limb, separated by these valleys, display different bedding and fracture orientations (Figure 2-5); in each segment the strike of one primary fracture set roughly parallels bedding. These valleys are therefore interpreted as faults. Valley trends indicate that the faults belong to the NE-striking fault set.

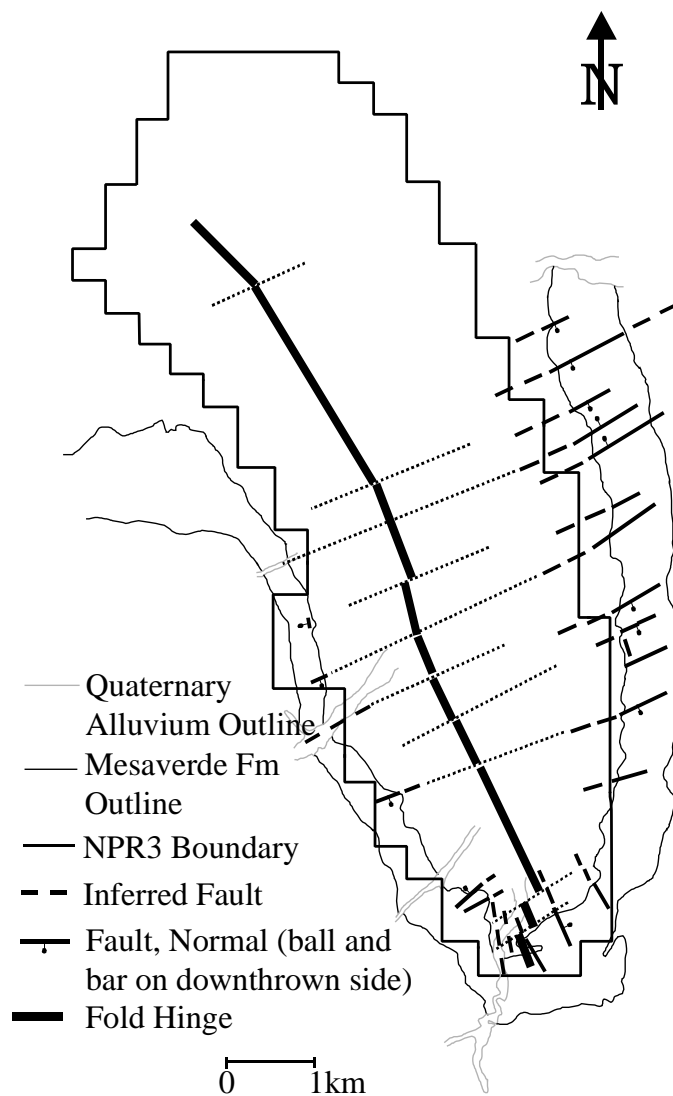


**Figure 2-4:** Primary faults observed at Teapot Dome, Wyoming. Because of poor exposure in the core of the dome, individual faults generally cannot be traced from the eastern to the western limb. Faults and fold hinge shown in the central portion of the anticline are inferred from a structure contour map on the top of the second Wall Creek Sandstone (Lawrence Allison, 1989) and field data.

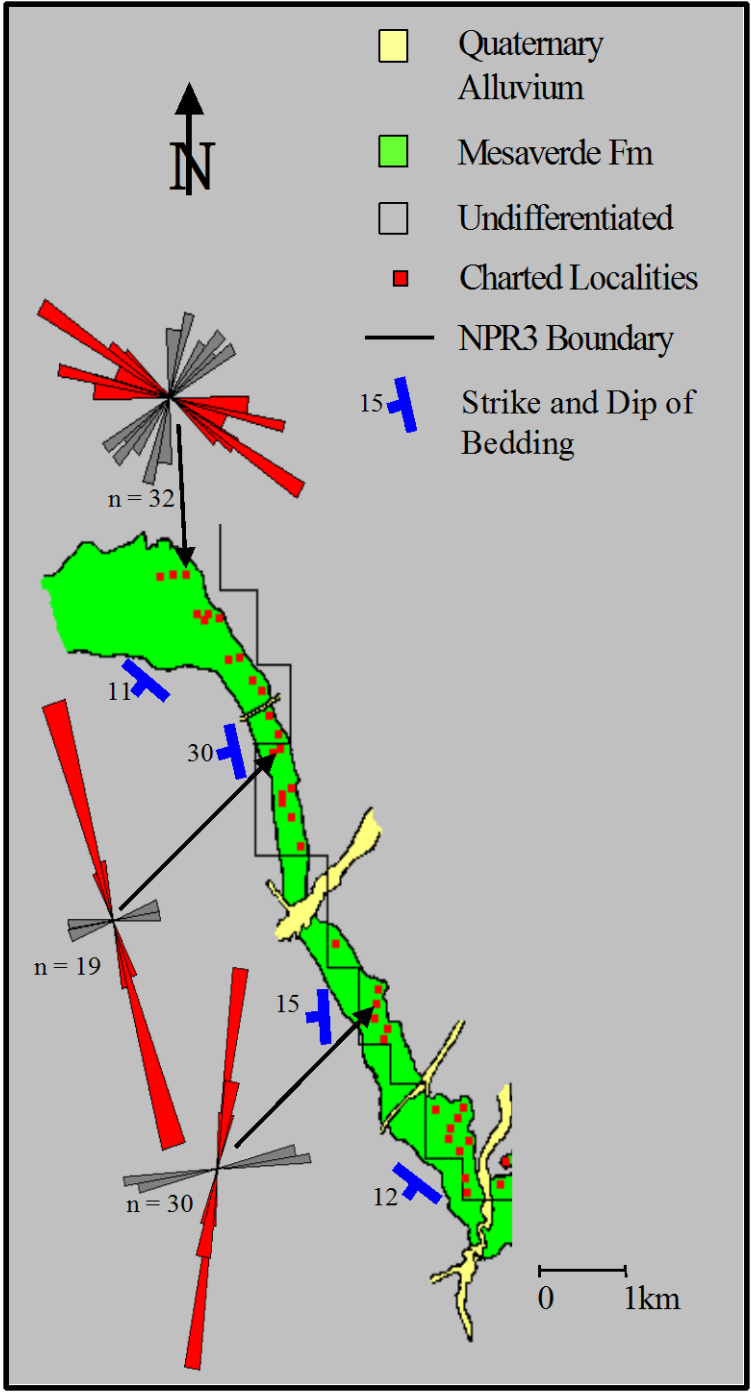


**Figure 2-5:** Map illustrating segmentation of the western limb. Fracture orientations of individual segments generally parallel bedding strike. Red sections of the rose diagrams illustrate the orientation of the throughgoing fracture sets.

Deformation bands (small-displacement faults characterized by pore collapse and cataclasis; Aydin, 1978) are observed primarily within poorly-cemented sandstones. Lithologic controls on deformation band formation are discussed in Part I. They commonly occur as conjugate pairs near the southern and southwestern margins of the anticline and as non-conjugate faults in other areas. The conjugate pairs are oriented such that there is a vertical bisector to the acute angle between a given pair. These small-displacement faults strike parallel to each of the three primary fracture orientations recorded at Teapot Dome. Normal separation associated with deformation bands ranges from indiscernible to approximately 20cm. The larger separations are associated with multiple (up to 20) inosculating deformation bands (inosculating deformation bands approach and diverge from each other but do not cross). Where displacement can be constrained, individual bands generally have 1-3 cm of normal separation. At four sites, deformation bands occurred within the same bed as fractures. At a single site, deformation bands were nearly perpendicular to the throughgoing extension fracture set and terminated where they intersected the fracture set (Chart 33, Appendix C). Therefore, at this site the deformation bands post date fracture formation. The age of the deformation bands relative to fracture formation at the other sites is undetermined.

## Fractures

Three throughgoing fracture sets were documented at Teapot Dome (Figure 2-6). One fracture set includes fractures oblique to the fold hinge. Most of these strike roughly NW to WNW; a small number are roughly perpendicular to these, and thus strike NNE. A second set is subparallel to the fold hinge.

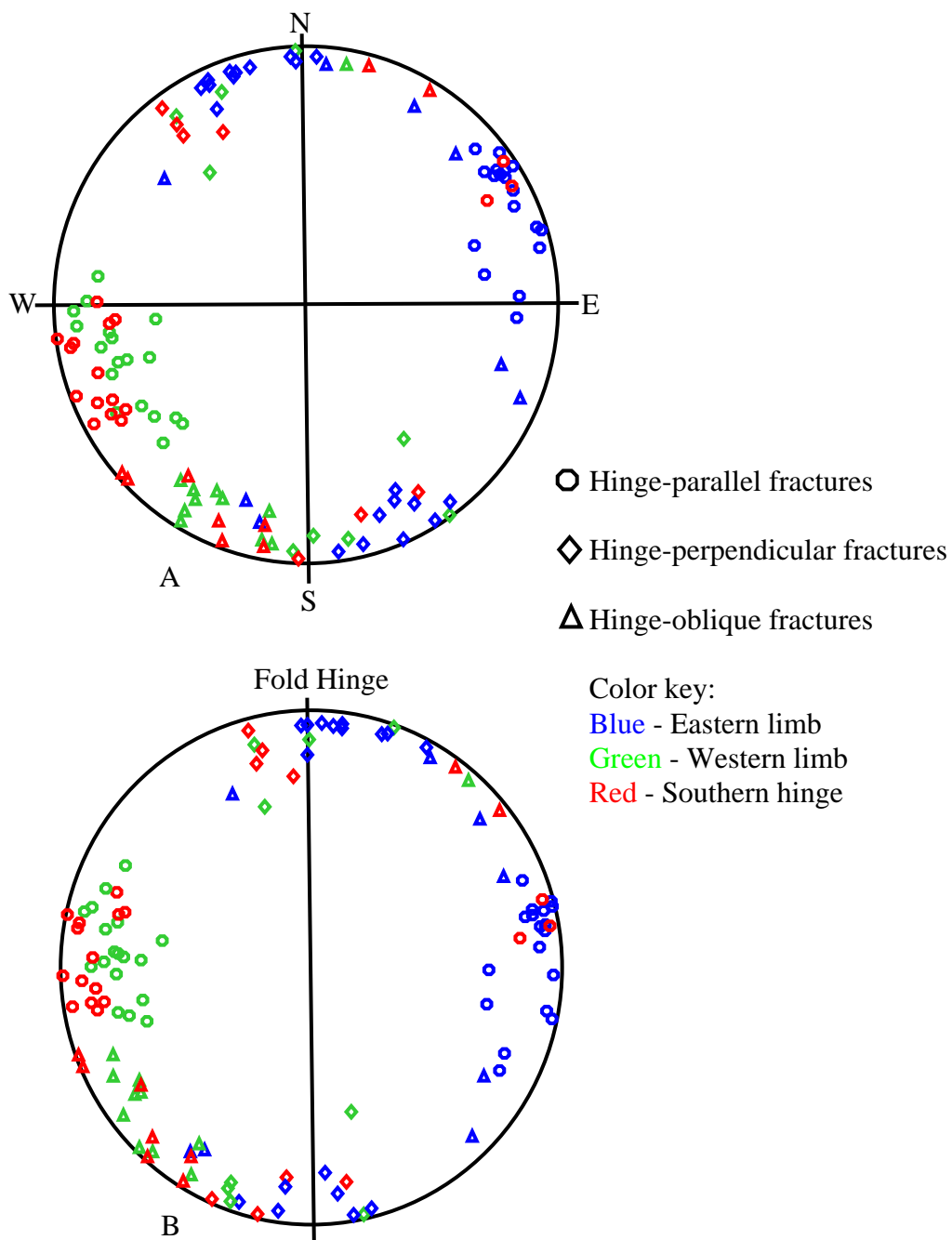


**Figure 2-6:** (A) Lower hemisphere equal area net plot of poles to 129 representative throughgoing fractures from 87 locations around Teapot Dome (Appendix F). (B) The same data set used in A, normalized to the fold hinge (data rotated so that fold hinge has orientation shown). Fractures are considered hinge-parallel if they strike  $\pm 20^\circ$  from the hinge; hinge-perpendicular fractures strike  $90^\circ \pm 20^\circ$  from the hinge.

The third fracture set is roughly perpendicular to the fold hinge. Forty-four percent of the documented fractures are parallel to the fold hinge, 32% are perpendicular to the fold hinge and 24% are oblique to the fold hinge.

The set of fractures which strikes oblique to the fold hinge is found at 28 sites throughout the fold and is equally distributed among the various lithologic units of the Mesaverde Formation (Figure 2-7; Appendix E). Three additional sites record deformation bands with the same general strike as the fracture set. At almost all sites this is the oldest set of fractures or deformation bands relative to the other throughgoing fracture sets as determined by abutting relationships. At only one site is the oblique set younger than one of the other two fracture sets. At another site, the oblique fracture set is the only fracture set recorded. There are two oblique fracture sets with an approximate  $10^\circ$  difference in strike at two locations. One of the sets at these locations is younger than the other. However, relative age between oblique fractures and hinge parallel and/or hinge-perpendicular fractures could not be determined, because the later two fracture sets are not present at either of these two sites.

Data collected at a distance from Teapot Dome shows that the oblique set (Figure 2-8; Appendix F), that strikes predominately NW to WNW, can be found at surrounding locations. Fracture orientation data from Oil Mountain are from Hennings et al. (1997). Three sites at Teapot Dome have hinge-oblique fractures that strike NNE. Fractures striking N to NNE were also observed at three sites at a distance from Teapot Dome, including Oil Mountain.

The two dominant, younger, throughgoing fracture sets parallel the two fault sets described previously. Most of these are bed-normal extension fractures.

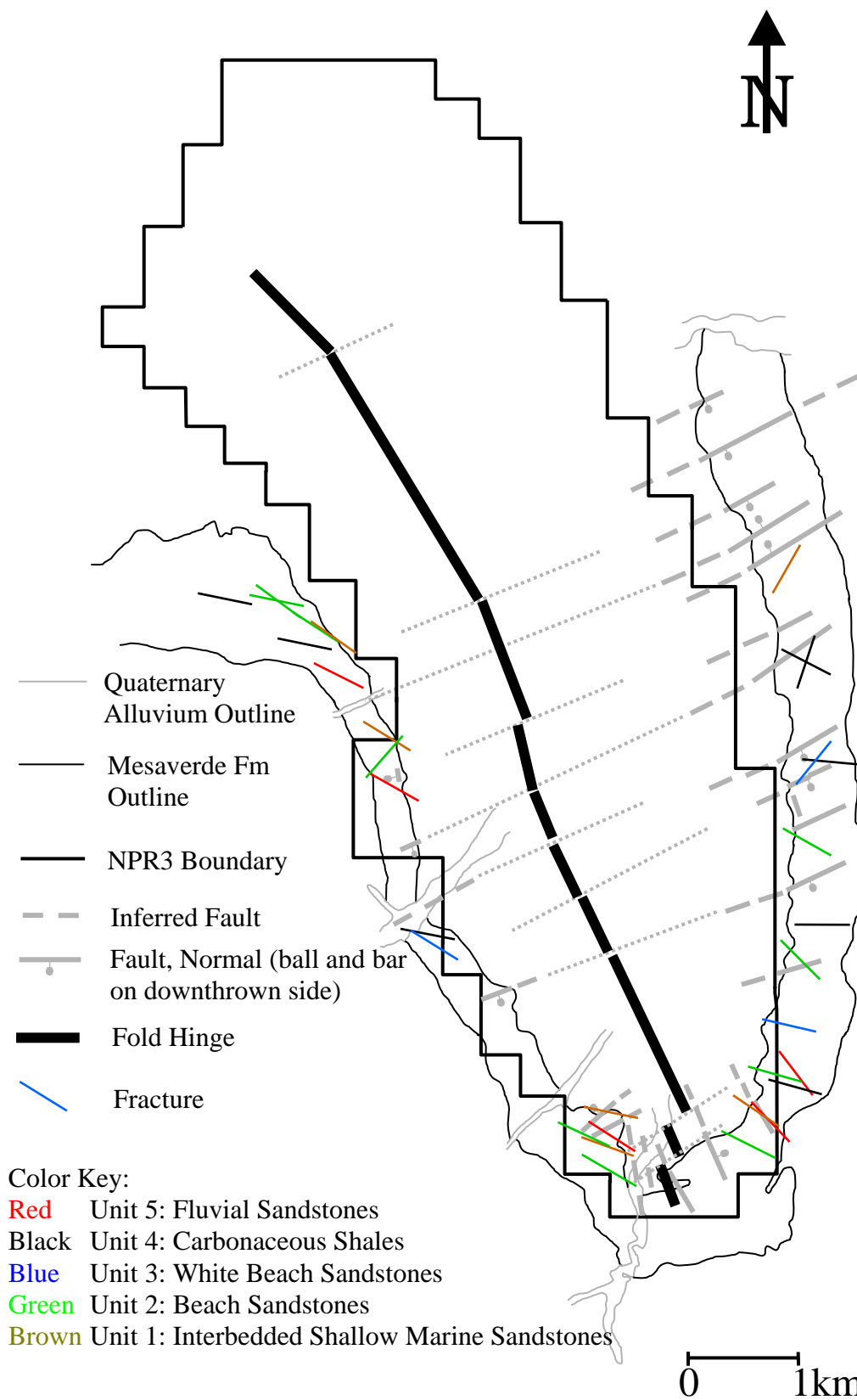


**Figure 2-7:** Map of representative fractures striking oblique to the fold hinge at Teapot Dome. Based on data in Appendix C.

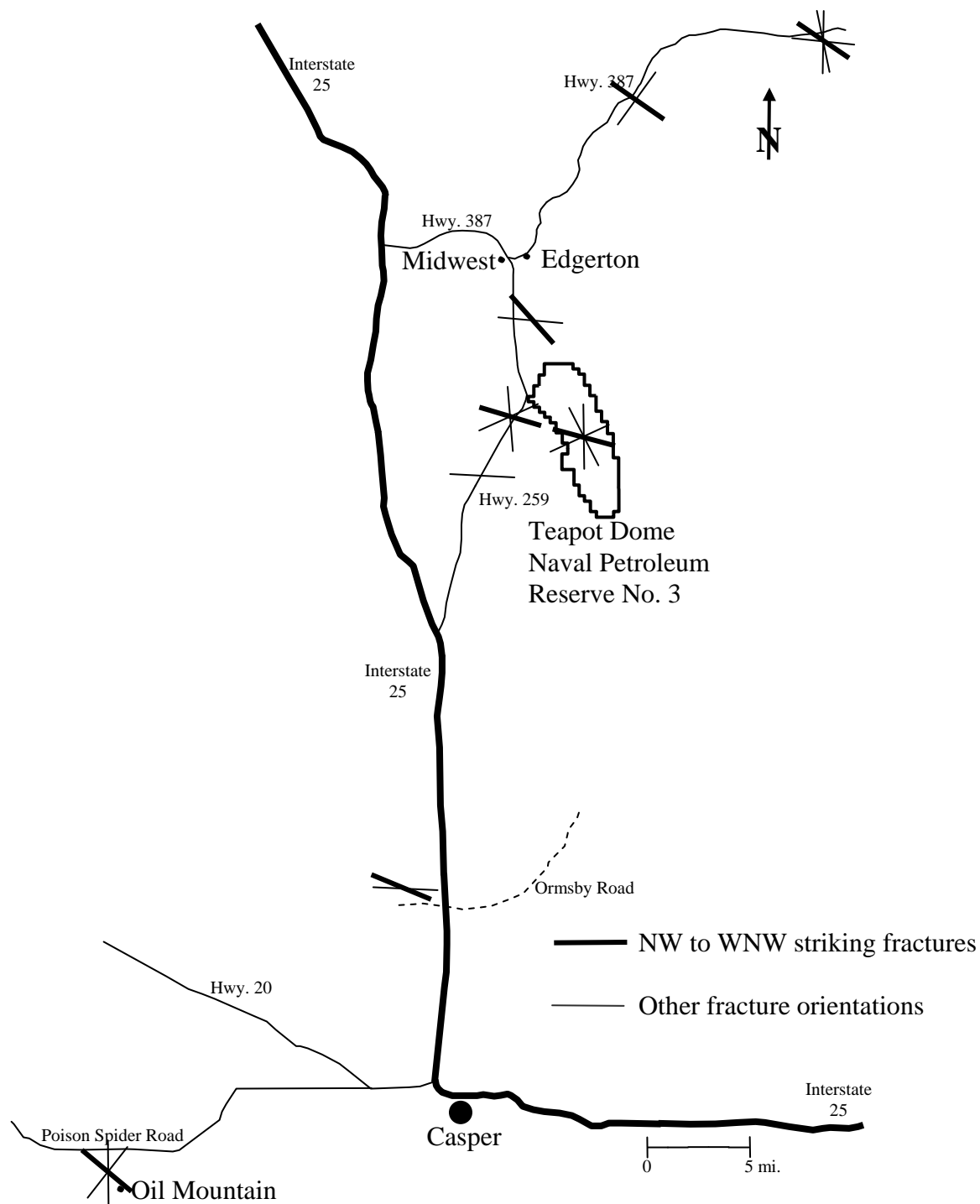


**Figure 2-8:** Representative fracture data from locations near and at a distance from Teapot Dome. Oil Mountain data are from Hennings et al. (1998).

The hinge-perpendicular fracture set was recorded at 35 sites around the anticline. Six



additional sites exhibit hinge-perpendicular deformation bands, but no fractures.

Fractures and deformation bands of this orientation are best developed along the eastern limb where normal faults are common (compare Figures 2-4 and 2-9). The hinge-parallel fracture set is found at 51 sites throughout the fold (Figure 2-10). Six additional sites exhibit deformation bands without fractures of similar orientation. Locally, bed normal extension fractures are replaced by conjugate shear fractures of the same strike.

Outcrops of the fold hinge are generally absent due to erosion of the fold core. A portion of the hinge remains near the southern exposure of the dome, where it records an increase in fracture density relative to the eastern and western limbs. Spacing between hinge-parallel fractures that are not associated with faults evidence this increase. Eight sites along the southern hinge of the anticline record a mean fracture spacing of 34.7cm (n=71). Ten sites along the central limbs of the anticline, in contrast, record a mean fracture spacing of 57.3cm (n=78).

Where pavement surfaces were large enough, both hinge-parallel and hinge-perpendicular fractures were observed to extend for lengths of up to 100m. Locally, these two dominant fracture sets typically meet at T-intersections. At certain outcrops around the anticline, hinge-parallel fractures terminate at hinge-perpendicular fractures. In other locations, hinge-perpendicular fractures terminate at intersections with hinge-parallel fractures (Figure 2-11). The fracture set that does not terminate at T-intersections (or junctions) is interpreted to be the oldest fracture set. These relationships indicate that the two fracture sets were contemporaneous.

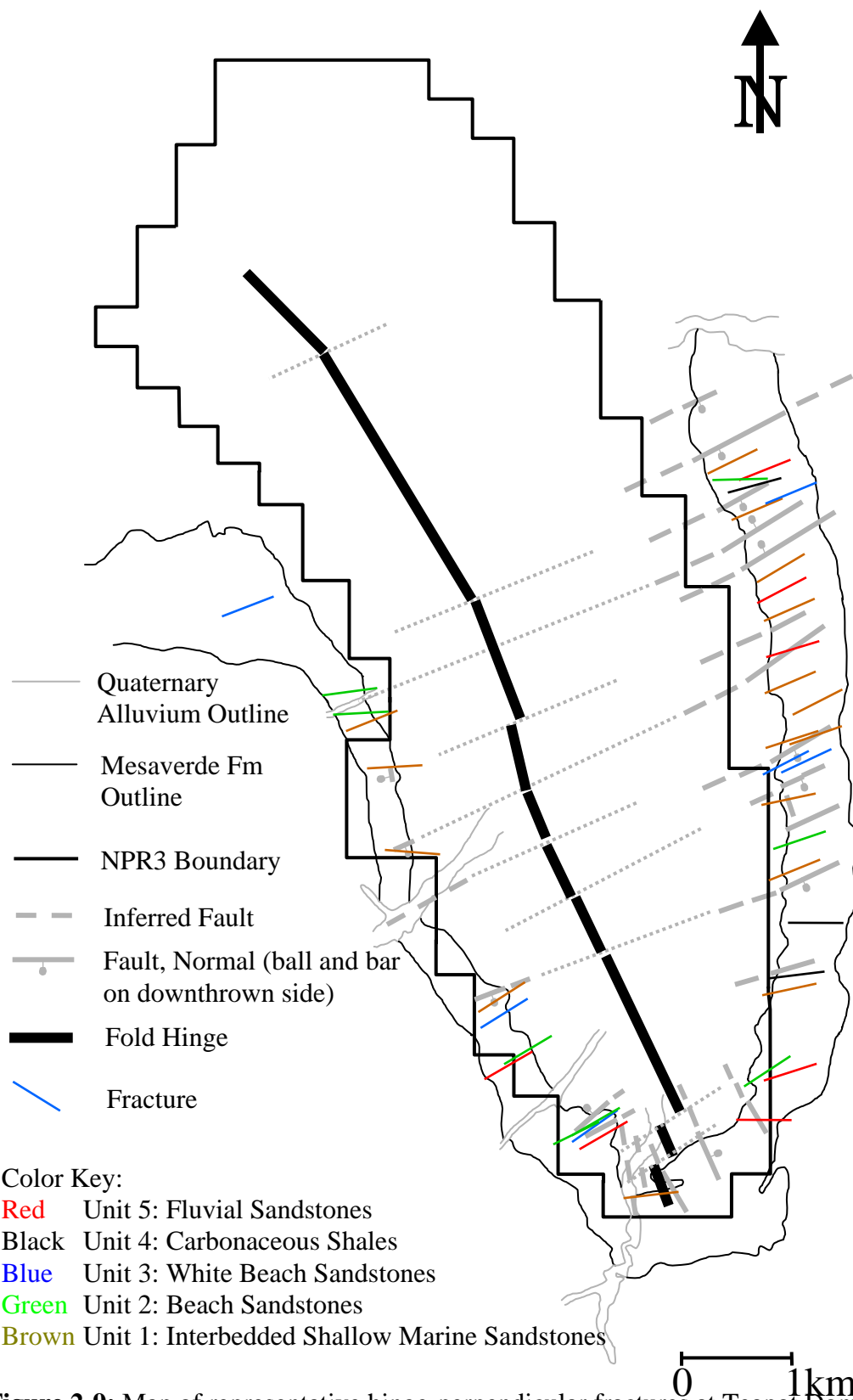


**Figure 2-9:** Map of representative hinge-perpendicular fractures at Teapot Dome. Based on data in Appendix C.

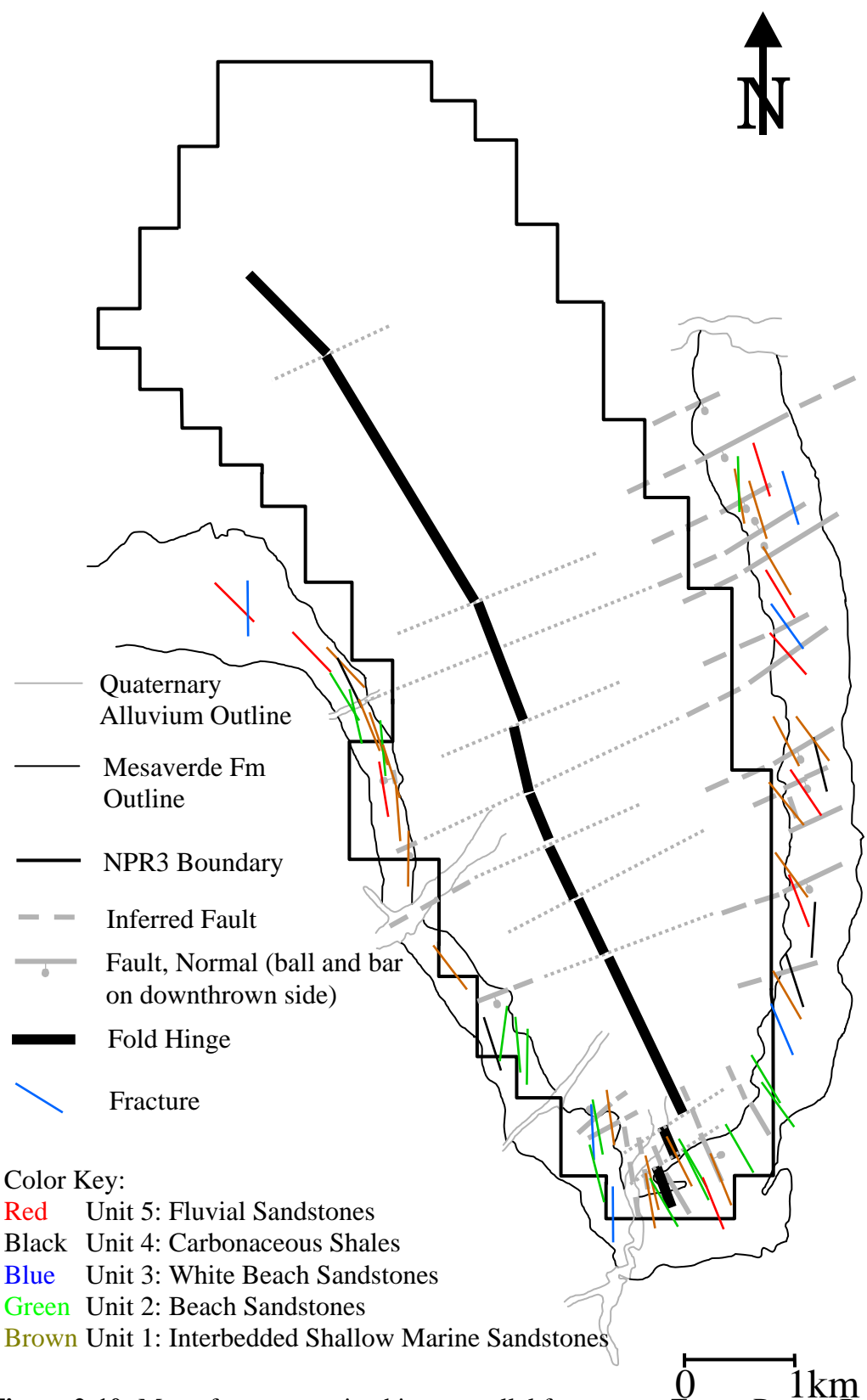
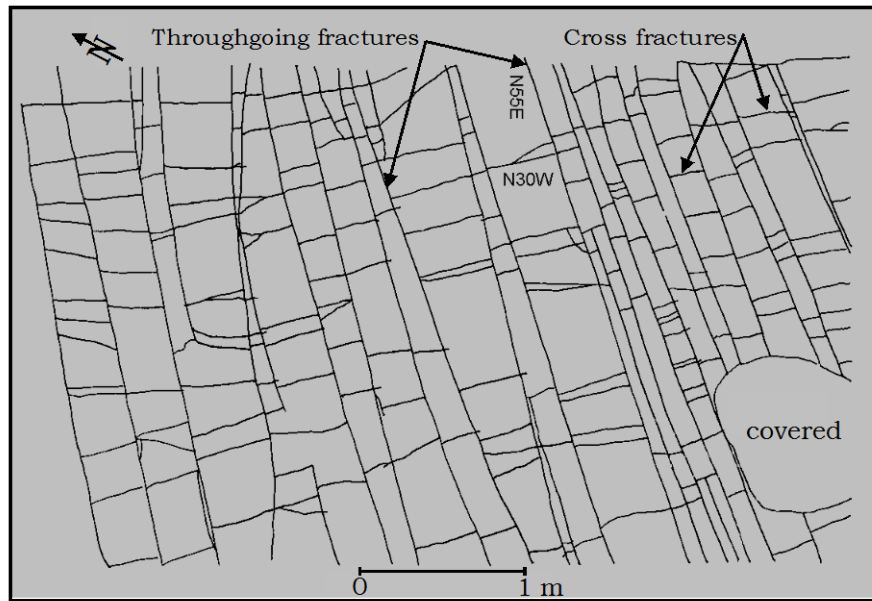


**Figure 2-10:** Map of representative hinge-parallel fractures at Teapot Dome. Based on data in Appendix C.



A



B

**Figure 2-11:** A) Plan view fracture map illustrating throughgoing fractures and cross fractures on a pavement surface. B) Photograph of a pavement surface illustrating bed-normal extension fractures parallel and perpendicular to the hinge of the Teapot Dome anticline (tape aligned perpendicular to the hinge of the anticline). Note termination of the hinge-perpendicular fracture set against the hinge-parallel set in this outcrop.

### ***Spatial relationship between faults and fractures***

As mentioned above, the two dominant fracture sets at Teapot Dome are generally parallel to faults. That is, one set of bed-normal extension fractures is subparallel to hinge-parallel faults, and the second set of bed-normal extension fractures is subparallel to NE-striking faults (and thus perpendicular to the fold hinge). There is also a close spatial relationship between hinge-perpendicular faults and fractures. The density of these fractures increases near the faults (Figure 2-12). At the location illustrated in Figure 2-12, hinge-perpendicular fractures are only present within a narrow zone adjacent to hinge-perpendicular faults. Hinge-parallel fractures are limited to the area outside this narrow zone, suggesting that the fault-related fractures formed first in this location.

### **Discussion**

Structures observed within the Cretaceous Mesaverde Formation at Teapot Dome include extension fractures, normal conjugate shear fractures, deformation bands, hinge-parallel normal faults and hinge-perpendicular normal oblique faults. The dominant fracture sets strike roughly parallel to the fault sets. The majority of the fractures are bed-normal extension fractures. These observations agree, in general, with those made by Thom and Speiker (1931). The single exception is in regard to fractures oblique to the fold hinge which they did not recognize. Fischer and Wilkerson (2000) suggested that hinge-oblique fractures could be formed in a fold associated with basement-involved thrusting. Because these hinge-oblique fractures may form early in the folding process they may predate both hinge-parallel and hinge-perpendicular fracture sets and still be related to the folding process.

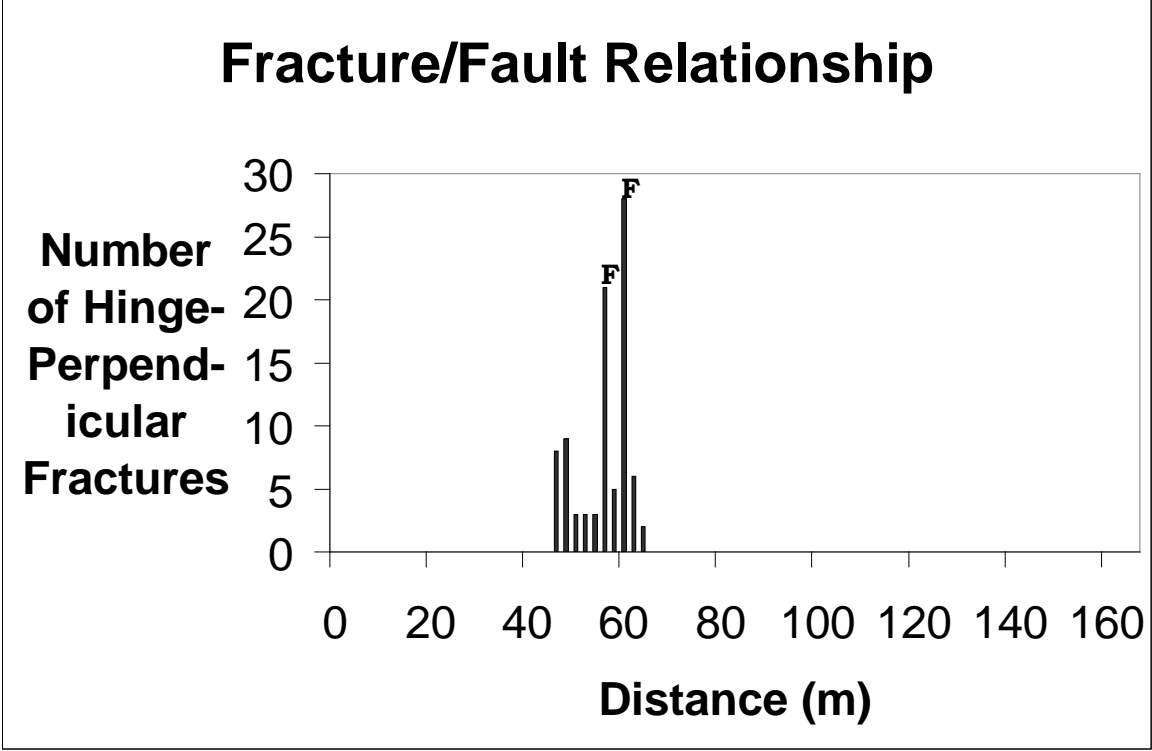


**Figure 2-12:** Histogram of an outcrop transect across a faulted area on the northeastern limb of Teapot Dome. The two F's on the histogram are the locations of hinge-perpendicular faults within the transect. From 0 to 46 m and 68 to 168 m the fractures are hinge-parallel in orientation; from 46 m to 68 m fractures are subparallel to the two hinge-perpendicular faults.

However, at Teapot Dome, the fact the hinge-oblique fractures are older than the other dominant fracture sets and that fractures with the same strike are recorded at sites away from the anticline suggests they predate folding.

In contrast, hinge-parallel and hinge-perpendicular fracturing and faulting are interpreted to be broadly contemporaneous with basement-involved thrusting and folding at Teapot Dome. This interpretation is based on several observations. Fracture abutting relationships indicate that the two fracture sets were broadly contemporaneous. The dominant fracture sets strike roughly parallel and perpendicular to the fold hinge, suggesting that they are related to the folding event. The fracture sets are parallel and spatially related to the fault sets. Evidence that NE-striking normal-oblique faults are temporally related to folding comes from the observed spatial relationships. These NE-striking faults are oriented roughly perpendicular to the fold hinge, even where it bends, and terminate toward the SW limb of the anticline.

As mentioned earlier, seismic data show that a basement-involved blind thrust terminates within the lower Paleozoic section. Therefore, regional compression resulted in shortening at the crustal level, manifest in the formation of basement-involved thrusts. The normal-oblique movement recorded on some of the NE-striking faults indicates they may have a transfer fault component related to differential movement across segments of the basement-cored thrust. As noted by Gay (1999), shortening parallel and perpendicular to the fold is required to develop four-way closure. Also using coseismic displacements after the Northridge earthquake of 1994 to model strain in a blind thrust, Unruh and Twiss (1998) determined that horizontal shortening ( $d_3$ ) was perpendicular to the fold hinge, maximum lengthening ( $d_1$ ) was horizontal and parallel to the fold axis and

$d_2$  was vertical. Each of these concepts are evidenced by the two dominant fracture and fault sets and their orientation with respect to the fold hinge at Teapot Dome and by the fold form itself. Specifically, hinge-perpendicular fractures and faults record extension parallel to the hinge of Teapot Dome; the fold itself evidences shortening normal to the hinge. The normal faults, extension fractures and conjugate shear fractures parallel to the fold hinge are interpreted to have accommodated extensional strains related to bending of the brittle sandstone beds. It is also possible that folding was accommodated by flow of the more ductile units within the folded sedimentary section. Further work is required to model possible variations in orientation and type of faults or fractures with increasing depth to basement and decreasing distance to the thrust.

The orientation of structures, such as hinge-parallel and hinge-perpendicular faults and fractures, at Teapot Dome is similar to those described by DeSitter (1956), Murray (1967), Garrett and Lorenz (1990), Engelder et al. (1997) and Hennings et al., (1998). Two of the studies, Garrett and Lorenz (1990) and Hennings et al. (1998), noted fracture sets that predated folding. In most of these studies, the fractures and/or faults striking parallel or perpendicular to the fold hinge were attributed to the folding process.

Structures at Oil Mountain for example are similar to those at Teapot Dome, with fractures striking both parallel and perpendicular to the fold hinge and an increase in fracture density in the southern plunging regions of both anticlines (Hennings et al., 1998). However, the hinge-parallel fractures at Oil Mountain were interpreted to predate folding; also the increase in fracture density in southern exposures at Oil Mountain is greater. It is possible the hinge-parallel fractures at Oil Mountain are related to the folding process because the pavement surfaces used as a comparison at a distance from



Oil Mountain are still part of the Casper arch, which strikes subparallel to Oil Mountain. Therefore, fractures at both locations may have formed in response to folding. It should be noted however, that the fracture set determined to predate folding at Oil Mountain is subparallel to the fracture set determined to predate folding at Teapot Dome. Therefore, the age relationship between hinge-parallel fracturing and fold formation at Oil Mountain is undetermined. The difference in fracture density between the two anticlines may be due to Oil Mountain being a tighter fold, evidenced by the forelimb being slightly overturned.

The structures described by Engelder et al. (1997) at Elk Basin anticline are perhaps most similar to those at Teapot Dome. Two fracture sets, one parallel and the other perpendicular to the fold, were documented. Changes in strike of hinge-parallel fractures observed on the forelimb of the anticline were attributed to local faulting as they are at Teapot Dome. At Elk Basin anticline, as at Teapot Dome, a significantly higher percentage of hinge-parallel fractures was observed relative to hinge-perpendicular fractures. Hinge-perpendicular fractures were also observed to extend for considerable lengths in a few areas and to terminate against hinge-parallel fractures in other areas at Elk Basin anticline.

### ***3-D conceptual model of basement-cored anticlines***

The observed fracture trends and interpreted genetic relationships from Teapot Dome and similar folds have been used to create a conceptual model of fault and fracture development in an anticline above a basement-cored thrust. The two main through-going fracture sets incorporated into this 3-D model are: 1) bed-normal extension fractures

striking subparallel to NE-striking oblique normal faults and perpendicular to the fold hinge, and 2) bed-normal extension fractures and normal faults striking parallel to the fold hinge (Figure 2-13a). The fracture set determined to predate folding at Teapot Dome is not incorporated into this conceptual model, as pre-existing regional fracture sets will vary in orientation with location.

A comparison between this and an earlier conceptual model (Stearns and Friedman, 1972) that describes fracturing associated with folding (based on data from Teton anticline) shows significant differences as well as some similarities in the fracture patterns (Figure 2-13). Conjugate fractures in the Stearns and Friedman (1972) model are oriented such that the bisector of the acute angle is parallel to the plane of bedding, while the Teapot Dome model illustrates conjugate fractures that have a vertical bisector to the acute angle. These shear fractures obliquely transect the anticline in the Stearns and Friedman (1972) model. The shear fracture sets in the Teapot Dome model strike either parallel or perpendicular to the hinge. However, the extension fractures in both models strike both parallel and perpendicular to the fold hinge in the vicinity of the culmination. Near the plunging nose of the anticline, where bedding strike is not parallel to the fold hinge, differences in extension fracture patterns become apparent. Bedding strike rotates through a 180° turn around the hinge at this point. Here the Stearns and Friedman (1972) fracture sets, by remaining parallel to bedding strike, change orientation with respect to the fold hinge, whereas the fracture sets within the Teapot Dome model remain parallel and perpendicular to the fold hinge (compare Figures 2-13a and b). Each of these observations suggests a significant difference in permeability anisotropy between models, as noted in the following section.

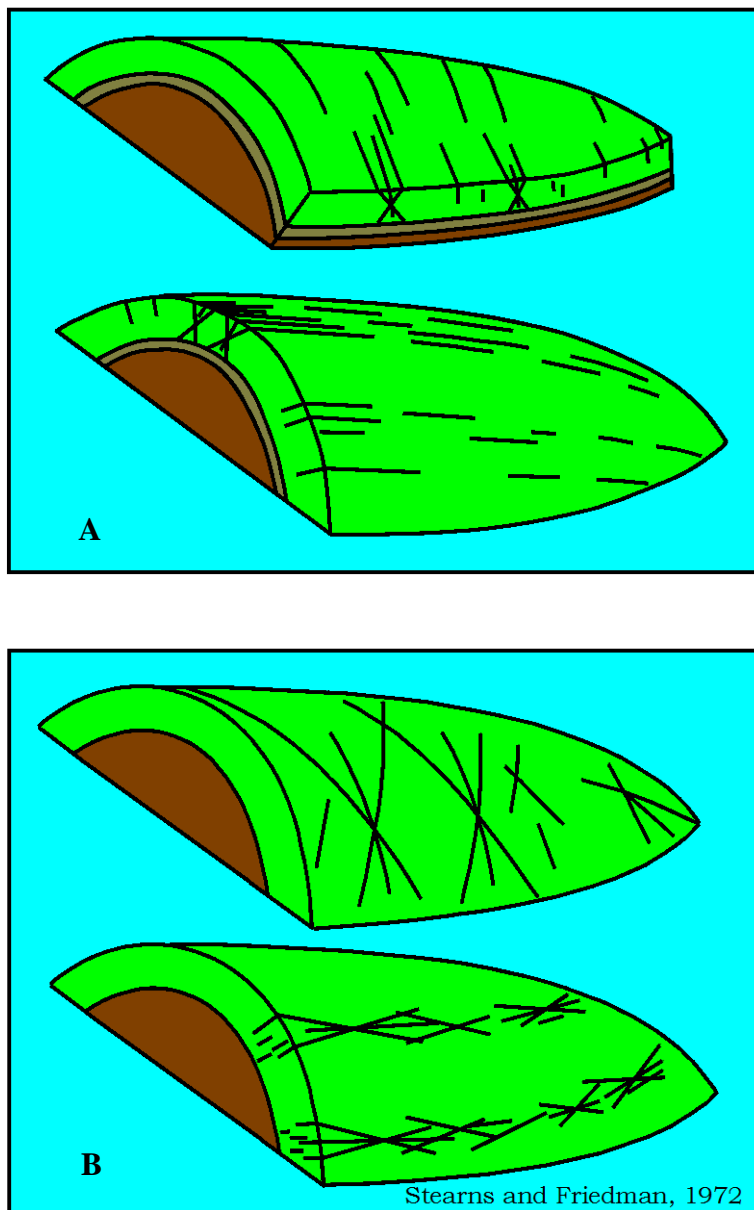


**Figure 2-13:** Two conceptual 3-D models of primary fracture patterns associated with anticlines. Different fracture sets are shown separately for clarity. A. Model developed from Teapot Dome data. B. Model developed by Stearns and Friedman (1972).

It is important to note that there may be a structural explanation for the differences between these two 3-D models. The two anticlines are distinctly different both in terms of the depth of the thrust relative to the fractured strata on which the models are based and in the type of folding process. Teapot Dome is situated above a deep-seated, basement-cored thrust. The sedimentary layers over the area of faulting are interpreted to be essentially draped over the thrust. In contrast, Teton anticline is cored by a thin-skinned thrust that propagated through the sedimentary section. As described by Sinclair (1980), the Teton Anticlines, separated by an unfaulted syncline, are essentially buckle folds in the form of a wave train over the thin-skinned thrust. It may be that bedding-parallel shortening is significantly greater in the latter case as evidenced by conjugate fractures with a horizontal (parallel to bedding) bisector to the acute angle. This may also hold true for the fault propagation and fault-bend folds documented by Cooper (1990), wherein fracture orientations representative of the Stearns and Friedman (1972) model were recorded. Conversely, brittle sandstones at Teapot Dome indicate lengthening in the area of flexure (drape) over the deep-seated thrust as evidenced by conjugate fractures and faults with a vertical bisector to the acute angle. The majority of folds that have fracture patterns similar to those at Teapot Dome are those associated with deep-seated blind thrusts. It should also be noted that Stearns (1964) observed a conjugate fracture set with a vertical bisector to the acute angle at Teton Anticline, which was not considered a dominant fracture set by Stearns and Friedman (1972). This fracture set was attributed to folding; bedding was visualized as a bent beam, wherein the upper arc would be an area of extension but the lower arc would be an area of shortening.

## Fluid flow implications

There are a number of implications of the fracture patterns that are incorporated into the conceptual fracture model (Figure 2-14). Since the dominant set of throughgoing fractures is parallel to the fold hinge, significant permeability anisotropy is expected, with maximum permeability generally parallel to the fold hinge across the entire anticline. Areas of greatest change in dip of bedding (i.e. the fold hinge) are areas of increased fracture density, with fractures generally parallel to the fold hinge. The increase in hinge-parallel fractures near the hinge of the anticline should be associated with an increase both in permeability and permeability anisotropy. NE-striking normal faults and associated fractures may locally cause the direction of maximum permeability to be perpendicular to the fold hinge. Intersections of hinge-perpendicular with hinge-parallel faults and associated fractures should be areas of enhanced permeability, where increased interconnectivity may allow for locally increased production. The permeability anisotropy will depend on the number of faults and fractures of each set and degree of interconnectivity, and will thus vary from site to site.

A preexisting fracture and deformation band set oblique to the fold hinge is specific to Teapot Dome. This fracture and deformation band set is found throughout the fold and in all lithologies and will have an influence on fluid flow. Doll et al. (1995) describe this fracture set, which strikes N65°W, as providing the most significant flow directionality with respect to water response and rapid oil response time during steam flooding.

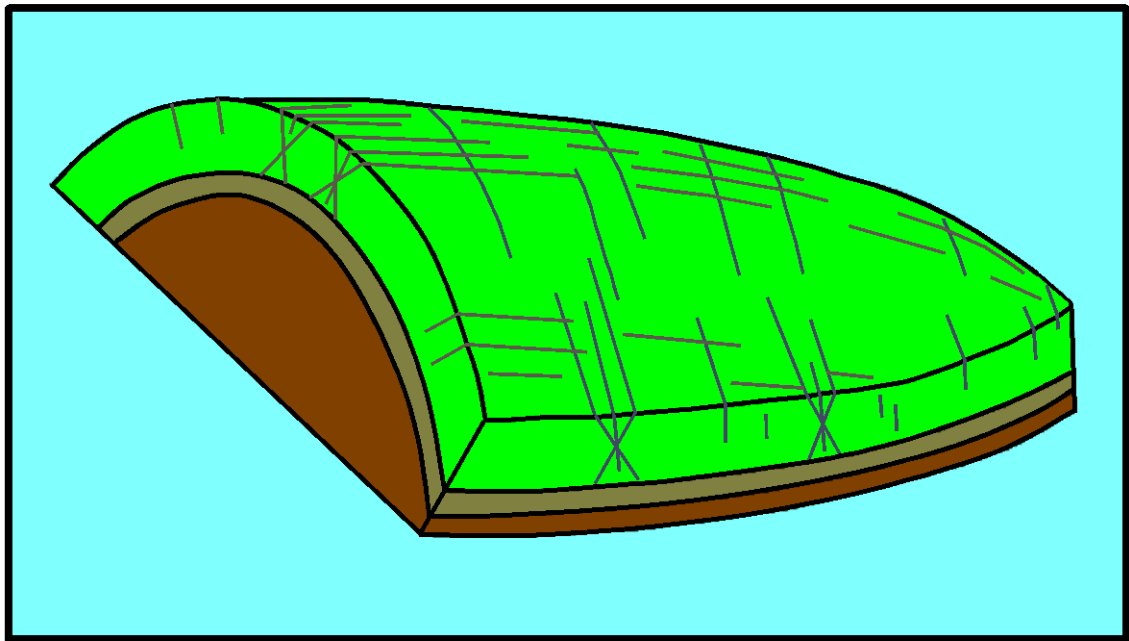


**Figure 2-14:** Conceptual 3-D model of fracture patterns developed at Teapot Dome. Implications of these fracture patterns on fluid flow include: significant permeability anisotropy, with maximum permeability generally along the fold hinge due to numerous hinge-parallel fractures near the apex of the anticline; NE-striking normal faults and associated fractures may cause the direction of maximum permeability to be locally perpendicular to the fold hinge; and intersections between hinge-perpendicular and hinge-parallel faults and fractures may allow for increased production.

It should be noted that mineralization within the faults and fractures will play an important role in all of the previous assessments. Highly mineralized fractures and faults will reduce the overall permeability within a volume of rock. They would still result in a direction of maximum permeability parallel to the mineralized fault or fracture set, but in this case, the zone of highest permeability would be the matrix and not the fracture or fault plane. The majority of fractures and faults studied were relatively unmineralized. However, localized areas of moderate mineralization were observed. Detailed information regarding mineralization is included in Part I: Lithologic Controls.

## **Conclusions**

Fractures and faults associated with folding within the Cretaceous Mesaverde Formation at Teapot Dome display variable patterns associated with structural position, including: 1) fracture density increases near faults, 2) conjugate fractures and deformation bands, oriented such that they have a vertical bisector to the acute angle, and faults striking subparallel to the axis of the anticline, are common in the exposed hinge of the anticline, 3) NE-striking normal-oblique faults and associated fractures are generally perpendicular to the fold hinge, and are more closely spaced near the culmination of the dome, and 4) extension fractures and faults that are parallel to the fold hinge, and are more closely spaced near the hinge.

The deformation process that formed the faults, fractures and fold is interpreted to have been a dynamic interactive system, wherein progressive folding was driven by displacement on the basement-involved thrust fault. Variable displacement along the thrust front was accommodated by transfer faults (the NE-striking normal oblique faults) at roughly right angles to the thrust fault. These faults also accommodated a component

of extension associated with bending of beds across the fold. Normal faulting perpendicular to the fold hinge accommodates the fold form in this direction. Hinge-parallel normal faults formed to accommodate the fold form and are roughly parallel to the thrust fault. In addition, fractures formed in brittle sandstones and carbonaceous shales in response to the fold form (driven by the basement thrust) and to displacements along faults (also driven by the basement thrust) while more ductile marine shales are interpreted to have responded to shortening through flow.

These observations indicate that maximum horizontal permeability associated with these fractures and faults will generally be hinge-parallel, especially near the apex of the anticline. Localized areas of maximum permeability that are perpendicular to the fold hinge may be found within the damage zones of NE-striking normal faults. A preexisting NW-WNW fracture set specific to Teapot Dome will also influence fluid flow. This set was observed in outcrop and inferred by Doll et al. (1995) from data collected during steam flooding of Shannon reservoirs.

Given the importance of correctly modeling permeability and fluid flow anisotropy it is essential to use the most appropriate reservoir analog. This study provides a conceptual model of fault and fracture distribution that is in many ways similar to previous descriptions of basement-involved anticlines, including a previous study at Teapot Dome (Thom and Speiker, 1931; DeSitter, 1956; Murray, 1967; Garrett and Lorenz, 1990; Cooper, 1992; Engelder, 1997; Hennings, 1998; Unruh and Twiss, 1998). The model is, however, significantly different from Stearns and Friedmans (1972) model, which has been widely applied to all anticlines regardless of the folding process. I believe that the model developed from the Teapot Dome data set is best applied to



basement-cored structures while the Stearns and Friedman (1972) model would be a better analog for folds developed above thin-skinned thrusts. In other words, fracture analogs are best applied with knowledge of the tectonic setting of the structure of interest. Using the wrong model could result in a poorly designed secondary recovery system, wherein early breakouts occur and/or production is not enhanced.

## APPENDIX A

### Brittle Deformation of Clastic Sediments

#### *Deformation Bands*

Deformation bands are roughly planar features that record some small amount of displacement (i.e. small-displacement faults) (c.f. Aydin 1978). These structures are narrow (1mm wide average) with along strike lengths from a few centimeters to some tens of meters in length. Displacements are in the range of a few millimeters to a few centimeters. Areas where larger amounts of displacement have been accommodated are typified by wider zones of deformation bands (Aydin, 1978; Aydin and Johnson, 1983; Antonellini et al., 1994). This observation, that a single deformation band can accommodate only a limited amount of displacement, suggests the possibility of strain hardening (Rudnicki and Rice, 1975; Aydin and Johnson, 1983; Antonellini et al., 1994; Wong et al., 1997). Strain hardening leads to the sequential formation of more deformation bands adjacent to the original band (Rudnicki and Rice, 1975; Antonellini et al., 1994). Because their laboratory data were inferred to lack evidence for strain hardening, Mair et al. (2000) suggest a different mechanism for the sequential formation of deformation bands. The authors suggest that friction along the first deformation band makes slip more and more difficult, conversely nearby grains are preferentially loaded until a new sequential band is formed. This mechanism results in slip along a new band rather than the older band without strain hardening.

Antonellini et al. (1994) described some deformation bands as more resistant to weathering than the surrounding rock. They inferred that this difference was related to

preferential cementation. Preferential cementation is inferred to be related to the relatively small pore spaces within a deformation band, since nucleation is facilitated as the pore space decreases (Antonellini et al., 1994). Weather resistant deformation bands can, however, also result from grain and pore size reduction and associated compaction without cementation (Sigda et al., 1999).

### ***Fracture initiation and propagation: Theory***

A fracture occurs when a rock unit breaks along a more or less planar surface and separates into discrete parts (Stearns and Friedman, 1972). Fractures can be divided into the following major groups based on the type of displacement observed, 1) dilating fractures/joints, and 2) shearing fractures/faults (Long et al., 1997). A genetic subdivision into modes of fracture is based on the relative movement of the fracture walls with respect to each other and to the fracture front (Figure C-1). Mode I fractures have displacements perpendicular to the fracture surfaces and are termed either extension, tensile or dilation fractures. Mode II (shear) fractures have displacements that are parallel to the fracture surface and perpendicular to the fracture front. Mode III (shear) fractures have displacements that are parallel to the fracture surface and the fracture front. These shear fractures are called faults if displacement is measurable (Pollard and Aydin, 1988; Long et al., 1997).

Generally, a fracture can initiate and propagate when the strength of the rock is equaled or surpassed by an applied stress. However, experimentation by Griffith (1921) showed that glass samples fractured at an applied stress level lower than their theoretical strength. Griffith's explanation for this observation is that stresses become amplified around preexisting flaws or microcracks within the samples. These flaws or microcracks propagate when optimally aligned to the applied stress (Figure C-2; Griffith, 1921;

Weijermars, 1997).

Both extension and conjugate shear fractures can form in laboratory compression tests (Figure D-3). Extension (opening) fractures form perpendicular to the least compressive stress and bisect the acute angle between the conjugate shear fractures (Peng and Johnson, 1972; Long et al., 1997). In accordance with Griffith's theory, macroscopic failure is generally found to be preceded by microfracturing (Griffith, 1921; Jaeger and Cook, 1969; Hallbauer et al., 1973; Nelson, 1985).

#### Fluid-pressure effects on fracture initiation

One of the more important controls on the strength of brittle rocks is pore pressure (Hubbert and Rubey, 1959; Secor, 1965). Work by Hubbert and Rubey (1959) shows that effective normal stress ( $\sigma$ ) acting on a plane of interest is related to pore fluid pressure ( $p$ ) and the total normal stress ( $S$ ).

$$\text{Equation 1:} \quad \sigma = S - p$$

As described by Secor (1965), the importance of this relationship is that fracturing within brittle rocks is a direct function of the effective stress.

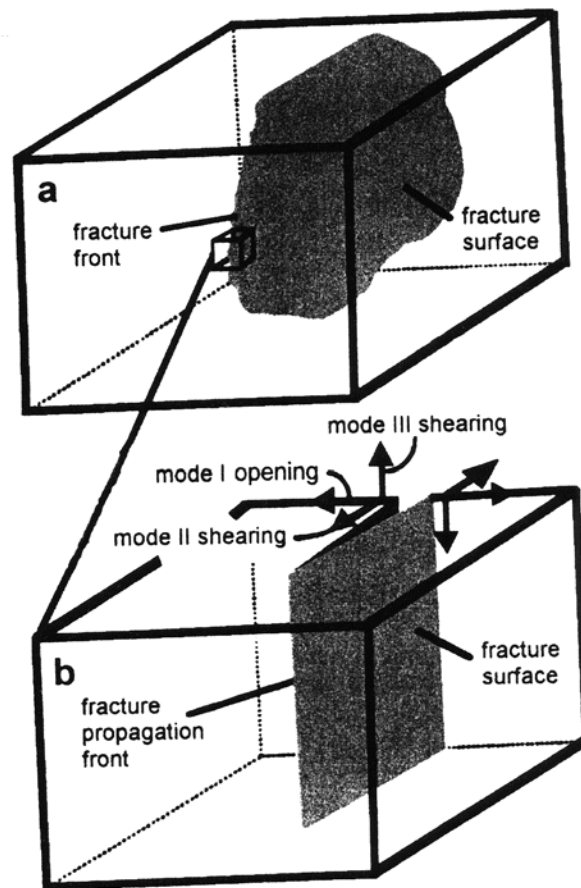


**Figure A-1:** (a) Diagram illustrating the propagation front of a fracture. (b) Illustration of fracture modes. Mode I fracture - opening displacements are perpendicular to the fracture surface. Mode II fracture - shearing displacements are parallel to the fracture surface and perpendicular to the fracture front. Mode III fracture - shearing displacements are parallel to the fracture surface and the fracture front (Pollard and Aydin, 1988).

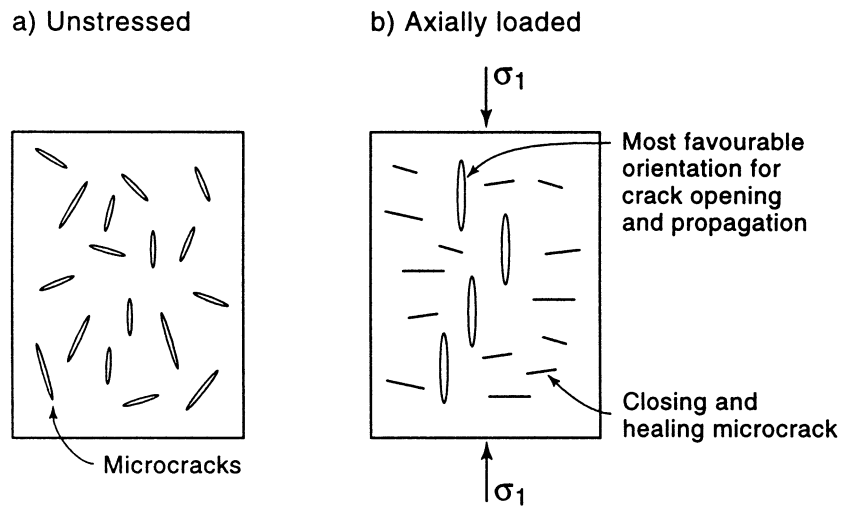


**Figure A-2:** Griffith's crack propagation model. (a) Randomly orientated flaws in an unstressed sample. (b) Under an applied stress (axial loading) the flaws orientated parallel to the maximum stress propagate while other microcracks are sealed (Weijermars, 1997).

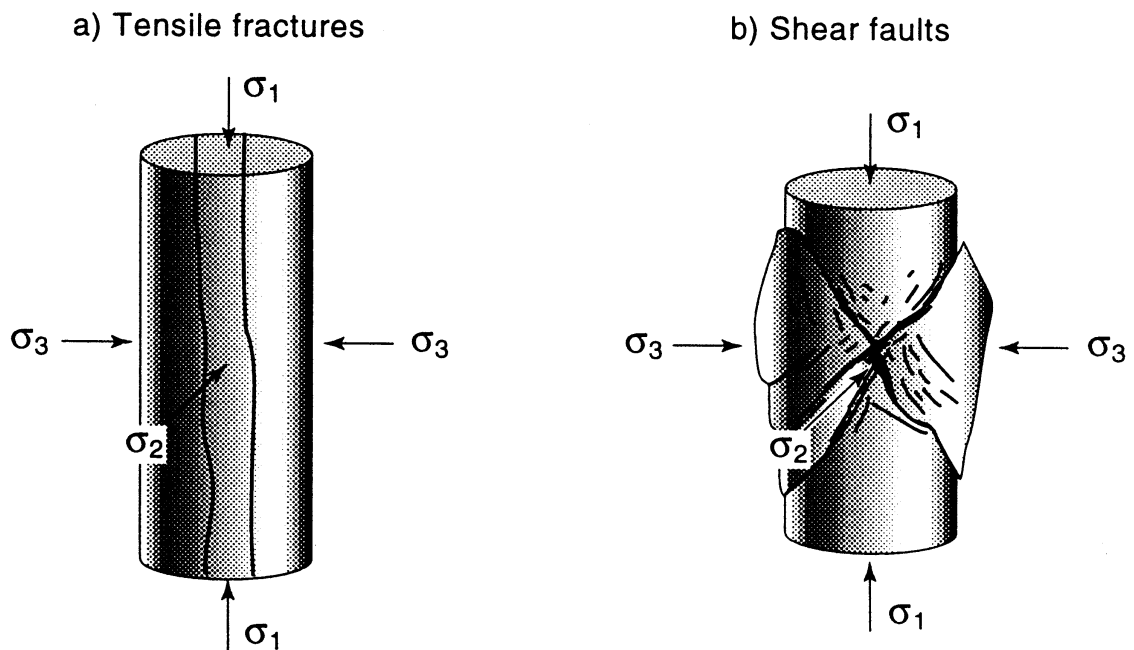


**Figure A-3:** Formation of tensile (extension) fractures and conjugate shear fractures/faults in laboratory compression tests (Weijermars, 1997).  $\sigma_1$  – maximum principal stress;  $\sigma_2$  – intermediate principal stress;  $\sigma_3$  – least principal stress.

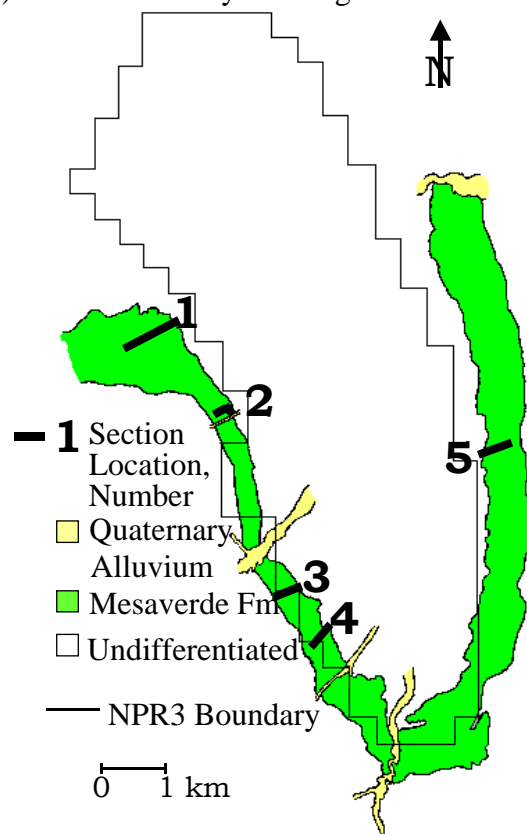
## APPENDIX B

### *Measured Stratigraphic Sections*

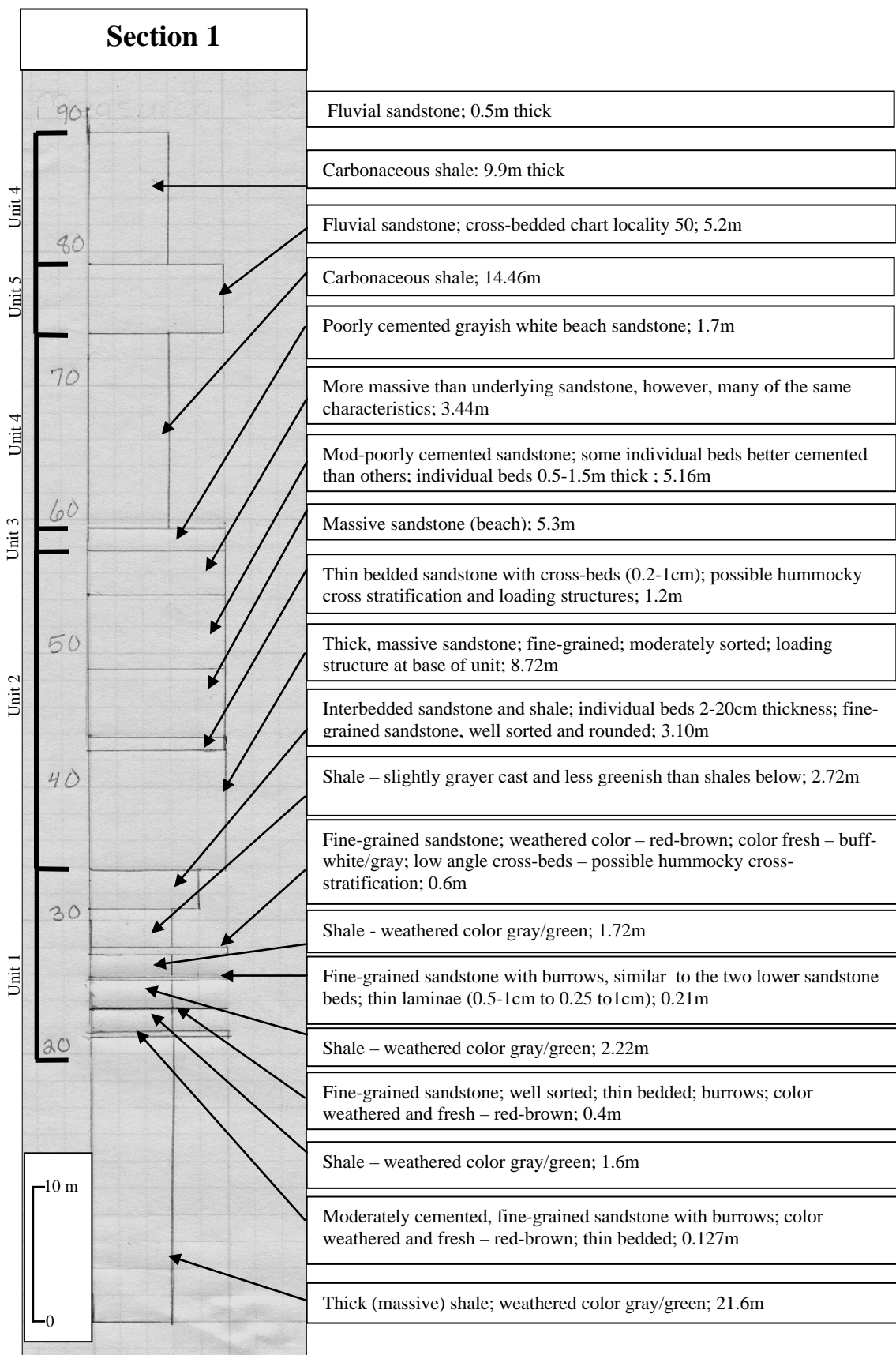
Stratigraphic sections were measured from five areas around Teapot Dome (Figure B-1). Measured sections begin within the interbedded sandstones and shales (Unit 1) and terminate within the fluvial sandstones and carbonaceous shales (Units 4 and 5) of the Mesaverde Formation. A brief lithologic description and thickness is provided for each measured bed. Larger scale (Unit) divisions are keyed to Figure 1-2.

Two stratigraphic sections (sections 2 and 4) contain fracture data obtained while measuring those sections. Fracture descriptions are included in this section to simplify the comparison of lithologic characteristics and fracture characteristics within each bed.

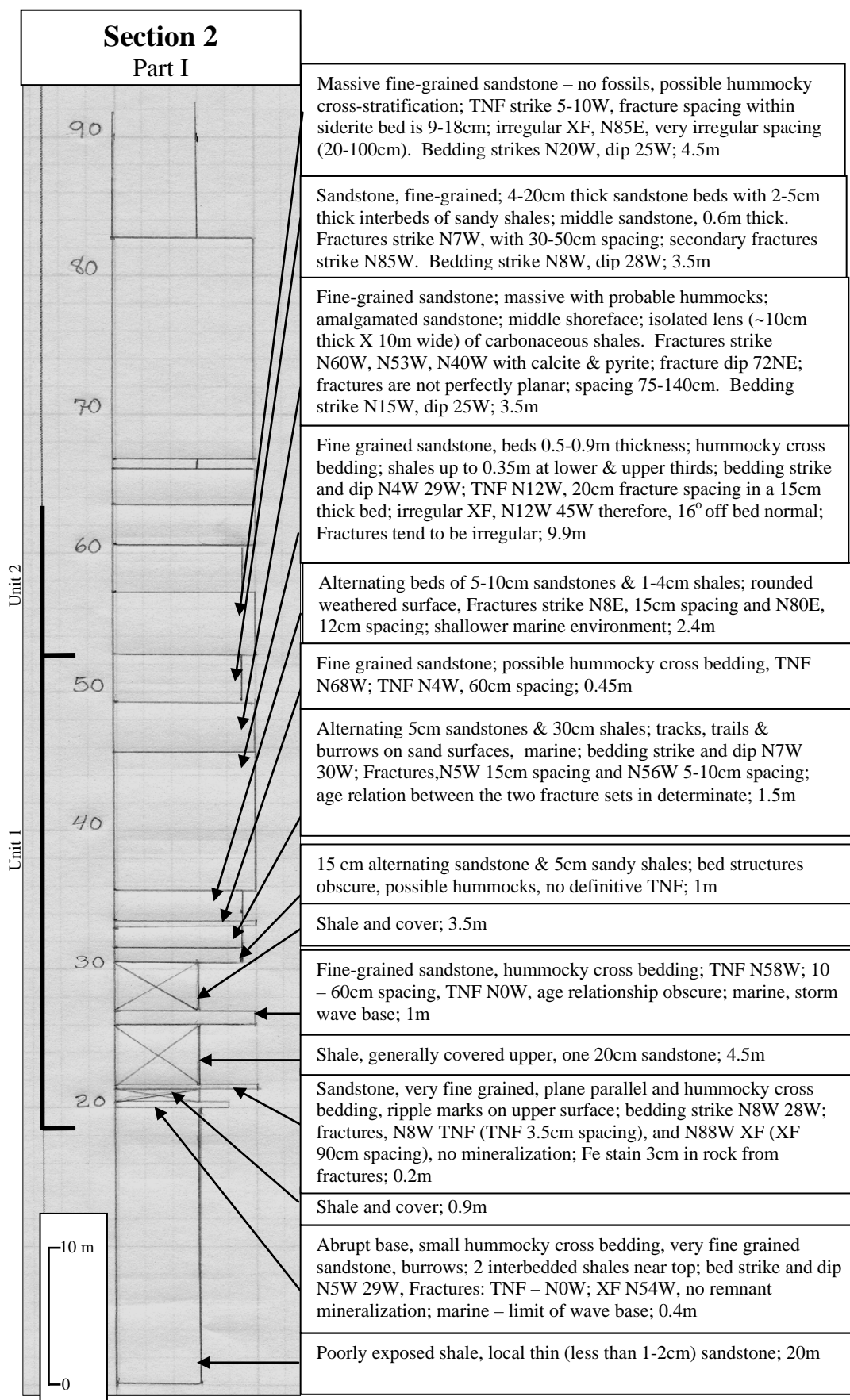
Large-scale (Unit) divisions are keyed to Figure 1-2.

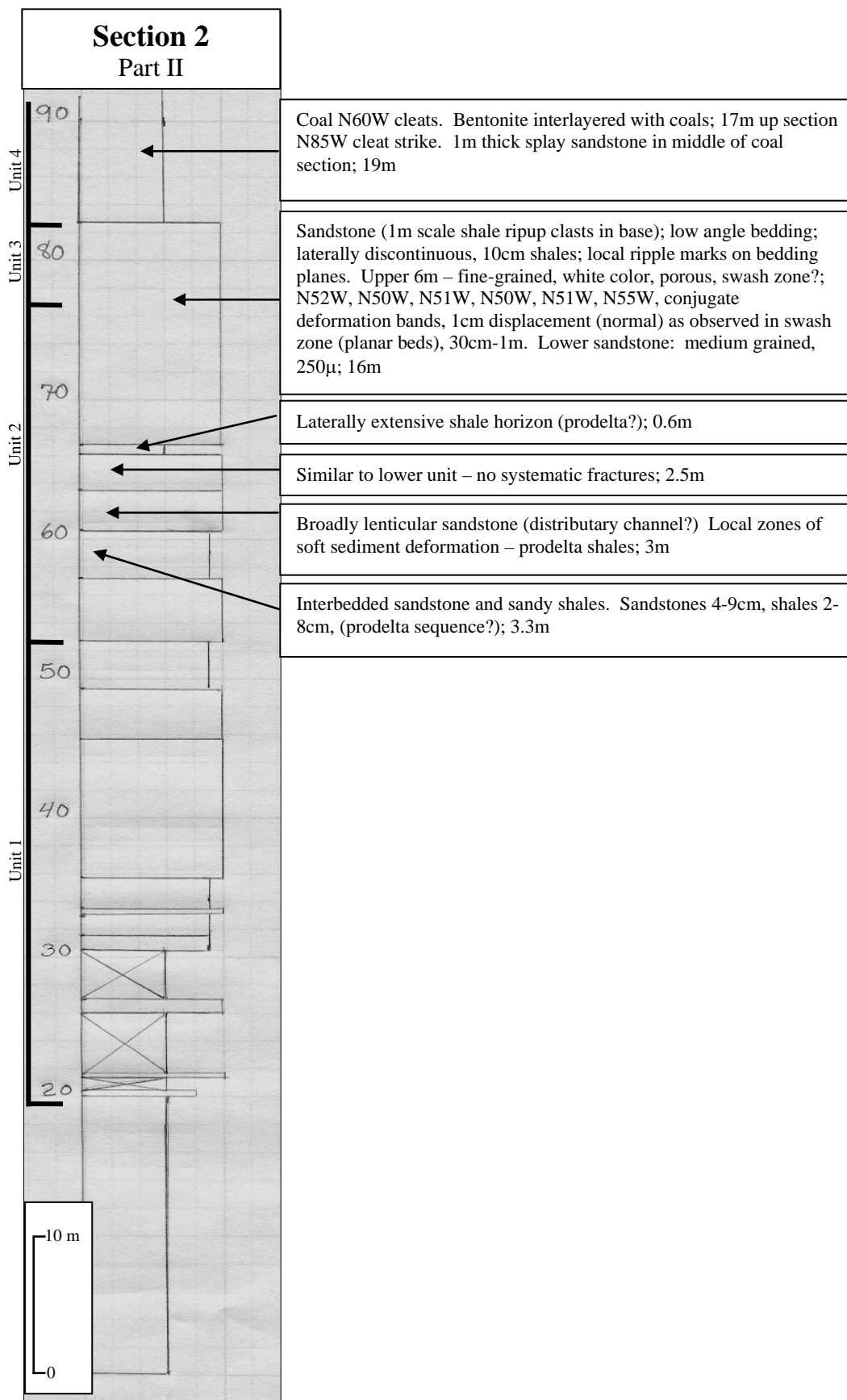


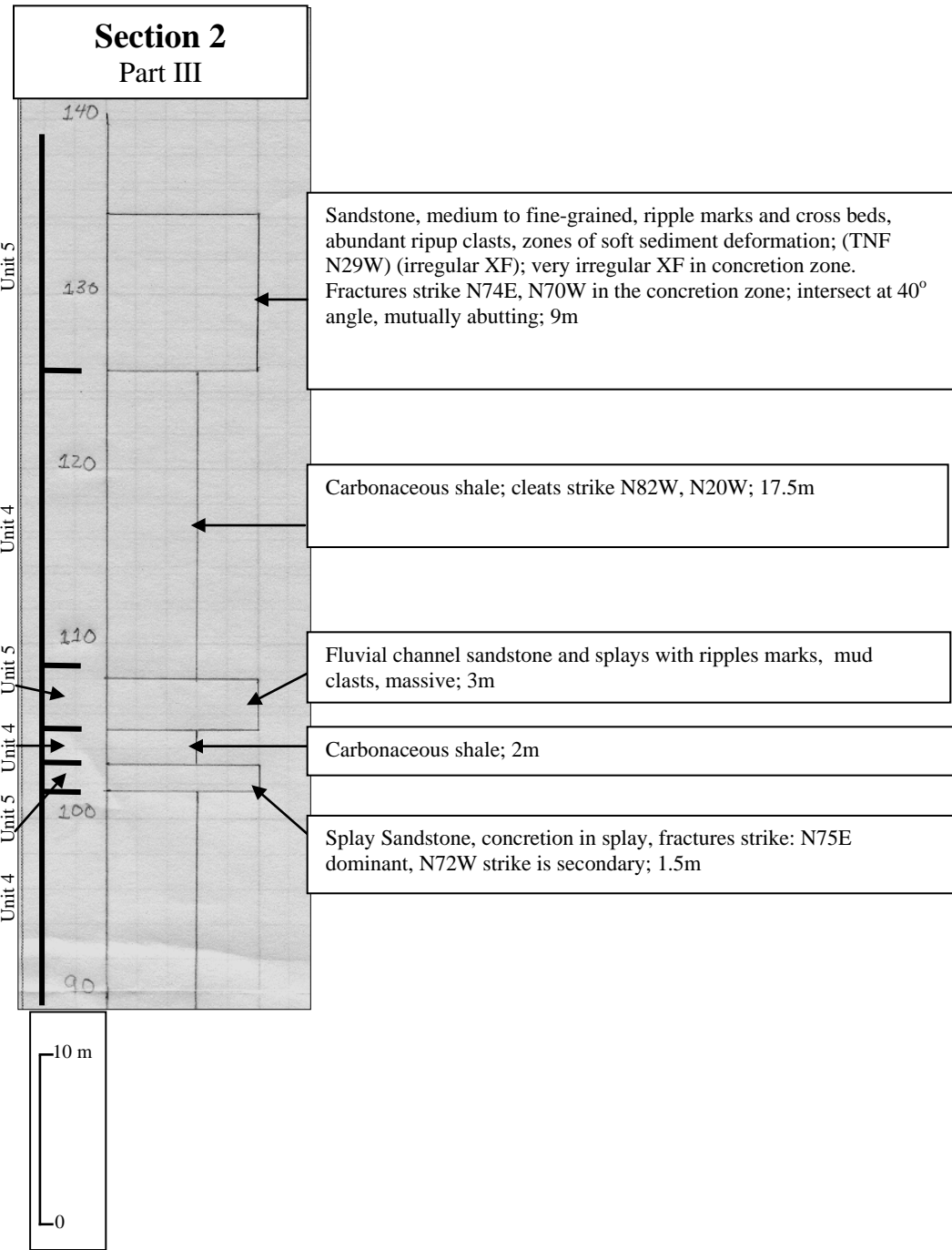
**Figure B-1:** Locations of measured sections at Teapot Dome.

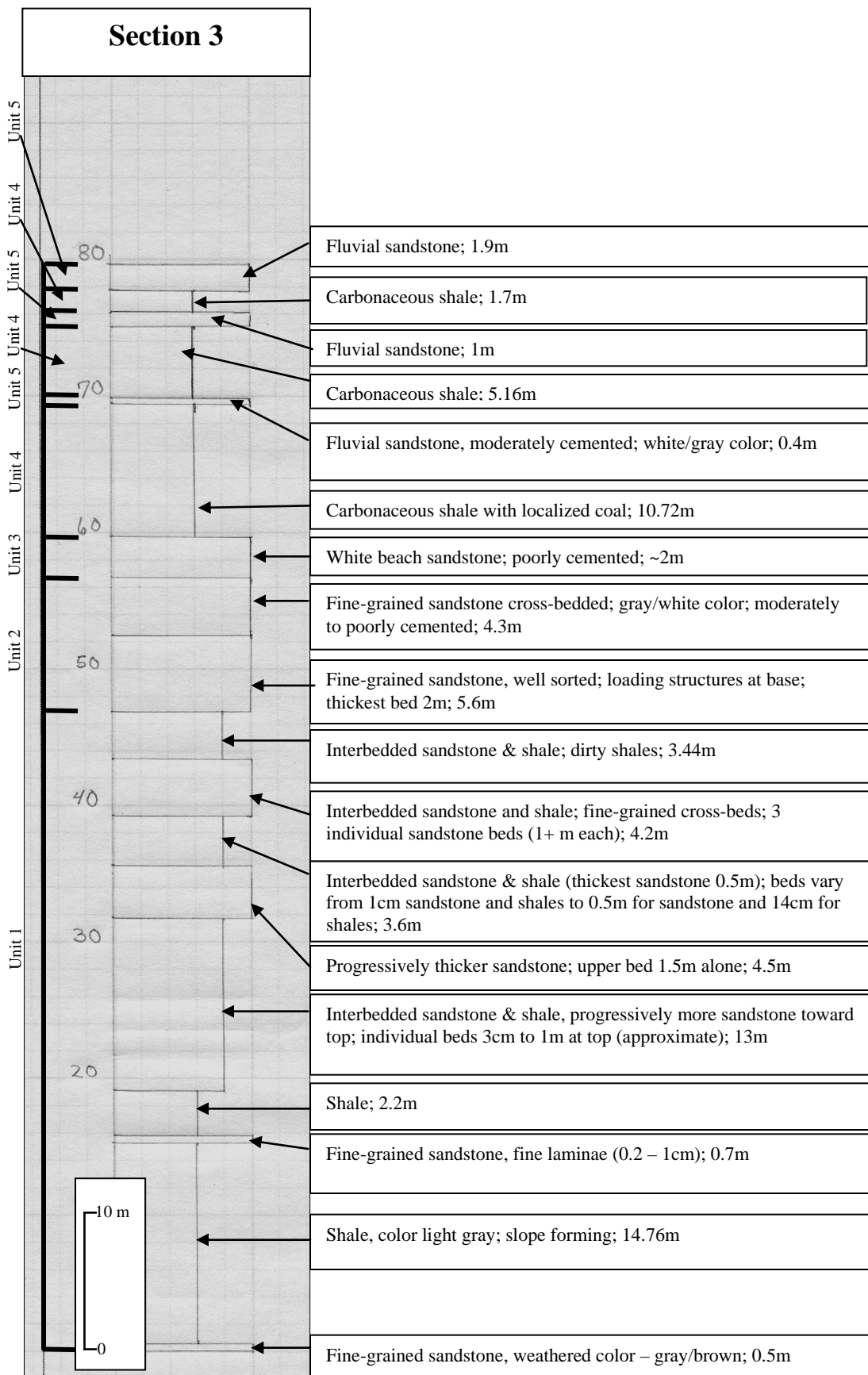


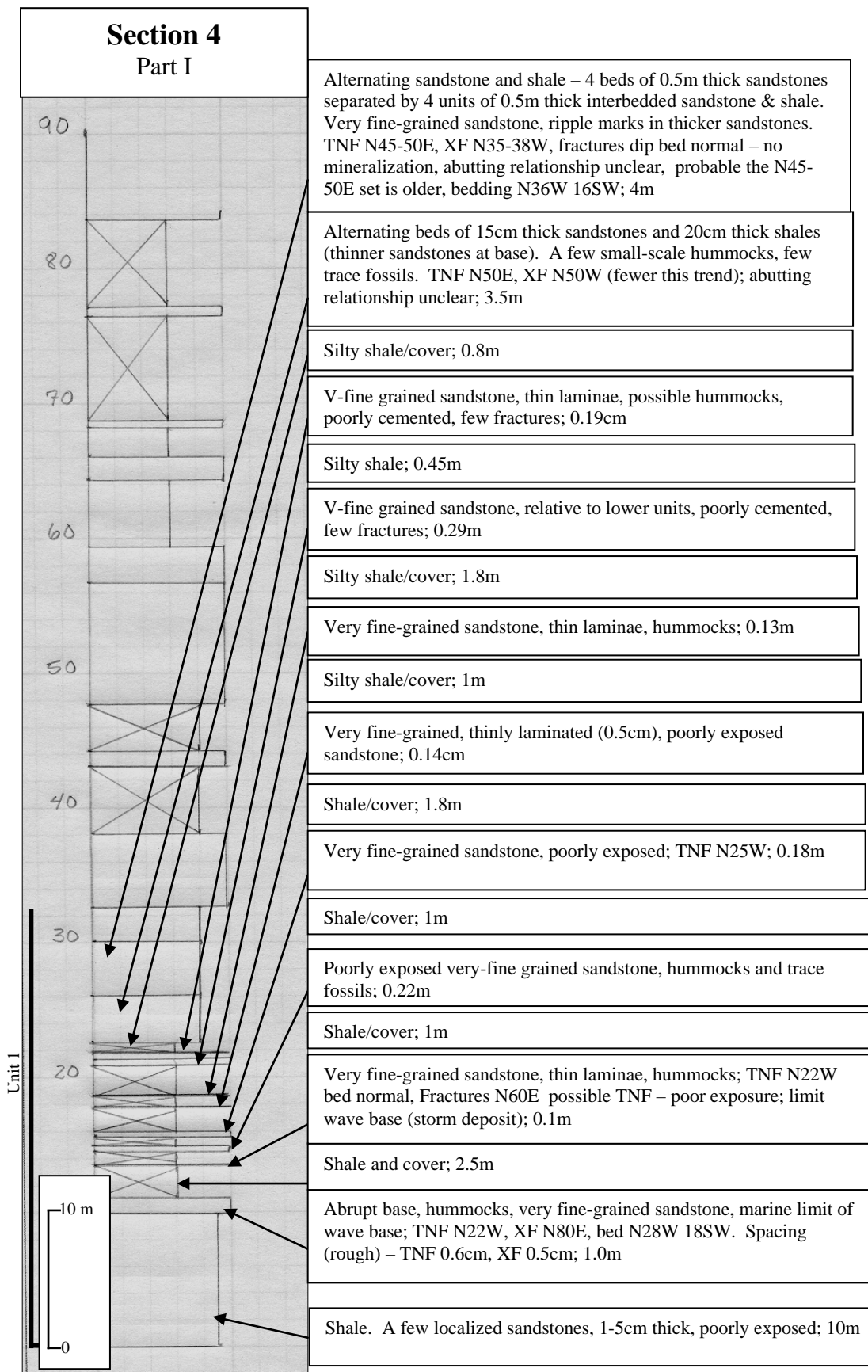


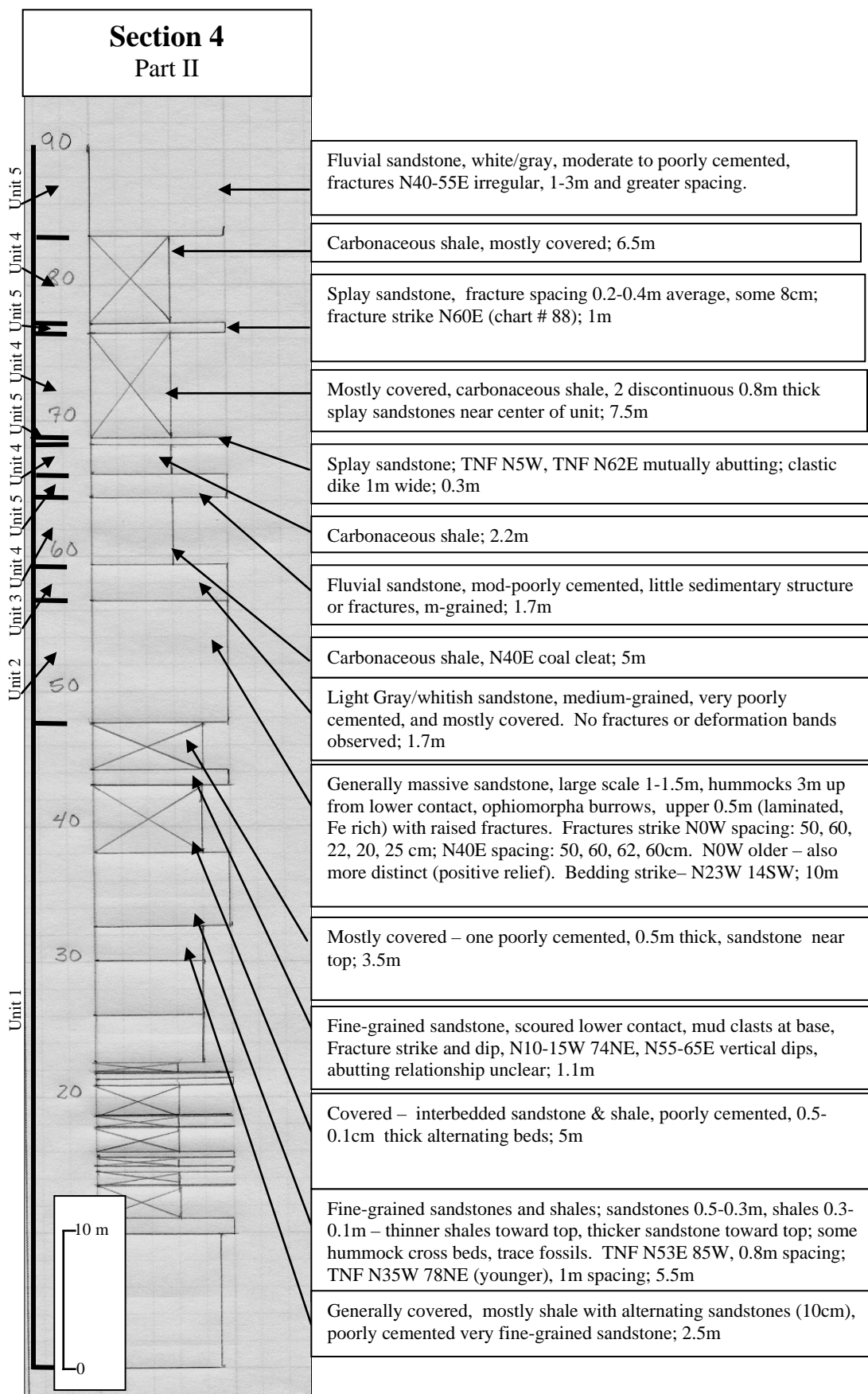


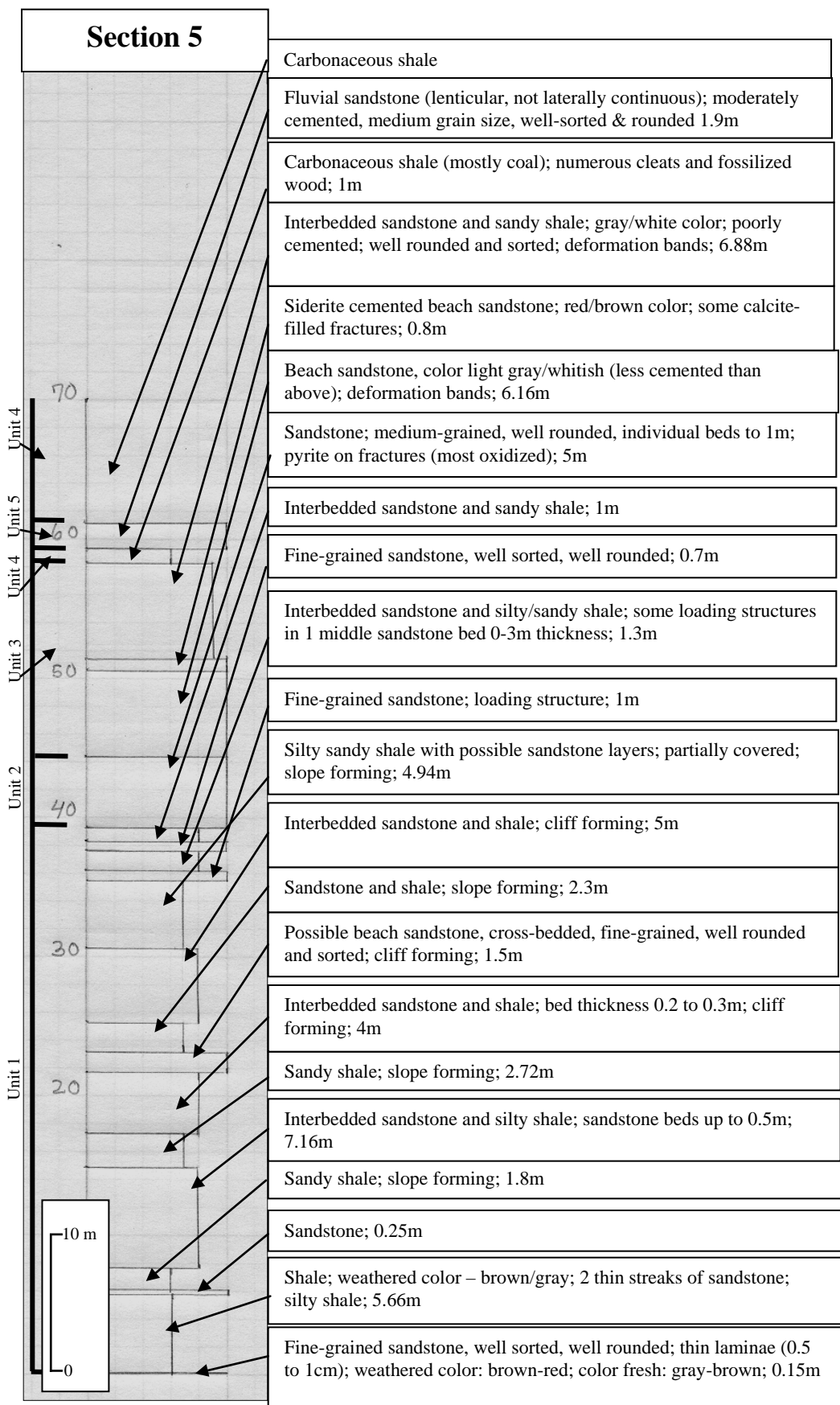












## APPENDIX C

This appendix primarily comprises fracture data compiled from the various sites at Teapot Dome. A key to the charts for each data collection site is given below. Locations are provided in Figure D-1.

**Chart #:** Location and whether this is a plan or cross-sectional view. Relationship to nearby charts is also included (if necessary).

**Location:** e.g., SW1/4 SE1/4 Sec# T#N R#W

**Lithology:** Cretaceous Mesaverde Formation (Kmv) in ascending order as shown in Figure 1-2.

**Size of Area:** Given in meters or acres.

**Grain Size, Cementation:** Visual estimate using grain-size chart. Field observations of cementation are recorded and placed on the following subjective scale: very poor (friable using fingers), poor (easily friable with a knife, which will leave a deep scratch mark), moderate (partially friable with knife and leaves scratch mark), well (leaves slight mark when scratched with knife), very well (few to no scratches with knife and produces ringing sound when struck with a rock hammer).

**Bed Thickness:** Measured in centimeters or meters; if possible, bracketing units are also measured.

### Structure

**Strike and Dip:** Recorded two or more bedding plane measurements (where possible).

**Curvature:** Estimated radius, in meters, of plan view structural curvature.

**Faulting:** Description of large-scale faults and associated fracture swarms. Recorded fault strike and dip and the same general descriptions as for fractures (see below).

### Fracture Characteristics

**Type, Orientation:** Fractures divided into sets (A, B, C, etc.) based on characteristics and orientations. Obtained as many readings as possible (at least ten for each set). Strike and dip readings given in quadrants.

Types: Abbreviations and types from John Lorenz (written. com., 1997).

CF: Conjugate shear fractures.

VCF: Vertical conjugate shear fractures (CF with vertical bisector of the acute angle).



HCF: Horizontal conjugate shear fractures.

XF: Cross fracture (short connecting fractures that terminate at throughgoing fractures).

VE: Vertical extension fractures, typically bed normal.

TNF: Throughgoing fractures have generally longer trace lengths relative to other fracture sets. Other fracture sets generally terminate at this set.

**Spacing:** Fracture spacing measurements were taken in traverses across the outcrop perpendicular to strike (i.e. fracture spacing for set A measured perpendicular to strike A, spacing for set B measured perpendicular to strike of set B). Where possible a minimum of ten measurements were made of fractures from each set.

**Separation:** Measured amount of separation, strike and type of fracture or fault.

**Surface Characteristics:** Recorded characteristics can include slickenside stria and surfaces, plumose structures, and rib marks. Observed steps or risers will be described using terminology of Norris and Barron (1968) and Petit (1987).

Accretion steps: steps formed by gouge or crystallized material.

Congruous fracture steps: risers facing away from movement of the opposite block.

Incongruous fracture steps: risers facing movement of the opposite block.

Sense of movement of the opposing block is determined by stratigraphic separation.

**Relative Ages:** Determined relative age using abutting or crosscutting relationships.

These relationships can help determine relative ages. A fracture that curves to intersect another is interpreted as younger. A fracture set that generally terminates against a throughgoing fracture set is interpreted as younger.

**Apertures:** Measured width of fracture opening. Determined if fracture apertures are recent. Mineralized fractures suggest open fractures at some stage in fracture history.

**Mineralization:** Type of fracture mineralization. Measured width of crystals if possible and width of mineralized zone.

**Deformation Bands (width):** Measured width of bands and described anastomosing or inosculating nature of bands including number of each.

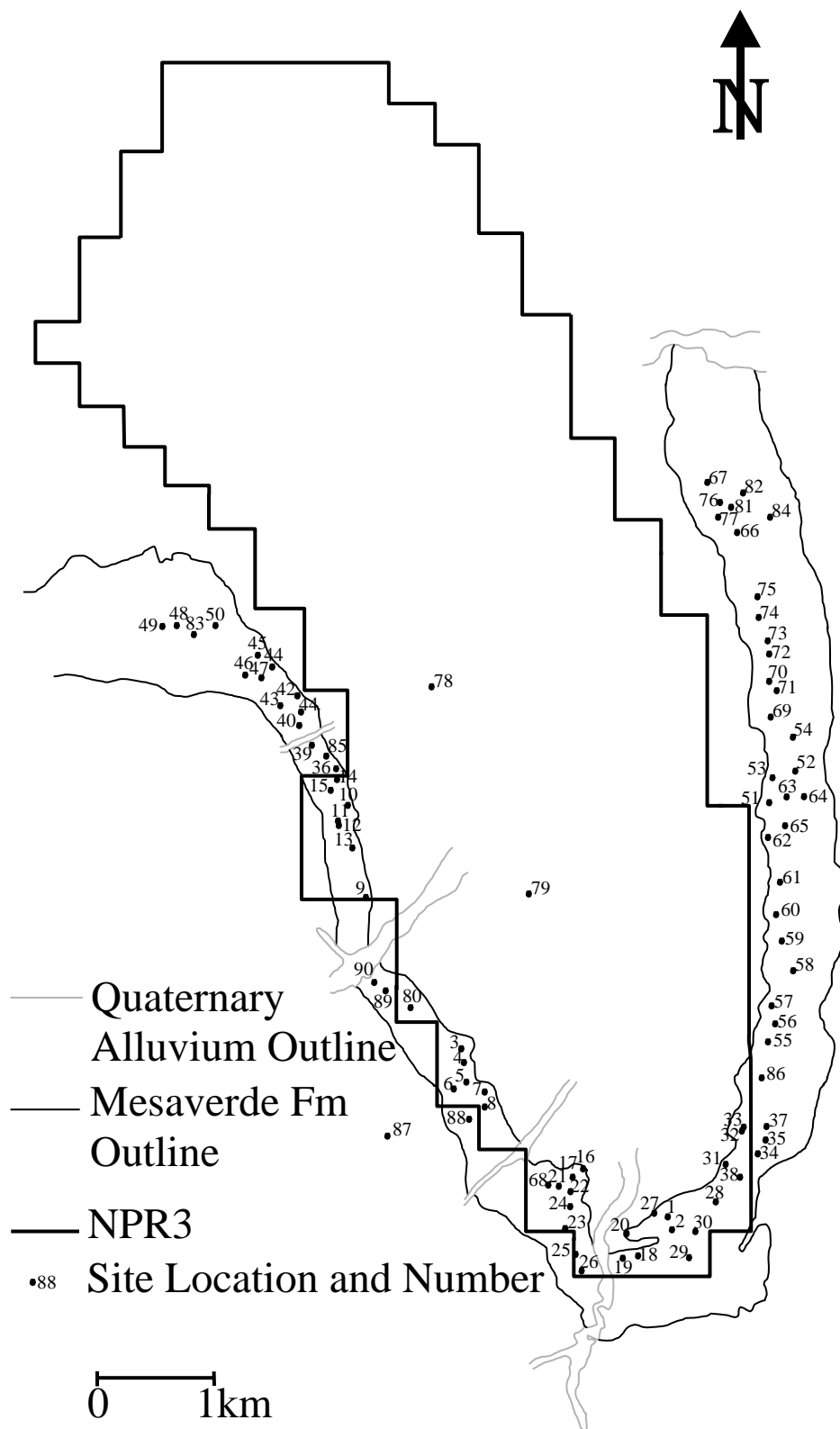


Figure D-1: Locations of charted areas.

**Chart #: 1**

Cliff exposure

**Location:** SW1/4 SE1/4 Sec 23 T38N R78W**Lithology:** Unit 2: beach sandstone - base shows major rip-up storm clasts w/coal; some trace fossils (*Ophiomorpha*)**Grain size, Cementation:** 250  $\mu$ ; rounded grain, moderate cement (calcite)**Bed thickness:** Approximately 10m**Structure****Strike and dip of bedding:** N46E 8SE; N45E 9SE**Structural curvature** (estimated): 1000-1500m**Faulting:** No rock exposed in gap; gap approximately 60 ft wide by 60 ft deep; Gap area shows general N23W 68NE**Fracture Characteristics****Type, Orientation:** TNF (VCF); measured on cliff face, south side of gap – both east and west faces

N24W 61SW

N15W 50SW

N32W 76NE

N40W 75SW – 1mm aperture – Incongruous fracture steps

N56W 59NE

N33W 66SW - undulatory

N44W 76NE

**Spacing:** 1-5m (average 2m)**Separation:****Mineralization:** none**Surface characteristics:** Cuspate incongruous fracture steps noted on one surface**Relative ages:****Apertures:** Generally none**Deformation Bands (width):** NA

**Chart #: 2**

Plan and side views

**Location:** SW1/4 SE1/4 Sec 23 T38N R78W**Lithology:** Unit 2: beach sandstone; 10m below carbonaceous shale**Grain size, cementation:** 177-250 $\mu$ ; calcite cement**Bed thickness:** 10m – not completely exposed**Structure****Strike and dip of bedding:** estimate – N60E 15SE**Structural curvature** (estimated): 1500m**Faulting:** Fault zone; projects trace of fault into gap in chart 1; general trend N25W 75NE; width 7m; continues south along trend 30m to carb shale/bss. Contact approximately 1.5m offset this location**Fracture Characteristics****Type, Orientation:** Fault-zone related fractures (TNF?)

Set A	Set B
N25W 84NE	N65E
N28W 81NE	N55E
N20W 76SW	N49E
N24W 80NE	N54E
N18W 64NE	N53E
N27W	
N28W 60NE	
N20W 90	
N26W	
N22W	

**Spacing:** Average .6m**Separation:** 1.5m offset 30m to south**Mineralization:** None observed**Surface characteristics:****Relative ages:** A set older than set B**Apertures:** erosional apertures**Deformation Bands (width):**

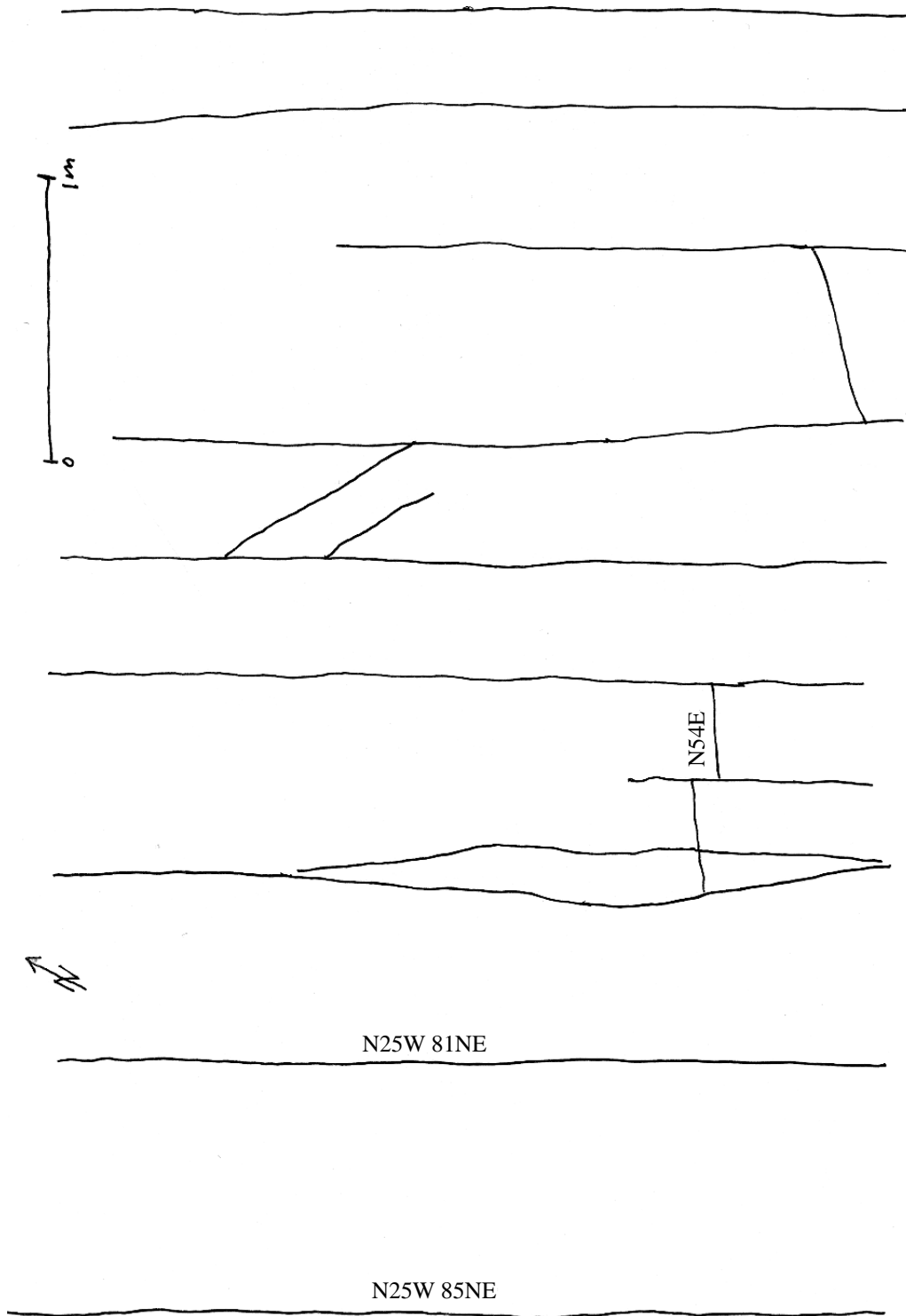


Chart 2: Outcrop map

**Chart #:** 3: plan view

**Location:** SE1/4 SW1/2 Sec 15 T38N R78W

**Lithology:** Unit 1: marine sandstone

**Grain size, cementation:** 125 $\mu$ ; rounded, moderate sorting, well cemented (calcite, siderite)

**Bed thickness:** 22cm

**Structure**

**Strike and dip of bedding:** N22W 16SW; N26W 16SW; N19W 15SW

**Structural curvature** (estimated):

**Faulting:**

**Fracture Characteristics**

**Type, Orientation:** A set: VNF; average between N55-60E.

B set: VXF; average between N30-35W, bed normal.

A set	B set
N52E	N5W
N58E 90	N13W
N56E 90	N34W 74NE
N52E 88SW	N33W 76NE
N52E 88SW	N30W
N48E 88SW	N29W 78NE
N52E 88SW	N20W
N61E	N15W
N55E	N30W 75NE
N58E 85SW	N27W
N57E	N13W
N60E	N20W
N72E 90	N16W
N59E	N22W
N68E 90	N30W 73NE
N55E	N27W
N58E 90	N31W
N60E	N21W
N55E	N27W 76NE
N62E	N25W
N57E	N38W 78NE
N58E	N36W
N57	N29W
N60E	N30W
N55E	N35W 74NE
	N27W

**Spacing:** A set average 4.2/m; B set average 4.0/m

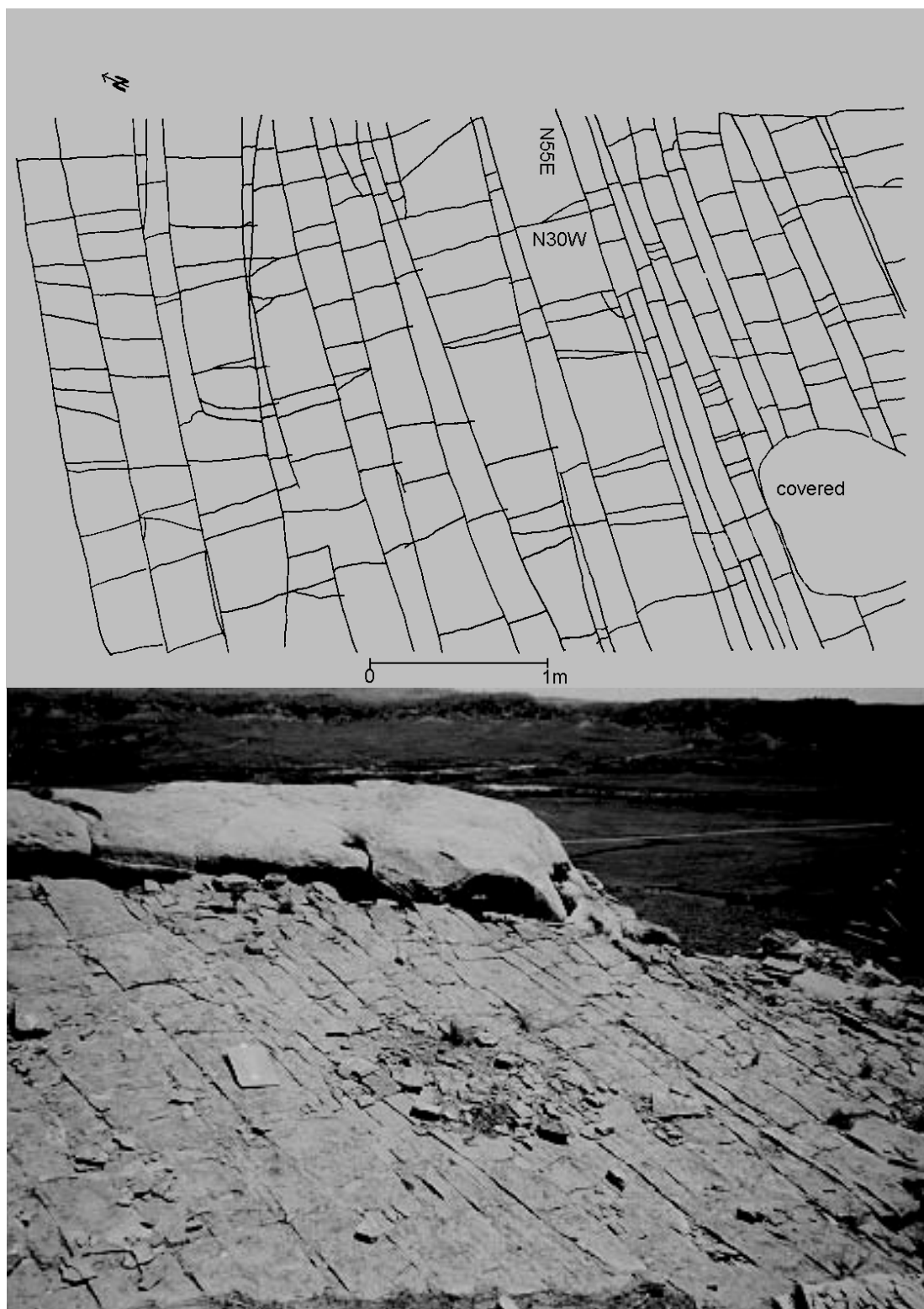
**Separation:**

**Mineralization:**

**Surface characteristics:**

**Relative ages:** A set older

**Apertures:**

**Deformation Bands (width): NA****Chart 3:** Photograph and outcrop map.

**Chart #: 4**

Plan and side views

**Location:** SE1/4 SW1/4 Sec 15 T38N R78W**Lithology:** Unit 3: white beach sandstone (wbss); directly below carbonaceous shale**Grain size, cementation:** 350 $\mu$ ; poorly cemented; easily cut with knife; little calcite**Bed thickness:** 3m**Structure****Strike and dip of bedding:** N33W 18SW; N28W 20SW; N28W 18SW**Structural curvature (estimated):** West limb**Faulting:** NA**Fracture Characteristics****Type, Orientation:** Vertical conjugate (VC) deformation bands

Set A	Set B
N60E 55SE	N55E 52NW
N55E 55SE	N55E 55NW
N58E 55SE	N58E 54NW
N58E 48SE	N58E 48NW
N55E 48SE	N50E 55NW
N58E 55SE	N55E 52NW
N58E 48SE	N55E 56NW
N52E 52SE	N55E 50NW
N56E 48SE	N58E 50NW
N55E 50SE	N58E 48NW
N58E 50SE	N52E 55NW
N58E 50SE	
N52E 55SE	

**Spacing:** 47 individual bands in 20m**Separation:** None observed**Mineralization:** Iron staining within conjugate sets; deformation bands provide the plane of discontinuity in staining.**Surface characteristics:****Relative ages:** Conjugate pairs same age**Apertures:****Deformation Bands (width, mm):** 2,2,2,2,2,2,2,1,2,2,



**Chart #: 5**

Plan and side views

**Location:** NE1/4 NW1/4 Sec 22 T38N R78W**Lithology:** Unit 2: bss; light tan color, 4m below carbonaceous shale; moderately to poorly cemented; better cemented than wbss at chart 4**Grain size, cementation:** 350 $\mu$ **Bed thickness:** 1.5m**Structure****Strike and dip of bedding:** N5E 16NW; N1E 16NW; N2W 20NW**Structural curvature** (estimated): west limb nearer to southern end perhaps 2000m**Faulting:** Fault zone on north cliff face in thick-bedded sandstone; seen at a distance on leaving outcrop**Fracture Characteristics****Type, Orientation:** Set A: average strike N5E, mineralized bed normal fractures, evidenced in thin section.

Set B: cross fractures; average strike N80W

Set A	Set B
N6E	N80W 90
N5E 72SE	N85W
N2E 73SE	N80W
N3E 74SE	N78W 90
N12E	N78W 90
N8E	N80W
N8E	N78W
N8E	N80W
N5E	N78W 90
N15E	N80W90
N12E	
N8E	
N12E	
N6E	
N5E	
N6E	
N10E 69SE	
N7E 82SE	
N15E 80SE	
N5E 75SE	

**Spacing:** Set A: two scan lines (29 fractures in 6m and 25 fractures in 4m) average of 5.4frac/m

Set B; 10 fractures in 18m; 0.55frac/m

**Separation:** none observed**Mineralization:** Resistant to erosion indicating mineralization. Type of mineralization could not be ascertained.**Surface characteristics:****Relative ages:** Set A oldest**Apertures:** none

Deformation Bands (width): NA

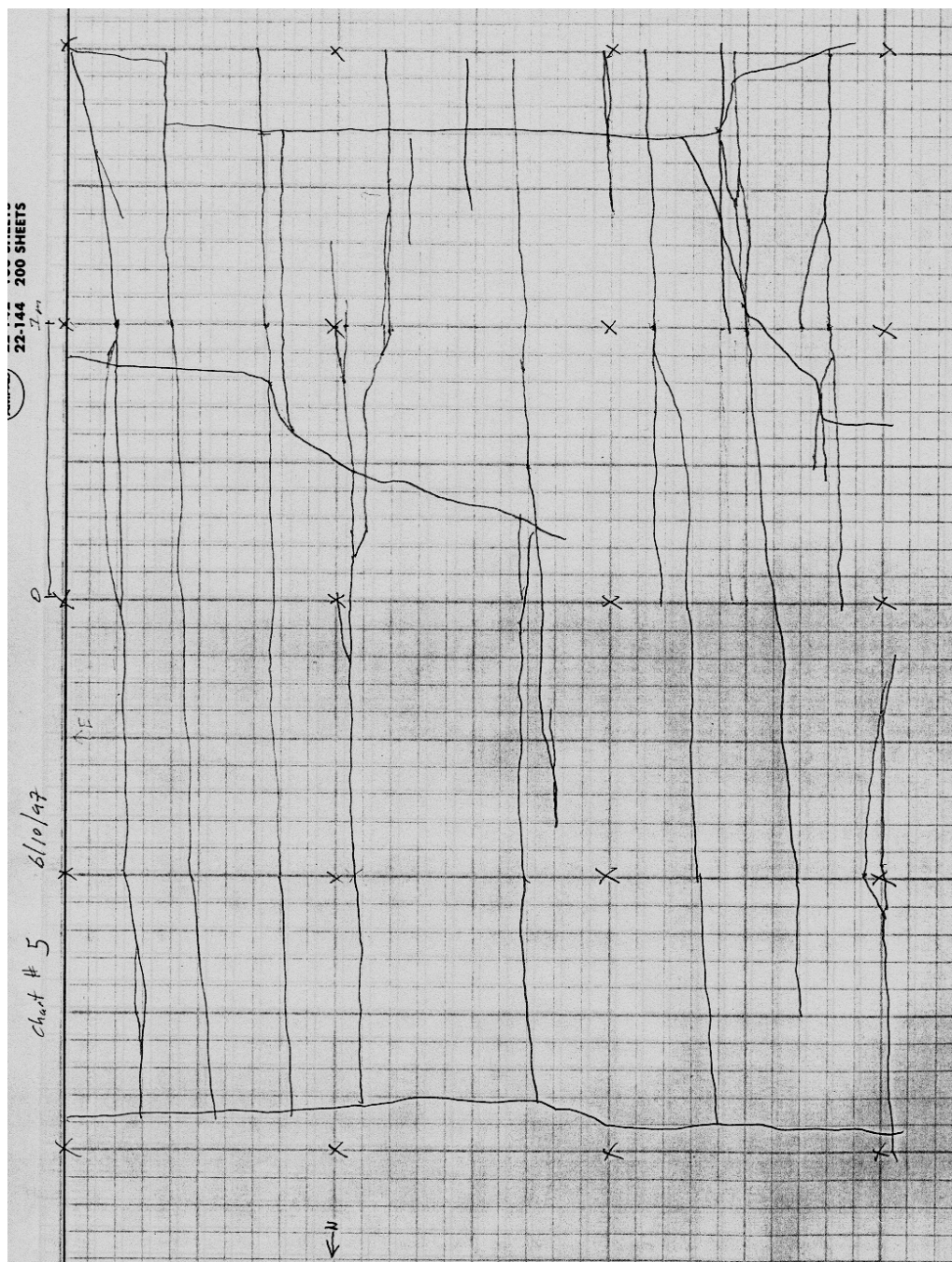


Chart 5: Fracture map.

**Chart #: 6**

Plan and side views

**Location:** NE1/4 NW1/4 Sec 22 T38N R78W**Lithology:** Unit 4: carbonaceous shale**Grain size, cementation:** very fine-grained**Bed thickness:** 2m of thinly laminated carbonaceous shale (1-2mm)**Structure****Strike and dip of bedding:** approximately N23W 10SE**Structural curvature (estimated):** 2000m**Faulting:****Fracture Characteristics****Type and Orientation:** Cleats in carbonaceous shale, bed normal. Set A: average N18W

Set A	Set B	Set C
N15W 53NE	N58E 62NW	N37W 65NE
N18W 60NE	N60E 66NW	N50W 90
N20W58NE	N52E 65NW	
N18W	N55E 65NW	
N8W	N55E 65NW	
N18W 56NE	N55E 65NW	
N18W 56NE	N50E 90	
N15W	N46E 70NW	
N12W	N50E 70NW	
N5W 75SW	N50E 70NW	
	N65E 60SW	
	N60E 60SW	
	N75E 90	
	N70E 90	
	N70E 74 SW	

**Spacing:** Set A 30cm average spacing; Set B spacing 5-20cm, average 10cm**Separation:****Mineralization:** Iron staining along Set A**Surface characteristics:****Relative ages:** Set A older**Apertures:** 1 aperture, 1cm wide**Deformation Bands (width):**

**Chart #: 7**

Plan and side views

**Location:** NE1/4 NW1/4 Sec 22 T38N R78W**Lithology:** Unit 2: beach sandstone, 5m above interbedded unit**Grain size, cementation:** 100-175 $\mu$ , moderately cemented, calcite; note – bed 1/2m directly above this unit is less well cemented and displays fewer fractures**Bed thickness:** .8m-1m (3x8m area)**Structure****Strike and dip of bedding:** N15W 12SW; N20W 15SW**Structural curvature** (estimated): 1500m**Faulting:****Fracture Characteristics****Type, Orientation:** Set A: TNF bed normal. Set B: XF

Set A	Set B
N15E	N72W
N10E	N85E
N10E	N88W
N10E	N85E
N11E	N80E
N3E	N80E
N5W	N80E
N5W	N88E
N5W	N60E
N10W	N60E
N2W	
N15W	
N3W	
N28W	
N28W	
N28W	

**Spacing:** cm; 15,20,30,15,25,20,20,20,5,5,5 (last three measurements are a small fracture swarm). Measurements at this locality are a combination of fracture sets A and B.**Separation:** None**Mineralization:** none**Surface characteristics:** Fractures are eroded/weathered (negative relief)**Relative ages:** Set A older**Apertures:** erosional apertures only.**Deformation Bands (width):** Some deformation bands in less consolidated unit above this measured bed.

**Chart #: 8**

Plan and side views

**Location:** NE1/4 NW1/4 Sec 22 T38N R78W**Lithology:** Unit 2: beach sandstone; stratigraphically 2-4m below carbonaceous shale**Grain size, cementation:** 177-250 $\mu$ , calcite, poor to moderate cementation**Bed thickness:** Entire unit 2m, individual laminae 2-4cm; pavement surface at top of ridge; area 15mX40m**Structure****Strike and dip of bedding:** N35W 11SW; N34W 10SW; N40W; 14SW**Structural curvature** (estimated): 1000m**Faulting:** Two fault zones (normal displacement)

1: fault zone; 1.5m wide; N65E 70SE; down on east side 1m (normal displacement); cuspsate incongruous fracture steps

2: fault zone, 1m wide, located 20m SW of fault zone 1, N65E 70SE, down 1m on south side (normal displacement)

**Fracture Characteristics****Type, Orientation:** Set A: TNF, bed normal; Set B: TNF

Set A	Set B
N3E 76SE	N50E 84SE
N3E	N55E
N3W 78NE	N55E
N1E	N36E
N2W	N44E
N1W	N45E
N3E	N48E
N9W	N53E
N2W	N56E
N5W	N50E
N3E	N60E
N3E	N55E
N4E	N44E
N1E	N52E
N6E	N48E 69SE
N5E 68SE	

**Spacing: (cm)**

Set A	Set B
40	25
10	20
50	9
17	40
45	10
55	35
57	25
45	25
18	10

**Separation:** none observed on fractures

**Mineralization:** mineralized fractures more resistant to weathering; width of mineralized/resistant fracture plane (mm)

Set A	Set B
5	1
5	1
2.5	1
5	1
	2.5
	2

**Surface characteristics:** weathering resistant

**Relative ages:** difficult to determine; Set A is more resistant

**Apertures:** none

**Deformation Bands (width):**

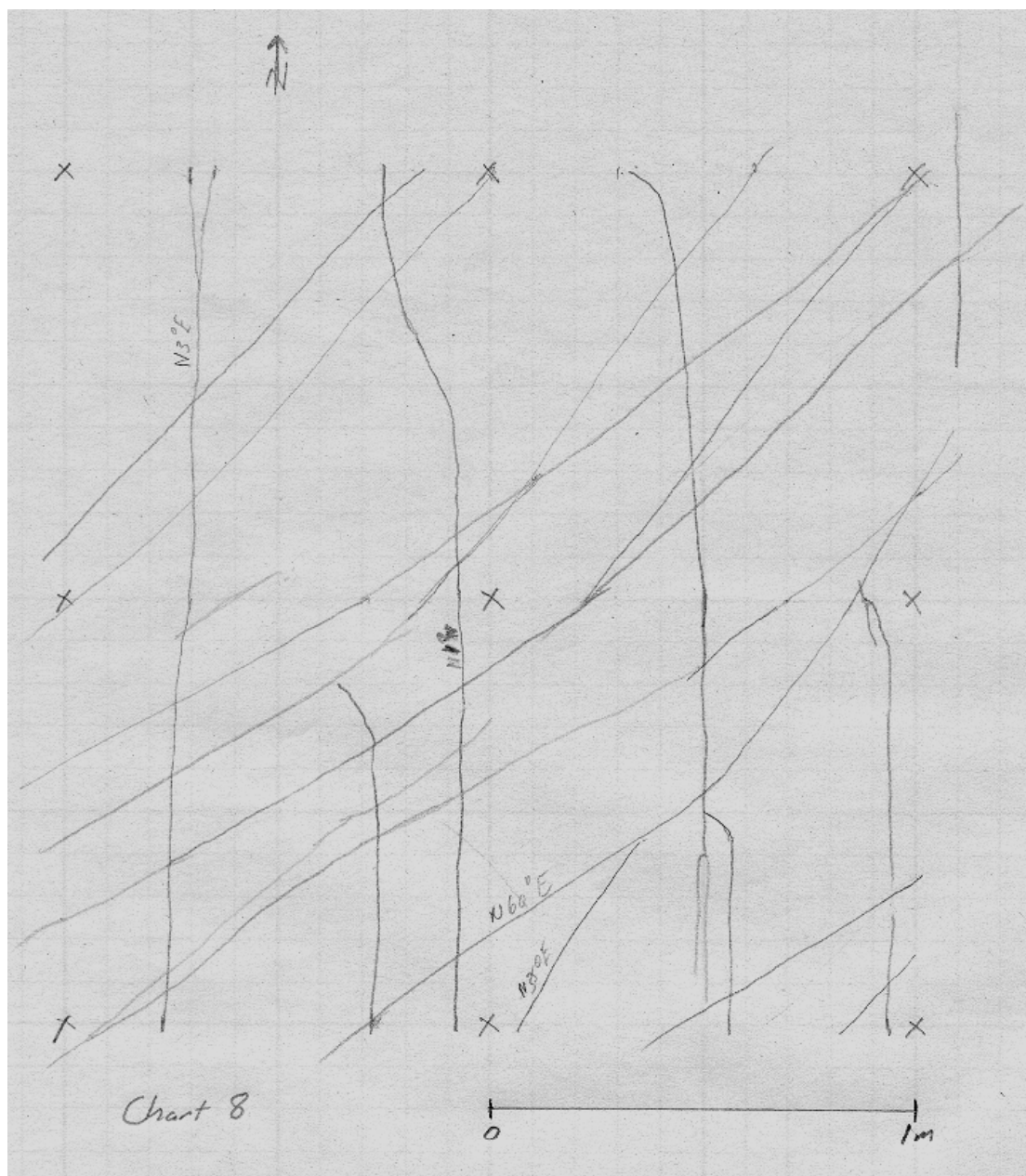


**Chart 8:** Fracture map.

**Chart #: 9**

Plan and side views

**Location:** SE1/4 SE1/4 Sec 9 T38N R78W**Lithology:** Unit 1: Interbedded marine sandstone and shale; numerous trace fossils; 5m thick shale above this unit, 2m thick shale below this unit**Grain size, cementation:** 62-88 $\mu$ ; moderately to well cemented (calcite, siderite)**Bed thickness:** 7cm, area 2x5m**Structure****Strike and dip of bedding:** N3W 24SW; N3W 24SW**Structural curvature** (estimated):**Faulting:****Fracture Characteristics****Type, Orientation:** Set A: TNF bed normal; Set B: TNF bed normal

Set A	Set B
N84W 90	N3E 80SW
N84W 90	N5E 81SW
N85E 88SW	N1W 82NE
N87W 88NE	N8W 80NE
N87W	N3W
N87E 90	N2E 82SW
N88W 88NE	N5E
N86W	N1E80SW
	N2E
	N8W
	N20W
	N2E

**Spacing: (cm)**

Set A	Set B
9	34
2	11
8	12
10	22
4	16
3	13
3	20
8	

**Separation:** none observed**Mineralization:** calcite fills 80% of both fracture sets**Surface characteristics:** calcite filled**Relative ages:** Set A older**Apertures:** (mm) 2,2,1,2,1,2**Deformation Bands (width):** NA



**Chart #: 10**

Cliff exposure

**Location:** SW1/4 NE1/4 Sec 9 T38N R78W**Lithology:** Unit1: shallow marine interbedded sandstone and shale**Grain size, cementation:** 88-125 $\mu$ , calcite cement, moderate to well cemented, reddish bed perhaps some siderite or iron oxide**Bed thickness:** 35cm, area – 13m along cliff face**Structure****Strike and dip of bedding:** N10W 21SW**Structural curvature** (estimated):**Faulting:** None observed**Fracture Characteristics****Type, Orientation:** Fracture spacing increases greatly above and below this bed – due to bed thickness difference? Thinner beds above and below. Fractures in other beds have the same general strikes.

Set A: TNF, bed normal, average trend approximately N70E 80SE

Set B: TNF, bed normal, average trend approximately N15W 65NE

Set A	Set B
N75E 84NW	N15W 64NE
N88W 84SW	N18W 65NE
N81E 85SE	N16W 64 NE
N77E 90	N17W 61 NE
N88E 90	N12W 65NE
N85W	N18W 64NE
N88W	N12W 65 NE
N86E 90	N18W
N84W	N20W 63 NE
N75E	N20W 64NE
N72E	N15W

**Spacing: (cm)**

Set A	Set B
32	45
24	30
8	10
8	15
30	70
9	8
20	30
30	30
30	

**Separation:** NA

**Mineralization:** Mineralized on fracture surfaces. Both fracture sets are mineralized.

1. euhedral calcite crystals
2. Tabular white crystals (does not react with HCl) possibly gypsum or anhydrite
3. black to very dark red cubic crystals (1mm x 1mm x 1mm) hard, pyrite in center
4. Manganese dendrites

**Surface characteristics:** some rib and plumose structures indicating fracture propagation both into and out of cliff along both fracture sets

**Relative ages:** With cliff face exposure age relationship is difficult to determine.

**Apertures:** Set A; 1-3mm, 2mm average, 1 aperture is 2cm – this could be recent.  
Set B; 0-1mm 2mm average, 1 aperture is 1cm – this could be recent.

**Deformation Bands (width):** NA

**Chart #: 11**

Plan and side views

**Location:** NW 1/4 SE 1/4 Sec 9 T38N R78W**Lithology:** Unit 5: Reddish/brown, fluvial sandstone, siderite-enriched lens.**Grain size, cementation:** 88-125 $\mu$ , moderate to well cemented, siderite**Bed thickness:** 18cm, area – 10m X 6m**Structure****Strike and dip of bedding:** N5E 23NW  
N5E 23NW**Structural curvature** (estimated): west limb, curvature not apparent**Faulting:** larger scale faulting not apparent**Fracture Characteristics****Type, Orientation:**

Set A: TNF, N55W, 90° dip – some curvature in a few (8 approx.) of these, not all are completely through going. Fractures do not continue in less cemented sandstone underneath.

Set B: XF, N12E, somewhat oblique to fracture set A. Fractures continue into underlying sandstone

Set A	Set B
N70W Near vertical dips	N11E 62SE
N65W	N12E 62SE
N50W	N7E
N60W	N9E 58SE
N62W	N28E
N52W	N10E
N62W	N15E
N52W	N10E
N70W	
N60W	
N63W	
N67W	
N55W	
N70W	
N65W	
N72W	

**Spacing: (cm)**

Set A	Set B
27	95
26	105
40	50
32	100
21	
20	
15	
5	

10 17 30 15 23	
----------------------------	--

**Separation:** NA

**Mineralization:** none

**Surface characteristics:** not apparent

**Relative ages:** A is older due to abutting relationships.

**Apertures:** No apertures on fractures furthest away from cliff edge. Some fractures are open to 1-2cm near edge. Therefore, fracture apertures are recent.

**Deformation Bands (width):** none

**Chart #: 12**

Plan and side views

**Location:** NW1/4 SE1/4 Sec 9 38N R78W**Lithology:** Unit 5: Light brown fluvial sandstone in carbonaceous shale unit.**Grain size, cementation:** 125-177 $\mu$ , poor to moderate cementation, very little cementation**Bed thickness:** 1m – dark (black) carbonaceous shale directly underneath sandstone bed**Structure****Strike and dip of bedding:** N2W 22SE; N1E 24NW**Structural curvature** (estimated): west limb, curvature not apparent**Faulting:** no larger scale faulting observed**Fracture Characteristics****Type, Orientation:** Set A: TNF, bed normal, N15W 62NE

Set B: XF, N85E, vertical

Set A	Set B
N5W bed normal	N83E vertical
N10W 68NE	N76E
N5W bed normal	N78E
N5W	N82E
N6W bed normal	N83E
N9W	N87E
N12W	N68E
N10W	N75E
N16W bed normal	N73E
N8W 62NE bed normal	N72E

**Spacing: (cm)**

Set A	Set B
60	120
30	70
45	90
20	60
35	60
20	70
25	85
19	110
65	37

**Separation:** not apparent**Mineralization:** none**Surface characteristics:** not apparent**Relative ages:** Set A is older.**Apertures:** Open approaching outcrop edge. No apertures going into hillside (down dip direction).**Deformation Bands (width):** NA

**Chart #: 13**

Plan and side views

**Location:** NW1/4 SE1/4 Sec 9 T38N R78W**Lithology:** Unit 1: Interbedded sandstone and shale. Bed directly overlying this sandstone bed is shale. Sandstone above is approximately 8m thick, the base of which exhibits sedimentary loading features.**Grain size, cementation:** 175-177 $\mu$ , moderate to poor cementation (very little calcite)**Bed thickness:** 1 to 1.4m, area – 30m of cliff exposure**Structure****Strike and dip of bedding:** N1W 23SW; N3W 21SW**Structural curvature** (estimated): west limb, curvature not apparent**Faulting:** No large scale faulting observed. Note inferred fault through pond and valley to the south. NE1/4 Sec 16**Fracture Characteristics****Type, Orientation:** Set A: TNF, N3W 46NE. Set B: XF, N89W 60NE

Set A	Set B
N5W 45NE	N64E 82NW
N14W 46NE	N82W 60NE
N17W 45NE	N89W 59NE
N4W 46NE	N89E 72NW
N14W 57NE	N88W 81NE
N1W 47NE	N88E 84NW
N3W 49NE	N87E 59SE
N4W 53NE	Other (cross fractures)
N0 54E	N35W 45E
	N56E 81SE

**Spacing:** (cm)

Set A	Set B
80	90
35	29
65	70
40	180
80	130
60	60
55	60

**Separation:** Set A; N3W 46NE down 1cm NE**Mineralization:** none – apertures generally filled with shale/clay**Surface characteristics:** Somewhat conchoidal on some surfaces (Set B) to smooth**Relative ages:** Set B – does not have direct extension into cliff face and are therefore younger. (They do not cut Set A.)**Apertures:** Set A – apertures common from 0-1cm (0.3cm average) and are filled with clay/shale. Not mineralized.

Set B - undetermined

**Deformation Bands (width):** NA

**Chart #: 14**

Plan and side views

**Location:** SW1/4 NE1/4 Sec 9 T38N R78W**Lithology:** Unit 2: Pavement in beach sandstone, light reddish brown. White poorly cemented beach sandstone directly on top of this pavement. One deformation band, N70E 90°, in the light colored sandstone.**Grain size, cementation:** average 125-177 $\mu$ , some grains 177-250 (10%), moderate to well-cemented (lots of calcite, probably some siderite (reddish color))**Bed thickness:** 10cm overall – this bed is thinly laminated with laminae width varying 3½ cm, 2cm, 4½ cm, some are thinner laminae - 0.5–1cm**Structure****Strike and dip of bedding:** N11W 26SW; N14W 22SW**Structural curvature** (estimated): west limb curvature not apparent**Faulting:** Possible larger scale fault through valley and Conley Res. separating the limbs.**Fracture Characteristics****Type, Orientation:** Set A: VEF (TNF) bed normal – a) N10W 68NE, bed normal, b) N24W 62NE, bed normal. Set B: oblique XF (TNF?), N62W dip vertical to 85NE.

Set A	Set B
N1W bed normal	N60W 90
N4W bed normal	N62W 88NE
N8W 68NE	N62W
N22W 66NE	N62W
N20W 66NE	N63W
N5W bed normal	N68W
	N63W
	N68W
	N65W
	N62W
	N62W

**Spacing: (cm)**

Set A	Set B
55	30
45	33
102	19
	30
	34
	49
	14
	18

Note: Spacing appears to increase down dip – limited exposure to prove this, but is suggestive.

**Separation:** Offset undetermined.**Mineralization:** none

**Surface characteristics:** Some Set B fractures have an en echelon pattern. Some Set B fractures turn parallel to Set A at intersection. Some Set B fractures curve to intersect Set A at a 90° angle. See drawing.

**Relative ages:** Set A is older due to the abutting relationship.

**Apertures:** 0-0.5cm apertures decrease to 0cm with distance from edge of outcrop (to west) down dip.

**Deformation Bands (width):** 2m in white sandstone, NA to pavement.

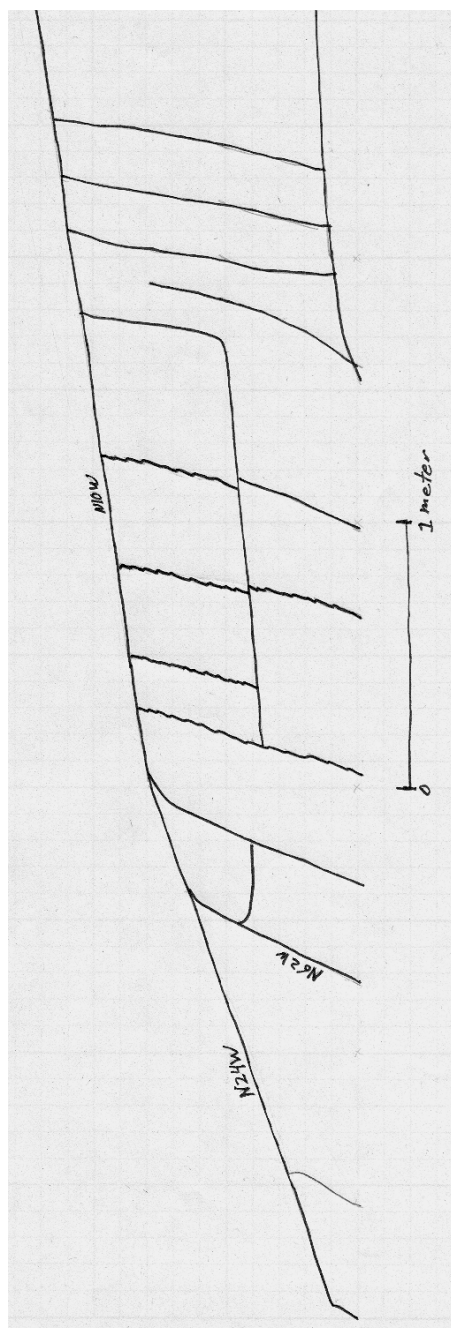


**Chart 14:** fracture map



**Chart #: 15**

Plan view

**Location:** SW1/4 NE1/4 Sec 9 T38N R38W**Lithology:** Unit 2: Dark reddish brown – iron (siderite)-enriched zone in upper layer of beach sandstone.**Grain size, cementation:** generally 125-177 $\mu$ , approximately 20% 177-259 $\mu$ ; well cemented**Bed thickness:** 10cm (white beach sandstone above this bed), area – 10m X 3m, irregular, caps whitish beach sandstone, isolated**Structure****Strike and dip of bedding:** N13W 24SE

N14W 27SE

**Structural curvature** (estimated): west limb, curvature not apparent**Faulting:** Not observed (large scale)**Fracture Characteristics****Type, Orientation:** Set A: TNF (VE). Set B: XF (oblique). Set C: other.

Set A	Set B	Set C
N26E 55SE	N60W 90	N4W 76NE bed normal
N45E 65SE	N63W 88SW	N4W 76NE bed normal
N42E	N60W 90	
N36E 54SE	N64W	
N50E 53SE	N64W	
N40E 59SE	N60W	
N36E 50SE	N55W 90	
N35E	N55W	
N33E 64SE	N63W	
N33E	N60W	
N36E 61SE		

**Spacing: (cm)**

Set A	Set B	Set C
82	20	
28	28	
28	23	
55	150	
32	55	
45	20	
25	10	
18	15	
29	20	
25	100	
	40	

**Separation:** not observed**Mineralization:** none

**Surface characteristics:** generally smooth

**Relative ages:** Set A is older than Set B due to abutting relationship. Set C only 2 of these in outcrop and are not extensive.

**Apertures:** Some aperture opening near outcrop edges to 1cm (recent).

**Deformation Bands (width):** NA

**Other observations:**

Set C fractures are 5cm apart. Neither continues through the outcrop. Longest is 2m from outcrop edge to end. Fracture extends into less cemented beach sandstone below.

One Set A fracture abuts a set C fracture. This single abutting relationship is interpreted as occurring recently or during set C formation.

One Set B fracture abuts set C fractures turning to intersect perpendicularly.

One Set B cross fracture curves to intersect Set A fractures and cuts 2 of them first.

**Chart #: 16**

Side view

**Location:** NW1/4 SW1/4 Sec 9 T38N R78W**Lithology:** Unit 1: thin-bedded shallow marine sandstone with some ripple marks and trace fossil evidence, light brown**Grain size, cementation:** 66-88 $\mu$ , fine grained, moderate calcite cementation**Bed thickness:** 30cm overall – individual beds (laminae) 1/2 cm – 4cm; 1/2 - 1cm average, area – 0.5m (enters under shale) X 15m, continues around nose of ridge to N.**Structure****Strike and dip of bedding:** Broken blocks may have shifted due to shales above and below. Therefore, these may not be highly accurate.

N47W 11SW; N50W 15SW; N48W 10SW

**Structural curvature** (estimated): 500m radius**Faulting:** Large-scale (probable) N-S through bottom of draw and South terminal**Fracture Characteristics****Type, Orientation:** Set A: TNF, N85W 85SW. Set B: TNF, N5W 68NE.

Set B	Set A
N85W 85SW	N5W 68NE
N74W	N8W
N80W	N5E
N75W	N3E
N82W vertical	N4E 77SE
N79W	N1E 81SE
N80W vertical	N7E 81SE
N79W 87NE	N7E 73SE
N88W 90	N10W 72SE
N64W 90	N6E
	N4W 78NE
	N4W

\* Due to differential weathering of laminae dips hard to obtain.

**Spacing:** (cm)

Set B	Set A
30	35
30	35
40	25
30	70
70	30
30	60
20	

\* Spacing hard to measure due to infilling (alluvial cover) around blocks.

**Separation:** Hard to evaluate with silty shales filling most apertures.

**Mineralization:** Loose slabs have iron (Fe) staining 3cm into matrix from the fracture surface.

**Surface characteristics:** Rough – some laminae are more resistant than others are. No fracture surface characteristics.

**Relative ages:** Very hard to determine, but it appears that some Set B fractures terminate against Set A. Therefore, Set A older.

**Apertures:** 0-8cm – sandy brown shales from above and below fill apertures. Therefore, apertures may have widened recently.

**Deformation Bands (width):** NA

**Chart #: 17**

Plan view. 100m SW of Chart 16.

**Location:** NE1/4 SE1/4 Sec 22 T38N R78W**Lithology:** Unit 2: Base of beach sandstone (Kmv), medium tan/brown beach sandstone**Grain size, cementation:** 177-250 $\mu$ , moderate cementation**Bed thickness:** 1 1/2 m – unit below light tan, poorly cemented sandstone (Kmv beach sandstone). Unit above light tan poorly cemented – some iron cemented trace fossils.

Area – 20m X 30m

**Structure****Strike and dip of bedding:** N52W 9SW; N90W 8S; N60W 9SW

\* Cross beds make finding true strike and dip surface difficult.

**Structural curvature** (estimated): 200m R**Faulting:** One large-scale fault observed on east-facing cliff to west of this outcrop across draw. Appears to be 1-1 1/2 m offset down on N side into anticline.**Fracture Characteristics****Type, Orientation:** Set A: TNF, N10W 81NE bed normal\*. Set B: TNF, N55E 86SE\*. Set C: XF, N70W vertical\*. Set D: XF, N24W vertical\*. \* one example of each – not an average.

Set A	Set B	Set C	Set D
N10W 81NE	N55E 86SE	N70W vertical	N24W vertical
N8W 90	N50E 88NW	N80W	N10W
N2W 88NE	N55E 78SE	N55W	N20W
N2E 88SE	N50E 86SE	N75W	N28W
N5W 85NE	N50E 90	N89W	
N9W 83NE	N52E		
N8W 85NE	N56E		
N4E 82SE	N50E		
N8W 86NE			
N10W 75NE			
N8W			
N8W			

**Spacing: (cm)**

Set A	Set B	Set C	Set D
Extensive throughout outcrop	Swarms of 2 or 3 every 2m	Closely spaced 5-30cm, average is 20	Closely spaced 5-30cm, average is 20
45			
20			
10			
40			
10			
12			
5			
10			

40			
10			
30			
20			

**Separation:**

**Mineralization:** none

**Surface characteristics:**

**Relative ages:** Cross fractures are younger. Set A younger than Set B (but highly speculative).

**Apertures:** apertures to 1cm - more at outcrop edges

**Deformation Bands (width):**

**Other observations:** This is a very confusing outcrop, with possibly 2 TNF and XF sets. Some of XF curve to intersect TFN perpendicularly.

Some of the fracture curving may be due to siderite nodules.

**Chart #: 18**

Side view

**Location:** NW1/4 NW1/4 Sec 26 T38N R78W**Lithology:** Unit 2: beach sandstone**Grain size, cementation:** 177-250 $\mu$ , poorly cemented, very little calcite, if any**Bed thickness:** Entire cliff face approx. 20m. Individual beds 1/2m to 2m (1½m average in sandstone). Area – 26m long X 20m high.**Structure****Strike and dip of bedding:** (Taken from west to east along cliff face)

N77E 85SE; N40E 5SE; N77E 65SE

**Structural curvature** (estimated): Southern tip – 200m R approx.**Faulting:** Inferred fault in valley, striking parallel to anticline hinge. West limb down relative to east limb, with approximately 20 m of normal separation with displacement decreasing toward the south.**Fracture Characteristics****Type, Orientation:** Set A: VCF, N30W 66NE. Set B: VCF, N25W 72SE.

Set A	Set B	Other
N34W 76NE N30W 67NE N28W 72NE	N10W 85SW N28W 72SW N35W 76SW N15W 66SW	N0E vertical

\* Majority of VCF sets too high on cliff for measurement.

**Spacing:** (cm) approximate spacing 1-2cm**Separation:** is normal, varies from 0-20cm**Mineralization:** none**Surface characteristics:** some incongruous fracture steps observed.**Relative ages:** VCF sets same age**Apertures:** none**Deformation Bands (width):** In poorly to very poorly cemented sandstone, deformation bands 1-2mm wide.**Other observations:** Small anticlinal structure, SE of South terminal S facing cliff.

Slide of offset fracture zone with incongruous fracture steps – part of larger conjugate fracture set.

**Chart #: 19**

Plan and side view

**Location:** NW1/4 NW1/4 Sec 26 T38N R38W, approximately 60 meters south of south terminal.**Lithology:** Unit 1: interbedded sandstone and shale, light tan, light tan shales below**Grain size, cementation:** 88-125 $\mu$ , poor – moderate cementation**Bed thickness:** 20cm, area – 6 X 8m pavement**Structure****Strike and dip of bedding:** N48W 75SW, N43W 80SW

Note – – why this strike? Perhaps fold at Chart 18 is apex of anticline?

**Structural curvature** (estimated): South end**Faulting:** Inferred fault in valley, striking parallel to anticline hinge. West limb down relative to east limb, with approximately 20 m of normal separation with displacement decreasing toward the south. Same inferred fault as described in chart 18.**Fracture Characteristics****Type, Strike:** Set A: TNF, N75E vertical. Set B: XF, N5W 90. Set C: TNF. Set D: XF.

Set A	Set B	Set C	Set D
N82E 90	N5W 90	N5W 90	N85E 85SE
N75E 90	N2E	N8W 90	N85W 90
N85E90	N10W	N8W 90	N88E 90
N88E	N5W	N5W 90	
N85E	N1E		
N82E	N3E 85NW		
N78E			
N81E vertical			

**Spacing:** (cm)

Set A	Set B	Set C	Set D
20	215	15	30
40	80	15	35
30	70	30	25
88			28
45			25
35			75
150			

**Separation:** not observed**Mineralization:** none**Surface characteristics:** planar**Relative ages:** Set A older than Set B. Set C older than Set D. Can draw no relationship between Sets A and B and Sets C and D.**Apertures:** Set A – 2-3m average**Deformation Bands (width):**



**Chart #: 20**

Plan and side views

**Location:** NW1/4 NW1/4 Sec 26 T38N R78W**Lithology:** Unit 1: interbedded sandstone and shale**Grain size, cementation:** fine grained sandstone 62-88 $\mu$ , poor to moderate cementation**Bed thickness:** 25cm in bed where most readings were taken, area – approximately 26m long X 4m wide (average) X 10m high**Structure****Strike and dip of bedding:** N45W 7SW; N55W 5SW**Structural curvature** (estimated): 100m**Faulting:** Fault bounded. This is assumed to be a fault sliver – view to south. From this view, axis of anticline could be to east of valley near charts 18 and 19. This is interpreted to be part of the inferred fault as described in charts 18 and 19.**Fracture Characteristics****Type, Orientation:** Set A: TNF. Set B: XF.

Location I: The fracture set A is expressed as the cliff face on SW side of this block.

Set A	Set B
N20W	N85E vertical
N18W	N68E
N24W 85SE	

Location II: Siderite enriched pavement 10m north of previous measurements and 4m down

Set A	Set B
N8W 72NE	N75E vertical
N18W 76NE	N85E
N15W 76NE	N78E
N15W	N85E
	N70W
	N82E
	N80E

**Spacing:** (cm)

Location I: Set A: 20cm. Set B: 30cm.

Location II:

Set A	Set B
25	90
45	35
35	43
39	39
	35
	30

**Separation:** 0-10cm down west, normal movement**Mineralization:** NA**Surface characteristics:** rough to planar**Relative ages:****Apertures:****Deformation Bands (width):** NA

**Chart #: 21**

Plan view

**Location:** NE1/4 SE1/4 Sec 22 T38N R78W**Lithology:** Unit 3: white to very light tan, beach sandstone, numerous cross-beds (very rounded, eroded surface)**Grain size, cementation:** 80% 177-250 $\mu$ , 20 % 250-350 $\mu$ , very poorly to poorly cemented**Bed thickness:** 3m approx., area – 10 X 15m**Structure****Strike and dip of bedding:** N35W 5SW\* ; N40W 13SW\*

\* Due to cross bedding, strike and dip are difficult to obtain with accuracy.

**Structural curvature** (estimated): 300m approximate**Faulting:** One of the deformation bands in a better cemented reddish overlying bed has 6cm normal separation down on NE. No larger scale faulting observed.**Fracture Characteristics****Type, Orientation:** Set A: deformation bands. Set B: deformation bands

Set A	Set B
N2W 90	N55E
N1W 69NE	N55E
N5W	N54E 77SE
N6W	
N2E 63NW	
N3W	
N3W 88NE	
N8W	
N4W 66NE	
N2W 90	
N8W 64NE	
N6E	
N7W	

**Spacing:** (cm) Set A: spacing of clusters – average 2m between clusters - see drawings  
Set B: spacing 80 and 90 cm. Few other cross fractures in exposure. Therefore, larger spacing than number has shown.**Separation:** One band 6cm normal offset, down on NE, see faulting data above.**Mineralization:** NA**Surface characteristics:** not observed**Relative ages:** Set A is older.**Apertures:** none**Deformation Bands (width):** (mm) 1-2mm average

1, 2, 4, 2, 1, 3, 1, 2

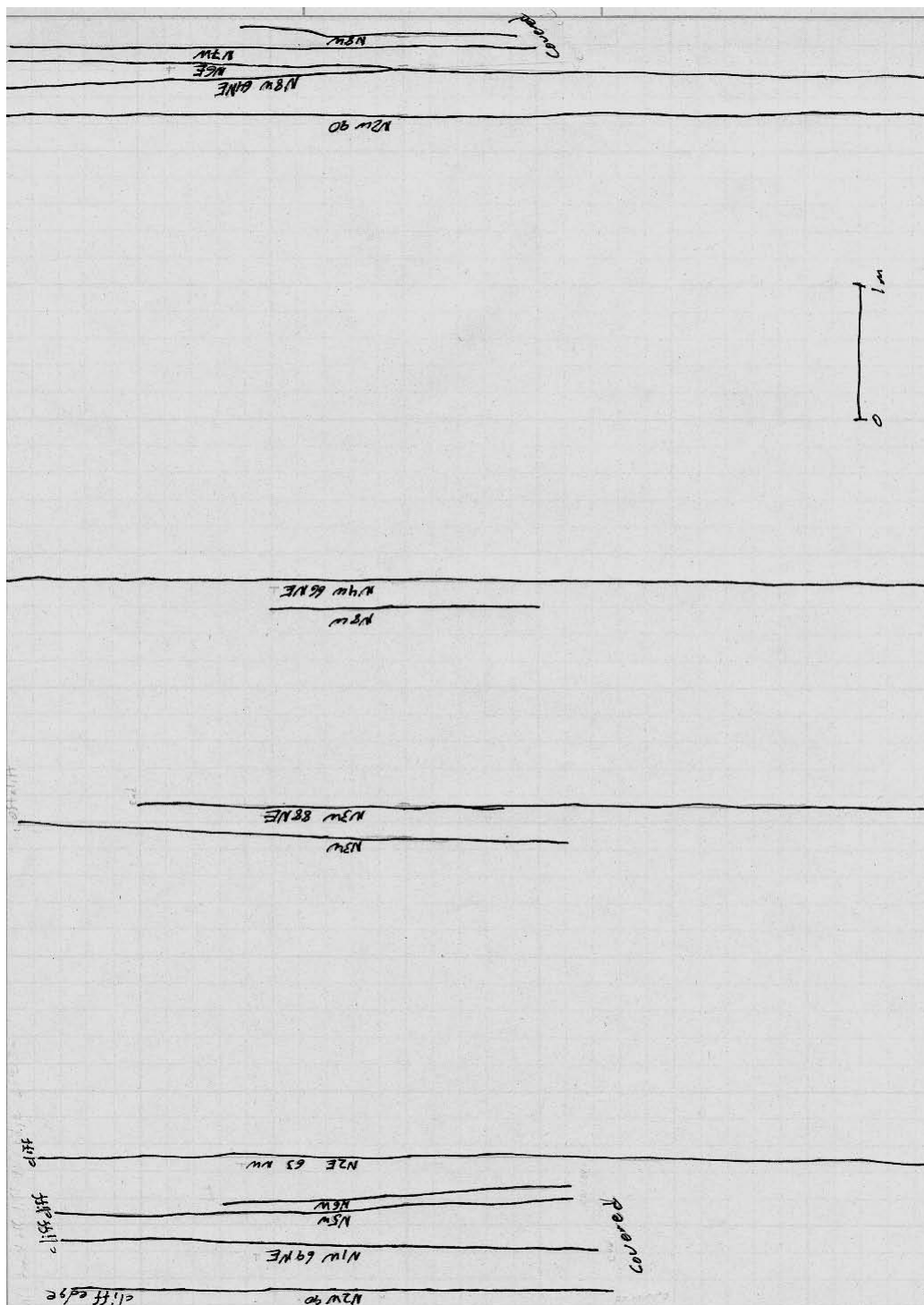


Chart 21: Map of set A deformation band clusters.

**Chart #: 22**

Plan and side view

**Location:** SE1/4 SE1/4 Sec 22 T38N R78W**Lithology:** Unit 5: fluvial sandstone, light tan**Grain size, cementation:** 122-175 $\mu$ , poor cementation**Bed thickness:** 2-3m, 2 1/2 m average, area – whole area approx. 2 acres**Structure****Strike and dip of bedding:** N65W 10SW – this is an estimate, due to lack of reliable bedding surfaces**Structural curvature (estimated):** 500m R**Faulting:** NA**Fracture Characteristics****Type, Orientation:** Set A: TNF, N55W 69NE. Set B: TNF, N60E 77SE  
85% (visually) of A and B are deformation bands.

Set A*	Set B*
N55W 69NE	N60E 77SE
N55W	N55E
N58W	N58E
N40W	N55E 72SE
N48W 72NE	N45E 86SE
N50W 70NE	N55E 72SE
N65W 76NE	N56E 70SE
N53W 85SW	N50E
N56W 72NE	N52E
N70W 71NE	N55E
N65W 89NE	N52E
N55W	N55E 72SE
N58W	

\* Appears to be same number of each, although Set A are generally more developed/noticeable.

**Spacing:** (cm) Set A - estimate 70cm average. Set B - estimate 90cm average.

Set A	Set B
30	95
60	40
10	45
20	110
100	30
20	90
50	90
15	
70	
140	
70	

65	
70	

**Separation:** none observed

**Mineralization:** none observed

**Surface characteristics:** no observable features.

**Relative ages:** Slight displacement on Set B (in some places – none in others) suggests Set A older.

Note: One place suggests Set B older – one Set A ends at one Set B.

**Apertures:** none

**Deformation Bands (width):** 1-2mm average for both sets. Largest width of Set B is 4mm and is actually an anastomosing set of 3 deformation band (individual bands are approximately 1mm wide).

**Chart #:** 23

Plan view

**Location:** SE1/4 SE1/4 Sec 22 T38N R78W

**Lithology:** Unit 2: upper beach sandstone

**Grain size, cementation:** 125-177 $\mu$ , poorly to moderately cemented

**Bed thickness:** 2m, area – 1 acre

**Structure**

**Strike and dip of bedding:** N64W 10SW

**Structural curvature (estimated):** 250m

**Faulting:**

**Fracture Characteristics**

**Type, Orientation:** Set A: TNF, N5-10W 65NE. Set B: TNF, N55-60W 65NE. North to south traverse, fracture strike changes as follows/ all dips “appear” NE

Set A	Set B
N10W	N50W 58NE
N20W 70NE	N52W
N30W	N40W
N28W 62NE	N45W
N20W	N50W 46NE
N13W 64NE	N50W
N5W 58NE	N70W
N15W	N72W
N12W	N60W

**Spacing:** (cm) very closely spaced, 5-10cm

**Separation:** Not observed

**Mineralization:**

**Surface characteristics:** vertical slickensides north end

**Relative ages:**

**Apertures:** none

**Deformation Bands (width):**

**Other observations:** This is a very confusing area for me. Fractures appear to change strike with no overlapping or abutting relationships between the fracture sets. These fractures may be a pavement surface representation of a small scale fault that curves along strike or they could be two separate sets as shown above.

**Chart #:** 24

**Location:** SW1/4 SW1/4 Sec 23 T38N R78W

**Lithology:** Unit 1: thin-bedded marine sandstone, may be equivalent unit to chart 16.

**Grain size, cementation:** Fine-grained sandstone, 62-88 $\mu$ , possible 10% 88-125 $\mu$ , moderate cementation, calcite

**Bed thickness:** 20cm, thick units of shale above and below – 5m above – total extent below unknown - at least 5m, area – 30m long X 2m wide

**Structure**

**Strike and dip of bedding:** N50W 10SW; N48W 8SW

**Structural curvature (estimated):** 300m

**Faulting:**

**Fracture Characteristics**

**Type, Orientation:** Set A: TNF. Set B: TNF

Set A	Set B
N72W 90	N5W 85NE *
N69W 90	N4W 81NE *
N70W 90	N13W 78NE *
N71W 90	N8W 85NE **
N62W 90	N10W 83NE **
N70W86SW	N15W 83NE **
N70W 90	N10W
N70W 86SW	N15W
N67W	
N80W	
N85W 90	
N85E 90	

\* These are 10m north of measured Set A fractures – calcite mineralization on these 3 fracture surfaces, 1mm thick.

\*\* spatially located with Set A fracture exposure – calcite mineralization, 1-2mm thick.

**Spacing:** (cm)

Set A	Set B
49	25 (none for 1m either side – no exposure left in that area)
57	
52	40
110	45
100	40
47	15
10	30
65	55

**Separation:** none observed

**Mineralization:** Some calcite mineralization on fracture surfaces – suggesting open apertures. Calcite vein widths perpendicular to fracture surface; mineralization mainly on Set B. Crystals, in float, up to 3-4mm wide.

**Surface characteristics:** not apparent

**Relative ages:** Set A is possibly older than Set B. Could not find an area to determine age relationship between Sets A and B – one area suggests Set A older than Set B, but is partially covered. Set A more prominent, especially at south end of exposure.

**Apertures:** Set A – [8cm, 2cm, 4cm, 1cm – probably recent due to movement down slope.] [5mm, 3mm, 0,0]

Set B – [0, 1mm, 2mm, 3mm, 2mm, 1cm]

**Deformation Bands (width):** NA



**Chart #: 25**

Side view

**Location:** NW1/4 NW1/4 Sec 23 T38N R78W**Lithology:** Unit 4: carbonaceous shale – just above beach sandstone contact**Grain size, cementation:** clay size, dark black carbonaceous shale, very poor cementation, very fissile**Bed thickness:** 1-1 ½ m, area – 25m long X 1m wide**Structure****Strike and dip of bedding:** N42W 12SW**Structural curvature** (estimated): 150m R**Faulting:****Fracture Characteristics****Type, Orientation:** very irregular, could not determine type

Set A	Set B	Set C	Set D
N89W N75W 90 N75W 90 N85W 85SW N85E 65SE N70W 86NE N60W 85NE	N6W N2E 68SE N2W 72NE N5W 90 N8W 80NE N1W 74NE	N15E 55SE	N45E 50NW N70E 75SE N65E

Magnitude of A to B – 3 :2; Set D is rare – 1 in 10; Set C is rarest – 1 in 30?

**Spacing:** (cm)

Set A: 20-40cm spacing with larger intervals – not uniformly found

Set B: 5-10cm spacing with 8cm average, but not uniformly found

**Separation:** unable to determine**Mineralization:** iron staining on 1/3 to 1/2 of surfaces**Surface characteristics:****Relative ages:** unable to determine**Apertures:** possibly 1mm (this could be recent)**Deformation Bands (width):** NA

**Chart #: 26**

Plan and side views

**Location:** NW1/4 NW1/4 Sec 26 T38N R78W**Lithology:** Unit 3: upper beach sandstone, cross-bedded**Grain size, cementation:** 125-177 $\mu$ , poorly cemented**Bed thickness:** Measurements taken on a 1m thick cross-bed set. Total thickness here of sets approximately 15m. Area – 4m X 7m**Structure****Strike and dip of bedding:** N45W 11SW**Structural curvature** (estimated): 100m R**Faulting:** Larger scale fault evidenced by displacement, across axis of anticline – from one limb to the other, of the beach sandstone. The deformed rock exposure 8m north of this site may be evidence for that fault.**Fracture Characteristics****Type, Strike:** Set A: systematic deformation bands – appear to become fractures in Fe enriched, better cemented beds below. Fractures have decreased spacing (20cm average) relative to deformation bands of set A.

Set B: deformation bands, perpendicular to bedding, discontinuous.

Set A	Set B	Other
N7E 80SE N3W 78NE N2W 88NE N2W 78NE N3E 73SE N4E 78SE N8E 80SE N3E N8E 83SE N1E 72SE N6E 78SE	N45E 67SE N50E 58SE	N30E 70NW

**Spacing:** (cm) Fractures in a better cemented sandstone bed exhibits decreased spacing relative to the deformation bands.

Set A – 45, 50, 78, 45, 39, 64, 50 cm

Set B – 2 bands spaced 1m apart

**Separation:** none observed**Mineralization:** none observed**Surface characteristics:** raised (resistant to erosion) deformation bands**Relative ages:** Set A is older. See drawing.**Apertures:** none**Deformation Bands (width):** Set A – 1mm, 2mm, 3mm, 4mm, 1mm, 2mm, 2mm

Set B – 1mm, 3mm

**Other observations:** General observation of fractures within Unit 2 (beach sandstones) near this area indicates that fractures generally strike north and dip to the east.

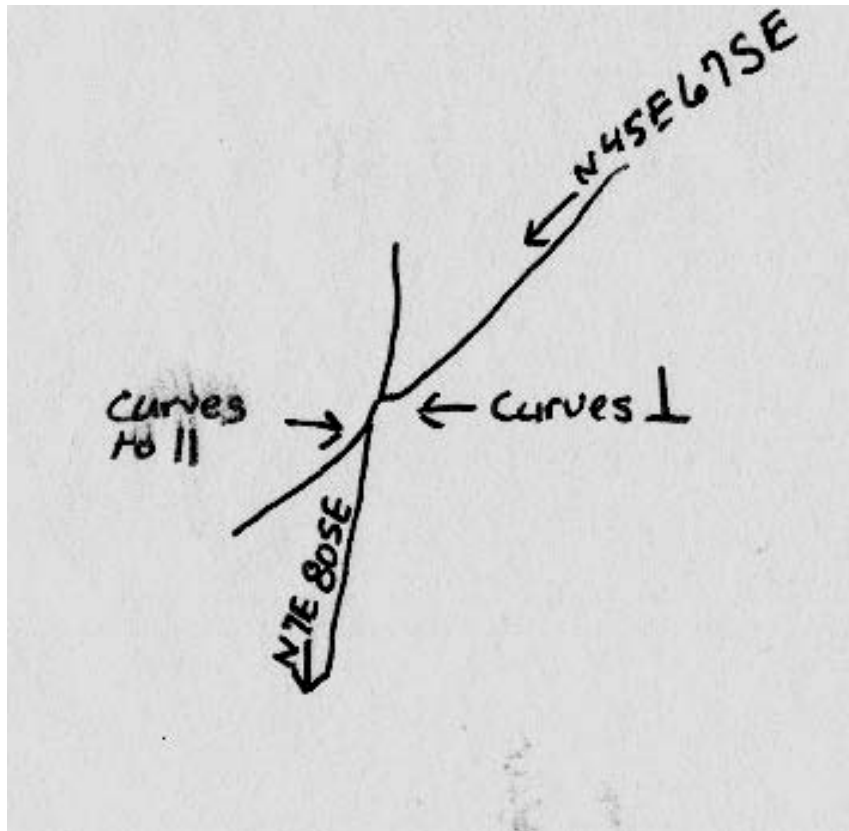


**Chart 26:** One example of abutting relationship.

**Chart #: 27**

Plan and side views

**Location:** SW1/4 SE1/4 Sec 23 T38N R78W**Lithology:** Unit 1: interbedded sandstone and shale**Grain size, cementation:** Of the measured sandstone bed 90% of grains 88-125 $\mu$ , and 10% of grains 125-177 $\mu$ , moderate cementation at base, poor cementation toward top – possibly due to weathering, however some fractures do not continue into the more poorly cemented section, others cut through sandstone and shale above and below.**Bed thickness:** 1m, entire cliff at tallest point 6-7m, area – cliff face exposure approximately 15m long.**Structure****Strike and dip of bedding:** Good bedding surfaces hard to find  
N60E 14SE; N50E 12SE**Structural curvature (estimated):** 400m R**Faulting:** One fault down 2cm, N25W 68NE, normal separation.**Fracture Characteristics****Type, Orientation:** Set A: TNF, N25W 68NE

Set B: possible XF – not well exposed, N50E 70NW

Set A	Set B	Other
N25W 65NE N30W 75NE N28W 74NE N25W 68NE N25W 71NE N26W 64NE N26W 75NE N24W 81NE	N50E 70NW N40E 69NW N45E 82NW	N5E 81NW

**Spacing:** (cm)

Set A: (measured E to W perpendicular to strike); 80, 90, 16, 15, 23, 94, 34

Set B: irregular, approx. 80cm – 1m

**Separation:** Set A: see faulting**Mineralization:** Set A; calcite mineralization most generally filling apertures 1-2mm, calcite crystals up to 1cm on each fracture surface growing toward center**Surface characteristics:****Relative ages:** Set A older**Apertures:** Set A – calcite filled generally 1-2mm, largest 2cm

Set B – not observed

**Deformation Bands (width):** NA

**Chart #: 28**

Plan and side views

**Location:** NE1/4 SE1/4 Sec 23 T38N R78W**Lithology:** Unit 2: upper beach sandstone – fine cross bedding**Grain size, cementation:** 90% 88-125 $\mu$ , 10% 125-177 $\mu$ , poorly to mod cemented – some reddish color - Fe**Bed thickness:** 70 cm, area – 10m X 2m**Structure****Strike and dip of bedding:** N42E 5SE – This is approximate due to poorly defined bedding planes.**Structural curvature (estimated):** 800m**Faulting:****Fracture Characteristics****Type, Orientation:** Set A: TNF, N65W 78NE

Set B: TNF, N25W 67NE

Set A	Set B
N65W 78NE	N25W 67NE N30W N26W 77NE N35W 79NE N28W 74NE N60W 64NE N31W 78NE N26W 78NE N28W 85SW N25W 76NE N30W 86NE N30W 88SW N28W 78NE

**Spacing: (cm)**

Set A; only 1 fracture

Set B; 2 fracture zones 3m apart spacing 2-25cm within fracture zones – 15cm average. Fewer fractures in 2m thick very poorly cemented white sandstone underlying this bed, fracture spacing 50-100cm.

**Separation:** One Set B fracture/fault [N25W 67NE] shows normal offset approximately 8cm down on east side**Mineralization:** none**Surface characteristics:****Relative ages:** Set A oldest. Set B fractures curve to intersect the one Set A fracture. Intersections are perpendicular.**Apertures:** none**Deformation Bands (width):** NA

**Chart #: 29**

Plan and side views

**Location:** NW1/4 NE1/4 Sec 26 T38NR78W**Lithology:** Unit 5: fluvial (splay) sandstone in carbonaceous shale unit. White color.**Grain size, cementation:** 62-88 $\mu$ , very fine-grained, moderate cementation.**Bed thickness:** 70cm, area – 30m of total vertical side exposure and 20-30cm of pavement exposure.**Structure****Strike and dip of bedding:** N55E 9SE; N60E 12 SE**Structural curvature (estimated):** 800m**Faulting:****Fracture Characteristics****Type, Orientation:** Set A: TNF and VCF, most fractures dip to NE, but some dip to SW  
3 NE dipping fractures for every 2 SW dipping fractures. Set B: XF, few – possibly recent

Set A – NE dip	Set A – SW dip	Set B
N28W 72NE	N36W 79SW	N50E 80 NW
N30W 71NE	N32W74SW	N70E 50NW
N31W 86NE	N34W 72SW	
N31W 71NE	N32W81SW	
N34W 72NE	N30W 73SW	
N28W 79NE	N33W 76SW	
N31W 76NE	N29W 75SW	
N32W 75NE	N34W 85SW	
N29W 84NE		
N30W 78NE		
N34W 70NE		
N25W 72NE		

**Spacing: (cm)**

Set A – NE dip	Set A – SW dip
60	70
55	75
60	70
30	50
20	40
30	75
10	60
10	35
30	
10	
50	
45	
70	

**Separation:** not able to determine

**Mineralization:** Some fracture surfaces Fe stained (red) – some fractures continue into carbonaceous shale unit underneath with Fe staining perpendicular from fracture surface into carbonaceous shale – average 4cm of staining into carbonaceous shales.

**Surface characteristics:** not clearly observed due to erosion.

**Relative ages:** Set A older

**Apertures:** (mm)

2, 2, 1, 5, 20, 6, 2, 0, 0, 0, 1, 2, 8, 10, 4 – average estimate 3mm – some apertures distinctly larger than average and interpreted to be recent.

**Deformation Bands (width):** NA

**Other Observations:** Shear component of this conjugate set undetermined.



**Chart 29:** Outcrop photograph illustrating conjugate nature of fracture set A.

**Chart #:** 30

Plan and side views

**Location:** NW1/4 NE1/4 Sec 26 T38N R78W**Lithology:** Unit 1: interbedded marine Ss/Sh unit**Grain size, cementation:** Fine-grained sandstone, grains 88-125 $\mu$ , moderate cementation, reddish color possibly due to Fe, area of exposure 15m X 3m.**Bed thickness:** 45cm**Structure****Strike and dip of bedding:** N52E 5SE**Structural curvature (estimated):** 800m**Faulting:****Fracture Characteristics****Type, Orientation:** Set A: TNF, major through-going set. Set B: XF

Set A	Set B
N18W 84NE	N71E
N22W 78NE	N62E
N22W 89NE	N74E 85NW
N22W 89NE	N52E 82NW
N28W 86NE	N15E 90
N20W 86NE	N65E 76NW
N19W	N55E
N32W	N56E
N35W	N66E 85NW
N32W 81NE	
N36W 84NE	
N33W	
N28W 86NE	

**Spacing: (cm)**

Set A	Set B
28	90
38	69
40	45
40	64
38	116
28	22
30	20
26	10
30	56
20	58
34	
25	
22	
12	
20	



**Separation:** none observed

**Mineralization:** none

**Surface characteristics:** no recognizable features

**Relative ages:** Set A older

**Apertures:** At outcrop edge (side exposure), 2mm-3cm (interpreted to be recent). Away from outcrop edge 1mm wide apertures to no apertures.

**Deformation Bands (width):** NA

**Chart #: 31**

Plan and side views

**Location:** SE1/4 NE1/4 Sec 23 T38N R78W**Lithology:** Unit 1: sandstone within the interbedded sandstone and shale unit, 2-3m shale overlying and 5-6m shale underlying this sandstone bed.**Grain size, cementation:** Fine-grained sandstone 88-125 $\mu$ , ripple marks, moderately to well cemented (reddish tint suggests Fe enriched cement)**Bed thickness:** 25cm total bed thickness, individual laminae are 5-2cm thick**Structure****Strike and dip of bedding:** N23E 9SE, N25E 7SE**Structural curvature (estimated):** 800m**Faulting:****Fracture Characteristics****Type, Orientation:** Set A: TNF

Set B: XF

Set A	Set B
N64W 84NE	N12W 90
N60W 90	N52E90
N55W 90	N4E
N56W 82NE	N75E 90
N53W 90	N44E 84NW
N70W 90	N60E
N65W 90	N57E
N66W 90	N32E
N60W 87SW	
N62W 90	
N64W 90	
N72W 90	
N58W 88SW	
N60W 90	
N64W 90	
N64W 90	
N68W 90	

**Spacing: (cm)**

Set A	Set B
30	70
28	165
24	70
19	120
17	60
25	28
33	105
22	40
25	

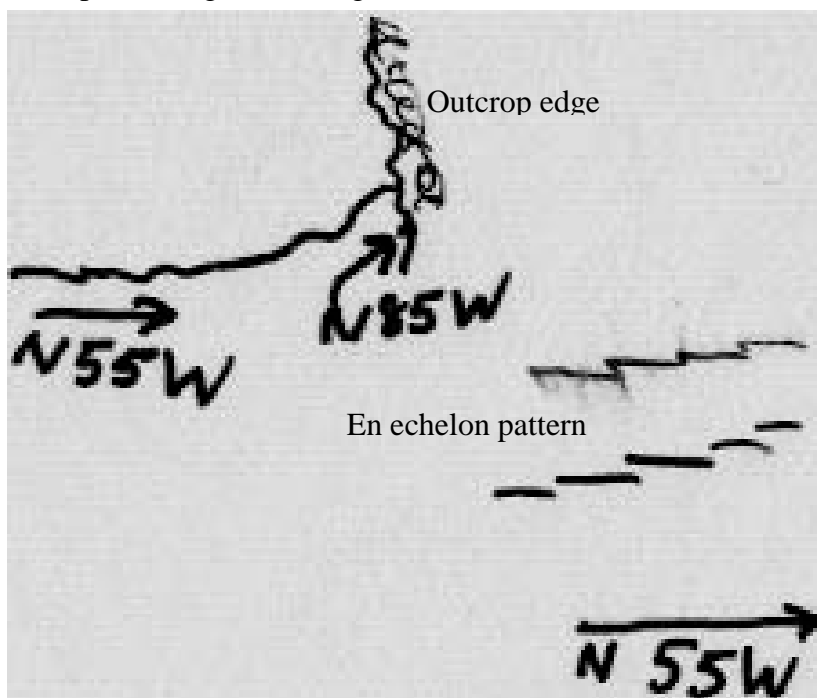
80	
80	
75	
65	
55	
20	
20	
18	
25	
60	

Distinctly larger spacing values for set B relative to set A.

**Separation:** None observed

**Mineralization:** In general Set A has 1mm wide calcite coating on the fracture surfaces.

**Surface characteristics:** in plan view 3-4 surfaces exhibit an en echelon pattern, also 2-3 are curved at exposure edge. See diagram below:



**Relative ages:** Set A older

**Apertures:** wider at outcrop edge to 8-10cm on some Set A

Set A: 0, 1mm, 1mm

Set B: 1-2mm average

**Deformation Bands (width):** NA

**Chart #: 32**

Plan and side views

**Location:** SE1/4 NE1/4 Sec 223 T38N R78W**Lithology:** Unit 2: upper beach sandstone, light tan**Grain size, cementation:** Distribution of grain sizes in this bed is 80% 88-125 $\mu$ , 20% 125-177 $\mu$ . poorly to moderately cemented, not as poorly cemented as Unit 3 white beach sandstones.**Bed thickness:** 60cm, approximate area – 10m X 8m.**Structure****Strike and dip of bedding:** N5E 7SE, N5E 8SE, N10E 7SE  
(undulatory surface – leveled out and measured on clipboard)**Structural curvature (estimated):** 1000m-1500m**Faulting:****Fracture Characteristics****Type, Orientation:** Set A: TNF – exposure not great for mapping, but fractures of similar strike to set A continue through ridge.

Set B: XF

Set A	Set B	Set C
N81W 84NE	N40W	N60E
N80W 87NE	N5E 78NW	N62E
N82W 81NE	N8E	N53E 75NW
N79W 79NE	N6E	3 fractures 50cm apart –
N83W 79NE	N30W 82SW	appear generally through-
N73W 84NE		going – 1 ends at a Set A
N78W		fracture
N77W		
N78W		
N77W		
N79W		

**Spacing: (cm)**

Set A	Set B
5	Where set A is closely spaced (i.e. less than 40 cm spacing) set B is also closely spaced (40cm average). Where set A is more widely spaced (i.e. greater than 40 cm) set B is also more widely spaced (2-3 m spacing).
16	
7	
8	
10	
48	
30	
38	
85 covered	
24	
25	
68	
145	

22 25 108 23	
-----------------------	--

**Separation:** none observed

**Mineralization:** none

**Surface characteristics:** no distinctive characteristics

**Relative ages:** Set A is older than Set B. One abutting relationship suggests set A is also older than set C.

**Apertures:** maximum 1-2mm, generally none

**Deformation Bands (width):** A few (3) deformation bands exist, widths 1-2mm.

**Chart #: 33**

Plan view

**Location:** SE1/4 NE1/4 Sec 23 T038N R78W, 20m west of chart 32**Lithology:** Unit 2: upper beach sandstone**Grain size, cementation:** Size distribution of grains in sandstone 40% 125-177 $\mu$  and 60% 177-250 $\mu$ , poorly cemented.**Bed thickness:** 1.5m approximate, area – 5m X 2m at widest point.**Structure****Strike and dip of bedding:** taken from chart 32 given proximity and inability to obtain good surface on this exposure for strike and dip.

N5E 7SE, N5E 8SE, N10E 7SE

**Structural curvature (estimated):** 1000-1500m**Faulting:****Fracture Characteristics****Type, Orientation:** Set A: TNF. Set B: deformation bands striking perpendicular to Set A

Set A	Set B
N38W 80SW	N52E 59NW
N34W	N53E 61SE
N32W 72SW	N51E 68SE
N39W	
N40W	
N38W 73NE	
N32W 72NE	
N38W 73SW	
N40W	
N12W 70NE	
N10W 74SW	
N30W 85SW	
N34W 85NE	

**Spacing:** (cm)

Set A: 25, 12, 12, 46, 10, 47, 12, 14, 42, 12, 14, 30, 68, 15

**Separation:** none observed**Mineralization:** none**Surface characteristics:** no distinctive characteristics**Relative ages:** Set A older**Apertures:** none**Deformation Bands (width):** 1cm, 4mm, 6mm**Other observations:** One set A fracture (N38W) does extend into a better cemented overlying bed, however, fracture spacing generally decreases in the better cemented unit. One of the few locations where fractures and deformation bands are found together and here it is suggestive (due to abutting relationships) that fractures are older than deformation bands (see field map).

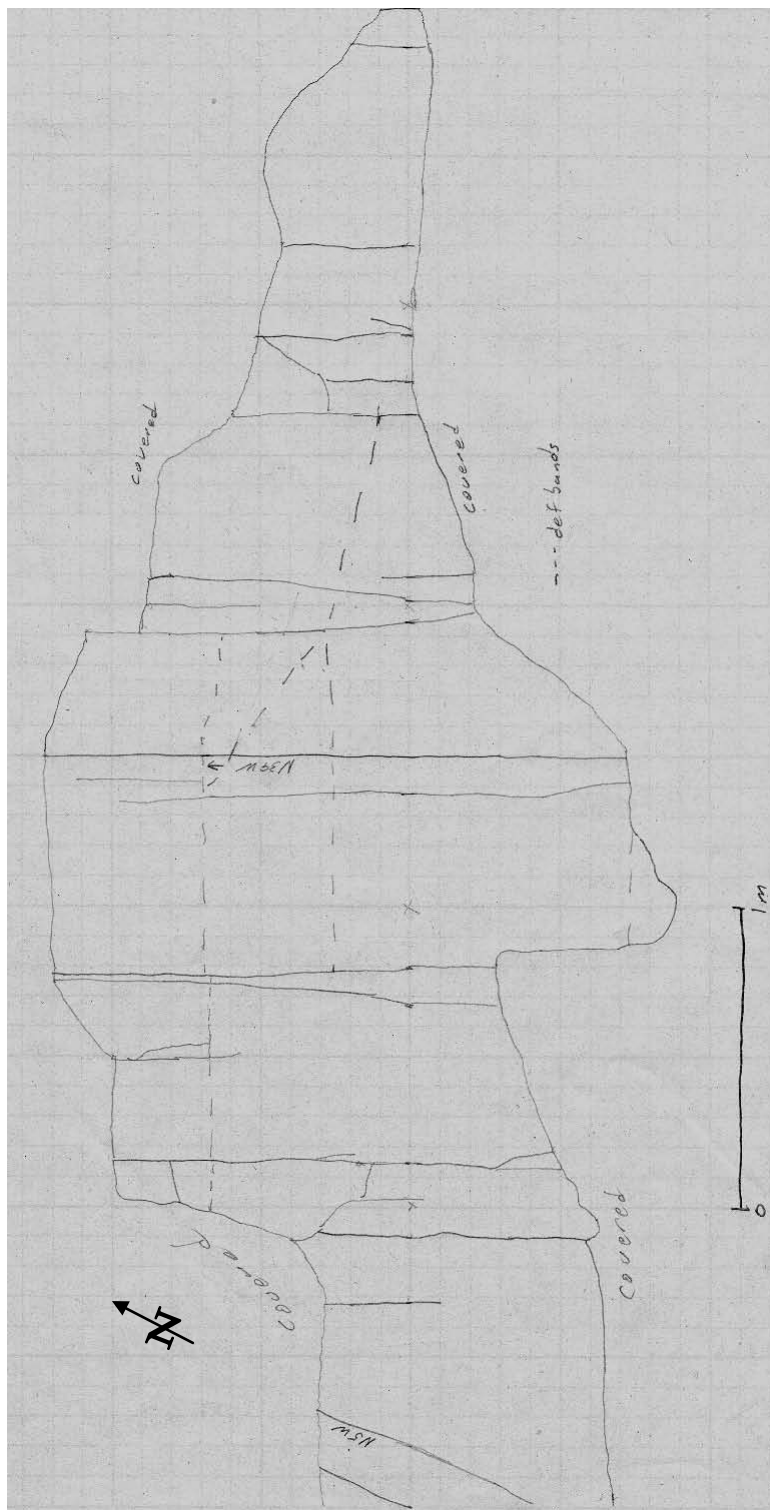


**Chart 33:** Field map illustrating relationship between fractures (solid lines) and deformation bands (dashed lines).

**Chart #: 34**

Plan view

**Location:** SE1/4 NE1/4 Sec 23 T38N**Lithology:** Unit 2: beach sandstone, numerous cross beds.**Grain size, cementation:** Grain size distribution within this sandstone bed is 20% 125-177 $\mu$  and 80% 177-250 $\mu$ , poor to moderate cementation.**Bed thickness:** 2m – 1 ½ m, area – The whole hummocky pavement surface is approximately 3 acres – area measured is 20m X 20m.**Structure****Strike and dip of bedding:** N16E 10SE**Structural curvature** (estimated): 1000m**Faulting:** Along the N35-40W strike there is undoubtedly some displacement – this particular fracture zone extends southward and across a major E-W gully and into the opposing hillside with approximately 50cm of normal separation observed in the cliff exposure. These fracture zones control drainage for this pavement. The fracture zones extend along strike for over 100m.**Fracture Characteristics****Type, Orientation:** Set A: throughgoing and VCF, general strike of fracture zones is N39W.

Set B: TNF, this set generally terminates at Set A, and is observable across all 3 acres of exposure. Set A is more pervasive with an estimated 3 set A fractures for every 1 set B fracture.

Set A	Set B
N33W 87SW	N86W 85NE
N36W 86SW	N84W 89NE
N40W 86NE	N83W 82NE
N39W 86NE	N84W
N35W 83SW	N89W 90
N38W	
N38W 76SW	
N40W 72SW	
N43W 79NE	
N34W 86SW	
N39W 86NE	

**Spacing: (cm)**

Set A*	Set B
25	20
40	70
75	80
12	95
27	
18	
24	



35	
35	
39	
30	
13.9	

\* Spacing between set A fracture zones 15-20m.

**Separation:** not visible on pavement surface but is visible in gully to the south (see notes on faulting).

**Mineralization:** In depression formed by this fracture zone euhedral calcite crystals can be found lying loose. After intensive search calcite crystals were found on fracture walls of Set A. Crystals grew on opposite walls toward each other. The largest crystals are 2.5mm long as measured perpendicular to fracture surface. Apertures are cemented closed with no current openings.

**Surface characteristics:** no obvious characteristics

**Relative ages:** Set A older

**Apertures:** Generally none, some to 5mm (see mineralization).

**Deformation Bands (width):** NA

**Chart #: 35**

Plan and side view

**Location:** SE1/4 NE1/4 Sec 23 T38N R78W**Lithology:** Unit 4: carbonaceous shale, black, very fissile**Grain size, cementation:** very fine grain size “shale”, very poorly cemented**Bed thickness:** 1.8m, area – 8m X 3m**Structure****Strike and dip of bedding:** N24E 7SE – This was measurement was difficult to obtain due to irregular bedding surfaces in the carbonaceous shale.**Structural curvature** (estimated): 1000m**Faulting:** NA**Fracture Characteristics****Type, Orientation:** Set A: cleats, maximum extent of cleat along strike 0.5m.

Set B: cleats, terminate at Set A.

Set A	Set A – 10m up ridge (3m up stratigraphically-still carbonaceous shale unit)	Set B
N70W 90	N80W 85SW	N43E 90
N62W 90	N80W 90	N24E 90
N32W 80SW	N81W 85SW	N21E
N65W 84SW	N79W 85SW	N14E 71NW
N82E	N80W 85SW	N30E 81NW
N85E	N76W 86SW	N20W 90
N80W 89SW	N77W	N6W
N75W	N75W 87SW	N1E 90
N65W 86SW	N79W	N11E
N67W 88SW	N77W	10m up ridge (3m up stratigraphically – still carbonaceous shale unit)
N65W 88SW	N78W	N5W
N82W 83SW	N79W 79SW	N12W
N80W 58SW		
N60W		
N55W 90		
N42W 90		
N70W 86SW		
N67W 85SW		

**Spacing:** (cm)

Set A: 18, 20, 18, 12, 10, 6, 5, 35, 2, 4, 15, 15, 5, 5, 8, 5, 8

**Separation:** none observed**Mineralization:** some red, Fe staining on surfaces**Surface characteristics:** planar**Relative ages:** Set A older**Apertures:** none**Deformation Bands (width):** NA**Other observations:** Some set A and set B cleats are iron stained 1cm into matrix.

**Chart #: 36**

Plan and side views

**Location:** NW1/4 NE1/4 Sec 9 T38NR78W**Lithology:** Unit 1: interbedded sandstone and shale**Grain size, cementation:** Grain size of sandstone bed is 62-88 $\mu$ , poor to moderate cementation.**Bed thickness:** 4-6cm thick sandstone, area – 8m X 3m**Structure****Strike and dip of bedding:** Note: distinct increase in dip from Chart 35.

N11W 31SW, N15W 30SW, N11W 26SW

**Structural curvature** (estimated):**Faulting:****Fracture Characteristics****Type, Orientation:** Set A: TNF

Set B: TNF, in general Set B has perpendicular intersections with set A. Some fractures tend to curve near the point of intersection to accommodate this relationship.

Note: spacing and strike generally the same in other sandstone beds near this location.

Set A	Set B
N60W	N2W
N55W 13NE	N10W 63NE
N57W 74NE	N16W 74NE
N57W 72NE	N11W
N56W 70NE	N12W
N60W 78NE	N11W 72NE
N59W 76NE	N25W 74NE
N58W 72NE	N9W 76NE
N62W 83NE	N24W 67NE
N58W 76NE	
N54W 79NE	

**Spacing: (cm)**

Set A - N to S	Set B
40	35
28	41
40	60
18	30
33	34
66	
40	
44	
47	
30	
70	
55	

**Separation:** none

**Mineralization:** none  
**Surface characteristics:** not apparent  
**Relative ages:** Set A older  
**Apertures:** aperture could be recent  
Set A: 2,1,1,2,2,3,2,2,3 (mm)  
Set B: 3,1,2,1,2,2,2,1 (mm)  
**Deformation Bands (width):** NA

**Chart #: 37**

Plan and side views

**Location:** SE1/4 NE1/4 Sec 23 T38N R78W**Lithology:** Unit 5: fluvial sandstone interbedded in carbonaceous shale**Grain size, cementation:** Grain size distribution within the sandstone is 90% 88-125 $\mu$  and 10% 125-177 $\mu$ . Moderate cementation, calcite cement (strongly reactive in HCl), some Fe given reddish brown color and rounded siderite nodules nearby. Note fractures curve to parallel the edges of these round nodules.**Bed thickness:** 1.4m, area – 20m X 4m**Structure****Strike and dip of bedding:** N30E 16SE – Difficult to find a good bedding surface for measurement of strike and dip.**Structural curvature** (estimated): 1000-1500m**Faulting:** no large-scale faults**Fracture Characteristics****Type, Orientation:** Set A: TNF. Set B: TNF

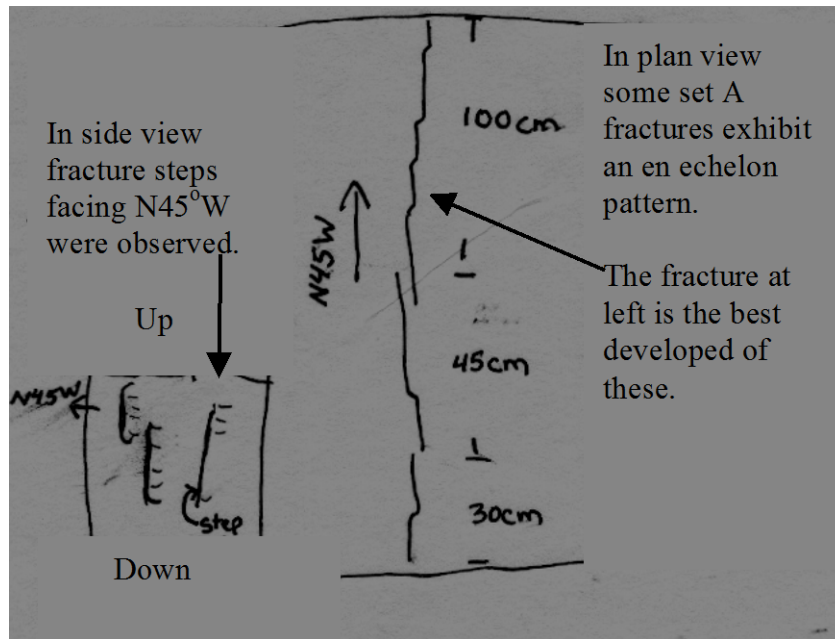
Set A	Set B	XF
N45W 90	N76E 75NW	N55E 90
N45W 90	N66E	
N42W 90	N77E 78NW	
N42W 90	N77E 77NW	
N41W 90	N73E 80NW	
N39W 90		
N44W 90		
N41W 90		
N44W 90		
N42W 90		
N43W 90		

**Spacing:** (cm)

Set A	Set B
75	85
35	165
50	
85	
75	
70	
105	
15	
20	
155	

**Separation:** none observed**Mineralization:** none

**Surface characteristics: Set A:**



**Relative ages:** Set A older

**Apertures:** 0-3cm – 0.5cm average (interpreted to be recent).

**Deformation Bands (width):** NA

**Chart #: 38**

Plan and side views

**Location:** NW1/4 SW1/4 Sec 24 T38N R78W**Lithology:** Unit 5: fluvial sandstone interbedded in carbonaceous shale, light tan color.**Grain size, cementation:** Grain size distribution within the fluvial sandstone is 60% 88-125 $\mu$  and 40% 125-177 $\mu$ . Moderate cementation, very reactive with HCl.**Bed thickness:** 1.4m, area – 30m long X 3m wide**Structure****Strike and dip of bedding:** N18E 14SE, N16E 9SE, N22E 13SE**Structural curvature** (estimated): 1000-1500m**Faulting:** no large scale faulting**Fracture Characteristics****Type, Orientation:** Set A: TNF. Set B: TNF. Set C: one fracture. Set D: XF.

Set A	Set B	Set C	Set D
N48W 90	N88W 90	N45E 71NW	N55E
N48W 90	N89W 87NE	One Set A fracture	N60E 70NW
N48W 90	N89W	terminates at	
N45W	N86W	intersection with	
N40W 90		this fracture	
N36W 90			
N47W			
N42W 90			
N44W 90			
N46W 90			

**Spacing: (cm)**

Set A	Set B
175	205
88	168
85	205
92	
58	
150	
68	
123	
65	
74	

**Separation:** none observed**Mineralization:** Set A – calcite mineralization on fracture surface to 2mm wide. Some 1mm fractures sealed with calcite. Almost all are mineralized.

Set B – no mineralization

**Surface characteristics:****Relative ages:** Set A older than B or D. Set C possibly the oldest fracture set.

**Apertures:** Apertures appear to have recently expanded in exposures near the cliff edge.  
Set A: Apertures near the cliff edge 0-4cm, 3 fractures away from the edge are cemented with calcite, apertures away from cliff edge between 0-2mm

Set B: Few good exposures away from outcrop edge, 1-4cm at cliff edge; 0-1mm away from edge.

**Deformation Bands (width):** NA



**Chart #: 39**

Plan and side views

**Location:** NW1/4 NE1/4 Sec 9 T38N R78W**Lithology:** Unit 2: Fe-enriched pavement in upper portion of beach sandstone.**Grain size, cementation:** Grain size distribution in this sandstone bed is 90% 177-250 $\mu$  and 10% 250-350 $\mu$ . Poor to moderate cementation, units overlying and underlying this bed are very poorly cemented. Fractures do not extend into the less-cemented units.**Bed thickness:** 60cm. Area – 10m X 2m**Structure****Strike and dip of bedding:** N10W 25SW, N9W 23SW, N10W 22SW**Structural curvature** (estimated): NA**Faulting:** Possible large-scale fault separating this section of the western limb and the section to the north. This fault would strike through the valley between these two sections of the western limb and would be covered by Quaternary alluvium. Conley reservoir is located in this valley.**Fracture Characteristics****Type, Orientation:** Set A: TNF, N89E 80NW

Set B: TNF/VE; N15W 68NE bed normal.

Set C: XF. Generally perpendicular to Set B.

Set A	Set B	Set C
N89E 80NW	N14W 68NE N17W 67NE N18W N16W 69NE N15W 72NE N18W N14W N17W 65NE N16W N19W 66NE N18W 67NE N18W N20W 69NE N19W 65NE N18W	N75E 90 N73E 90 N68E 90

**Spacing:** (cm) Set A: only one fracture, spacing at least 3m.

Set B: Measured west to east perpendicular to strike, 72, 24, 35, 28, 13, 19, 19, 4, 9, 37, 20, 59, 22, 17, 48

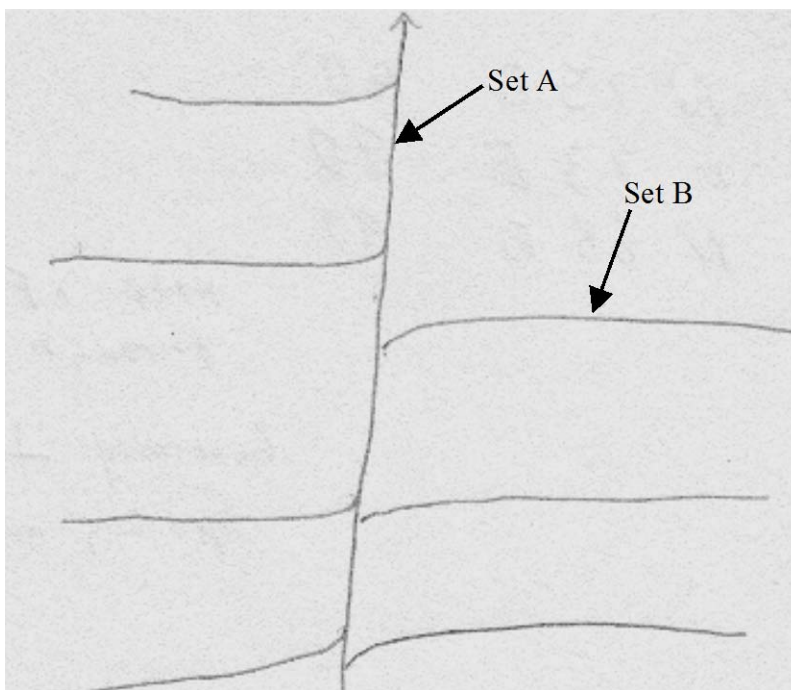
Set C: spacing average 0.5cm

**Separation:** no visible separation**Mineralization:** none

**Surface characteristics:** Abutting relationship between Set A and Set B is such that Set B curves to parallel Set A near points of intersection. Due to the plan view nature of this outcrop, study of surface features on the fracture walls was not possible.

Two possibilities exist for the observed abutting relationship. First possibility, the Set A fracture is a fault and the Set B fractures are bent or dragged suggesting left lateral displacement in plan view. Second possibility, is that as the Set B fractures propagated either toward or away from the Set A fracture they were influenced by localized compressive stress near the Set A fracture.

Evidence for the Set A fracture being a fracture is 1) no visible fault gouge, 2) the set A fracture is no wider than set B fractures and 3) there are no fractures parallel to the single set A fracture observed in this outcrop. In other outcrops faults generally have an associated fracture zone. However, it is possible any displacement on possible set A fault is small and therefore did not develop gouge material or a fracture zone. For this study the set A fracture with the abutting relationship illustrated below is interpreted to be a fracture and not a fault.



**Relative ages:** Set A older

**Apertures:** Apertures of up to 3cm at cliff edge. At a distance of 1 ½ m from edge apertures range between 0-5mm, 2mm average. Apertures decrease continually away from cliff edge. Upon removing some of the material covering the outcrop away from the cliff edge, it is apparent that fractures have no apertures when at a distance of 3m from the cliff edge. Therefore, the apertures are interpreted to be recent.

**Deformation Bands (width):** NA

**Chart #: 40**

Plan view

**Location:** SW1/4 SE1/4 Sec 4 T38N R78W**Lithology:** Unit 2: upper portion of beach sandstone – Fe enriched pavement**Grain size, cementation:** Grain size distribution for the sandstone bed is 90% 88-125 $\mu$  and 10% 125-177 $\mu$ . Moderate cementation, calcite (strong reaction to HCl), also reddish-tan color suggesting some Fe.**Bed thickness:** 30cm, area – 6m X 2m**Structure****Strike and dip of bedding:** N22W 23SW, N26W 23SW, N22W 25SW**Structural curvature** (estimated):**Faulting:** After digging away some of the covering alluvium it is apparent there is no large-scale fault at this stratigraphic level through the bottom of Conley Reservoir draw. However it should be noted that there is a 12° –16° change in bedding strike from one side of this valley to the other. Chart 39 details data for the immediate south side of this east-west striking valley and Chart 40 details data for the immediate north side.**Fracture Characteristics****Type, Orientation:** Set A: TNF/VE. Set B: TNF

Set A	Set B
N31W 68NE	N80E 82NW
N34W 65NE	N77E 85NW
N32W 66NE	N81E
N32W 68NE	N80E 80NW
N33W 65NE	N80E 83NW
N30W 62NE	N84E 80NW
N32W 75NE	
N31W 72NE	
N33W 67NE	
N30W 62NE	

**Spacing: (cm)**

Set A	Set B
30	160
18	146
8	213
34	70
10	12
4	40
32	
30	
45	
26	
30	
21	
28	

**Separation:** none observed

**Mineralization:** Set A: Iron stained 4cm into matrix from fracture plane in numerous fractures.

Set B: Iron stained although not as extensively as Set A

**Surface characteristics:** generally planar

**Relative ages:** Set A generally older. However, age determinations were not easy to make. A couple of abutting relationships suggest Set B is older. These fracture sets may be penecontemporaneous.

**Apertures:** (mm)

Set A: 0, 1, 2, 1, 1, 1, 1

Set B: 0, 1, 1

1mm average aperture width for both sets. Note: aperture width increases to 1cm with increased proximity to outcrop edge.

**Deformation Bands (width):** NA

**Chart #: 41**

Plan and side views

**Location:** SE1/4 SW1/4 Sec 4 T38N R78W**Lithology:** Unit 4: carbonaceous shale**Grain size, cementation:** very fine (black carbonaceous shale), very poorly cemented**Bed thickness:** 1m thick, 4-5m stratigraphically above Unit 2: beach sandstone.**Structure****Strike and dip of bedding:** Obtained from nearby Unit 2: beach sandstone

N12W 25 SW, N18W 25SW

**Structural curvature** (estimated):**Faulting:** No large scale faulting observed**Fracture Characteristics****Type, Orientation:** Set A: (TNF) cleats, N35-40W. Set B: (XF) cleats, N80W

Set A	Set B	Set C
N35W 70NE*	N82W 62NE	N30E 40SE
N28W 64NE	N85W 60NE	N35E 53SE
N24W 67NE	N70W 82NE	
N30W 64NE	N80W 71NE	
N32W	N80W 80NE	
N23W 84SW	N85W	
N35W 74NE	N85W 87NE	
N28W 75NE	N80W	
N30W 76NE	N86W 87NE	
N36W 75NE	N75W 85NE	
N30W 69NE		

\* Extends for 3m, Set B cleats terminate at this cleat. Note: Generally most cleats do not extend very far. 5-10cm along dip, ½ - 1m along strike, average along strike 0.5m.

**Spacing:** (cm)

Set A	Set B
11	22
34	27
50	30
60	30
35	4
4	6
35	8
20	3
	5

**Separation:** none observed**Mineralization:** Fe staining directly on fracture surface.**Surface characteristics:** planar**Relative ages:** Set A older**Apertures:** None**Deformation Bands (width):** NA

**Chart #:** 42

Plan and side views

**Location:** NE1/4 SW1/4 Sec 4 T38N R78W (pavement)**Lithology:** Unit 1: interbedded sandstones and shales, light tan sandstone**Grain size, cementation:** Grain size distribution within the measured sandstone bed is 10% 62-88 $\mu$ , 80% 88-125 $\mu$ , and 10% 125-177 $\mu$ . Poor to moderate cementation (moderate reaction to HCl).**Bed thickness:** 40cm total thickness, thin 1cm laminae/cross-beds, area – 10m X 16m**Structure****Strike and dip of bedding:** N30W 23SW, N30W 22SW, N38W 23SW, N39W 24SW**Structural curvature (estimated):** Northwestern limb, estimate of curvature unavailable due to poor exposure of northern plunge as expressed within the Mesaverde section.**Faulting:** No large-scale faulting observed.**Fracture Characteristics****Type, Orientation:** Set A: VE. Set B; XF

Set A	Set B
N41W 52NE	N48E 89NW
N44W 58NE	N45E 90
N42W 59NE	N46E
N45W 57NE	N46E 90
N43W 57NE	N42E 90
N46W	N35E
N44W 59NE	N25E 85SW
N44W 55NE	N48E 90
N44W 54NE	
N43W 46NE	

**Spacing:** (cm)

Set A	Set B
1.4	4.4
1.73	1.7
1.00	2.9
0.87	2.4
0.50	2.1
1.46	1.2
1.94	some spacing greater than 5m – average is
1.70	approximately 3m

**Separation:** No visible offset on pavement surface, partial side view suggests no offset.**Mineralization:** none**Surface characteristics:** planar on VE Set A**Relative ages:** Set A older**Apertures:** 0-1mm, generally no apertures**Deformation Bands (width):** NA

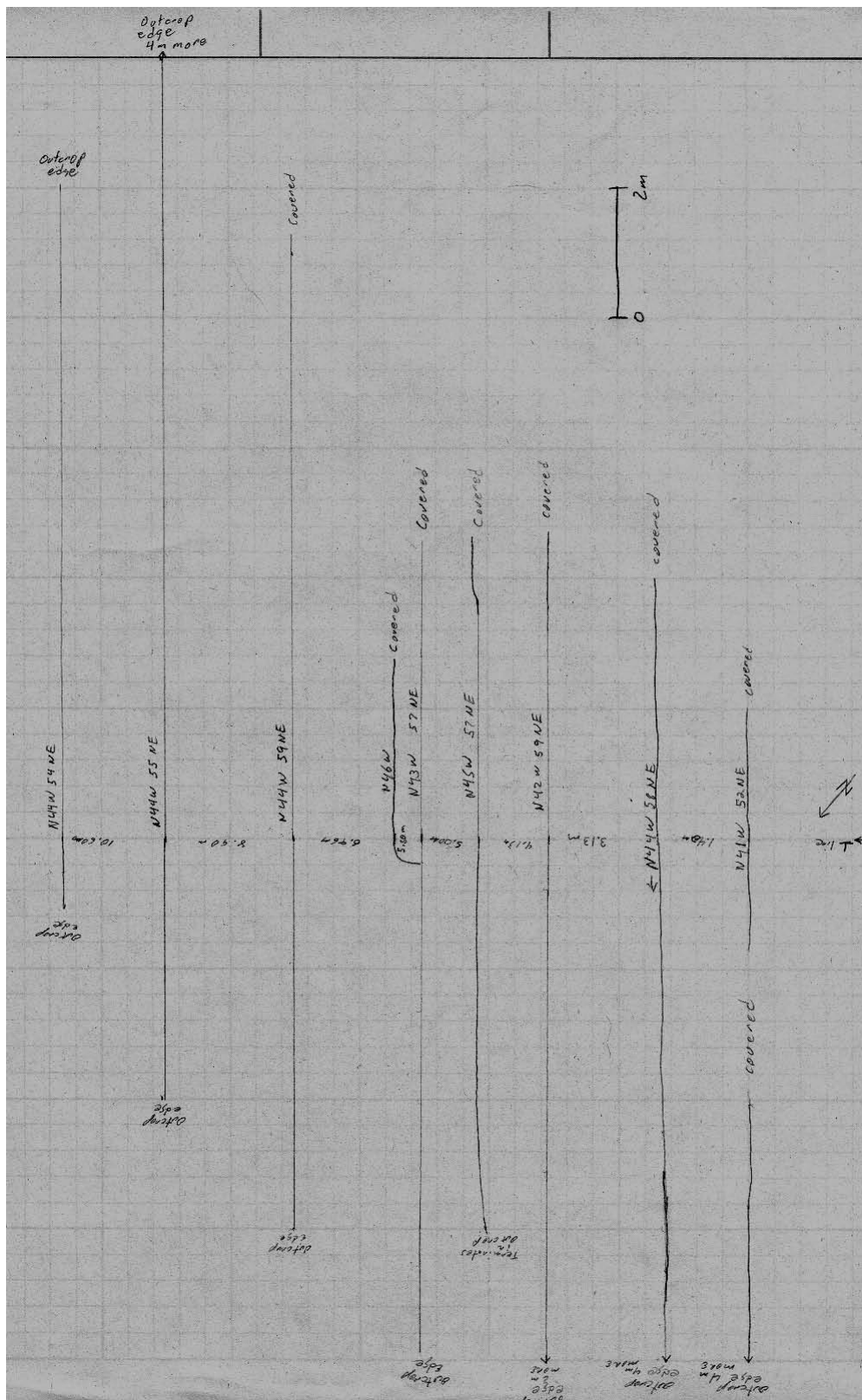


Chart 42: fracture map – scan line drawn perpendicular to Set A.

**Chart #:** 43

Plan and side view

**Location:** SE1/4 SW1/4 Sec 4 T38N R78W**Lithology:** Unit 5: fluvial sandstone interbedded in carbonaceous shale**Grain size, cementation:** Grain size distribution with fluvial sandstone bed 40% 62-88 $\mu$  and 60% 88-125 $\mu$ . Moderate cementation, light tan/red suggesting Fe enrichment, moderate to strong reaction with HCl.**Bed thickness:** 50cm thick; underlying sandstone is Unit 3: white beach sandstone, poorly cemented, approximately 1/3 of these fracture continue into this unit as either fractures or deformation bands, area – 4m X 6m.**Structure****Strike and dip of bedding:** Difficult to measure strike and dip due to very broken, undulatory surface. N39W 23SW, N39W 25SW**Structural curvature (estimated):** Northwestern limb, estimate of curvature unavailable due to poor exposure of northern plunge as expressed within the Mesaverde section.**Faulting:** No large scale faulting observed**Fracture Characteristics****Type, Orientation:** Set A: TNF. Set B: XF, this set does not extend into underlying unit.

Set A	Set B
N68W 63NE	N15E 90
N66W 79NE	N24E 76NW
N67W 73NE	N28E 90
N69W 73NE	N25E
N68W 65NE	N18E
N64W 69NE	N18E 90
N69W 71NE	N43E 80NW
N67W 67NE	N25E
N68W 68NE	N13E 62SE
N65W 70NE	N8W 65SE
N66W 60NE	
N65W	
N71W 66NE	
N73W 87SW	

**Spacing:** (cm) Set A; readings taken E-W perpendicular to fracture trend

Set A	Set B
82	75
15	95
9	25
35	66
9	70
30	40
24	50
20	
28	



32 113 29 76	
-----------------------	--

**Separation:** On side view “possible” 1cm normal offset on 1Set A fracture, dip to NE. Separation may be recent due to gravity sliding at edge of outcrop.

**Mineralization:** none

**Surface characteristics:** Very rough pavement surface. No characteristic fracture surface features observed.

**Relative ages:** Set A older

**Apertures:** 0-5mm in Set A

0-5mm in Set B. Both possibly recent

**Deformation Bands (width):** Deformation bands up to 3mm wide in underlying Unit 3: white beach sandstone.

**Chart #: 44**

Plan and side views

**Location:** NW1/4 NW1/4 Sec 4 T38N R78W**Lithology:** Unit 1: interbedded sandstone and shale**Grain size, cementation:** Fine-grained sandstone, grain size distribution for this measured sandstone bed is 62-88 $\mu$ . Moderate cementation, calcite; red-brown color indicates some Fe.**Bed thickness:** 8cm thick sandstone, 5m of shale overlying and 2m of shale underlying this bed, area – 10m X 1m**Structure****Strike and dip of bedding:** Strike and dip measurements difficult due to rough surface. N33W 20SW, N31W 20SW, N36W 22SW**Structural curvature** (estimated):**Faulting:** no large-scale faulting observed**Fracture Characteristics****Type, Orientation:** Set A: TNF, this set is the most distinct and pervasive fracture set at this locality. Set B: XF

Set A	Set B	Set C
N64W 81NE	N25E 85NW	N89W 76NE
N66W 81NE	N14E 76SE	N90W 78NE
N64W 71NE	N15E 85NW	N89W 81NW
N67W 71NE	N15E 79SE	N87E
N65W 82NE	N10E 75SE	N87E
N70W 76NE	N15E 70SE	N87W 74NE
N68W 77NE	N15E 77SE	N75W 85NE
N65W 71NE		N76E 82NW
N65W 83NE		N5W 77NE
N72W 81NE		
N70W 70NE		
N68W 82SW		
N69W 82NE		

**Spacing: (cm)**

Set A	Set B	Set C
14	30	11
26	37	7
14	28	9
35	87	25
20	54	8
38	61	28
19	39	
	53	
	43	

**Separation:** none observed

**Mineralization:** Fe staining on fracture surface

**Surface characteristics:**

**Relative ages:** Set A oldest, Set C next oldest, Set B youngest.

Note – 1 intersection suggests Set C older than Set A.

**Apertures:** (mm) Large apertures are interpreted to be recent.

Set A	Set B	Set C
5	20	0
2	20	10
10	38	0
4	15	1
4	5	0
20	5	0
0	5	1
0	8	2
1		2
8		

**Deformation Bands (width):** NA

**Chart #: 45**

Plan and side views

**Location:** SW1/4 NW1/4 Sec 4 T38N R78W**Lithology:** Unit 2: upper portion of beach sandstone**Grain size, cementation:** Grain size distribution within this measured sandstone bed is 90% 88-125 $\mu$  and 10% 125-177 $\mu$ . Moderate cementation, very reactive to HCl, red-brown color – Fe enriched (siderite) pavement.**Bed thickness:** 20cm average thickness, laminae 0.5-1cm.**Structure****Strike and dip of bedding:** N35W 18SW, N29W 18SW, N35W 19SW, N29W 17SW**Structural curvature** (estimated):**Faulting:** no large-scale faulting observed**Fracture Characteristics****Type, Orientation:** Set A: TNF. Set B: XF.

Set A	Set B
N50W 74NE	N25E 88SE
N59W 74NE	N29E
N61W 74NE	N41E 83NW
N52W 74NE	N28E
N53W 82NE	N35E 89NW
N62W 85NE	N35E 81SE
N48W 74NE	N23W 84SE
N56W 74NE	N34E 81SE
N60W 79NE	N21W 84NW
N64W 76NE	
N53W 76NE	
N55W 71NE	
N64W 78NE	
N62W 73NE	

**Spacing: (cm)**

Set A	Set B
19	160
25	120
25	154
31	160
25	65
39	61
44	211
6	110
18	231
55	265
17	355
56	390
24	124

20 35 55 8	Note – distinctly wider spacing in Set B
---------------------	--

**Separation:** none observed

**Mineralization:** none

**Surface characteristics:** Set A does not have as a uniform strike as observed in chart 44.

**Relative ages:** Set A is older.

**Apertures:** Apertures are only at outer (cliff side) edge of outcrop. Therefore, apertures are interpreted to be recent.

**Deformation Bands (width):** Unit 3: white poorly cemented (2m thick) beach sandstone stratigraphically above this measured bed contains deformation bands with a variety of orientations.

**Other observations:** 1m stratigraphically below this unit is a 14cm thick pavement, poorly cemented. Separating the 2 units is a very poorly cemented white Ss (Unit 2: beach sandstone). A 3m wide broken zone separates the 14cm thick pavement into 2 exposures (N and S). No mineralization observed in fractures. Recent apertures to 1cm at exposure edge, otherwise no apertures.

N exposure (no XF)	S exposure	S exposure XF (oblique)
N67W N68W 79NE N66W 84NE	N89E 84NW N86E 86NW N85E 85NW N76E 86NW N81E 81NW N85E 81NW N86E 82NW Spacing average 15cm	N68W N70W N66W 82NE N64W 80NE Spacing average 18cm

**Chart #: 46**

Plan and side views

**Location:** SW1/4 NW1/4 Sec 4 T38N R78W**Lithology:** Unit 4: carbonaceous shale (black)**Grain size, cementation:** very fine-grained, very poorly cemented**Bed thickness:** 1m average thickness, area – 11m X 2m.**Structure****Strike and dip of bedding:** N10E 18NW – hard to find good pavement surface. This reading is probably erroneous. More accurate measurements are described below.

N36W 14SW – Taken on Unit 2: bss 15m below charted area.

N38W 13SW – Taken on Unit 2: bss 15m below charted area.

Also see chart 45 - readings are relatively close to this charted area.

**Structural curvature** (estimated):**Faulting:** No large-scale faulting observed.**Fracture Characteristics****Type, Orientation:** Set A: cleats in carbonaceous shale.

Set A	Set A - continued
N83W 83SW	N40W 86NE
N81W 86NE	N81W 85NE
N83W 86NE	N83W 85NE
N51W 80NE	N80W 90
N79W 79NE	N79W 85NE
N86W	N81W 89NE
N86W	N79W 84NE
N84W	N44W 74NE
N52W	N76W 78NE
N77W 81NE	N76W 85NE
N64W 87SW	N46W 74NE
N80W 85NE	N84W 85NE

**Spacing: (cm)**

Set A	Vertical extent	Length along strike
12	10cm – 1m	30
10	average 20cm	45
21		30
54		10
36		45
10		35
15		23
6		21
13		20
27		25-30 average
22		
8		
2		

34		
8		
10		
14		
17		
4		

**Separation:** none observed.

**Mineralization:** Fe staining on fracture surfaces.

**Surface characteristics:** planar

**Relative ages:** N75-85W older than other fractures where abutting relationships exist.

**Apertures (mm):** 1, 1, 1, 1, 1, 1, 2, 1, 1, 4, 2, 1, 2, 1, 1, 2, 3, 8, 10 (1mm average for most)

**Deformation Bands (width):** Deformation bands in poorly cemented Unit 5: fluvial sandstone directly overly the Unit 4: carbonaceous shale measured here.

1mm - N60E 37SE, 22cm spacing

4mm – N62E 38SE, 18cm spacing

2mm – N60E 39SE

3mm – N45W 45NE

**Chart #: 47**

Side view (cliff exposure)

**Location:** SW1/4 NW1/4 Sec 4 T38N R78W**Lithology:** Unit 5: fluvial sandstone, within Unit 4: carbonaceous shales, approximately 20m above the Unit 4: carbonaceous shale and Unit 3: beach sandstone contact.**Grain size, cementation:** 122-173 $\mu$ , poor-mod cementation, non-reactive to HCl**Bed thickness:** 3-6m thick, area – 30m along cliff face**Structure****Strike and dip of bedding:** N34W 13SW, N32W 15SW**Structural curvature** (estimated):**Faulting:** No large-scale faulting observed. However, some of the fractures do have some displacement.**Fracture Characteristics****Type, Orientation:** Set A: TNF

Set A	Spacing - Set A
1-N40W 55NE 6cm norm displacement	5m
2-N45W 56NE	1.5m
3-N45W 59NE 2cm norm displacement	4m
4-N45W 53NE 8cm norm displacement	0.9m
5-N43W 54NE 1cm norm displacement	5.0m
6-N42W 58NE 1cm norm displacement	2.2m
7-N40W 61NE	0.2m
8-N36W 60NE (A-1)	2.3m
9-N40W 65NE (A-2)	5.3m
10-N45W 50NE (A-3)	

The last 3 measured fractures apparently curve in the upper 2m of outcrop the following strikes: A-1: N60W 84NE; A-2: N61W 81NE; A-3: N62W 81NE; see drawing.

**Separation:** data provided in above table**Mineralization:** none**Surface characteristics:** See drawing. Other surface characteristics include a few incongruous fracture steps.**Relative ages:** Set A older**Apertures:** 0, 0, 5cm, 2cm, 0, 0. Apertures probably recent**Deformation Bands (width):** NA



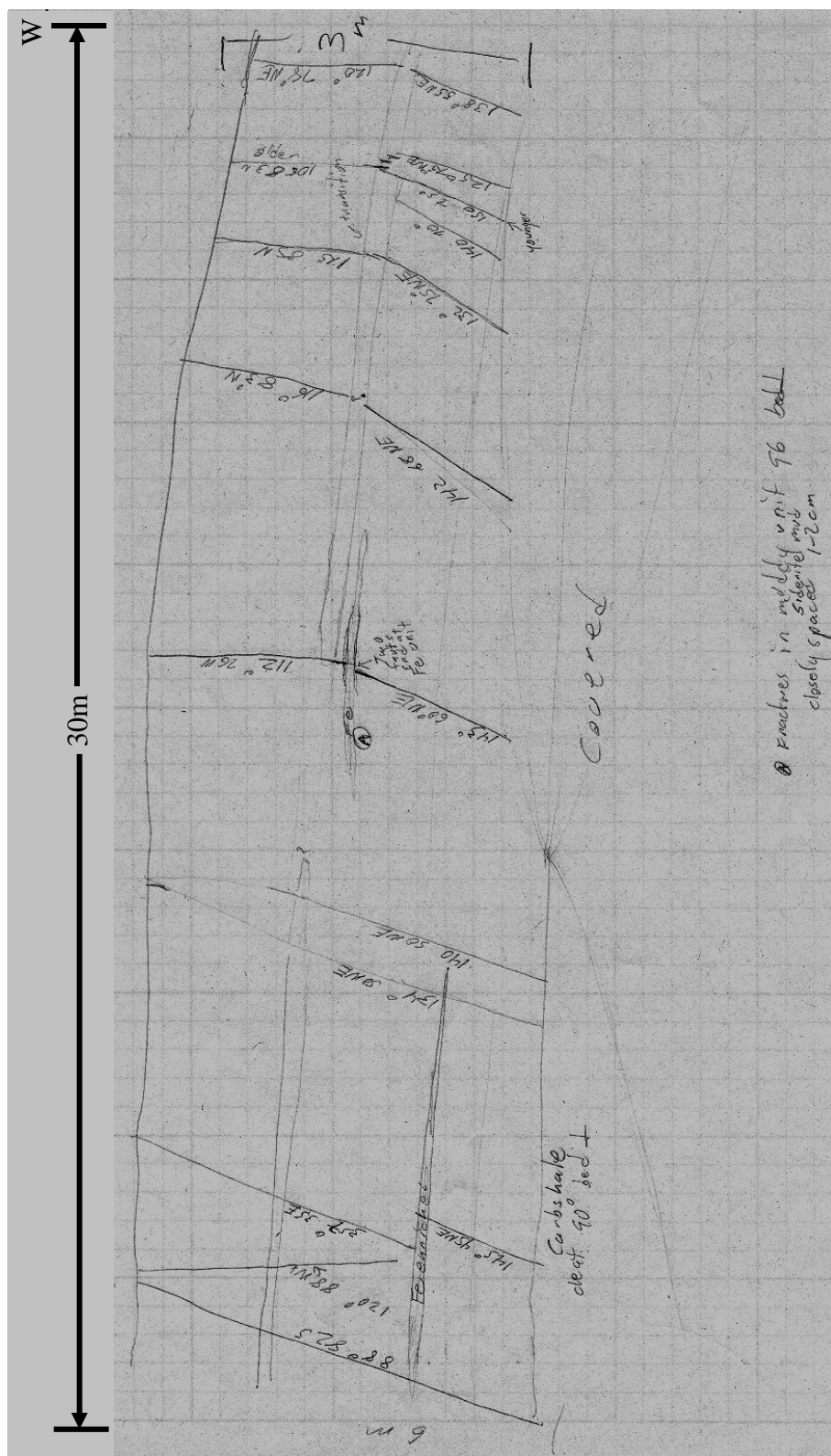


Chart 47: fracture map (cross sectional view)

**Chart #: 48**

Plan and side views

**Location:** NE1/4 NE1/4 Sec 5 T38N R78W**Lithology:** Unit 5: fluvial sandstone within the carbonaceous shales of Unit 4.**Grain size, cementation:** Grain size distribution within the measured Unit 5 fluvial sandstone bed is 125-177 $\mu$ . Poor to moderate cementation (generally moderate), strong reaction to HCl.**Bed thickness:** 4m thick (massive, Unit 5: white fluvial sandstone), area – 1 acre**Structure****Strike and dip of bedding:** A good bedding surface to measure strike and dip is almost impossible to find. Estimate N50W 11SW. See chart 50 for measurements at that locality.**Structural curvature (estimated):** Northwestern limb, estimate of curvature unavailable due to poor exposure of northern plunge as expressed within the Mesaverde section.**Faulting:** No large-scale faulting observed.**Fracture Characteristics****Type, Orientation:** Set A: TNF. Set B: XF.

Set A	Set B
N44W 68NE	N36E 88SE
N42W 80SE	N46E 86SE
N43W 62NE	N54E 80SE
N45W 63NE	N43E 64SE
N45W 62NE	N55E
N46W 68NE	N30E 87SE
N41W 64NE	N65E 76SE

**Spacing: (m)**

Set A (meters)	Set B (meters)
6.30	4.3
5.25	5.1
4.85	4.9
3.9	2.6
4.5	4.2
	3.6
	4.3

**Separation: (cm)****Mineralization:** None.**Surface characteristics:** Generally planar surface.**Relative ages:** Set A older**Apertures:** (cm) Set A – 1.1, 4.0, 3.0, 2.0, 1.2, 1.5

Set B – 2.5, 2.5, 2.0, 3.0, 2.5, 2.0, 1.1, 0

Determined to be recent.

**Deformation Bands (width):**

**Other observations:** Two thin (6-7 cm thick) Fe enriched cross-beds in the measured unit are oriented N50E 5SE. TNF orientations in these siderite (Fe) enriched cross-beds are provided below:

TNF	Spacing, cm
N60W 80SW	10
N63W 82SW	15
N68W 90	10
N60W 84SW	15
N63W 85SW	13
N68W	15
90	14
N63W	22
N65W 84SW	10
N63W	18
	average 15

These fractures do not extend into the less cemented massive sandstone that encases these Fe enriched cross-beds.

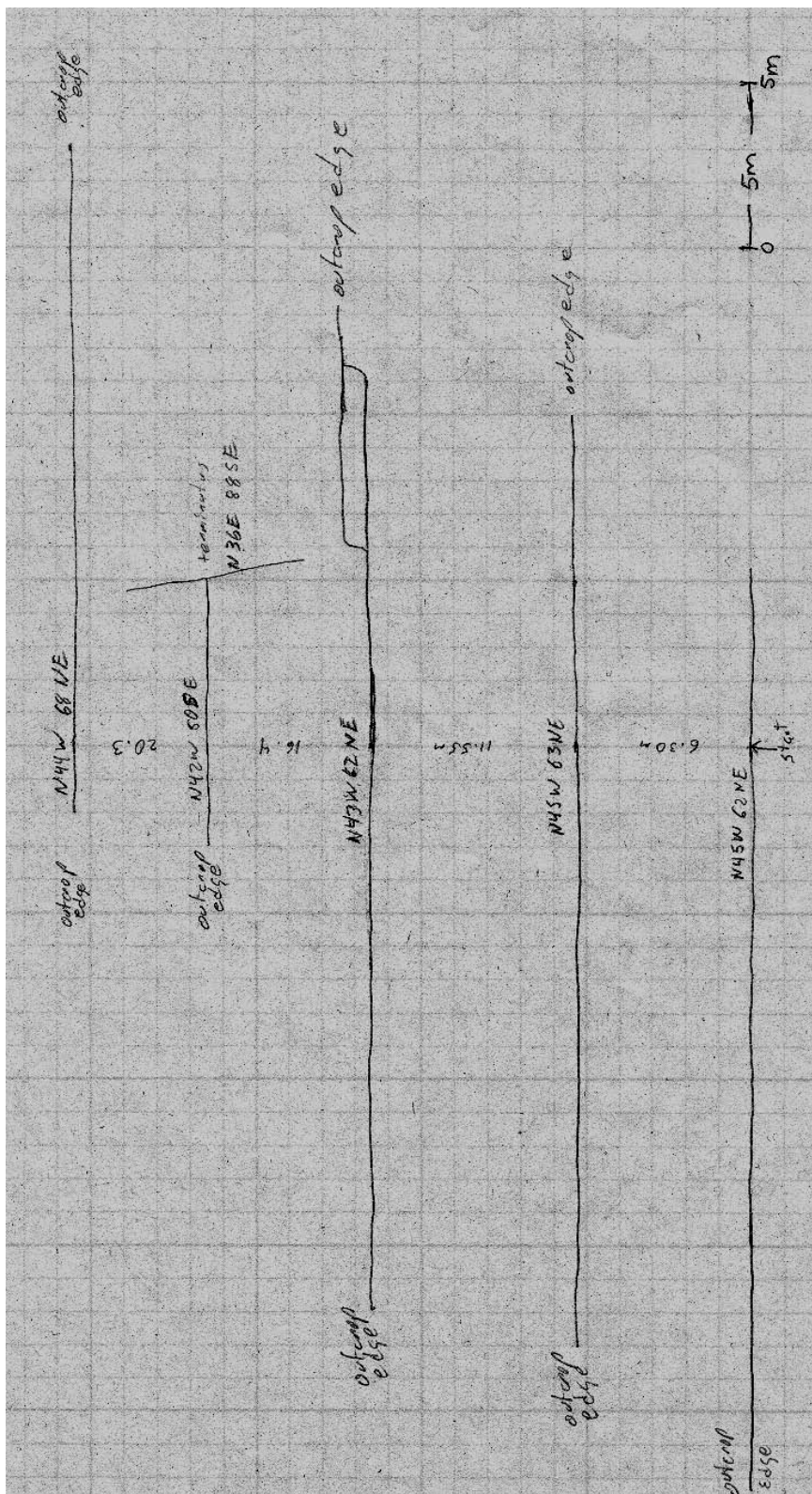


Chart 48: Pavement map detailing Set A fracture trace lengths, spacing and orientations.

**Chart #: 49**

Plan and side views

**Location:** NE1/4 NE1/4 Sec 5 T38N R78W**Lithology:** Unit 4: carbonaceous shale**Grain size, cementation:** very fine-grained (carbonaceous shale), very poorly cemented (fissile)**Bed thickness:** 20cm thick, area – 5m X 2m**Structure****Strike and dip of bedding:** Estimate N50W 10SW. See chart 50.**Structural curvature (estimated):** Northwestern limb, estimate of curvature unavailable due to poor exposure of northern plunge as expressed within the Mesaverde section.**Faulting:** No large-scale faulting observed.**Fracture Characteristics****Type, Orientation:** Set A: cleats, most easily distinguished through-going set in this outcrop. Set B: cleats, generally terminate at Set A.

Set A	Set B
N81W 85SW	N1E 80NW
N79W 86SW	N4E 76NW
N80W 85SW	N30W 82SW
N81W 90	N8E
N83W 89SW	N8E 87NW
N80W 90	N3W 74NE
N78W 87SW	N8E 88NW
N80W 85SW	N10E 84SE
N81W	N5E 90
N79W 86SW	N5E 84NW
N82W 89SW	N8W 80NE
N79W 90	
N78W 88SW	
N79W 90	

**Spacing: (cm)**

Set A	Set B
22	40
25	32
24	90
40	94
39	57
6	20
35	24
33	25
24	30
25	
44	

44	
30	
29	
26	
26	
15	
19	

**Separation:** None observed

**Mineralization:** Fe staining on cleat surfaces

**Surface characteristics:** planar

**Relative ages:** Set A older

**Apertures:** (mm)range 0-5mm, 3mm average

Set A: 3, 2, 1, 5, 2, 4, 6, 4, 3, 4

Set B: 5, 4, 2, 2, 1, 2, 2

**Deformation Bands (width):** NA

**Chart #: 50**

Plan and side views

**Location:** NE1/4 NE1/4 Sec 5 T38N R78W**Lithology:** Unit 2: upper section of beach sandstone, Fe (siderite) enriched pavement (dark red/brown), poorly to moderately cemented white bss overlying and underlying the measured pavement.**Grain size, cementation:** Grain size distribution within the measured bed 40% 125-177 $\mu$ , 55% 177-250 $\mu$ , and 5% 250-350 $\mu$ . Moderately to well cemented.**Bed thickness:** 18cm thick, area – 6m X 11m**Structure****Strike and dip of bedding:** Note – This is the best area found for obtaining strike and dip for this area and should be used for charts 48 and 49 considering lack of good bedding planes in those areas. N47W 11SW, N49W 11SW, N59W 11SW, N49W 11SW**Structural curvature (estimated):** Northwestern limb, estimate of curvature unavailable due to poor exposure of northern plunge as expressed within the Mesaverde section.**Faulting:** No large-scale faulting observed.**Fracture Characteristics****Type, Orientation:** Set A: TNF. Set B: TNF. Set C; XF. Some fractures (not many and no XF's) extend into the poorly cemented unit underlying this pavement.

Set A	Set B	Set C
N45W 75NE	N85W 73NE	XF to Set A
N65W 75NE	N75W	N40W 83NW
N55W 75NE	N80W 87NE	N36W 86NW
N60W 74NE	N80W	N50E 86NW
N55W	N70W	N32E 88NW
N55W 65NE	N78W	N52E 89NW
N59W 75NE	N75W 75NE	N46E
N53W 72NE	N85W 77NE	N42E
N55W		
N58W 75NE		XF to Set B
N50W 73NE		N5E
		N4E 78SE
		N16E
		N10E
		N10E 83SE

**Spacing:** (cm)

Set A	Set B	Set C ( XF to Set A)	Set C (XF to Set B)
45	90	80	40
92	95	43	44
95	130	53	45
94	90	62	54
19	110	92	44
110	90	34	

43		65	
95		35	
		45	
		55	

**Separation:** none observed

**Mineralization:** none observed

**Surface characteristics:** Set B generally terminates at contact with Set A.

**Relative ages:** Set A oldest, Set B next oldest, Set C (XF's) youngest

**Apertures:** 0-10mm – apertures open at outcrop edge; 0 into outcrop, therefore apertures are interpreted to be recent.

**Deformation Bands (width):** NA



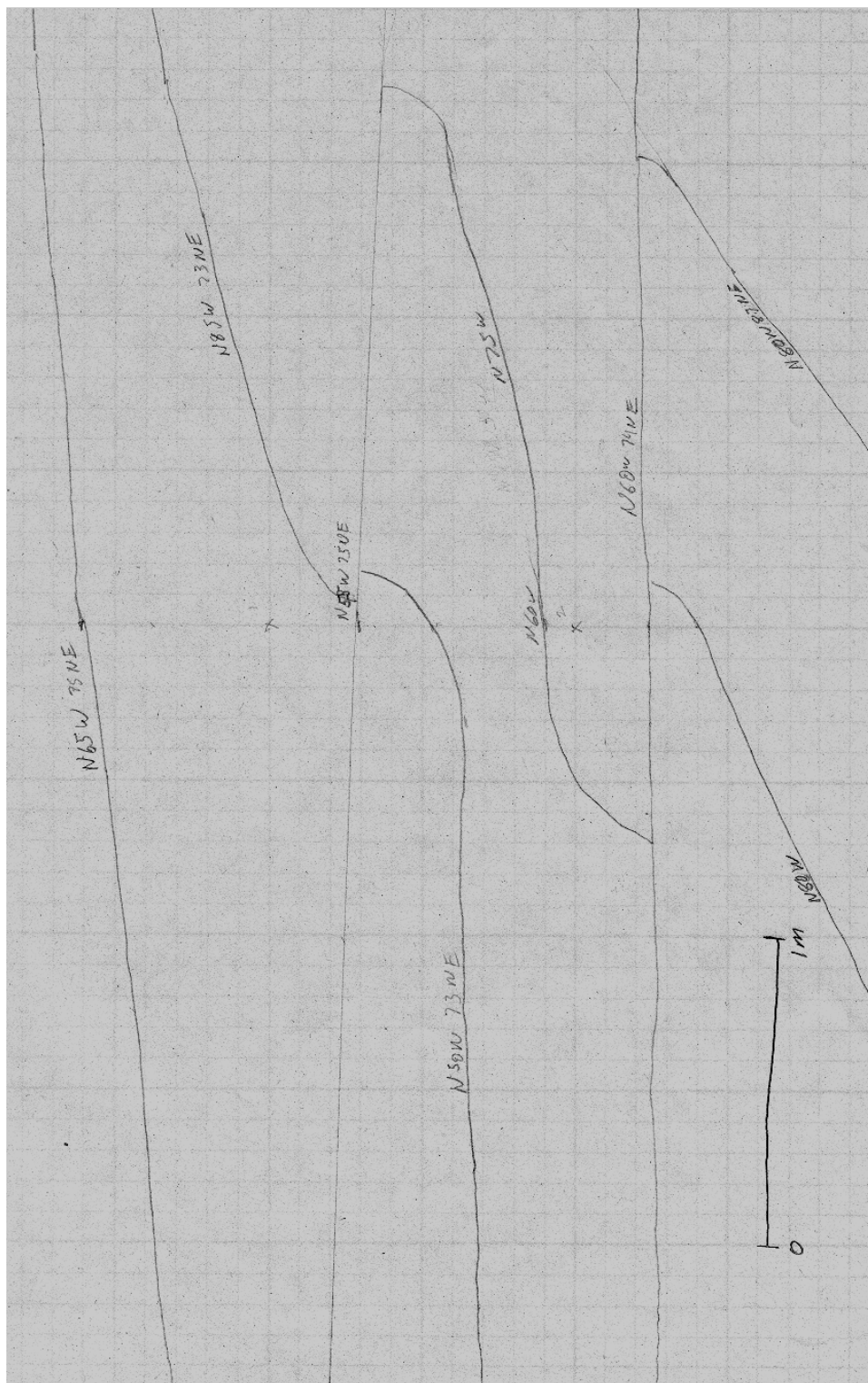


**Chart 50:** Fracture map, fracture sets A and B only, cross fractures are excluded to more clearly illustrate the abutting relationship between Sets A and B.

Sample number	A	B	C	D	E	F	G
Quartz (monocrystalline)	110	89	108	129	128	122	106
Quartz (polycrystalline)	7	0	1	2	1	1	3
Chert	35	28	37	30	17	43	22
Feldspar	14	5	4	6	7	9	8
Muscovite	0	3	2	3	2	4	2
Cement (hematite)	81	23	56	20	130	20	127
Cement (calcite)	0	34	10	2	0	6	0
Cement (chert)	0	2	2	0	0	1	0
Macroporosity (intergranular)	34	99	69	92	8	82	22
Macroporosity (intragranular)	5	4	2	5	0	1	0
Microporosity (intragranular)	5	9	4	9	4	8	6
Microporosity (cement)	9	4	5	2	3	3	4
Number of point counts	300	300	300	300	300	300	300
Percent cement	27.0	19.7	22.7	7.3	43.3	9.0	42.3
Percent porosity	17.7	38.7	26.7	36.0	5.0	31.3	10.7
Cementation (microscopic observations)	mod-well	poor-mod	mod	poor	well	poor	well
Porosity (microscopic observations)	mod	high	mod	high	low	mod	low
Cementation (macroscopic field observations)	well	poor	mod	poor	well	poor	well

**Table Chart 50:** Thin section data from seven distinct beds at Chart 50 location.

**Chart #: 51**

Fault zone, plan and cross-sectional views. Measurements taken as a traverse (from west to east) along strike of the fault.

**Location:** SE1/4 NE1/4 Sec 11 T38N R78W

**Lithology:** The three units from which fracture measurements were obtained along this traverse are Unit 1, Unit 2, and Unit 3.

**Grain size, cementation:** Grain size distribution within sandstones of Unit 1 is 20% 88-125 $\mu$  and 80% 125-177 $\mu$ . The sandstones of Unit 1 are poorly to moderately cemented.

**Bed thickness:** Total thickness of measured Unit 1 sandstones and shales is 5m.

Sandstones of Unit 1 have thicknesses up to 2m. Area where faulting and fracturing was measured within Unit 1 was 20m X 30m.

**Structure**

**Strike and dip of bedding:** N10E 12SE estimate (no reliable bedding surfaces)

**Structural curvature (estimated):** NA

**Faulting:** 5m wide fault zone. N65E 65NW, N58E 84SE. At Stop 1 normal separation along two fault planes 4m northern plane, 2m southern plane, 6m overall separation.

**Fault Characteristics**

**Type, Orientation:** Stop 1: This was the first stop along a fault parallel traverse.

Measurements here are within sandstones and shales of Unit 1. Increased fault parallel fracture spacing with increased distance from the fault was noted at this stop.

Stop 2: Following strike of the fault (150m east of stop 1) into center of a drainage, there is approx. 2m normal separation within sandstone beds of Unit 2 at this locality.

Set 3: Continuation of the fault parallel traverse (50-70m east of stop 2). At this locality the fault is expressed as subparallel deformation bands within the poorly cemented white beach sandstones of Unit 3. One deformation band (striking N75 E 58SE) has slickenlines, with a 25° rake to west, recording sense of slip. Orientation of deformation bands: N56E 80SE, N58E 84NE, N60E 84SE, N58E 82SE, N55E 81SE, N55E 65SE, N65E 81SE, N80E 75SE, N88E 80SE

**Spacing:** (cm)

**Separation:** Varies along strike – 2m at Stop 2 and 6m at Stop 1. Amount of separation at Stop 3 is undetermined.

**Mineralization:** none

**Surface characteristics:** Vertical slickensides and incongruous fracture steps on fault surfaces within sandstones of Units 1 and 2 at stops 1 and 2.

**Relative ages:** NA

**Apertures:** NA

**Deformation Bands (width):**

**Chart #: 52**

Plan view

**Location:** SW1/4 NW1/4 Sec 12 T38N R78W**Lithology:** Unit 1: interbedded sandstone and shale – Unit 3 white beach sandstones are estimated to be ½ m stratigraphically above this location.**Grain size, cementation:** Grain size distribution within the measured sandstone pavement is 80% 88-125µ and 20% 125-177µ. Moderately cemented, dark reddish tan (Fe enriched), highly reactive with HCL.**Bed thickness:** 8-10cm thick, area – 10m X 20m**Structure****Strike and dip of bedding:** N6W 11NE, N6W 11NE, N1W 10NE**Structural curvature** (estimated): NA**Faulting:** 50m north and east of the fault (Stop 3) described in chart 51.

200m south of a large-scale fault located behind the 3 black storage tanks of the Teapot Oil Co.

**Fracture Characteristics****Type, Orientation:** Set A: TNF. Set B: TNF

Set A	Set B
N64E 74NW	N38W 86NE
N66E	N39W 90
N63E 80SE	N34W 89SW
N76E 84NW	N34W 89SW
N72E 84NW	N42W
N76E	N45W 87SW
N73E 83SE	N43W
N73E 85SE	N38W 88SW
N76E 86SE	N39W 80NE
N74E 84SE	N47W 84SW
N74E	N41W 85SW
N60E	N42W
N70E 87SE	N31W
N75E	N54W 1mm wide aperture, calcite filled
N72E 82NW	N32W 1mm wide aperture, calcite filled
N78E 85NW	N35W 81SW
N74E 1mm wide aperture, calcite filled	

**Spacing:** (cm)

Set A	Set B
60	15 *
50	10 *
48	15 *
34	10 *
33	15 *
75	100

85	35
38	25
40	75
73	55
28	56
	68
	75
	38
	102
	68

\* Fracture zone – fracture spacing decreases within this zone and increases away from this zone in both directions.

**Separation:** NA

**Mineralization:** 6 fractures with 1mm wide apertures within Sets A and B are filled with calcite.

**Surface characteristics:** planar

**Relative ages:** Set A older

**Apertures:**

**Deformation Bands (width):** NA

**Chart #: 53**

Plan view and outcrop edge exposures.

**Location:** SE1/4 NE1/4 Sec 11 T38N R78W

**Lithology:** Unit 1: Interbedded marine sandstones and shales (ripple Ss).

**Grain size, cementation:** Grain size distribution within the measured sandstone bed is 60% 62-88 $\mu$  and 40% 88-125 $\mu$ . This tan sandstone is moderately cemented.

**Bed thickness:** 25cm thick, area – 5m X 10m

**Structure**

**Strike and dip of bedding:** N4W 11 NE (overall estimate) poor surface

**Structural curvature (estimated):** NA

**Faulting:** A fault 150-200m to the northeast has approximately 45m of normal separation.

**Fracture Characteristics**

**Type, Orientation:** Set A: TNF. Set B: TNF

Set A	Set B
N74E 75NW	N46W 83SW
N72E 77NW	N26W 86SW
N71E 67NW	N42W 85SW
N77E 67NW	N48W 78SW
N76E 78NW	N25W 81SW
N71E 68NW	N41W 82SW
N68E 77NW	N26W 86SW
N74E 74NW	N26W 88SW
N65E 74NW	N58W
N77E 78NW	N34W 84SW
N74E	N36W
N76E	N24W
N80E	N27W 79SW
N79E 88NW	N52W
N72E 75NW	

**Spacing: (cm)**

Set A	Set B
45	55
11	45
33	42
25	15
5	50
3	27
17	37
17	25
13	26
19	57
22	90

20	23
5	
30	
36	
15	
17	
30	
18	
37	

**Separation:** none

**Mineralization:** Up to 1mm of calcite on some Set A fracture surfaces. Mineralization of similar type also found on Set B fractures. Approx. 50% of fractures have mineralized surfaces (others may have eroded off or not deposited). Some fracture surfaces do exhibit evidence for erosion of calcite surface, such as thin (less than 1mm) patchy coatings of calcite.

**Surface characteristics:** planar

**Relative ages:** Set A older

**Apertures:** Apertures to 2cm. These wider apertures are interpreted as recent. A calcite coating on some fracture surfaces indicates possible 2mm wide apertures at depth.

**Deformation Bands (width):** NA

**Chart #:** 54 – Fault Zone

**Location:** NW1/4 NW1/4 Sec 12 T38N R78W

**Lithology:** Fault places Unit 4 (carbonaceous shale) against Unit 1 (interbedded sandstone and shale)

**Grain size, cementation:**

**Bed thickness:** size of recorded area - 11/2 – 2 acre

**Structure**

**Strike and dip of bedding:** N5W 13NE (approx. – few good bedding planes)

**Structural curvature (estimated):** NA

**Faulting:** Approximately 40m of normal stratigraphic separation, down to S, pipeline placed on fault, disturbing the contact.

**Fault Characteristics**

**Type, Orientation:** Major fault zone is generally covered and bulldozed over due to pipeline emplacement. Fault strike is estimated as N45E 75SE.

Fractures near the fault in Unit 1: Interbedded sandstones and shales and Unit 2: beach sandstones	Coal cleats (Fe stained cleat surfaces) in Unit 4 near the fault
N69E 81NW N62E 67NW N67E 87SE * N79E 75NW N60E 87SE N52E 84NW N81E 57NW N42E 71NW N39E 76NW N62E 75NW N53E 86NW	N80W 76NE N52W 83SE N54E 70SE N63W 72NE N74E 78SE N58E 79SE N72W 76SW N42W 60NE N68E 82SE N85E 67NW

\* 20cm normal separation, note dip

**Spacing: (cm)**

Spacing of fractures within Unit 2: sandstones on the north side of the fault. Fracture spacing measured perpendicular (south to north) from the fault.	Coal cleat spacing in Unit 4
10 5 5 5 28 3 10 22 22 24	2-10 cm, 4cm average



40 10 42 68 110 20 25 100 35 40 87 120 123	
--	--

**Separation:**

**Mineralization:** not observed

**Surface characteristics:**

**Relative ages:** Fracture formation penecontemporaneous with fault formation.

**Apertures:** none

**Deformation Bands (width):**

**Chart #: 55**

Plan and side views

**Location:** SW1/4 SW1/4 Sec 13 T38N R78W**Lithology:** Unit 1: interbedded sandstone and shale. Fractures measured in the sandstones.**Grain size, cementation:** Grain size distribution within the measured sandstone bed 50% 88-125 $\mu$  and 50% 125-177 $\mu$ . Moderately cemented (calcite), tan/brown colored sandstone.**Bed thickness:** 85cm thick, area – 20m X 30m**Structure****Strike and dip of bedding:** N4E 10SE**Structural curvature** (estimated): NA**Faulting:** no large-scale faulting observed**Fracture Characteristics****Type, Orientation:** Set A: TNF – generally more distinct than fracture Set B.

Set B: TNF, fractures less distinct than Set A.

Set C and D: 50cm shale overlying the sandstone bed where set A and B fractures were measured. Sets C and D are measured in the sandstone bed overlying the 50cm thick shale. Within this Unit 1 sandstone bed there are two TNF sets (Sets C and D), measured area – 4m X 15m.

Set D fractures have perpendicular intersections with Set C.

Set A	Set B	Set C	Set D
N85E 83SE	N45W 86SW	N25W 90	N85W 86SW
N82E 89SE	N36W 81SW	N25W 89NE	N72W 83SW
N81E	N36W 82SW	N33W	N76W
N82E 90	N34W 83SW	N28W 83SW	N83W
N81E	N35W	N26W 85SW	N77W 84SW
N81E	N31W	N29W 86SW	N84W 86SW
N78E 88NW	N37W	N26W 90	N76W 82SW
N77E 87NW	N36W 79SW		N76W 83SW
N86E 86NW	N34W 85SW		
N85E 90	N33W 84SW		
N82E 90	N31W 86SW		
N77E 84NW	N31W 79SW		

**Spacing: (cm)**

Set A (measured N to S)	Set B (measured W to E)
150	62
95	15
93	70
48	26
129	45
covered	33
132	28

58	88
72	38
91	97
94	26
	116
	18
	77
	85

**Separation:** none apparent

**Mineralization:** 2/3 of Set B fractures are calcite filled – 1mm average up to 2mm.

Set C fractures have 1-2mm calcite mineralization, filling original apertures.

**Surface characteristics:** indistinct, planar

**Relative ages:** Set A older than Set B. Some Set B fractures intersect Set A perpendicularly. In second area, Set C older, perhaps related to Set B trend from above.

**Apertures:** Calcite mineralization suggests 1-2mm apertures originally in Set B and Set C fractures, alternatively these could be displacive cements. No mineralization on Set A and Set D fracture surfaces.

**Deformation Bands (width):** NA

Note: numerous oyster shells above 8cm thick sandstone interbedded in shales. Also thin lenses of coal 2m stratigraphically above 8cm thick sandstone, then into Unit 3: white beach sandstones. The coals are an anomaly in this part of the stratigraphic section and in this case are interpreted as part of a storm deposit (rip-up clasts).

**Chart #: 56**

Plan and side views

**Location:** NW1/4 SW1/4 Sec 13 T38N R78W**Lithology:** Unit 4: carbonaceous shale**Grain size, cementation:** very fine grained (sh), very poorly cemented**Bed thickness:** 50cm thick, estimate 1 ½ m stratigraphically above Unit 2: bss, area – 4m X 8m**Structure****Strike and dip of bedding:** N1E 11SE (estimate)**Structural curvature** (estimated): NA**Faulting:** no large-scale faults observed**Fracture Characteristics****Type, Orientation:** Cleats in Unit 4, two sets, Set A and Set B.

Set A	Set B
N85E 88SE	N18W 86SW
N85E 86SE	N16W
N88E 86SE	N15W 83SW
N86E 86NW	N14W
N87E 90	N18W
N84E 88NW	N20W 86SW
N88W 89NE	N16W 74SW
N85W	N12W 81SW
N88E 88NW	
N86E 90	
N88W	
N87E	
N87E 86SE	

**Spacing: (cm)**

Set A (N to S)	Set B (E to W)
42	20
8	25
2	30
10	43
42	73
45	56
43	47
6	
5	
4	
11	
11	
68	
15	

**Separation:** none observed

**Mineralization:** Cleat surfaces are Fe stained.

**Surface characteristics:** planar

**Relative ages:** There exist examples of Set A terminating at Set B and Set B terminating at Set A. Generally more Set B fractures terminate at Set A fractures.

**Apertures:** (mm) few apertures; 1, 2, 2, 1, 4, 1, 5, 1, 2

**Deformation Bands (width):** NA

**Chart #: 57****Location:** NW1/4 SW1/4 Sec 13 T38N R78W**Lithology:** Unit 2 beach sandstones**Grain size, cementation:** 20% 125-177 $\mu$ , 80% 177-250 $\mu$ , poor-mod cement, whitish-tan**Bed thickness:** 5m approx., area – 2 acres – large pavement area**Structure****Strike and dip of bedding:** N1E 10SE (estimate)**Structural curvature** (estimated):**Faulting:** no large-scale faulting observed**Fracture Characteristics****Type, Orientation:** Set A: TNF and deformation bands.

Set B: deformation bands.

Key to data chart: db = deformation bands, next db width; F = fracture – (subjective) these designations are somewhat interpretive on my part with well exposed planar surfaces as F, lines with little relief interpreted as deformation bands. Distinguishing between deformation bands and fractures at this outcrop is problematic.

Set A – from S to N end of outcrop	Set A – far N end of ridge/outcrop – fracture zone	Set B
N55W 67SW db 1mm N55W 85NE db 1mm N45W 73SW F N45W 90 F N48W 90 F N49W 68SW F N45W 82SW F N38W 80SW db 1mm – 2 bands N50W 75NE F N47W 86SW F N47W db 11mm 4 bands N44W db 11mm 4 bands N51W db 2mm N62W 80SW F N54W 70NE F N52W 77SW F	N36W 89SW F N42W 86SW F N36W 90 F N34W 86NE F N35W F N48W 84 NE F N44W 66SW F N24W 72SW db 5mm 3 bands N26W 72SW db 3mm 2 bands	N75E 68SE db 2mm N68E 52SE db 3mm N55E 74SE db 2mm N52E db 2mm N45E 68SE db 4mm 1 band, but wide

**Spacing:** (cm)

Set A (measured S to N perpendicular to Set A)	Set B
190 92 10 30 20	

20	
70	
3m	
10	
40	
2	
40	
35	
100	

**Separation:** No separation observed on pavement, although large cliff face below should be examined. Thursday a.m., 8/7/97- Hiked to base of cliff to check for offset. Two distinct sections of different cementation within this bed – the upper section is better cemented than the lower section. Most fractures do not extend into the lower unit – estimate 1 out of 5 possibly less. In this cliff view some separation is observed.

2cm normal offset N42W 75NE

2cm normal offset N40W 86NE

maximum of 1mm normal offset N40W 74NE – incongruous fracture steps.

**Mineralization:** none

**Surface characteristics:** generally planar

**Relative ages:** relationships indeterminate, possible that Set A is older

**Apertures:** none

**Deformation Bands (width):** See type/strike chart above.

**Chart #: 58**

Plan and side views

**Location:** SW1/4 NE1/4 Sec 13 T38N R78W**Lithology:** Unit 4: carbonaceous shale**Grain size, cementation:** very fine grained shale, very poorly cemented , lt. gray shale (bentonite rich) above and below measured unit**Bed thickness:** 1.3m, area – 3m X 10m**Structure****Strike and dip of bedding:** N4W 10NE (estimate)**Structural curvature** (estimated):**Faulting:** no large-scale faulting observed**Fracture Characteristics****Type, Orientation:** cleats

Set A: thoroughgoing cleats

Set B: thoroughgoing cleats, Fe staining extends into shale average 3-5mm. Estimate 1 out of 4 cleats exhibit this trait.

Set A	Set B
N85W 89NE	N4E 73NW
N88W 84SW	N6E 55NW
N86W 77NE	N4E 74NW
N85W 90	N6E 59NW
N87W 84NE	N4E 72NW
N83W 87NE	N1E 83NW
N85W 85SW	N5E 68NW
N82W 87NE	N1W 66SW
N87W 88SW	N4W 65SW
N90W 85SW	N11E 5SW
N87W	N6E 54NW
N89W 90	
N86W	
N88W 90	

**Spacing: (cm)**

Set A (S to N)	Set B (W to E)
20	18
18	10
13	8
17	22
2	8
17	24
15	24
3	18
6	12
8	6
10	9
10	30



19	9
13	

**Separation:** none

**Mineralization:** some Fe staining on surfaces

**Surface characteristics:** planar

**Relative ages:** Set A older

**Apertures:** recent apertures near outcrop edge to 0.5cm

**Deformation Bands (width):** NA

**Chart #: 59**

Mostly cliff exposure, upper surface is generally covered.

**Location:** NW1/4 NW1/4 Sec 13 T38N R78W

**Lithology:** Unit 5: fluvial sandstone

**Grain size, cementation:** Grain size distribution within this sandstone is 10% 125-177 $\mu$ , 80% 177-250 $\mu$  and 10% 250-350 $\mu$ . Poorly to moderately cemented sandstone.

**Bed thickness:** 3½ m to 4m thick, measured area – 15m long X 3 ½ to 4m high

**Structure**

**Strike and dip of bedding:** N3W 11NE (estimate)

**Structural curvature** (estimated):

**Faulting:** no large-scale faulting observed

**Fracture Characteristics**

**Type, Orientation and Spacing (cm):** Set A TNF (VE)

Set A - Strike	Set A – Spacing (measured W to E)
N21W 61SW	90
N19W 60SW	35
N22W 61SW	160
N24W 45SW	5
N24W 54SW	
N21W 59SW	15
N25W 55SW	130
N19W 56SW	100
N18W 51SW	210
N11W 52SW	30
N14W 58SW	95
N16W 58SW	38

**Separation:** none observed

**Mineralization:** One fracture has small vein of gypsum

**Surface characteristics:** planar, some anastomosed surfaces, possible deformation bands in less well cemented areas.

**Relative ages:** only one set observed.

**Apertures:** none

**Deformation Bands (width):** 3 bands (anastomosed) total 8mm

**Chart #:** 60

**Location:** NW1/4 NW1/4 Sec 13 T38N R78W

**Lithology:** Unit 1: interbedded sandstone and shale (measured bed is sandstone)

**Grain size, cementation:** Grain size distribution within the sandstone bed is 90% 88-125 $\mu$  and 10% 125-177 $\mu$ . Moderately cemented (calcite).

**Bed thickness:** 70cm thick – Unit 3: white bss stratigraphically above the measured area. Unit 2 sandstones are absent to very thin (less than 1m) and there is a laterally extensive carbonaceous shale (20cm thick) at base of the Unit 3: white bss - observed while traversing from chart 59 to 60.

**Structure**

**Strike and dip of bedding:** N4W 12NE

**Structural curvature** (estimated):

**Faulting:** no large-scale faulting observed

**Fracture Characteristics**

**Type, Orientation:** Set A: TNF. Set B: TNF.

Set A	Set B
N62E 90	N32W 85SW
N68E 79SE	N34W 89SW
N76E 90	N31W 82SW
N74E 82SE	N34W 87SW
N74E 87SE	N28W 84SW
N67E 84SE	N35W 84SW
N68E 85SE	N44W 78SW
N66E 84SE	N33W 86SW
N68E 90	N33W 89NE
N59E 89NW	N30W 84SW
N70E 86NW	N35W 85SW
N71E 84SE	N37W 80SW
N67E	
N66E	

**Spacing:** (cm)

Set A (measured N to S)	Set B (measured E to W)
134	95
79	95
50	64
50	45
60	53
35	103
45	85
90	84
42	69
92	150
65	58
37	
26	

**Separation:** none observed

**Mineralization:** Some Set B fractures are observed to be filled with calcite, up to 2mm.

**Surface characteristics:** Planar.

**Relative ages:** 70% of Set B fractures terminate at intersection with Set A fractures.

30% of Set A fractures terminate at intersection with Set B fractures. Formation of the two fracture sets maybe broadly contemporaneous at this locality.

**Apertures:** Up to 2mm (calcite filled) in Set B fractures

**Deformation Bands (width):** NA

**Chart #: 61**

Pavement with partial side (cross-sectional) views.

**Location:** SW1/4 SW1/4 Sec 12 T38N R78W

**Lithology:** Unit 2: upper beach sandstone pavement underlying Unit 3: white bss. Note: the anomalous carbonaceous shale found below Unit 3 (white bss) at the Chart 60 location does not exist at this locality. Therefore, the carbonaceous shale pinches out between Chart 60 location and Chart 61 location.

**Grain size, cementation:** Grain size distribution within this sandstone is 20% 125-177 $\mu$ , 70% 177-250 $\mu$  and 10% 250-350 $\mu$ . Grains are well rounded. Moderately to well cemented, light tan sandstone pavement.

**Bed thickness:** 25cm thick, measured area – 2m X 6m

**Structure**

**Strike and dip of bedding:** N5W 12NE

**Structural curvature (estimated):** NA

**Faulting:** no large-scale faulting observed

**Fracture Characteristics**

**Type, Orientation:** Set A: TNF. Set B: TNF.

Set A	Set B
N74E 79SE	N60W 82SW
N78E 70SE	N64W 80SW
N77E 82SE	N62W
N68E	N63W 77SW
N72E 86SE	N70W
N72E 84SE	N58W
N69E 87SE	N61W 78SW
N71E 84SE	
N73E 85SE	
N73E 85NW	
N74E 88NW	
XF to A (not mineralized)	
N19W 81SW	
N19W 83SW	
N17W 84SW	

**Spacing: (cm)**

Set A (measured S to N)	Set B (measured W to E)
26	42
12	68
24	74
25	20
12	18
13	13
12	47
20	25
15	

13	
14	
17	
12	
15	
7	
11	

**Separation:** none

**Mineralization:** 1-2mm wide calcite mineralization within some fractures (in both sets) that fill the fracture apertures completely.

**Surface characteristics:** none visible.

**Relative ages:** Set A fractures older interpreted from abutting relationships.

**Apertures:** 1-2mm. Pavement in road 10m to the NE has numerous mineralized (calcite) fractures; most apertures are 1-2mm and calcite filled. One 10mm wide aperture has 3mm thick calcite on each opposing fracture face.

**Deformation Bands (width):**

**Chart #:** 62

Plan and side views.

**Location:** NW1/4 SW1/4 Sec 12 T38N R78W**Lithology:** Unit 1: light tan sandstone within thick shales (sandstone is very bioturbated).**Grain size, cementation:** Grain size distribution within the moderately cemented (calcite) sandstone is 30% 62-88 $\mu$  and 70% 88-125 $\mu$ .**Bed thickness:** 22cm thick sandstone (3m shale above and 3m shale below), area – 2m X 5 1/2 m.**Structure****Strike and dip of bedding:** N4W 11NE**Structural curvature** (estimated): NA**Faulting:** no large-scale faulting observed in area**Fracture Characteristics****Type, Orientation:** Set A: TNF. Set B: TNF.

Set A	Set B
N82E	N36W 79SW
N77E 87NW	N40W
N84E 86NW	N57W 77SW
N77E 90	N39W 81SW
N82E 90	N56W 86SW
N80E 89SE	N42W 83SW
N79E	N36W
N83E 88NW	N37W 77SW
N82E 89NW	N38W
N81E	N34W
N73E 90	N32W 80SW
N80E 88SE	N32W 75SW
N88E 90	
N88E 89SE	
N89W 90	
N89E 86SE	

**Spacing:** (cm)

Set A (measured S to N)	Set B (measured W to E)
78	20
30	65
26	17
25	30
18	50
12	64
18	
19	
31	
13	
27	
10	

26	
20	
14	
31	
19	
23	

**Separation:** none observed

**Mineralization:** Fe stained surfaces. Some calcite on Set A fracture walls, 1mm thick or less. Not extensively mineralized (most fractures are unmineralized).

**Surface characteristics:** Planar

**Relative ages:** Set A older.

**Apertures:** Current apertures of 1-2mm on Sets A and B near the outcrop edge.

**Deformation Bands (width):** NA



**Chart #:** 63

Pavement with partial side exposures.

**Location:** SW1/4 NW1/4 Sec 12 T38N R78W

**Lithology:** Unit 3: white beach sandstone

**Grain size, cementation:** Grain size distribution within this poorly cemented sandstone is 10% 88-125 $\mu$ , 80% 125-177 $\mu$  and 10% 177-125 $\mu$ .

**Bed thickness:** 120cm thick , measured area – 15m X 15m

**Structure**

**Strike and dip of bedding:** N8W 11NE

**Structural curvature** (estimated):

**Faulting:** Fault 80m - 100m to the north is described in chart 51. Chart 54 details a large-scale fault further to the north.

**Fracture Characteristics**

**Type, Orientation:** Set A: deformation bands. Set B: deformation bands.

Set A	Set B
N32E 57SE	N66E 74SE
N36E 57SE	N67E 76SE
N39E 54SE	N66E 74SE
N42E 64SE	N64E 70SE
N52E 65SE	
N52E 69SE	N33W 64SW
N51E 70SE	
N49E 64SE	
N48E 67SE	

**Spacing:** (cm)

Set A (measured S to N)	Set B
8	4.7m (spacing between N66E 74SE deformation band to the N67E 76SE deformation band)
39	
40	
36	3.5m (spacing between the N67E 76SE deformation band and the N66E 74SE deformation band)
77	
77	
26	
35	
34	

**Separation:** none

**Mineralization:** none

**Surface characteristics:** deformation bands

**Relative ages:**

**Apertures:** apertures exist up to 5mm, generally 1mm or less – to zero aperture width.

**Deformation Bands (width):** (mm) 1, 1, 2, 1, 2, 1, 2, 1, 3, 2, 1

**Other observations:** This area was also charted to detail an observed hexagonal (elephant skin) weathering pattern (Howard and Kochel, 1988). Small hexagons penetrate the surface of this bed up to 30cm. These features are not all hexagons, pentagons and squares are also exist. These features are interpreted as recent and not included in the fracture study. These features are primarily found in Units 2 and 3 at a variety of locations around the rim of Teapot Dome. Larger, to 3m diameter, similar structures are found in other locations. This outcrop contains smaller hexagons within larger hexagonal structures. Fractures and deformation bands found in areas with these weathering features can be difficult to distinguish.

Trends of hexagonal margins	Trends of hexagonal margins
N40E	N82W
N63W	N29E
N15W	N3E
N83W	N15E
N10W	N64W
N64E	N36W
N39W	N30E

**Chart #:** 64

Mostly side exposures with some plan view exposure.

**Location:** SW1/4 NW1/4 Sec 12 T38N R78W

**Lithology:** Unit 4: carbonaceous shale

**Grain size, cementation:** very fine-grained (shale), very poorly cemented

**Bed thickness:** 110cm thick, measured area – 20m X 2m

**Structure**

**Strike and dip of bedding:** N5W 10NE (estimate)

**Structural curvature (estimated):** NA

**Faulting:** no large-scale faulting observed.

**Fracture Characteristics**

**Type, Orientation:** Set A: cleats extend vertically 1m and laterally into outcrop (extensive, well-developed cleats, the dominant set of cleats)

Set B: measurements taken N to S across the outcrop, this set is more widely spaced and fewer in number relative to Set A

Set A	Set B
N86W 80SW	N28W 64SW
N84W 84SW	N18W
N84W 85SW	N10E 88NW
N85W 85SW	N13W 85SW
N85W 84SW	N7E 81NW
N88W 84SW	
N81W 84SW	
N84W 84SW	
N84W 90	
N84W 90	
N88W 90	
N85W 90	
N89W 98NE	
N88W 90	

**Spacing:** (cm) Set A – 12, 3, 15, 14, 17, 16, 5, 18, 15, 17, 12, 20, 11

**Separation:** none observed

**Mineralization:** Some Fe staining on cleat surfaces.

**Surface characteristics:** planar

**Relative ages:** Few other cleats; Set A older

**Apertures:** Up to 3mm at outcrop edge, interpreted as recent.

**Deformation Bands (width):** NA

**Chart #: 65**

Plan view with side exposure

**Location:** NW1/4 SW1/4 Sec 12 T38N R78W**Lithology:** Unit 5: fluvial sandstone (channel)**Grain size, cementation:** Grain size distribution within the measured sandstone is 5% 88-125 $\mu$ , 10% 125-177 $\mu$ , 80% 177-250 $\mu$  and 5% 250-350 $\mu$ . This is a moderately cemented, light tan sandstone with some Fe enrichment.**Bed thickness:** 2m thick, measured area – 5m X 15m**Structure****Strike and dip of bedding:** N4W 11NE (estimate)**Structural curvature** (estimated): NA**Faulting:** no large-scale faulting observed**Fracture Characteristics****Type, Orientation:** Set A: TNF (possible VE). Fractures extend completely across the outcrop. Set B: XF (fewer in number relative to Set A)

Set A	Set B
N36W 85SW	N53E 65NW
N35W 89SW	N46E 73NW
N32W 86SW	N55E 68NW
N21W 90	N59E 68NW
N34W 82SW	N57E 67NW
N27W 84SW	
N38W 85SW	
N38W 87SW	
N40W 90	
N38W 87SW	
N38W 85SW	
N32W 87SW	
N35W 85SW	
N34W 83SW	
N35W 85SW	

**Spacing:** (cm)

Set A (measured E to W across outcrop)	Set B
66	185cm spacing between the fracture striking N55E 68NW and the fracture striking N59E 68NW. Spacing between the other fractures was undetermined due to exposure. Spacing on these is inferred to be greater than 2m.
116	
86	
50	
106	
142	
78	
64	
129	
108	
110	
110	

105	
92	

**Separation:** Possible 1cm offset (normal) on 2 Set A fractures. However, this is observed along a very rugged cliff exposure. Therefore these displacements maybe recent.

**Mineralization:** none – looking at cliff exposure 1 fracture has splotchy (1mm wide) coating of calcite on the fracture wall. Calcite coatings on the other fracture surfaces may have eroded off or is not visible in plan view.

**Surface characteristics:** Planar

**Relative ages:** Set A older.

**Apertures:** none

**Deformation Bands (width):** NA

**Chart #:** 66

Graben

**Location:** SE1/4 SE1/4 Sec 35 T38N R78W

**Lithology:** Unit 4: Carbonaceous shale down dropped to stratigraphic level of Unit 1: interbedded Ss and shale. Both fractures and cleats of Units 1 and 4 respectively were measured at this location.

**Area:** approximately ¼ section

**Structure**

**Strike and dip of bedding:** Measured on a Unit 1 sandstone, N45W 14NE.

**Structural curvature** (estimated): NA

**Faulting:**

Finger ridge on N end is composed of fault slivers of Unit 1: interbedded sandstone and shale. Fracture orientations along this ridge include N65E 88SE, N67E 85SE, N69E 86SE. Slickenlines with 20° rake to west are recorded on a fault plane striking N65E 88SE within this ridge. Some fracture patterns (see diagram below) and slickensides indicate right lateral shear. At the far northeastern corner of this ridge a major fault is observed with 40-45m stratigraphic separation. Orientation of this fault is N65E 85SE.



**Fracture Characteristics**

**Type, Orientation:** Set A: top of ridge NE corner, fractures measured S to N from the large-scale fault within a 160cm thick Unit 1 sandstone. The sandstone is moderately cemented with a grain size distribution of 90% 88-125µ and 10% 125-177µ.

Set A - strike	Set A – spacing (cm)
N62E	20
N66E 74NW	46
N65E 70SE	65
N68E 75NW	72
N67E 80NW	96
N66E 62SE	125
N65E 82NW	345
N65E 73NW	365
N63E 73NW	1130
N65E 79NW	1258
N66E 70SE	1319
N66E 84NW	1637
N69E 85SE	1706
N56E 77NW	

Set B: Same sandstone bed described above for Set A fractures, these TNF's curve to have near perpendicular intersections with the large-scale fault, the actual area of fracture fault intersection is covered therefore the intersection angle is inferred. Curving begins 6-8m out from the fault. Fractures measured E to W across the outcrop.

Set B - strike away from fault	Set B – near fault
N13W 74SW	N42W 75SW
N14W 68SW	N33W 83SW
N11W 87SW	N50W 84SW

Coal (carbonaceous shale cleats in fault block)	Continued
N56E 73SE	N26W 70NE
N59E	N15W 84SW
N58E 77SE	Note – carbonaceous shale bent upward at fault margin
N58E 86SE	
N72E90	
N64E 68SE	
N76E 76SE	

**Spacing:** Set A fracture spacing measured in a second transect starting at the large-scale fault, 3, 1, 3, 20, 25, 20, 5, 22, 29, 28, 45, 52, 4, 800 (cm).

Set B – 3.4m (N42W 75SW fracture to N33W 83SW fracture)

6.3m (N33W 83SW fracture to N50W 84SW fracture).

**Separation:** 40-45m normal offset on graben. 5+m offset on some fault slivers

**Mineralization:** Most fractures are not mineralized however some fracture surfaces coated with calcite (up to 2.5mm on a single fracture wall) and cubic pyrite.

**Surface characteristics:** One area - slickensides on fault sliver.

**Relative ages:** Set A older.

**Apertures:** Generally none

**Deformation Bands (width):** NA

**Other observations:** Stratigraphic units appear to have same elevation on opposite sides of graben.

South side of graben:

- Good pavement for taking fracture measurements unavailable, unlike N side.
- Coal beds bend upward at fault zone.
- Ss and shale – possibly bend down into fault.
- Ss and shale very broken, extensive calcite mineralization 1-3mm width average.
- Fault orientation at ridge top is N65E 85NW (dip approx.).
- Fault orientation to E, estimate at N55E 85NW.

**Chart #:** 67

Plan and side views

**Location:** NW1/4 SE1/4 Sec 35 T38N R78W

**Lithology:** Unit 1: sandstone interbedded in shale

**Grain size, cementation:**

**Bed thickness:** area – fault zone extends approx. ½ mile to E

**Structure**

**Strike and dip of bedding:** N40W 11NE

**Structural curvature (estimated):** beginning N end curvature 1km?

**Faulting:** This is a description of a large-scale fault. Fault zone approx. 10m wide.

**Fracture Characteristics**

**Type, Strike:** N65E 85SE

**Spacing:** (cm)

**Separation:** Normal displacement down approx. 20m to south as estimated from stratigraphic separation of Unit 3 white sandstones and Unit 1 sandstones and shales.

**Mineralization:** calcite mineralization in some fractures

**Surface characteristics:**

**Relative ages:**

**Apertures:**

**Deformation Bands (width):** NA



**Chart #:** 68

**Location:** SE1/4 SE1/4 Sec 22 T38N R78W

**Lithology:** Fractures on north side of fault are in light tan Unit 5 fluvial sandstone (channel), with moderate cement.

**Grain size, cementation:** 10% 88-125 $\mu$ , 80% 125-177 $\mu$ , 10% 177-250 $\mu$ , poor-mod cementation in bss

**Bed thickness:** Area – 10-acre approx.

**Structure**

**Strike and dip of bedding:** N35W 14SW

**Structural curvature** (estimated): entering southern hinge, approx. 1km curvature.

**Faulting:**

Graben: 1m offset, 20-25 yards wide, N60E 86° dip. Fractures are TNF's.

Set A	Set B
N58W 73NE	N14W 84NE
N60W 84NE	N13W 85NE
N61W 85NE	N6W 88NE
N57W 85NE	N11W 78NE
N58W 81NE	N12W 87NE
N56W 80NE	N14W 85NE
N60W 81NE	N7W 84NE
	N9W 83NE
	N7W 86NE

Set A trend more abundant on W end of outcrop.

**Fracture Characteristics**

**Type, Orientation:** Fracture orientation in \* area of map – Unit 2 bss, 30cm average spacing in a 8m square area.

Set A	Set B
N64W 86NE	N65E 65SE
N74W 71NE	
N72W 85NE	
N68W 90	
N68W 83NE	
N78W 78NE	

**Spacing:** (cm) 30cm average

**Fracture Characteristics**

**Type, Strike:** Fault zone North end, orientation N45E 85NW, wide area 25-30m, two isolated blocks in zone each down to North. The following are orientations in Unit 2 bss.

Set A- measurements S to N from fault zone that shows shear	Set B	Set C – deformation bands in Unit 3 sandstone Same general orientation as Set A	Along cliff face Some surfaces show incongruous fracture steps
N45E 71NW	N15W 70NE	N47E	N46E 67SE
N43E 78NW	N16W 68NE	N44E 50SE	N42E 74NW
N43E 52NW	N13W 80NE	N50E 90	N41E 73SE

N45E 72SE N47E 86SE	N15W 78NE N15W 74NE N15W 72NE N9W 78NE N10W 72NE N45W 82NE	N49E 70SE N45E 79NW N44E 80NW N47E 67NW N46E 83SE N54E	N29E 72SE N52E 75SE N46E 73NW N53E 83NW N43E 81NW N30E 67NW** N33E 66NW N47E 77NW
------------------------	---	---	--

\*\* 28° rake to east measured on slickenlines.

**Spacing: (cm)**

Set A	Set B	Set C
30	25	35
300	35	85
40	10	18
45	10	60
	28	65
	100	80
	18	100
	670	

**Separation:** 5m total normal separation

**Mineralization:**

**Surface characteristics:**

**Relative ages:**

**Apertures:**

**Deformation Bands (width):** (mm) Set C – 3 (2 bands), 3 (2 bands), 2, 2, 2, 2, 2, 2

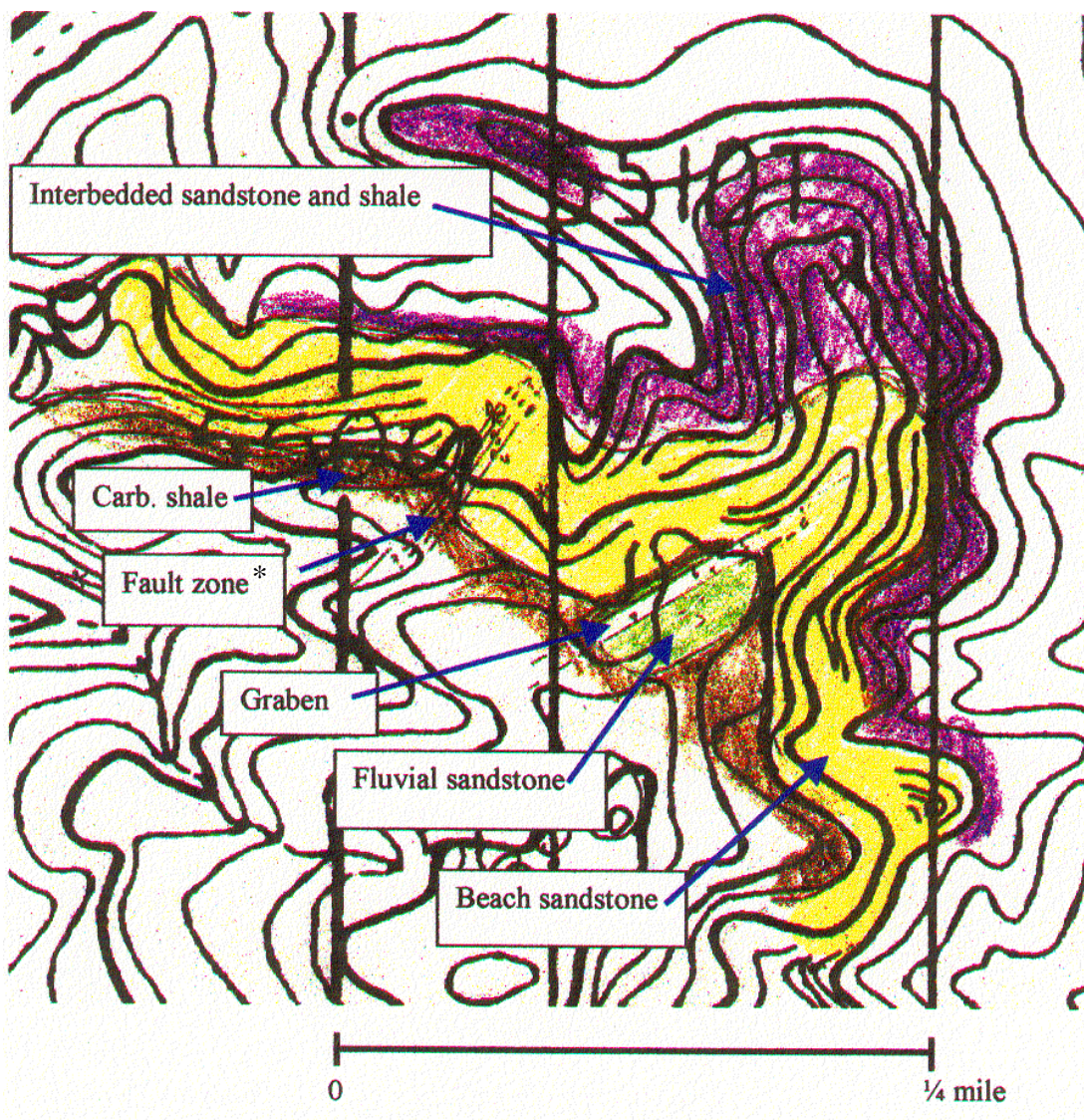


**Chart 68:** Field map

**Chart #: 69**

Plan and side views

**Location:** NW1/4 NW1/4 Sec 12 T38N R78W**Lithology:** FGRSs within Unit 1: interbedded sandstones and shales.**Grain size, cementation:** Grain size distribution within the sandstone 85% 62-88 $\mu$ , 10% 88-125 $\mu$  and 5% 125-177 $\mu$ . Moderate to well cemented (reddish color, Fe enriched).**Bed thickness:** 35cm thick; measured area – 10m X 10m**Structure****Strike and dip of bedding:** N10W 10NE

N9W 9NE

**Structural curvature** (estimated): NA**Faulting:** 40m to E of charted area a fault places unit 4 carbonaceous shales against Unit 3 white sandstones, orientation N65E 54NW.

Fracture orientations within Unit 1 sandstones near the fault are:

N67E 55NW \*

N65E 57NW \*

N64E 57NW \*

\* N end of fault zone; spacing 25cm average for these three fractures

South side of main fault zone a subsidiary fault oriented N55W 69NE has 25cm normal stratigraphic separation within Unit 1 interbedded marine sandstones and shales.

**Fracture Characteristics****Type, Orientation:** Set A: TNF, measured S to N across outcrop, perpendicular to fracture strike.

Set B; XF, measured E to W, irregular strike, dips difficult to obtain due to irregular pavement surface.

Set A	Set B
N52E 90	N37W 90
N54E 90	N52W
N57E 90	N29W 84SW
N58E	N24W
N48E 89SE	N34W 88SW
N83E 89NW	N2W 88SW
N51E 90	N4W
N57E 90	N22W
N58E 88NW	N23W
N60E 89NW	N29W 90
N51E	N11W 85SW
N62E	N50W 85SW
N65E	N22W 88NE
N64E 84SE	N36W
N65E 90	N31W
N69E 90	N8W 78SW
N67E	N12W 83SW
N64E 90	

**Spacing:** (cm)

Set A (measured S to N)	Set B (measured E to W)
34	20
20	10
25	20
27	45
45	30
39	38
26	60
24	30
33	33
19	35
3	43
59	55
17	
56	
5	
38	

**Separation:** not observed in fractures – see fault description.

**Mineralization:** near faulted area 1-2mm wide calcite on some surfaces, not extensive. No mineralization observed on fractures in FGRSs pavement.

**Surface characteristics:** Difficult to observe fracture surfaces due to very poor (irregular) pavement surface. Set A much better developed and extensive relative to Set B.

**Relative ages:** Set A older than Set B (cannot tell age relation between fault and Set A)

**Apertures:** generally none up to 2mm near outcrop edge

**Deformation Bands (width):** NA

**Chart #: 70**

Plan and side views

**Location:** NW1/4 SW1/4 Sec1 T38N R78W**Lithology:** Unit 5: fluvial (channel) sandstone**Grain size, cementation:** Grain size distribution within the measured sandstone bed 90% 62-88 $\mu$  and 10% 88-125 $\mu$ . Red colored, moderately cemented sandstone.**Bed thickness:** Total thickness of fluvial unit is 3.5m. The upper 50cm of this unit is relatively better cemented compared to the underlying 3m of sandstone. Measured bed thickness for this site is 50cm.**Structure****Strike and dip of bedding:** N14W 13NE**Structural curvature** (estimated): NA**Faulting:** no large-scale faulting observed**Fracture Characteristics****Type, Orientation:** Set A: TNF. Set B: TNF.

Set A	Set B
N44W 76SW	N75E 86SE
N40W 85NE	N76E 88SE
N42W 83SW	N74E 84SE
N46W 81SW	N83E 86SE
N43W 80SW	N74E 86NW
N48W 90	N74E 90
N26W 88NE	N72E 87SE
N47W 84SW	N76E 89SE
N51W 76SW	N73E 87SE
N14W 86NE	
N41W 89NE	
N54W 88SW	

**Spacing:** (cm) measured perpendicular to strike of each set

Set A	Set B
85	30
48	35
102	29
104	55
57	38
70	20
40	52
35	20
72	
50	

**Separation:** none observed

**Mineralization:** none observed at measured area – to north in the same lithologic unit, some calcite on Set A fractures was observed. 1mm wide calcite filled aperture.

**Surface characteristics:** no distinct surface characteristics

**Relative ages:** Set A older

**Apertures:** primarily recent openings at cliff edge

**Deformation Bands (width):** NA

**Chart #: 71**

Side and plan views.

**Location:** SW1/4 SW1/4 Sec 1 T38N R78W**Lithology:** Unit 4: carbonaceous shale**Grain size, cementation:** Very fine-grained, very poorly cemented.**Bed thickness:** 1m thick; measured area – 6m X 2m**Structure****Strike and dip of bedding:** N14W 12NE**Structural curvature (estimated):** NA**Faulting:** no large-scale faulting observed**Fracture Characteristics****Type, Orientation:** Set A: (TNF) cleats in Unit 4 carbonaceous shale and coal. Set B: (TNF) cleats.

Set A	Set B
N74W 90	N89E 90
N76W 86NE	N24E 77SE
N72W 75NE	N26E 79SE
N73W 70NE	N18E 70NW
N74W 81NE	N17E 65NW
N70W 81NE	N27E 84SE
N63W 79NE	N26E 82NW
N78W 78NE	N18E 90
N79W 76NE	
N53W 71NE	
N71W 84NE	

**Spacing:** (cm)

Set A	Set B
20	41
10	36
20	75
23	17
28	56
25	50
20	43
55	35
35	

**Separation:** none observed**Mineralization:** Fe staining on cleat surface**Surface characteristics:** planar**Relative ages:** Set A older.**Apertures:** recent apertures to 4mm at edge**Deformation Bands (width):** NA

Note: On transverse between Charts 69-70 few good cleats observed in the carbonaceous shale unit.



**Chart #:** 72

Plan and side views.

**Location:** SW1/4 NW1/4 Sec 1 T38N R78W

**Lithology:** Unit 3: white beach sandstone (snowy white)

**Grain size, cementation:** Grain size distribution within the measured bed is 10% 125-177 $\mu$ , 80% 177-250 $\mu$  and 10% 250-350 $\mu$ . Poorly cemented sandstone.

**Bed thickness:** 5m thick; measured area – 15m X 5m

**Structure**

**Strike and dip of bedding:** N18W 13NE

**Structural curvature** (estimated): NA

**Faulting:** no large-scale faulting observed

**Fracture Characteristics**

**Type, Strike:** Set A: deformation bands. N38W 84NE, N35W 80SW, N32W 76NE, N39W 78SW, N34W 76NE

**Spacing:** (cm) 40, 320, 135, 200

**Separation:** none observed

**Mineralization:** no mineralization

**Surface characteristics:** planar

**Relative ages:** only one set of deformation bands

**Apertures:** none

**Deformation Bands (width):** 2, 2, 2, 2, 1mm

Notes: Hexagonal (elephant skin) weathering pattern also observed (ignored during measurements of deformation bands).

**Chart #:** 73

Fault description.

**Location:** SW1/4 SW1/4 Sec 1 T38N R78W

**Lithology:** Unit 1 and Unit 2 sandstones

**Grain size, cementation:**

**Bed thickness:**

**Structure**

**Strike and dip of bedding:** N15W 14NE

**Structural curvature** (estimated): NA

**Faulting:** Fault zone is approximately 30m wide with one primary slip surface. 5m of normal stratigraphic separation, orientation of the primary slip surface is N65E 85NW.

**Fracture/Fault Characteristics**

**Type, Orientation:**

Fracture orientations within Unit 2 sandstones. These measurements are within the damage zone south of the primary fault surface. N66E 65NW, N69E 73NW, N65E 70NW, N64W 81SW, N64W 78SW, N64W 78NW

**Spacing:** (cm)

**Separation:** 5m displacement

**Mineralization:** calcite mineralization with associated fractures

**Surface characteristics:**

**Relative ages:**

**Apertures:** NA

**Deformation Bands (width):** NA

**Chart #: 74**

Plan and side views.

**Location:** NW1/4 NW1/4 Sec 1 T38N R78W**Lithology:** Unit 5: fluvial sandstone**Grain size, cementation:** Grain size distribution within the measured sandstone bed is 50% 88-125 $\mu$ , and 50% 125-177 $\mu$ .**Bed thickness:** The measured bed is 70cm thick, overall thickness of this fluvial sandstone package is 3.4m; measured area – 15m X 15m**Structure****Strike and dip of bedding:** N20W 11NE, N17W 12NE**Structural curvature** (estimated): NA**Faulting:** no large-scale faulting observed**Fracture Characteristics****Type, Orientation:** Set A: TNF bed normal, one en echelon left step. Set B: TNF

Set A	Set B
N40W 75SW	N51E 85SE
N44W 86SW	N62E 79NW
N35W 82SW	N47E 71NW
N28W 88NE	N63E 80NW
N32W	N64E 89SE
N35W	N63E 80NW
N35W 80SW	N53E 73NW
N25W 80SW	N63E 83NW
N26W	N66E 84SE
N36W 76SW	N62E
N33W 78SW	
N44W 85SW	
N32W 83SW	
N28W 84SW	
N30W	

**Spacing: (cm)**

Set A (measured E to W)	Set B (measured S to N)
75	125
18	39
78	95
16	160
20	100
40	102
55	100
95	
80	
55	
40	
82	

**Separation:** none observed

**Mineralization:** no visible mineralization; however, fracture surfaces are raised (erosion resistant)

**Surface characteristics:** none observed

**Relative ages:** Set A older

**Apertures:** recent apertures to 1mm

**Deformation Bands (width):**

**Chart #: 75**

Pavement

**Location:** NE1/4 NE1/4 Sec 2 T38N R78W**Lithology:** Unit 1: interbedded sandstone and shale. Measured bed is sandstone.**Grain size, cementation:** Grain size distribution within the measured sandstone bed is 20% 88-125 $\mu$ , 40% 125-177 $\mu$  and 40% 177-250 $\mu$ . This light tan sandstone is moderately cemented, not as Fe stained as some pavements.**Bed thickness:** 90cm thick, approximately 3-4m stratigraphically below Unit 3: white beach sandstone.**Structure****Strike and dip of bedding:** N25W 10NE, N18W 11NE, N20W 11NE

These are possible cross beds overall orientation estimate N20W 10NE.

**Structural curvature (estimated):** Nearing area of northern plunge.**Faulting:** No large-scale faulting observed between charts 74 and 75.**Fracture Characteristics****Type, Orientation:** Set A: TNF. Set B: TNF. Set C: XF (possible TNF).

Set A (S to N)	Set B (S to N)	Set C (E to W)
N25E 72NW	N56E 90	N32W 79SW
N25E 82NW	N58E 85NW	N25W
N29E 81NW	N55E 86NW	N30W 83SW
N29E 76NW	N56E	N33W 83SW
	N60E 90	N32W
	N52E	N32W 82SW
	N48E 88NW *	N32W
	N42E	N30W 81SW
	N55E 86NW	N28W 85SW
	N57E 88NW	
	N53E 90	
	N54E	

\* curves to parallel Set A at intersection

**Spacing: (cm)**

Set A	Set B	Set C
107	20	152
125	3	25
125	3	118
	33	80
	18	22
	28	14
	22	30
	100	70
	80	
	24	
	14	

**Separation:** none observed

**Mineralization:** none

**Surface characteristics:**

**Relative ages:** Set A oldest. Set B next oldest. Set C is the youngest.

**Apertures:** Decrease to zeros away from outcrop edge. Recent apertures at outcrop edge to 3mm, 1mm average

**Deformation Bands (width):** NA

**Chart #: 76**

Plan view

**Location:** SE1/4 SE1/4 Sec 35 T39N R78W**Lithology:** Unit 2: upper beach sandstone**Grain size, cementation:** Grain size distribution within the measured sandstone bed is 15% 125-177 $\mu$ , 80% 177-250 $\mu$  and 5% 250-350 $\mu$ . This is a poorly to moderately cemented light gray sandstone.**Bed thickness:** 2.5m thick, measured area – 12m X 6m**Structure****Strike and dip of bedding:** N30W 14NE**Structural curvature (estimated):** North end of anticline curvature undetermined. This is due to the lack of Mesaverde Formation exposures along the northern plunge of the anticline.**Faulting:** Graben described in Chart 66 is 300-400m to the south of this charted (chart 76) location.**Fracture Characteristics****Type, Orientation:** Set A: TNF (VE). Set B: TNF (possible XF?)

Set A (W to E)	Set B (S to N)
N1W 73SW	N84E
N0W 76W	N85E
N1W 74SW	N84E 84SE
N2W 70SW	N86E
N1E 71NW	N87E 88SE
N0 81E	N87E 87SE
N4W 85SW	N86E 90
N1W 74SW	N87W 88SW
N0W	

**Spacing: (cm)**

Set A	Set B
220	105
55	258
170	85
73	57
41	86
66	90
65	
109	

**Separation:** no visible offset**Mineralization:** none**Surface characteristics:** none distinguishable**Relative ages:** Set A older**Apertures:** none**Deformation Bands (width):** NA

**Chart #: 77**

Side view (cliff exposure)

**Location:** SW1/4 SW1/4 Sec 35 T39N R78W**Lithology:** Sandstone within Unit 1: interbedded sandstones and shales.**Grain size, cementation:** Grain size distribution within the measured sandstone bed 80% 62-88 $\mu$  and 20% 88-125 $\mu$ . Moderately cemented sandstone.**Bed thickness:** 31cm thick; measured area – cliff exposure – 10m long X 6m high**Structure****Strike and dip of bedding:** N28W 11NE**Structural curvature (estimated):** North end of anticline curvature undetermined. This is due to the lack of Mesaverde Formation exposures along the northern plunge of the anticline.**Faulting:** Uphill and 20m south of the charted outcrop a fault is expressed in a 2m wide break in the rock unit. The 2m wide fault zone is a total of 20cm down (normal) to the south. Strike N65E near vertical dip.**Fracture Characteristics****Type, Orientation:** Set A: TNF (VE). Set B: XF.

Set A	Set B
N14W 53SW	N86W 76NE (cliff breakage?)
N7W 54SW	N83E 77NW
N8W 56SW	N75W 86SW
N10W 54SW	N86E 76SE
N13W 55SW	N81E 67SE
N8W 55SW	
N7W 59SW	
N9W 61SW	
N14W 56SW	
N9W 53SW	

**Spacing: (cm)**

Set A	Set B
47	5
57	5
47	
53	
26	
50	
17	
18	
20	

**Separation:** no visible offset**Mineralization:** none visible**Surface characteristics:** no distinguishable characteristics**Relative ages:** Set A older

Note: This is cliff exposure plan view, abutting relationships difficult



**Apertures:** (mm) 1, 1, 2, 3, 1, 1, 2

**Deformation Bands (width):** NA

Note: observed a lack of fractures in shale and increased fracture spacing with increased bed thickness.

Detailed spacing data of Set A fractures for several Unit 1 sandstone beds.

Beds listed from top to bottom.

A: shale 1cm thick (average)

B: sandstone 8 cm thick (average)

C: shale 4.5 cm thick (average)

D: sandstone 33 cm thick (average)

E: shale 1.5 cm thick (average)

F: sandstone 5.5 cm thick (average)

G: shale 1.5 cm thick (average)

Bed B thickness (cm)	Bed B spacing (cm)	Bed D thickness (cm)	Bed D spacing (cm)
3	8	32	31
1.5	8	30	32
1.3	8.5	15	33
2	8	18	34
4	8	19	33
1	8	36	33
5	7	26	32
5.5	6.5	56	36
7	7.5	49	33
12	8	36	34
11	8	44	32
15	8		
15	8		
16	10		
20	15		
19	16		
15	16		
25	15		
15	12		
12.5	10		
19	9.5		
11.5	7		
10.5	7.5		
5	6		
12.5	5		
11.5	5		
2.5	4		

6	5		
5	5		
3.5	5		
3	5		
5	5		
13	5		

Bed F thickness (cm)	Bed F spacing (cm)
10	5
19	5.5
14	6
9	6
4	4
5	4.5
1	4
3	4
3	3.5
4.5	4
17.5	5
12	5
11	5.5
13	5.5
6	5
9	5.5
6	6
5	5
8	5
19	6
8	6
15	6
5	6
17	8
10	7
30	7.5
11	5.5
8	5
13	5
10	4.5
6	4.5
8	5
10	5
11	5
15	6

**Chart #:** 78

**Location:** NW1/4 SW1/4 Sec 3 T38N R78W

**Lithology:** Steele Shale

**Grain size, cementation:** very fine-grained, very poorly cemented

**Bed thickness:** undetermined – at least 8m this location; area – 4 acres

**Structure**

**Strike and dip of bedding:**

**Structural curvature (estimated):** NA

**Faulting:**

**Fracture Characteristics**

**Type, Orientation:** Mineralized veins within the fault zone. Mineralized veins have calcite crystals that are inferred to grow on opposite walls toward the center. This is evidenced by crystal shape with points of crystals at the center of the vein.

Strike	Number of mineralized veins along a single fault plane.	Widths (mm)
1-N80W 81NE	5	16, 8, 8, 10, 10
2-N75W 70NE	10	10 (max) 5, 2, 1, 2, 10, 1, 5
3-N72W 68NE	10	5, 1, 5, 6, 5, 2, 22, 5, 4
4-N62W 70NE	11	6, 15, 2, 1, 1, 4, 10, 12, 3, 2, 2
5-N60W 70NE	3	7, 1, 2
5a-N60W 88NE	1	2

Data in the following chart are from an area 40m to SE of location from which the previous data was obtained – 1cm thick Ss (gray) in shale; poor to moderate cementation: grain size distribution 40% 88-125 $\mu$  and 60% 125-177 $\mu$ . Average fractures spacing ~5cm; Strike and dip of bedding N35W 15SW.

Set A	Set B – oblique younger set	Set C?
N64W 90	N14W 90	N30W 90
N60W 90	N15W 90	N31W 90
N60W 90	N20W 90	
N58W 90	N16W 90	
N54W 90	N8W 90	
N58W 90	N18W 90	
N56W 90	N13W 90	
N58W 90	N16W 90	
N61W 90	N14W 90	
N65W 90	N15W 90	
N62W 90		

**Spacing: (cm)**

Set A	Set B
8	10
7	6

10	4
5	5
5	6
10	3
6	12
4	3
4	
5	
5	
8	
10	
4	

**Separation:** unknown

**Mineralization:** calcite

**Surface characteristics:**

**Relative ages:** Set B is the younger set.

**Apertures:**

**Deformation Bands (width):** NA

**Chart #: 79**

Side view with limited plan view

**Location:** SE1/4 SE1/4 Sec 10 T38N R78W

**Lithology:** Steele Shale – sandstone in shale

**Grain size, cementation:** Grain size distribution of the measured sandstone bed is 10% 62-88µ, 80% 88-125µ and 10% 125-177µ. Moderately cemented sandstone.

**Bed thickness:** 40cm thick; measured area 20m X 2m

**Structure**

**Strike and dip of bedding:** N20W 8NE (estimate – rough and broken bedding surface)

**Structural curvature (estimated):** NA

**Faulting:** no large-scale faulting observed

**Fracture Characteristics**

**Type, Orientation:** Set A: bed normal VE (TNF). Set B: TNF. Set C: XF

Set A	Set B	Set C	Other
N30W 82SW N37W 84SW N35W 87SW	N75W 85SW N78W 81SW N88W 83SW N87W 85SW N78W 80NE N77W 90 N62W 84NE	N38E 90 N38E 84NW	N1E 90 N58E 85SE N57E 88NW* N62E 85NE *4mm calcite on one surface

**Spacing:** (cm) Set A – approximately 100cm

Set B - 100, 20, 70, 35 cm

Set C – 100 cm

**Separation:** none visible

**Mineralization:** Up to 1mm calcite on Set A fracture surfaces.

**Surface characteristics:** no distinguishing characteristics

**Relative ages:** Set A oldest, Set B next oldest, Set C youngest

**Apertures:**

**Deformation Bands (width):** NA

**Chart #: 80**

Plan view with partial side view

**Location:** NW1/4 SW1/4 Sec 15 T38N R78W**Lithology:** The measured bed is a light tan sandstone within Unit 1 interbedded sandstones and shales.**Grain size, cementation:** Grain size distribution within the measured bed is 10% 62-88 $\mu$ , 85% 88-125 $\mu$  and 5% 125-177 $\mu$ . Poorly to moderately cemented.**Bed thickness:** 40cm thick, measured area – 20m X 10m**Structure****Strike and dip of bedding:** N15W 20SW**Structural curvature (estimated):** NA**Faulting:** no faulting observed**Fracture Characteristics****Type, Orientation:** Set A; TNF (VE). Set B: XF.

Set A	Set B
N39W 70NE	N48E 90
N36W 64NE	N37E 90
N35W 73NE	N45E
N39W 88NE	N49E 90
N34W 89SW	N54E
N43W 62NE	N48E 89SE
N35W 86NE	N51E ~90
N29W 89NE	N47E ~90
N36W	N62E
N39W	N53E 87SE

**Spacing: (cm)**

Set A	Set B
63	120
117	137
80	105
52	45
86	88
20	130
143	140
40	335
	49
	260
	125
	150
	140

**Separation:** none**Mineralization:** none**Surface characteristics:** Planar, no other distinct characteristics**Relative ages:** Set A oldest**Apertures:** none**Deformation Bands (width):** none

**Chart #:** 81

Pavement view

**Location:** NE1/4 SE1/4 Sec 35 T39N R78W

**Lithology:** Unit 4: carbonaceous shale

**Grain size, cementation:** very fine-grained (shale), very poorly cemented

**Bed thickness:** ~1m thick; measured area – 10m X 5m,

**Structure**

**Strike and dip of bedding:**

**Structural curvature (estimated):** North end of anticline and curvature is undetermined due to the lack of Mesaverde Formation exposures along the northern plunge of the anticline.

**Faulting:** no large-scale faulting observed in this location

**Fracture Characteristics**

**Type, Orientation:** Set A: (TNF) cleats in carbonaceous shale. Set B: (XF) less numerous cleats

Set A	Set B
N84E 67SE	N31E 67SE
N86E 84SE	N62E 74SE
N85E 86SE	N49E
N79E 89SE	N45E
N76E 85SE	N56E 89SE
N72E 86SE	N59E 87SE
N84E 83SE	N66E 86SE
N75E 86SE	
N77E 86SE	
N71E 88SE	
N76E 88NW	
N75E 80SE	
N76E 88SE	

**Spacing: (cm)**

Set A	Set B
40	30
35	15
17	10
5	8
10	
10	
15	
10	

**Separation:** none

**Mineralization:** some Fe stain on cleat surface

**Surface characteristics:** planar

**Relative ages:** Set A older

**Apertures: (mm)** Set A cleats – 10, 0, 1, 10, 1, 5, 1, 0. Apertures probably recent – in particular a 2.3cm aperture has a root growing within the cleat.

**Deformation Bands (width):** NA

**Chart #: 82**

Plan view with partial side view

**Location:** NE1/4 SE1/4 Sec 35 T39N R78W**Lithology:** Unit 5: fluvial sandstone**Grain size, cementation:** Grain size distribution for the measured sandstone bed is 10% 62-88 $\mu$ , 85% 88-125 $\mu$  and 5% 125-177 $\mu$ . Poorly to moderately cemented sandstone.

The west side of outcrop more is reddish in color (more Fe?) than eastern side. Eastern side less well cemented relative to western side of charted outcrop.

**Bed thickness:** Measured area ~5m X 10m**Structure****Strike and dip of bedding:** ~N38W 15NE**Structural curvature** (estimated): North end of anticline where curvature undetermined due to the lack of Mesaverde Formation exposures along the northern plunge of the anticline.**Faulting:** none at this location**Fracture Characteristics****Type, Orientation:** Set A: TNF (VE), measured E to W, perpendicular to fracture strike.

Set B: TNF, fewer measurements due to outcrop orientation relative to fracture strike.

Set A	Set B
N15W 88SW	N67E 83SE
N18W 88SW	N69E 85SE
N26W 86SW	N67E 85SE
N19W 86SW	N69E 84SE
N34W 84SW	
N13W 87SW	
N18W 88SW	
N17W 86SW	
N10W 68SW*	
N17W 64SW*	
N12W 69SW*	

\*Measurements within eastern portion of the outcrop. This area is less well cemented relative to the western portion of the outcrop. Note the change in fracture dip.

**Spacing: (cm)**

Set A	Set B
45	58
61	17
143	70
17	
32	
29	
67	
5	
95	
87	



**Separation:** none

**Mineralization:** none

**Surface characteristics:** no distinguishing characteristics

**Relative ages:** Set A generally older; some abutting relationships indicate that Sets A and B maybe penecontemporaneous.

**Apertures:** none

**Deformation Bands (width):** NA

**Chart #:** 83

Plan and side views

**Location:** NE1/4 NE1/4 Sec 5 T38N R78W (located between charts 48 and 50)**Lithology:** Unit 3: white beach sandstone**Grain size, cementation:** Grain size distribution of the measured sandstone bed is 10% 125-177 $\mu$ , 80% 177-250 $\mu$  and 10% 250-350 $\mu$ . Poorly cemented sandstone.**Bed thickness:** 1.9m thick, measured area – 10m X 15m**Structure****Strike and dip of bedding:** N49W 11SW**Structural curvature** (estimated): NW corner – possible structural influence from Salt Creek anticline.**Faulting:** none observed**Fracture Characteristics****Type, Orientation:** Set A: Deformation bands, most extensive set, dip hard to find and quantify, qualitatively most deformation bands appear to dip to the NW with some dips to the SE. Set B: Deformation bands.

Set A	Set A - deformation band width, mm	Set B	Set B – deformation band width, mm
N65E	1	N5E	2
N65E	2	N2W	2
N66E	2	N1E	1
N85E	2	N2E	2
N80E	2		
N84E	1	N70W	2
N70E	2		
N65E	2		
N89E	1		
N72E (Fe stained)	3		
N67E	1		
N66E	2		
N71E	1		
N70E	2		
N68E	2		
N66E	2		
N70E	1		
N68E	4		
N85E	2		

**Spacing:** (cm)

Set A	Set B
0.5	76
18	
30	
35	
86	
60	

14 29 26 104 39 21 52 55 37 25	
---	--

**Separation:** none

**Mineralization:** none

**Surface characteristics:** One Set A orientation measurement is composed of at least 3 inosculating bands.

**Relative ages:** penecontemporaneous? Intersections between Sets A and B are generally simple crosses, therefore age determination is questionable.

**Apertures:** NA

**Deformation Bands (width):** see type and orientation data above.

**Chart #:** 84

Plan and side views

**Location:** NE1/4 SE1/4 Sec 35 T39N R78W**Lithology:** Unit 3: white beach sandstone**Grain size, cementation:** Grain size distribution within the measured sandstone is 5% 125-177 $\mu$ , 80% 177-250 $\mu$  and 15% 250-350 $\mu$ . Poorly cemented sandstone.**Bed thickness:** 5.46m thick; measured area – 10m X 20m**Structure****Strike and dip of bedding:** N28W 9NE, N30W 9NE**Structural curvature** (estimated): NA**Faulting:** eastside graben described in chart 66 is approximately 150m to the southwest of this outcrop.**Fracture Characteristics****Type, Orientation:** Set A: deformation bands several of which can be followed along strike for 20m. Set B: these are not as extensive relative to Set A, maximum of 4m in length, this set curves in outcrop and is not as well developed as Set A.

Set A	Set A – deformation band or zone width, mm	Set B	Set B – deformation band width, mm
N65E 70NW	1	N35W	1
N68E 60SE	1	N35W	1
N69E 74NW	1	N33W	1
N66E 53SE	3 (? bands)	N28W	1
N65E 78NW	2	N39W	
N65E 76NW	3 (2 bands)		
N62E 64SE	2		
N55E 65SE	1		
N56E 69SE	2		
N62E 74NW	1		
N67E 85SE	2		
N69E 72NW	2		
N71E 78NW	2		
N71E 78NW	1		
N68E 60SE	2		

**Spacing: (cm)**

Set A	Set B
52	30
23	43
45	30
13	
520	
115	
52	
50	

320 54 68 90 10 110	
------------------------------------	--

**Separation:** NA

**Mineralization:** none observed

**Surface characteristics:** none observed

**Relative ages:** Set A older

**Apertures:** NA

**Deformation Bands (width):** See type and orientation data above.

**Other observations:** Top of this outcrop has several octagonal “elephant skin” weathering features.

**Chart #: 85**

Plan and side views

**Location:** SE1/4 NW1/4 Sec 9 T38N R78W**Lithology:** Sandstones within Unit 1: interbedded sandstones and shale.**Grain size, cementation:** Grain size distribution within the lower measured beds is 10% 125-177 $\mu$ , 80% 177-250 $\mu$  and 10% 250-350 $\mu$ . These lower beds are poorly to moderately cemented.Grain size distribution within the upper measured bed is 10% 88-125 $\mu$ , 80% 125-177 $\mu$  and 10% 250-350 $\mu$ . This sandstone is moderately to well cemented and provides a good pavement surface.**Bed thickness:** Lower bed thicknesses (from top to bottom): 20, 85, 20, 5, 10, 3, 45, 15cm, approximately 2m total thickness. Upper bed thickness is 25 cm. Total measured area – 5m wide X 5m long X 2.5m high**Structure****Strike and dip of bedding:** N15W 23SW**Structural curvature** (estimated): West limb (no noticeable curvature).**Faulting:** N24W 86SW – 13cm normal stratigraphic separation. N33W 76NE – 2cm normal stratigraphic separation. These are hinge-parallel faults.**Fracture Characteristics****Type, Orientation:** Set A: TNF in pavement surface. Pavement surface of upper bed shows none of the displacement observed with the small-scale faults in the lower bed. However, there is a fracture zone on the pavement surface with decreased fracture spacing that is spatially located between the two faults observed in the lower beds.

Set B: TNF, generally terminates at intersection with set A, but is dominant for short distance in some areas of the outcrop

Set A	Set B
N20W 71NE	N78E
N24W 70NE	N68E
N22W 73NE	N69E
N25W 78NE	N72E
N22W	N72E
N21W 78NE	N72E
N23W 68NE	N66E
N18W	
N21W	
N20W 73NE	
N22W	
N25W	
N24W	
N25W	
N23W	
N12W	
N12W	
N23W	
N20W	
N18W	

N15W N19W N20W N17W N18W N18W N16W N12W N16W N22W 70NE N21W	
---	--

**Spacing: (cm)**

Set A	Set B
37	58
23	19
40	5
1	50
10	28
6	38
1	
2	
2	
31	
14	
16	
27	
8	
6	
4	
4	
4	
1	
3	
1	
3	
5	
2	
6	
10	
4	
7	
15	
11	
21	
9	

15	
46	

**Separation:** none observed in fractured pavement above faults. Normal stratigraphic separation observed in cross sectional views along two distinct planes. 13cm displacement on one, 2cm displacement on the other.

**Mineralization:** none

**Surface characteristics:**

**Relative ages:** Set A generally older.

**Apertures:** none

**Deformation Bands (width):** NA



**Chart #: 86**

Plan and side views

**Location:** NW1/4 NW1/4 Sec 24 T38N R78W**Lithology:** Unit 3: white beach sandstone**Grain size, cementation:** Grain size distribution within the measured bed is 10% 88-125 $\mu$ , 80% 125-177 $\mu$  and 10% 177-250 $\mu$ . Poorly cemented sandstone.**Bed thickness:** 3m thick; measured area – 5m X 10m**Structure****Strike and dip of bedding:** There are few bedding surfaces appropriate for strike and dip measurements at this location (estimate N10W 12NE).**Structural curvature (estimated):** No apparent curvature.**Faulting:** No large-scale faulting.**Fracture Characteristics****Type, Orientation:** Set A: Deformation bands. Set B: Deformation bands. Set C: deformation bands.

Set A	Set B	Set C – 2 deformation bands
N85W 75NE N85W 78NE N88W 80SW N85W vertical N83W 78NE N83W N78W N78W N72W N72W 78NE N78W vertical to 88SW N74W N68W N68W	N32W – curves to intersect Set A N28W – terminates in rock N28W – terminates in rock N25W – terminates at Set A N25W – curves to intersect Set A	N58E N56E

**Spacing: (cm)**

Set A	Set B	Set C
100 19 31 22 12 3 21 12 10 13 17 11 18	19 25 26 40	130

**Separation:** none observed

**Mineralization:** Concretions noted near to and within the deformation bands. Concretions are elongate along the deformation band plane. These concretions are associated with Set A deformation bands.

**Surface characteristics:** no kinematic indicators for determining displacement or sense of slip that may be associated with deformation bands.

**Relative ages:** Set A older than Set B – abutting relationship. Two Set B deformation bands terminate before intersection with Set A, 2 curve to parallel Set A, and 1 terminates at intersection with Set A. Set C oldest, the two deformation bands within this set cuts both Set A and Set B deformation bands.

**Apertures:** NA

**Deformation Bands (width):** (mm)

Set A	Set B	Set C
1	1	3
2	1	3
1	1	
1	1	
1	1	
1		
1		
1		
1		
1		
1		
1		
1		
1		
1		

**Other observations:** While traversing to this site, numerous fractures with N65E trend noted in Unit 1: marine sandstones.

**Chart #:** 87

Plan and side views

**Location:** NE1/4 NE1/4 Sec 21 T38N R78W**Lithology:** Kmv "Teapot Ss member"**Grain size, cementation:** Grain size distribution within this measured bed is 2% 88-125 $\mu$ , 13% 125-177 $\mu$ , 80% 177-250 $\mu$  and 5% 250-350 $\mu$ . Poorly cemented sandstone, yet forms a less extensive secondary ridge around Teapot Dome; very quartz rich, 95+%, rounded to subrounded grains.**Bed thickness:** Overall thickness 6m; individual beds 3cm – 1m. Cross-beds and current ripples noted.**Structure****Strike and dip of bedding:** N25W 18SW (very irregular surface).**Structural curvature (estimated):** SW corner – 1.5km curvature**Faulting:** none**Fracture Characteristics****Type, Orientation:** Set A: VCF. Set B: TNF

Set A	Set B
N32W 82SW	N80E 70NW
N20W 82NE	N75W 88SW
N20W 76SW	N88E vertical
N18W 76NE	N55E 70SE
N16W 75SW	N65E 72NW
N42W	N25E
N18W	
N33W 62NE	
N28W 58NE	
N10E vertical	
N25W 76NE	
N26W 70SW	
N32W 87NE	
N26W 88NE	
N32W 78NE	
N30W 78NE	
N28W 76SW	
N34W 62NE	
N28W 54NE	
N34W	
N20W	

**Spacing:** (cm) Set A: 0.6, 1.1, 0.4, 0.6, 38, 41, 31, 50, 55cm**Separation:** none**Mineralization:** none**Surface characteristics:** irregular**Relative ages:** Abutting relationship unclear**Apertures:** none/only recent apertures**Deformation Bands (width):** NA

**Chart #:** 88

Plan and side views

**Location:** NE1/4 NW1/4 Sec 22 T38N R78W

**Lithology:** Unit 5: fluvial sandstone

**Grain size, cementation:** fine grained, moderately cemented

**Bed thickness:** 30cm to 1m thick; measured area – 1.5m X 50m. Detailed bed thickness measurements are proved with the fracture type and orientation chart.

**Structure**

**Strike and dip of bedding:** N23W 14SW

**Structural curvature** (estimated): SW corner, 1-2km curvature

**Faulting:** NA

**Fracture Characteristics**

**Type, Strike:** TNF measured across outcrop from starting point 0 to 58 meters.

Measured in this fashion to describe orientation difference across the length of the outcrop.

Distance (m)	Strike	Bed Thickness (m)
0	N62E	1
5	N60E	1
10	N50E	0.7-0.8
15	N55E	0.7-0.8
20	N58E	0.7-0.8
25	N56E	0.7-0.8
30	Covered	0.7-0.8
35	N52E	0.7-0.8
40	Irregular maximum N63E minimum N48E	Possible divide between two splays
45	Poorly fractured N57E	0.2-0.3
50	Irregular maximum N63E minimum N38E	0.2-0.3
55	N48E	0.5-0.6
58	N58E	0.5-0.6

**Spacing:** (cm) 10-30cm, average 20cm

**Separation:** NA

**Mineralization:** none

**Surface characteristics:** none visible

**Relative ages:** Only one set of fractures.

**Apertures:** recent

**Deformation Bands (width):** NA

**Chart #: 89**

Plan view and partial side view

**Location:** NE1/4 SW1/4 Sec 16 T38N R78W**Lithology:** Unit 3: white beach sandstone.**Grain size, cementation:** Grain size distribution within the measured bed is 20% 88-125 $\mu$ , 70% 125-177 $\mu$  and 10% 177-250 $\mu$ . Poorly cemented sandstone.**Bed thickness:** 3m total thickness, bed from which deformation band measurements were taken 1m; measured area – 10m X 5m**Structure****Strike and dip of bedding:** N29W 22SW**Structural curvature (estimated):** NA**Faulting:** South of large valley with fault interpreted from seismic data.**Fracture Characteristics****Type, Orientation:** Set A: deformation bands. Set B: Deformation bands

Set A	Set B
N52W 62NE	N52E – younger
N50W 60NE	N51E – younger
N56W 60NE	N43E – younger
N62W 85SW	
N58W	
N58W	
N60W 60NE	
N66W 88SW	
N62W 74NE	
N60W	
N61W	
N64W	
N58W 80NE	
N60W 85NE	
N53W vertical	

**Spacing:** (cm) Set A – 12, 130, 45, 82, 9, 7, 27, 42, 3, 6, 103cm**Separation:** none**Mineralization:** none**Surface characteristics:** none visible**Relative ages:** Set B abuts Set A at near right angles. Neither Set terminates at intersection therefore age relationship is unclear.**Apertures:** NA**Deformation Bands (width):** All Set A and Set B deformation bands 1mm in width.

**Chart #:** 90

Plan and side views.

**Location:** SE1/4 NE1/4 Sec 16 T38N R78W

**Lithology:** Unit 4: carbonaceous shale

**Grain size, cementation:** Carbonaceous shale very fine-grained, very poorly cemented.

**Bed thickness:** 51cm thick; measured area – 2m X 15m

**Structure**

**Strike and dip of bedding:** A suitable bedding surface for strike and dip measurements unavailable. Data from Chart 89 indicates N29W 22SW for bedding strike and dip.

**Structural curvature** (estimated): NA

**Faulting:** Near valley with large-scale fault interpreted from seismic. It should be noted that large-scale movement/separation is not evident in outcrop.

**Fracture Characteristics**

**Type, Orientation:** Set A: coal cleats, measured N to S

Coal cleats – measured N to S	Coal cleats, continued
N88W	N65W
N86W	N82W 86NE
N82W	N85W 67NE
N78W 64NE	N88W 72NE
N82W 70NE	N85W 87SW
N77W 75NE	N80W 73NE
N78W 62NE	N79W 69SW
N82W 65NE	N89W 79NE
N86W 73NE	

**Spacing:** (cm) 18, 38, 28, 53, 37, 58, 18, 23, 52, 45, 5, 78, 33, 46, 31, 82cm

**Separation:** NA

**Mineralization:** none

**Surface characteristics:** none visible

**Relative ages:** NA – only one cleat set

**Apertures:** none

**Deformation Bands (width):** NA

**Chart #:** 91

Plan view with partial side view

**Location:** Road cut 1 mile west of Teapot Ranch on Hwy 259**Lithology:** Kmv Teapot Sandstone member**Grain size, cementation:****Bed thickness:** 3m in road cut; cliffs of S and N from Hwy approx. 9m

Area – 100m X 20m

**Structure****Strike and dip of bedding:** Difficult to obtain due to poor bedding surface, estimate is N90E 3SE.**Structural curvature (estimated):** NA**Faulting:** no faulting observed**Fracture Characteristics****Type, Strike:** Set A: VCF

VCF	VCF, continued
N89W 87SW	N82W 68SW
N89E 74SE	N82W 82SW
N89W 80NE	N86W 79SW
N87W 74SW	N87W 78NE
N85W 76SW	N76W 75SW
N88W 84NE	N75W 86NE
N78W 74SW	N72W 73SW
N68E 88NW	N74W 74SW
N88W 64SW	N85E 75SE
N88E 87SE	N87E 78NW
N82W 76SW	N82E 76NW
N84W 45SW	N88E 75SE

**Spacing:** (cm) 41, 28, 68, 50, 61, 43, 22, 28, 81, 34, 102, 23, 51, 15, 15, covered 2m, 10, 12, 18, 56, 20, 50, 24cm**Separation:** none**Mineralization:** none**Surface characteristics:** no visible kinematic indicators**Relative ages:** One VCF set.**Apertures:** none**Deformation Bands (width):** NA

## APPENDIX D

### ***Fracture Spacing and Bed Thickness Data***

This is a compilation of data from Appendix D used to generate bed thickness vs. fracture spacing charts. These data are from those locations where clear fracture age relationships were available. In many cases the fracture spacing of fracture sets of different ages is distinctly different. The spacing within the oldest fracture set at a given location was used for this comparison to avoid averaging spacings measured from different fracture sets.

Unit 5: Fluvial Sandstones						
Chart number	Bed Thickness (m)	Set A: Mean Fracture spacing (m)	Set A: n =	Set B: Mean Fracture spacing (m)	Set B: n =	Oldest fracture set
11	0.18	0.22	13	0.87	4	A
12	1	0.35	9	0.78	9	A
22	2.5	0.55	13	0.71	7	A
37	1.4	0.68	10	1.25	2	A
38	1.4	0.98	10	1.92	3	A
43	0.5	0.39	13	0.6	7	A
48	4	4.96	5	4.14	7	A
59	3.75	.73	11			A
65	2	0.97	14	1.85	1	A
70	0.5	.66	10	0.35	8	A
74	0.7	0.54	12	1.03	7	A
Unit 4: Carbonaceous Shales						
Chart number	Bed Thickness (m)	Set A: Mean Fracture spacing (m)	Set A: n =	Set B: Mean Fracture spacing (m)	Set B: n =	Oldest fracture set
35	1.8	0.11	17			A
41	1	0.31	8	0.15	9	A
46	1	0.17	19			A
49	0.2	0.28	18	0.46	9	A
56	0.5	0.22	14	0.42	7	A
58	1.3	0.12	14	0.15	13	A
64	1.1	0.14	13			A
71	1	0.26	9	0.44	8	A
81	1	0.18	8	0.16	4	A
90	0.51	0.4	16			A



Unit 2: Beach Sandstones						
Chart number	Bed Thickness (m)	Set A: Mean Fracture spacing (m)	Set A: n =	Set B: Mean Fracture spacing (m)	Set B: n =	Oldest fracture set
8	2	0.37	9	0.22	9	A
14	0.1	0.67	3	0.28	8	A
15	0.1	0.36	10	0.43	11	A
32	0.6	0.4	17			A
33	1.5	0.26	14			A
39	0.6			0.28	15	A
40	0.3	0.24	13	1.06	6	A
45	0.2	0.3	17	1.73	14	A
50	0.18	0.74	8	1	6	A
61	0.25	0.16	16	0.38	8	A
76	2.5	1	8	1.13	6	A
80	0.4	0.75	8	1.4	13	A
Unit 1: Interbedded Shallow Marine Sandstones						
Chart number	Bed Thickness (m)	Set A: Mean Fracture spacing (m)	Set A: n =	Set B: Mean Fracture spacing (m)	Set B: n =	Oldest fracture set
9	0.07	0.06	8	0.18	7	A
10	0.35	0.21	9	0.3	8	A
13	1.2	0.59	7	0.88	7	A
16	0.3	0.36	7	0.42	6	A
24	0.2	0.61	8	0.36	7	A
27	1	0.5	7			A
30	0.45	0.29	15	0.55	10	A
31	0.25	0.38	19	0.82	8	A
36	0.05	0.42	12	0.4	5	A
42	0.4	1.33	8	2.45	6	A
44	0.08	0.24	7	0.48	9	A
52	0.1	0.51	11	0.47	16	A
53	0.25	0.21	20	0.41	12	A
55	0.85	0.96	10	0.55	15	A
60	0.7	0.62	13	0.82	11	A
62	0.22	0.24	18	0.41	6	A
69	0.35	0.29	16			A
75	0.9	1.19	3	0.31	11	A
77	0.31	0.37	9	0.05	2	A
80	0.4	0.75	8	1.4	13	A
Total n =			594		360	

## APPENDIX E

### ***Representative fracture orientation data***

Compilation of representative throughgoing fracture orientation data compiled from Appendix C. Chart numbers correlate to Appendix C.



Chart #	Lithologic unit	Orientation	Hinge-parallel	Hinge-perpendicular	Other (oblique)	West limb	East limb	Southern exposure	Oldest fracture set (x = yes)	Chart fracture set	n =
51	3	N65E 81SE		x			x			A	9
52	1	N73E 85SE		x			x		x	A	17
53	1	N38W 88SW	x				x		x	B	16
54	1	N72E 77NW		x			x			A	15
55	1	N34W 84SW	x				x		x	B	14
56	1	N62E 75NW		x			x		x	A	11
57	1	N77E 87NW		x			x		x	A	12
58	1	N33W 84SW	x				x		x	B	12
59	4	N88E 88SE					x		x	A	13
60	4	N18W 86SW	x				x		x	B	8
61	2	N45W 73SW			x		x		x	A	23
62	4	N87W 88SW	x				x		x	A	14
63	4	N4E 73NW	x				x		x	B	11
64	5	N19W 60SW	x				x		x	A	12
65	1	N68E 90					x		x	A	14
66	1	N34W 89SW	x				x		x	B	12
67	2	N73E 85SE			x		x		x	A	11
68	2	N61W 78SW					x		x	B	7
69	1	N83E 88NW	x				x		x	A	16
70	1	N37W 77SW					x		x	B	12
71	3	N42E 84SE	x				x		x	A	9
72	3	N66E 74SE					x		x	B	4
73	4	N85W 84SW					x		x	A	14
74	4	N13W 85SW	x				x		x	B	5
75	5	N34W 82SW	x				x		x	A	15
76	1	N68E 74NW					x		x	A	14
77	1	N13W 74SW	x				x		x	B	3
78	1	N85E 85SE					x		x	A	1
79	2	N68W 83NE			x		x		x	A	6
80	2	N65E 85SE					x		x	B	1
81	1	N60E 89NW					x		x	A	18
82	5	N43W 80SW	x				x		x	A	1
83	5	N74E 86SE					x		x	A	12
84	4	N73W 70NE					x		x	B	9
85	4	N19E 70NW					x		x	A	11
86	3	N35W 80SW	x				x		x	B	8
87	1	N68E 70NW					x		x	A	5
88	5	N33W 80SW	x				x		x	A	6
89	4	N62E 79NW					x		x	A	15
90	1	N29E 84NW					x		x	C	4
91	1	N60W 83SW	x				x		x	A	9
92	2	N59E 86NW					x		x	B	12
93	2	N1W 74SW	x				x		x	A	9
94	2	N67E 86SE					x		x	B	8
95	1	N39W 81SW	x				x		x	A	10
96	4	N35W 84NE	x				x		x	A	10
97	5	N77E 86SE					x		x	A	13
98	5	N19W 86SW	x				x		x	A	11
99	3	N67E 85SE					x		x	B	4
100	3	N1E	x				x		x	A	19
101	3	N67E 85SE					x		x	B	4
102	3	N35W	x				x		x	A	15
103	3	N19W	x				x		x	A	5
104	1	N20W 71NE	x				x		x	B	31
105	1	N68E 78SE	x				x		x	A	7
106	3	N73W 78NE					x		x	B	14
107	3	N25W 80SW	x				x		x	A	5
108	5	N57E					x		x	A	13
109	3	N60W 85NE					x		x	A	15
110	4	N80W 73NE					x		x	A	17
total n =											
Number	n = 129		57	41	31						1413
Percentage			44.19	31.78	24.03						
Hinge-parallel and hinge-perpendicular (normalized)	n = 98		58.16	41.84							

## APPENDIX F

### ***Representative fracture orientation data for locations away from Teapot Dome***

Compilation of representative throughgoing fracture orientation data from locations at a distance from Teapot Dome. The data shown below were compiled from field observations.

Location	Description	Orientation	Type	
Site A				
Salt creek anticline	Shannon sandstone	N85W 80NE	TNF	
		N40W 90	TNF	
Site B				
Hiway 387 @ milepost 109	Tertiary fluvial unit	N25W 40 NE	TNF	
East of Midwest	approx. 10m thick	N15W 65NE	TNF	
	with 1/2 m thick	N10W 57 NE	TNF	
	well cemented	N8E 67NW	TNF	
	sandstone near top	N85E 90	TNF	
		N55W 90	TNF	
		N57W 85NE	TNF	
		N55W 85NE	TNF	
		N85W 80 NE	TNF	
		N5E 83 NW	TNF	
Site C				
Hiway 387 @ milepost 103	Mesaverde Fm	N35E bed normal	TNF	
East of Midwest	White sandstone	N55W bed normal	TNF	
	3m thick			
	underlain by			
	carbonaceous shale			
Site D				
1.5 miles southwest of NPR 3	Mesaverde Fm	N72E 80SE	TNF	
NPR 3 entrance	Fluvial Sandstone	N40E 70SE	TNF	
North side of Hiway 259	1.5m thick	N65E 84 SE	TNF	
		N75E 85SE	TNF	
		N35E 88SE	TNF	
		N50E 75SE	TNF	
		N5W 89SW	TNF	
		N5W 88SW	TNF	
		N72W 90	TNF	

Site E				
West 1/2 mile on Ormsby road	Mesaverde Fm	N80-90W	VCF	
off Interstate 25	White sandstone	N65W	TNF	
	Teapot Sandstone member			
Site F				
Road cut 1 mile west of Teapot Ranch on Hiway 259	Mesaverde Fm	N89W 87SW	VCF	
	White sandstone	N89E 74SE	VCF	
North side of road	Teapot Sandstone member	N89W 80NE	VCF	
		N87W 74SW	VCF	
		N85W 76SW	VCF	
		N88W 84NE	VCF	
		N78W 74SW	VCF	
		N68E 88NW	VCF	
		N88W 64SW	VCF	
		N88E 87SE	VCF	
		N82W 76SW	VCF	
		N84W 45SW	VCF	
		N82W 68SW	VCF	
		N82W 82SW	VCF	
		N86W79SW	VCF	
		N87W 78NE	VCF	
		N76W 75SW	VCF	
		N75W 86NE	VCF	
		N72W 73SW	VCF	
		N74W 74SW	VCF	
		N85E 75SE	VCF	
		N87E 78NW	VCF	
		N82E 76NW	VCF	
		N88E 75SE	VCF	

## REFERENCES

- Agarwal, B., Allen, L.R., and Farrell, H.E., 1997, Ekofisk reservoir characterization: Mapping permeability through facies and fractures intensity: Society of Petroleum Engineers Inc., Formation Evaluation, p. 227-233.
- Antonellini, M., and Aydin, A., 1994, Effect of faulting on fluid flow in porous sandstones: Petrophysical properties: American Association of Petroleum Geologists Bulletin, v. 78, p. 355-377.
- Antonellini, M., and Aydin, A., 1995, Effect of faulting on fluid flow in porous sandstones: Geometry and spatial distribution: American Association of Petroleum Geologists Bulletin, v. 79, p. 642-671.
- Antonellini, M., Aydin, A., and Pollard, D.D., 1994, Microstructure of deformation bands in porous sandstones at Arches National Park, Utah: Journal of Structural Geology, v. 16, p. 941-959.
- Aydin, A., 1978, Small faults formed as deformation bands in sandstone: Pure and Applied Geophysics, v. 116, p. 913-930.
- Aydin, A., and Johnson, A.M., 1983, Analysis of faulting in porous sandstones: Journal of structural Geology, v. 5, p. 19-31.
- Bai, T., and Pollard, D.D., 2000, Fracture spacing in layered rocks: a new explanation based on the stress transition: Journal of Structural Geology, v. 22, p. 43-57.
- Berg, R.R., 1962, Mountain flank thrusting in Rocky Mountain Foreland, Wyoming and Colorado: American Association of Petroleum Geologists Bulletin, v. 46, p. 2019-2032.
- Blackstone, D.L., Jr., 1940, Structure of the Pryor Mountains, Montana: Journal of Geology, v. 48, p. 590-618.
- Blackstone, D.L., Jr., 1980, Foreland deformation: compression as a cause: University of Wyoming Contributions in Geology, v. 18, p. 83-101.
- Bogdanov, A.A., 1947, The intensity of cleavage as related to the thickness of beds (in Russian): Soviet Geology.
- Caine, J.S., Evans, J.P., and Forster, C.B., 1996, Fault zone architecture and permeability structure: Geology, v. 24, p. 1025-1028.
- Cooper, M., 1992, The analysis of fracture systems in subsurface thrust structures from the Foothills of the Canadian Rockies, *in* McClay, K.R., ed., Thrust Tectonics, London, Chapman and Hall, p. 391-405.
- Curry, W.H., 1977, Teapot Dome - past, present and future: American Association of Petroleum Geologists Bulletin, v. 61, p. 671-697.
- DeSitter, L.U., 1956, Structural Geology: New York, McGraw-Hill, 552 p.
- DeSitter, L.U., 1964, Variation in tectonic style: Bulletin of Canadian Petroleum Geology, v. 12, p. 263-278.
- Doelger, M.J., Mullen, D.M., and Barlow & Haun, I., 1993, Nearshore marine sandstone, Atlas of Major Rocky Mountain Gas Reservoirs: Socorro, NM, New Mexico Bureau of Mines and Mineral Resources, p. 54-55.
- Doll, T.E., Luers, D.K., Strong, G.R., Schult, R.K., Sarathi, P.S., Olsen, D.K., and Hendricks, M.L., 1995, An update of steam injection operations at Naval Petroleum Reserve No. 3, Teapot Dome Field, Wyoming: A shallow

- heterogeneous light oil reservoir, SPE 30286, International Heavy Oil Symposium: Calgary, Alberta, Canada, Society of Petroleum Engineers, p. 1-20.
- Dunn, D.D., LaFountain, L.J., and Jackson, R.E., 1973, Porosity dependence and mechanism of brittle fracture in sandstones: *Journal of Geophysical Research*, v. 78, p. 2403-2417.
- Elkins, L.F., and Skov, A.M., 1960, Determination of fracture orientation from pressure interference: *Petroleum Transactions, American Institute of Mining Engineers*, v. 219, p. 301-304.
- Engelder, T., 1974, Cataclasis and the generation of fault gouge: *Geological Society of America Bulletin*, v. 85, p. 1515-1522.
- Engelder, T., Gross, M.R., and Pinkerton, 1997, An analysis of joint development in thick sandstone beds of the Elk Basin anticline, Montana-Wyoming, *in* Hoak, T.E., Klawitter, A.L., and Blomquist, P.K., eds., *Fractured reservoirs: characterization and modeling: Rocky Mountain Association of Geologists Guidebook*, p. 1-18.
- Fassett, J.E., 1991, Oil and gas resources of the San Juan basin, New Mexico and Colorado, *in* Gluskoter, H.J., Rice, D.D., and Taylor, R.B., eds., *Economic Geology, U.S., Volume P-2: The Geology of North America, Geological Society of America*, p. 357-372.
- Fausnaugh, J.M., and LeBeau, J., 1997, Characterization of shallow hydrocarbon reservoirs using surface geochemical methods: *American Association of Petroleum Geologists Bulletin*, v. 81, p. 1223.
- Fisher, M.P., and Wilkerson, M.S., 2000, Predicting the orientation of joints from fold shape: Results of pseudo-three-dimensional modeling and curvature analysis: *Geology*, v. 28, p. 15-18.
- Fjaer, E., Holt, R.M., Horsrud, P., Raaen, A.M., and Risnes, R., 1992, Petroleum related rock mechanics: New York, Elsevier Science Publishing Company Inc., 388 p.
- Fox, J.E., Dolton, G.L., and Clayton, J.L., 1991, Powder River Basin, *in* Gluskoter, H.J., Rice, D.D., and Taylor, R.B., eds., *Economic Geology, U.S.: Geological Society of America, The Geology of North America, P-2*, p. 373-390.
- Friedman, M., and Stearns, D.W., 1971, Relations between stresses inferred from calcite twin lamellae and macrofractures, Teton Anticline, Montana: *Geological Society of America Bulletin*, v. 82, p. 3151-3162.
- Garrett, C.H., and Lorenz, J.C., 1990, Fracturing along the Grand Hogback, Garfield County, Colorado, *in* Bauer, P.W., Lucas, S.G., Mawer, C.K., and McIntosh, W.C., eds., *New Mexico Geological Society Guidebook, 41st Field Conference, Southern Sangre de Cristo Mountains, New Mexico*, p. 145-150.
- Gay, S.P., Jr., 1999, An explanation for "4-way closure" of thrust-fold structures in the Rocky Mountains, and implications for similar structures elsewhere: *The Mountain Geologist*, v. 36, p. 235-244.
- Gill, J.R., and Cobban, W.A., 1966, Regional unconformity in Late Cretaceous, Wyoming: *United States Geological Survey Professional Paper 550-B*, p. B20-B27.
- Gribbin, D.J., 1952, Completion report exploratory well no. 1-G-10 at Naval Petroleum Reserve No. 3, Natrona County, Wyoming: *Casper*, p. 1-20.



- Gries, R., 1983, Oil and gas prospecting beneath Precambrian of foreland thrust plates in Rocky Mountains: American Association of Petroleum Geologists Bulletin, v. 67, p. 1-28.
- Gries, R.R., and Dyer, R.C., 1985, Seismic exploration of the Rocky Mountain foreland structures: Denver, Rocky Mountain Association of Geologists and the Denver Geophysical Society, p. 298.
- Griffith, A.A., 1921, The Phenomena of rupture and flow in solids: Royal Society of London Transactions, v. 221, p. 163-198.
- Gross, M.R., 1993, The origin and spacing of cross joints: examples from the Monterey Formation, Santa Barbara Coastline, California: Journal of Structural Geology, v. 15, p. 737-751.
- Hallbauer, D.K., Wagner, H., and Cook, N.G.W., 1973, Some observations concerning the microscopic and mechanical behavior of quartzite specimens in stiff, triaxial compression tests: International Journal of Rock Mechanics and Mineral Science, v. 10, p. 713-726.
- Haneberg, W.C., 1995, Steady state groundwater flow across idealized faults: Water Resources Research, v. 31, p. 1815-1820.
- Harding, T.P., and Lowell, J.D., 1979, Structural styles, their plate-tectonic habitats, and hydrocarbon traps in petroleum provinces: American Association of Petroleum Geologists Bulletin, v. 63, p. 1016-1058.
- Harris, J.F., Taylor, G.L., and Walper, J.L., 1960, Relation of deformation fractures in sedimentary rocks to regional and local structure: American Association of Petroleum Geologists Bulletin, v. 44, p. 1853-1873.
- Hennings, P.H., Olson, J.E., and Thompson, L.B., 1998, Using outcrop data to calibrate 3-D geometric models for prediction of reservoir-scale deformation: An example from Wyoming, *in* Hoak, T.E., ed., Fractured reservoirs: practical exploration and development strategies, Symposium Proceedings, The Rocky Mountain Association of Geologists, p. 91-95.
- Hobbs, D.W., 1967, The formation of tension joints in sedimentary rocks: an explanation: Geological Magazine, v. 104, p. 550-556.
- Hoshino, K., 1974, Effect of porosity on the strength of clastic sedimentary rocks, Advances in Rock Mechanics, Proc. 3rd Int. Soc. Rock Mech., Volume 2: Denver, Colorado, p. 511-516.
- Howard, A.D., and Kochel, R.C., 1988, Introduction to cuesta landforms and sapping processes on the Colorado Plateau, *in* Howard, A.D., Kochel, R.C., and Holt, H.E., eds., Sapping features of the Colorado Plateau - A comparative planetary geology field guide, National Aeronautics and Space Administration Special Publication 491, p. 6-56.
- Huang, Q., and Angelier, J., 1989, Fracture spacing and its relation to bed thickness: Geological Magazine, v. 126, p. 355-362.
- Hubbert, M.K., and Rubey, W.W., 1959, Role of fluid pressure in mechanics of overthrust faulting, I. Mechanics of fluid-filled porous solids and its application to overthrust faulting: Geological Society of America Bulletin, v. 70, p. 115-166.
- Huntoon, P.A., and Lundy, D.A., 1979, Fracture-controlled ground-water circulation and well siting in the vicinity of Laramie, Wyoming: Ground Water, v. 17, p. 463-469.

- Jaeger, J.C., and Cook, N.G.W., 1969, *Fundamentals of Rock Mechanics*: London, Methuen and Co., 513 p.
- Jamison, W.R., and Stearns, D.W., 1982, Tectonic deformation of Wingate Sandstone, Colorado National Monument: *American Association of Petroleum Geologists Bulletin*, v. 66, p. 2584-2608.
- Ji, S., and Saruwatari, K., 1998, A revised model for the relationship between joint spacing and layer thickness: *Journal of Structural Geology*, v. 20, p. 1495-1508.
- Kuenen, P.H., 1958, Experiments in geology: *Transactions Geological Society Glasgow*, v. 23, p. 1-28.
- Ladeira, F.L., and Price, N.J., 1981, Relationship between fracture spacing and bed thickness: *Journal of Structural Geology*, v. 3, p. 179-183.
- Lawrence Allison, 1989, Structure Contour Map, Top of the Second Wall Creek Sand, Naval Petroleum Reserve No. 3, Natrona County, Wyoming: Casper, Wyoming, Rocky Mountain Oilfield Testing Center.
- LeBeau, J., 1996, Preliminary geological characterization of the Dakota Formation, Naval Petroleum Reserve #3, Midwest, Wyoming, RMOTC/Halliburton multilateral test, October 1996: Rocky Mountain Oilfield Technology Center Internal Report, p. 25 p. plus appendices.
- Long, J.C.S., Aydin, A., Brown, S.R., Einstein, H.H., Hestir, K., Hsieh, P.A., Myer, L.R., Nolte, K.G., Norton, D.L., Olsson, O.L., Paillet, F.L., Smith, J.L., and Thomsen, L., 1997, *Rock Fracture and Fluid Flow*: Washington, D.C., National Academy Press, p. 551.
- Lorenz, J.C., 1997a, Heartburn in predicting natural fractures: The effects of differential fracture susceptibility in heterogeneous lithologies, *in* Hoak, T.E., Klawitter, A.L., and Blomquist, P.K., eds., *Fractured reservoirs: Characterization and modeling*: Rocky Mountain Association of Geologists Guidebook, p. 57-66.
- Lorenz, J.C., 1997b, Natural fractures and in-situ stresses in the Teapot Dome: Proposal for development of an analog to Rocky Mountain anticlines, 48th Annual Field Conference Technical Abstracts: Casper, Wyoming, Wyoming Geological Association, p. 5-6.
- Lorenz, J.C., and Finley, S.J., 1989, Differences in fracture characteristics and related production: Mesaverde Formation, Northwestern Colorado: *Society of Petroleum Engineers Formation Evaluation*, v. 4, p. 11-16.
- Lorenz, J.C., and Hill, R.E., 1991, Subsurface fracture spacing: comparison of inferences from slant/horizontal core and vertical core in Mesaverde reservoirs: *Society of Petroleum Engineers Paper 21877: Joint Rocky Mountain Section Meeting and Low-Permeability Reservoir Symposium*, p. 705-716.
- Lorenz, J.C., and Hill, R.E., 1992, Measurement and Analysis of fractures in core, *in* Schmoker, J.W., Coalson, E.B., and Brown, C.A., eds., *Geological studies relevant to Horizontal drilling: Examples from Western North America*, Rocky Mountain Association of Geologists, p. 47-59.
- Lorenz, J.C., Teufel, L.W., and Warpinski, N.R., 1991, Regional fractures I: A mechanism for the formation of regional fractures at depth in flat-lying reservoirs: *American Association of Petroleum Geologists Bulletin*, v. 75, p. 1714-1737.
- Lorenz, J.C., Warpinski, N.R., and Teufel, L.W., 1996, Natural fracture characteristics and effects: *The Leading Edge*, v. 15, p. 909-911.

- Mair, K., Main, I., and Elphick, S., 2000, Sequential growth of deformation bands in the laboratory: *Journal of Structural Geology*, v. 22, p. 25-42.
- Martinsen, O.J., Martinsen, R.S., and Steidtmann, J.R., 1993, Mesaverde Group (Upper Cretaceous), southeastern Wyoming: Allostratigraphy versus sequence stratigraphy in a tectonically active area: *American Association of Petroleum Geologists Bulletin*, v. 77, p. 1351-1373.
- McQuillan, H., 1973, Small-scale fracture density in Asmari Formation of southwest Iran and its relation to bed thickness and structural setting: *American Association of Petroleum Geologists Bulletin*, v. 57, p. 2367-2385.
- Merewether, E.A., 1990, Cretaceous formations in the southwestern part of the Powder River Basin, northeastern Wyoming: *American Association of Petroleum Geologists Bulletin*, v. 74, p. 1337.
- Muhlhaus, H.B., and Vardoulakis, I., 1988, The thickness of shear bands in granular materials: *Geotechnique*, v. 38, p. 271-284.
- Murray, F.N., 1967, Jointing in sedimentary rocks along the Grand Hogback Monocline, Colorado: *Journal of Geology*, v. 75, p. 340-350.
- Murray, G.H., Jr., 1968, Quantitative fracture study - Sanish Pool, McKenzie County, North Dakota: *American Association of Petroleum Geologists Bulletin*, v. 52, p. 57-65.
- Narr, W., and Suppe, J., 1991, Joint spacing in sedimentary rocks: *Journal of Structural Geology*, v. 13, p. 1037-1048.
- Nelson, R.A., 1985, *Geologic analysis of naturally fractured reservoirs*: Houston, Gulf Publishing Company, 360 p.
- Nicol, A., Watterson, J., Walsh, J.J., and Childs, C., 1996, The shapes, major axis orientations and displacement patterns of fault surfaces: *Journal of Structural Geology*, v. 18, p. 235-248.
- Oldow, J.S., Bally, A.W., Ave' Lallemand, H.G., and Leeman, W.P., 1989, Phanerozoic evolution of the North American Cordillera; United States and Canada, *in* Bally, A.W., and Palmer, A.R., eds., *The geology of North America; an overview*, Volume A: Boulder, Geological Society of America, p. 139-232.
- Olsen, D.K., Sarathi, P.S., and Hendricks, M.L., 1993, Case history of steam injection operations at Naval Petroleum Reserve No. 3, Teapot Dome Field, Wyoming: A shallow heterogeneous light-oil reservoir: SPE paper 25786, *International Thermal Operations Symposium*: Bakersfield, CA, Society of Petroleum Engineers, p. 93-110.
- Peng, S., and Johnson, A.M., 1972, Crack growth and faulting in cylindrical specimens of Chelmsford granite: *International Journal of Rock Mechanics and Mining Science*, v. 9, p. 37-86.
- Pollard, D.D., and Aydin, A., 1988, Progress in understanding jointing over the past century: *Geological Society of America Bulletin*, v. 100, p. 1181-1204.
- Potter, P.E., and Pettijohn, F.J., 1977, *Paleocurrents and Basin Analysis*: New York, Springer-Verlag, 425 p.
- Price, N.J., 1966, *Fault and joint development*: Oxford, Pergamon Press, 176 p.
- Prucha, J.J., Graham, J.A., and Nickelsen, R.P., 1965, Basement-controlled deformation in Wyoming Province of Rocky Mountains foreland: *American Association of Petroleum Geologists Bulletin*, v. 49, p. 966-992.

- Raghaven, R., Scorer, J.D.T., and Miller, F.G., 1972, An investigation by numerical methods of the effect of pressure-dependent rock and fluid properties on well flow tests: *Society of Petroleum Engineers Journal*, v. 12, p. 267-275.
- Rice, D.D., 1983, Relation of natural gas composition to thermal maturity and source rock type in San Juan basin, northwestern New Mexico and southwestern Colorado: *American Association of Petroleum Geologists Bulletin*, v. 67, p. 1199-1218.
- Roscoe, K.H., 1970, The influence of strains in soil mechanics: *Geotechnique*, v. 20, p. 129-170.
- Rudnicki, J.W., and Rice, J.R., 1975, Conditions for the localization of deformation in pressure-sensitive dilatant materials: *Journal Mech. Phys. Solids*, v. 23, p. 371-394.
- Secor, D.T., Jr., 1965, Role of fluid pressure in jointing: *American Journal of Science*, v. 263, p. 633-646.
- Sigda, J.M., Goodwin, L.B., Mozley, P.S., and Wilson, J.L., 1999, Permeability alteration in small-displacement faults in poorly consolidated sediments: Rio Grande Rift, central New Mexico, *in* Haneberg, W.C., Mozley, P.S., Moore, J.C., and Goodwin, L.B., eds., *Faults and Subsurface Fluid Flow in the Shallow Crust* AGU Monograph 113, p. 51-68.
- Sinclair, S.M., 1980, Analysis of Macroscopic Fractures on Teton Anticline, Northwestern Montana [M.S. thesis]: College Station, Texas A&M University.
- Stearns, D.W., 1964, Macrofracture patterns on Teton anticline, northwest Montana: *American Geophysical Union Transactions*, v. 45, p. 107-108.
- Stearns, D.W., 1967, Certain aspects of fracture in naturally deformed rocks, *in* Rieker, R.E., ed., *NSF Advanced Science Seminar in Rock Mechanics: Bedford, Air Force Cambridge Research Laboratories*, p. 97-118.
- Stearns, D.W., 1971, Mechanisms of drape folding in the Wyoming Province, *in* Renfro, A.R., Madison, L.W., Jarre, G.A., and Bradley, W.A., eds., *Symposium on Wyoming tectonics and their economic significance, Twenty-Third Annual Field Conference Guidebook*, Wyoming Geological Association, p. 125-143.
- Stearns, D.W., 1975, Laramide basement deformation in the Bighorn Basin - The controlling factor for structures in the layered rocks, *in* Exum, F.A., and George, G.R., eds., *Geology and mineral resources of the Bighorn Basin, Twenty-Seventh Annual Field Conference Guidebook*, Wyoming Geological Association, p. 149-158.
- Stearns, D.W., 1978, Faulting and forced folding in the Rocky Mountains foreland, *in* Matthews, V., III., ed., *Laramide folding associated with basement block faulting in the western United States, Volume Memoir 151*, Geological Society of America, p. 1-37.
- Stearns, D.W., and Friedman, M., 1972, Reservoirs in fractured rock, *in* King, R.E., ed., *Stratigraphic oil and gas fields - classification, exploration methods, and case histories, Volume Memoir 16*, American Association of Petroleum Geologists, p. 82-106.
- Teufel, L.W., and Farrell, H.E., 1992, Interrelationship between in situ stress, natural fractures, and reservoir permeability anisotropy: A case study of the Ekofisk Field, North Sea, *Fractures and Jointed Rock Conference: Lake Tahoe, CA*.

- Thom, W.T., Jr., and Speiker, E.M., 1931, The significance of geologic conditions in Naval Petroleum Reserve No. 3, Wyoming, United States Geological Survey Professional Paper 163, p. 64.
- Tillman, R.W., and Martinsen, R.S., 1984, The Shannon self-ridge sandstone complex, Salt Creek Anticline area, Powder River Basin, Wyoming, *in* Tillman, R.W., and Seimers, C.T., eds., Siliclastic shelf sediments: Society of Economic Paleontology and Mineralogy Special Publication, Volume 40, p. 85-142.
- Trexel, C.A., 1930, Compilation of data on Naval Petroleum Reserve No. 3 (Teapot Dome), Natrona County, Wyoming, p. 248.
- Unruh, J.R., and Twiss, R.J., 1998, Coseismic growth of basement-involved anticlines: The Northridge-Laramide connection: *Geology*, v. 26, p. 335-338.
- Wegemann, C.H., 1918, The Salt Creek oil field, Wyoming, United States Geological Survey Bulletin 452, p. 37-83.
- Weijermars, R., 1997, Principles of Rock Mechanics, Alboran Science Publishing, 360 p.
- Weimer, R.J., 1960, Upper Cretaceous stratigraphy, Rocky Mountain area: American Association of Petroleum Geologists Bulletin, v. 44, p. 1-20.
- Weimer, R.J., 1984, Relation of unconformities, tectonics, and sea level changes, Cretaceous of Western Interior, U.S.A., *in* Schlee, J.S., ed., Interregional unconformities and hydrocarbon accumulation, American Association of Petroleum Geologists Memoir 36, p. 7-35.
- Willis, J.J., and Brown, W.G., 1993, Structural interpretations of the Rocky Mountain Foreland: Past, Present, and Future, *in* Strook, B., and Andrew, S., eds., Jubilee Anniversary Field Conference Guidebook: Casper, Wyoming Geological Society, p. 95-119.
- Wong, T.-f., 1998, Dilatancy, compaction and failure mode in porous rocks, US Department of Energy Basic Sciences Geoscience Program, 1998 Research Symposium, Micromechanics and Flow: Santa Fe, NM, p. 14.
- Wong, T.-f., David, C., and Zhu, W., 1997, The transition from brittle faulting to cataclastic flow in porous sandstones: Mechanical deformation: *Journal of Geophysical Research*, v. 102, p. 3009-3025.
- Wong, T.-f., Szeto, H., and Zhang, J., 1992, Effect of loading path and porosity on the failure mode of porous rocks: *Applied Mechanical Review*, v. 45, p. 281-293.
- Zapp, A.D., and Cobban, W.A., 1962, Some Late Cretaceous strand lines in southern Wyoming: United States Geological Survey Professional Paper 45-D, p. D52-D55.